Optimizing Distillation Techniques for Isotopic Determinations in Beverages

Susiane Leonardelli, Julia Panozzo, Júlia Daneluz, Letícia Leonardelli,
Gilberto João Cargne, Regina Vanderlinde

Learn. Discover. Interact. Explore.

Welcome to the 4th Iberoamerican Conference on Mass Spectrometry website!

December 8 – 11, 2024

Venue: Grand Carimã Resort & Convention Center, Foz do Iguaçu, PR, Brazil

IBERO2024 brings together researchers, students, industry professionals and experts from around the world to discuss the latest advances and challenges in Mass Spectrometry.

It is a unique opportunity to share discoveries, exchange ideas, and foster new collaborations.

The scientific program will cover all aspects of mass spectrometry from fundamentals and instrumentation through to applied chemical, environmental, health, earth, forensic and biological sciences.

The coffee breaks and poster sessions will take place in the exhibition hall at the Grand Carimã Resort, providing ample opportunities for sponsors and exhibitors to engage with delegates and participants.

During the event, participants will be allowed to explore the company stands, where sponsors and exhibitors can highlight their latest innovations through technical presentations, product launches and Q&A sessions with their team. This setup ensures a dynamic and interactive environment for all involved.

BrJAC

Brazilian Journal of Analytical Chemistry

Aims & Scope

BrJAC is a double-blind peer-reviewed research journal, dedicated to the diffusion of significant and original knowledge in all branches of Analytical Chemistry and Bioanalytical Chemistry. It is addressed to professionals involved in science, technology, and innovation projects at universities, research centers and in industry. The **BrJAC welcomes** the submission of research papers reporting studies devoted to new and significant analytical methodologies, putting in evidence the scientific novelty, impact of the research, and demonstrated analytical or bioanalytical applicability. BrJAC **strongly discourages** those simple applications of routine analytical methodologies, or the extension of these methods to new sample matrices, unless the proposal contains substantial novelty and unpublished data, clearly demonstrating advantages over existing ones.

BrJAC is a quarterly journal that publishes original, unpublished scientific articles, reviews and technical notes. In addition, it publishes interviews, points of view, letters, sponsor reports, and features related to analytical chemistry.

For complete information on ethics and policies on conflicts of interest, copyright, reproduction of already published material and preprints, in addition to the manuscript submission and peer review system, please visit 'About us' and 'Author Guidelines' at www.brjac.com.br

Indexing Sources

Scopus

CiteScore$^{TM}_{2023}$ 1.6
SJR$_{2023}$ 0.229
SNIP$_{2023}$ 0.390
CiteScore^{TM} Tracker$_{2024}$ 2.0
Access source details

CiteScore trend

CiteScore value ■   Percentile in category ◆

CLARIVATE ANALYTICS — EMERGING SOURCES CITATION INDEX — INDEXED
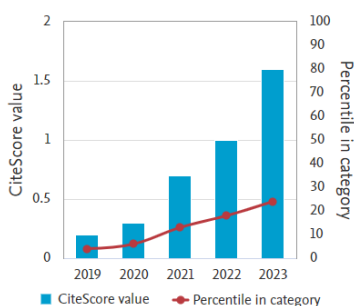
IF$_{2023}$ **1.1**
JCI$_{2023}$ **0.23**

C A P E S QUALIS

BrJAC is in the Qualis B3 stratum
according to preliminary list
published on 29 December, 2022

Google scholar

Cited by	All	Since 2019
Citations	783	683
h-index	12	12
i10-index	20	18
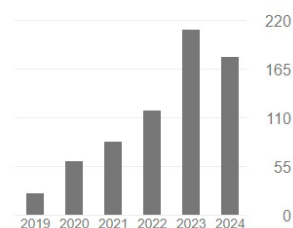
Last updated on 18 September, 2024

EDITORIAL ADVISORY BOARD (Continuation)

CONTENTS

CONTENTS *(Continuation)*

BrJAC

EDITORIAL

Highlighting the Importance of Data Treatment in Analytical Chemistry

Elcio Cruz de Oliveira (ID) ✉

Professor at the Pontifical Catholic University of Rio de Janeiro, and Master Professional at Petróleo Brasileiro S.A. – PETROBRAS, Rio de Janeiro, RJ, Brazil

In recent decades, statistical analysis and data processing have become essential tools in Analytical Chemistry, ensuring reliable results from experimental data treatment. Some of the main statistical techniques used in this field include descriptive statistics, hypothesis tests, quality control of analytical measurements, calibration methods in instrumental analysis with a focus on regression lines, nonparametric and robust methods, experimental design, response surface methodology associated with the optimization of analytical methods, uncertainty evaluation and its application for compliance assessment, and chemometrics for interpreting chemical data.

These transversal approaches are widely used for solving problems in medical scenarios, environmental research, food security, pharmaceuticals, and more. It is crucial to emphasize that proper data processing requires a solid knowledge of statistics that remains grounded in the core principles of Analytical Chemistry to ensure the correct interpretation and reliability of the results.

This issue of BrJAC includes one letter, four articles, and one technical note, each featuring at least one statistical analysis and data processing method mentioned earlier in this editorial. Professor Tarley from the University of Londrina believes that chemometrics practiced in Brazil is on par with world-leading research centers. Professor Edenir Rodrigues Pereira-Filho from Federal University of São Carlos discusses the practical application of academic training to professionals in Brazilian industry. Renowned Brazilian researchers shed light on the importance of correctly expressing units of measurement in Analytical Chemistry, particularly considering the updated definition of the mole based on Avogadro's constant, following the International System of Units guidelines.

Additionally, Indian and Rwandan researchers have investigated the toxicity of methanol and ethanol, seeking to identify the origin and the frequency of methanol contamination in illegal alcoholic beverages in Rwanda, supported by performance figures in method validation. Indian researchers have developed a voltammetric method for measuring acetaminophen in oral suspensions, in which the accuracy and precision parameters were essential for establishing the study's reliability. This issue also features two optimization studies: the first validates a new method for isotopic determinations in beverages, while the second utilizes Box-Behnken design and Response Surface Methodology to optimize a method that uses hollow fiber microextraction and gas chromatography coupled to mass spectrometry for determining the presence of pesticides in postmortem whole blood samples. Finally, by using parametric and nonparametric tests and Principal Component Analysis, it was possible to infer that consuming diacetyl as a flavoring agent may pose health risks.

BrJAC reaffirms the enduring relationship between data treatment and Analytical Chemistry in its publications. This focus may have contributed to the recent increase in our impact factor from 0.7 to 1.1, indicating that we are on the right track!

Elcio Cruz de Oliveira has a degree in Chemistry from the Rio de Janeiro State University (1990), a Master's degree in Metrology from the Pontifical Catholic University of Rio de Janeiro (2001), and a Doctoral degree in Analytical Chemistry from the Rio de Janeiro Federal University (2008). He is currently a Professor of the Postgraduate Programme in Metrology, Metrology for Quality and Innovation, Pontifical Catholic University of Rio de Janeiro, and a Researcher in Petrobras S.A. His research activities include all areas of chemical metrology, but mainly related to the oil and gas industry.

CV Web of Science ResearcherID: ABD-2058-2022

BrJAC

INTERVIEW

Professor César Ricardo Teixeira Tarley, a young researcher with a distinguished and internationally recognized career, kindly gave an interview to BrJAC

César Ricardo Teixeira Tarley ⓘD is Full Professor at the Department of Chemistry of the State University of Londrina (UEL, PR, Brazil), Research Productivity Fellow of the National Council for Scientific and Technological Development (CNPq) since 2007, has a Bachelor's degree in Chemistry from the State University of Maringá (UEM, PR, Brazil) (1998), a Master's Degree in Applied Chemistry from UEM (2001), a Doctorate in Natural Sciences (Analytical Chemistry) from the State University of Campinas (UNICAMP, SP, Brazil) (2004), and a postdoctoral fellowship in Analytical Chemistry from UNICAMP (2005) under the supervision of Prof. Lauro Tatsuo. Since 2019, Dr. Tarley has been considered one of the most influential researchers in the world (Plos Biology – https://doi.org/10.1371/journal.pbio.3000918) and among the top chemists in Brazil (research.com) in the 2022 and 2023 rankings. He was an Associate Professor at the Federal University of Alfenas (UNIFAL, MG, Brazil) (2005-2009) and at the Federal University of Uberlândia (UFU, MG, Brazil) (2009-2010). From 2006 to 2009, he was a member of the Board of Directors of the Master's Degree Programs in Chemistry and Pharmaceutical Sciences at UNIFAL, a member of the Board of Directors of the Doctoral Program in Chemistry associated with UEL, Central-Western State University (UNICENTRO) and Ponta Grossa State University (UEPG). Dr. Tarley was also a member of the Advisory Committee of the Research Promotion Foundation of the State of Minas Gerais (FAPEMIG) in 2009, Vice Head (2014-2016) and Head of the Chemistry Department at UEL (2016-2018), Representative of the Central Committee for Extension (CCE) in the Ethics Committee for Research with Human Subjects at UEL (2015), Member of the Committee of the Program of Innovation and Information Technology (PROITI) (2015-2018), Member of the Committee of the Program of Scientific Initiation (ProIC) (2018-2019), Vice Coordinator of the Exact Sciences Advisory Committee of the Araucária Foundation (2017-2019), Coordinator of the UEL Chemistry Graduate Program (2019-2021), Vice Secretary of the Regional Brazilian Chemical Society in the State of Paraná (2021-2022), Consultant of the Coordination for the Improvement of Higher Education Personnel (CAPES) (2017-2020). He is a Full Professor of Analytical Chemistry at the State University of Londrina (UEL), Coordinator of the Advisory Committee for the Exact Sciences Area of the Araucária Foundation, and supervises undergraduate, master's, and doctoral students in chemistry. He is also a permanent professor in the Postgraduate Program in Pharmaceutical Sciences and Food Science. He has been a coordinator and/or member of research projects financed by funding agencies (CNPq, Araucária Foundation of Paraná, FAPEMIG, CAPES, FINEP, and INCT-Bio). Dr. Tarley has experience in chemistry working on the following topics: development of chromatographic methodologies for the determination of contaminants and

toxicants in food and pharmaceutical samples; development of electroanalytical methodologies for the determination of compounds of forensic, environmental, food, and clinical interest; and development of analytical methodologies for the determination of metals and micronutrients in food and environmental samples by atomic spectrometric techniques. Emphasis is placed on the use of chemically imprinted polymers and nanomaterials and liquid-liquid microextraction methods in method development. Dr. Tarley has published more than 260 scientific papers in international and national journals, has an h-index of 41 in ISI and 42 in Scopus, and more than 5942 citations in Web of Science and 6670 in Scopus. He has supervised 75 undergraduate students, 30 master's students, and 21 Ph.D. students, and has supervised 5 postdoctoral fellows.

BrJAC: How was your childhood?
Prof. Tarley: I am a son of self-employed parents – my father was a truck driver, and my mother was a merchant (in memoriam). At 8 years old, I was already working in a coffee cooperative manufacturing coffee baskets. At 10 years old, I worked as a delivery boy for one year. At 12 years old up to 17 years old, I worked with my mother in a clothing store. Since I had to work during the day, I studied accounting at night in high school. It was a difficult time because to be approved for the university application, I had to borrow books from the Museum of Parapuã City and study on the weekends.

BrJAC: What early influences encouraged you to study chemistry? Did you have any influencers, such as a teacher?
Prof. Tarley: I clearly remember the teacher teaching about the atom in elementary school, in the eighth grade. Coincidentally or not, I did my PhD in atomic spectrometry. The Civil Engineering course was my first choice for a university course, but my application was not approved. Therefore, I opted for Chemistry at the State University of Maringá. Although it was a tough course, it was a turning point in my life, as I always liked studying and making discoveries. Chemistry provides this for us.

BrJAC: How was the beginning of your career in chemistry?
Prof. Tarley: After finishing my postdoctorate in 2004 at Unicamp, I applied for a public contest for an Analytical Chemistry Adjunct Professor role at Unifal-MG. I worked in this role from 2005 until 2009. Through another public contest, I was transferred to UFU in 2010 and then to UEL, where I am a Full Professor. At Unifal-MG, I initiated the guide for scientific initiation and graduate students; I also had the opportunity to participate in the creation of new undergraduate and graduate courses, and administrative activities.

BrJAC: What has changed in your profile, ambitions, and performance since the time you started your career?
Prof. Tarley: I hold a master's degree in gas chromatography, a doctorate degree in atomic spectrometry, and a postdoctoral in electroanalytics. Due to my graduate training subject, I have been working in different areas of Analytical Chemistry with emphasis on material synthesis, especially chemically imprinted polymers, and the development of preconcentration methods, electrochemical sensors, and liquid-liquid microextraction methods. From my point of view, the Analytical Chemist must be a versatile professional with extensive knowledge to develop and improve analytical methods.

BrJAC: Could you comment briefly on the recent evolution of analytical chemistry, considering your contributions?
Prof. Tarley: Over the years, Analytical Chemistry has evolved and contributed to solving different analytical challenges that directly impact the population and the production field. It is possible to mention the advent of sample preparation methods, chemometrics, chromatographic methods, miniaturized analytical

systems based on microfluidics, and electrochemical sensors, among others. In this context, I especially contributed to the development of new analytical methods. In 2004, at the beginning of my postdoctorate, after an exhaustive review of the literature, I found that no research group in Brazil carried out studies with molecularly imprinted polymers. My main contribution is based on the synthesis and use of these polymers in the development of preconcentration methods and electrochemical sensors. I have published more than 80 scientific papers in this field to date.

BrJAC: What are your lines of research? You have published many scientific papers. Would you highlight any?

Prof. Tarley: My line of research focuses on the development of chromatographic, electroanalytical, and electroanalytical methodologies to determine substances of forensic, environmental, food, and clinical interest. The emphasis is the use of chemically imprinted polymers and nanomaterials for preconcentration and sensor modification, as well as liquid-liquid microextraction methods for methodology development. The highlight is not just polymer use but the study of new polymer synthesis routes to obtain materials with superior selectivity and sensitivity. These studies resulted in the filing of some patents.

BrJAC: What is your opinion about the current progress of chemistry research in Brazil? What are the recent advances and challenges in scientific research in Brazil?

Prof. Tarley: Analytical Chemistry carried out in Brazil is of a high level, comparable to large research hubs around the world. Most Analytical Chemistry fields have researchers who stand out on the world stage, carrying out high-quality research in sample preparation, methods based on microfluidic devices, analytical devices based on 3D printing, point-of-care devices, chemometric methods, ohmic studies, and instrumentation development.

"From my point of view, Analytical Chemistry reaches its purpose when the development of analytical methods and/or use of analytical tools leaves the walls of universities and research centers and becomes technologies with practical applications."

BrJAC: For you, what have been the most important recent achievements in analytical chemistry research? What are the landmarks? What has changed in this scenario with the COVID-19 pandemic?

Prof. Tarley: Analytical Chemistry has been meeting the demands of chemical analysis in different areas for years. From my point of view, Analytical Chemistry reaches its purpose when the development of analytical methods and/or use of analytical tools leaves the walls of universities and research centers and becomes technologies with practical applications. In this sense, examples of recent achievements in Analytical Chemistry are routine analytical devices, especially point-of-care ones, screening methods based on chemometrics, portable electrochemical sensors used in forensic chemistry, and proteomic and metabolomic studies. Considering the COVID-19 pandemic, despite the development of different sensors for detecting the virus, I believe that Analytical Chemistry could be more proactive in anticipating new devices for detecting new virus variants that may emerge.

BrJAC: There are, in Brazil and the world, several conferences on chemistry. To you, how important are these meetings to the scientific chemistry community? How do you see the development of national chemistry meetings in Brazil?

Prof. Tarley: Conferences are essential for exchanging experiences between professors, technicians, and undergraduate and graduate students, as well as for establishing scientific partnerships. In Brazil, traditional congresses such as the Meeting of the Brazilian Chemical Society, the National Meeting of Analytical Chemistry, the Brazilian Symposium on Electrochemistry and Electroanalytics, and the Brazilian Meeting on Chemical Speciation are examples of success.

BrJAC: What is the importance of awards for the development of science and new technologies?
Prof. Tarley: Without a question, the recognition of the science and technology work provides encouragement to the researcher and contributes to more comprehensive dissemination of science in the media.

BrJAC: For you, what is the importance of the national funding agencies for the scientific development of Brazil?
Prof. Tarley: The foundation of developed countries is based on high-quality education and scientific and technological independence. The lack of large-scale investments through development agencies would negatively impact human resources training and lead to technological obsolescence. However, financial resources through partnerships between universities and the production sector are also welcome since they can promote the solution of real problems more quickly, leading to the well-being of the population.

BrJAC: At the moment, the situation for scientific research in Brazil is one of decreasing investment. How do you see this situation, and what would you say to young researchers?
Prof. Tarley: It is a very worrying situation since most of the Brazilian research is carried out by graduate students. It is necessary to increase the rating and number of scholarships. Graduate students should have rights and duties like any other working condition, and the essential infrastructure needed to carry out research should be provided. To young researchers, I recommend they prioritize human resource training and knowledge building throughout their careers, although the demands for scientific production are tough.

BrJAC: What advice would you give to a young scientist who wants to pursue a career in chemistry?
Prof. Tarley: It's a beautiful career that allows constant learning, considering either the production sector or the education and research field. Therefore, have a critical sense and be enthusiastic to produce more and more.

BrJAC: For what would you like to be remembered?
Prof. Tarley: Professionally, I would like to be recalled as a good teacher and a researcher concerned with human resource training; a teacher who works hard and demands excellent work from his students. When it comes to personal life, I would like to be remembered as a good son, a good father, and a good husband.

BrJAC

POINT OF VIEW

Interaction between Industry and Academia: Is the Chemical Professional Master a Possibility?

Edenir Rodrigues Pereira-Filho iD ✉

Full Professor in the Department of Chemistry at the Federal University of São Carlos (UFSCar), São Carlos, SP, Brazil

Between 2017 and 2020, the Brazilian chemical graduate education system comprised a total of 74 graduate programs spread over several states. However, a mere five of these (just 6.7%) were exclusively dedicated to professionals already engaged in industry or teaching in public and/or private schools.[1] This substantial underrepresentation reveals a significant imbalance within the system, suggesting that it is not fully aligned with the needs of the workforce and the educational sector. Unfortunately, as of 2024, the situation has only shown a slight improvement, as the proportion of professional-focused programs remains almost the same. The limited availability of these programs is particularly concerning given the critical role that professional master's programs play in bridging the gap between academic knowledge and practical application in industry. These programs equip industry professionals and educators with the advanced skills and knowledge they need to stay competitive in rapidly evolving national and international scenarios. Despite this need, the current offerings are insufficient to meet the demands of professionals seeking to enhance their expertise and to contribute more effectively to their respective fields.[2]

Moreover, the existing chemical professional programs are restricted to master's level courses, with no further opportunities for professional doctorates or specialized formation. This limitation further constrains the ability of professionals to pursue advanced, industry-relevant education within the chemical field. As a result, many may be unable to advance in their careers or are forced to seek opportunities abroad, leading to a potential brain drain and a weakening of Brazil's industrial and educational sectors. Considering these challenges, there is an urgent need to reassess and expand the professional education offerings within the Brazilian chemical graduate system. By doing so, professors and universities can be more active in supporting industry and educational professionals, fostering innovation, and driving economic growth. An increase in the number and diversity of chemical professional master's programs would address the current imbalance and ensure that the system is better aligned with the broader goals of national development and global competitiveness (e.g., Industry 4.0).[3]

One of the critical issues exacerbating this imbalance is the lack of awareness within the chemical industry, and related areas about the existence and benefits of chemical professional graduate programs. Many companies are unaware of these opportunities, which limits their ability to encourage employees to pursue further education that could enhance their skills and contribute to organizational growth. This lack of information impedes the fostering of stronger university–industry collaborations, which is essential for driving innovation and economic development. Based on a recent inquiry focusing on 48 former students from the Professional Master Graduation Chemical Program (PPGPQ)[4] located at the Chemistry Department of the Federal University of São Carlos (DQ/UFSCar), (i) all professionals are employed, indicating that the graduates of this program have a high level of employability, and (ii) around 80% indicated that their income had increased after finishing the course. Hence, the course has a clear positive impact on the former student's professional life. In addition, a second survey with 54 professionals on LinkedIn[5] revealed that

a significant majority (around 80%) acknowledged the positive impact of chemical professional master's programs (see Figure 1a) on their careers. However, many also recognized that companies (see Figure 1b), along with their leaders and managers (see Figure 1c), lack sufficient information about these types of courses.
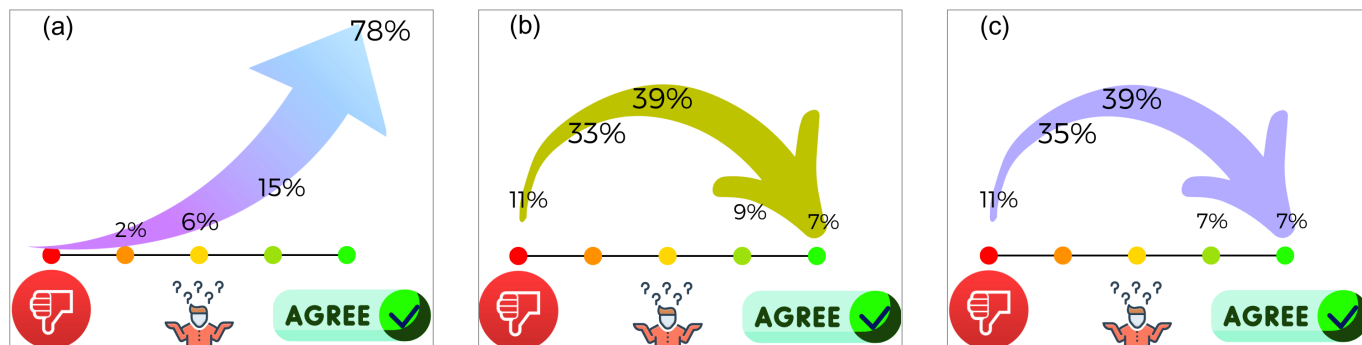
Figure 1. Professionals' opinions on the positive impact of these graduate programs on their lives (a), and the awareness of companies (b) and their leaders or managers (c) about such programs.

This issue is even more pronounced in teaching science, technology, engineering, arts/humanities, and mathematics (STEAM).[6,7] The current educational system does not sufficiently prepare educators to teach these critical subjects in a way that is both innovative and aligned with industry needs. As a result, there is a growing disconnection between the skills taught in schools and the skills required in the workforce. By expanding professional master's programs and enhancing the focus on STEAM education, universities can help bridge this gap, ensuring that students are better prepared to meet the demands of modern industries. Another important aspect is the involvement of various stakeholders, such as *Empresa Brasileira de Pesquisa e Inovação Industrial* (Embrapii)[8] and *Confederação Nacional da Indústria* (CNI), in promoting chemistry graduate programs.[9]

Considering these challenges, there is an urgent need to reassess and expand the professional education offerings within the Brazilian chemical graduate system. By doing so, universities can play a more active role in supporting industry and educational professionals, fostering innovation or tools, and driving economic growth. This expansion presents a significant opportunity for growth and improvement, instilling a sense of hope and optimism in the potential of the system. An increase in the number and diversity of professional master's programs in chemistry would address the current imbalance and ensure that the system is better aligned with the broader goals of national development and global competitiveness.

(1) "Coordenação de Aperfeiçoamento de Pessoal de Nível Superior (CAPES). Resultado da Avaliação Quadrienal 2017-2020". Available at: https://www.gov.br/capes/pt-br/acesso-a-informacao/acoes-e-programas/avaliacao/avaliacao-quadrienal/resultado-da-avaliacao-quadrienal-2017-2020 [accessed on August 2024].

(2) Franco, M.; Haase, H. University–industry cooperation: Researchers' motivations and interaction channels. *J. Eng. Technol. Manage.* **2015**, *36*, 41–51. http://dx.doi.org/10.1016/j.jengtecman.2015.05.002

(3) Moraes, E. B.; Kipper, L. M.; Kellermann, A. C. H.; Austria, L.; Leivas, P.; Moraes, J. A. R.; Witczak, M. Integration of Industry 4.0 technologies with Education 4.0: advantages for improvements in learning. *Interactive Technology and Smart Education* **2023**, *20*, 271-287. https://doi.org/10.1108/ITSE-11-2021-0201

(4) "Programa de Pós-Graduação Profissional em Química (PPGPQ) da Universidade Federal de São Carlos". Available at: https://www.ppgpq.ufscar.br/pt-br/front-page [accessed on August 2024].

(5)   LinkedIn. https://br.linkedin.com/ [accessed on August 2024].
(6)   Liu, C.-Y.; Wu, C.-J. Not Just for Decoration: How the Arts Complement Science, Technology, Engineering, and Mathematics Learning. *Psychology of Aesthetics, Creativity, and the Arts. Advance online publication* **2023**. https://doi.org/10.1037/aca0000634
(7)   Rodrigues-Silva, J.; Alsina, A. Conceptualising and framing STEAM education: what is (and what is not) this educational approach? *Texto Livre* **2023**, *16*, 1-13. https://doi.org/10.1590/1983-3652.2023.44946
(8)   "Empresa Brasileira de Pesquisa e Inovação Industrial (EMBRAPII)". https://embrapii.org.br/ [accessed on August 2024].
(9)   "Confederação Nacional da Industria (CNI)". https://www.portaldaindustria.com.br/cni/ [accessed on August 2024].

Edenir Rodrigues Pereira-Filho holds a B.S. degree in Chemistry from the Pontifical Catholic University of Campinas (PUC-Campinas) in São Paulo, Brazil. He earned his first M.Sc. in Chemistry in 1999 from the Chemistry Institute at Campinas State University (Unicamp) and a second M.Sc. in Mathematics in 2022 from the Federal University of São Carlos (UFSCar). In 1999, he began his Ph.D. studies at Unicamp, completing part of his research at the Institute of Spectrochemistry and Applied Spectroscopy (ISAS) in Dortmund, Germany, in 2001. He was awarded his Ph.D. in Sciences in 2003. Dr. Pereira Filho's research focuses on laser-induced breakdown spectroscopy (LIBS), sample preparation, the analysis of technological and environmental samples—including waste electric and electronic equipment (WEEE)—as well as digital and hyperspectral imaging and the application of chemometrics in analytical chemistry. He has published more than 190 scientific papers. Since August 2006, Dr. Pereira Filho has been a faculty member of the Chemistry Department at UFSCar, where he has supervised 29 master's students (14 academic and 15 professional) and 15 Ph.D. candidates. In 2023, he was promoted to Full Professor at UFSCar. He also runs a YouTube channel (https://www.youtube.com/c/EdenirPereiraFilho) dedicated to teaching design of experiments (DoE) and other key topics such as bibliometric application and WEEE characterization and recycling.

BrJAC

LETTER

Expressing the Unit of Measurement in Analytical Chemistry

Maycon Lucas de Oliveira[1] iD **, Maria das Graças Andrade Korn**[2] iD **, Márcia Andreia Mesquita Silva da Veiga**[1]* iD ✉

[1]Departamento de Química, Universidade de São Paulo, Av. Bandeirantes, 3900, Vila Monte Alegre, Ribeirão Preto,14040-900, SP, Brazil

[2]Instituto de Química, Universidade Federal da Bahia, Rua Barão de Jeremoabo, 147, Ondina, Salvador, 40170-115, BA, Brazil

Units in Analytical Chemistry

Analytical chemistry is a measurement science that provides both qualitative and quantitative data across various areas, including basic science, industry, medicine, and space exploration. The subject of analytical procedures in multiple fields of analytical instrumentation enables the determination of the composition of mixtures containing two or more components.[1] So, we not only detect the composition but also specify the amount of the compound of interest. An example is the analysis of a milk sample to quantify the calcium concentration. In this context, milk is the sample analyzed, while calcium is the analyte being determined.[2] In this sense:

A sample is analyzed.

An element or compound (analyte) is determined.

Chemical analysis should include a numerical value, and a corresponding unit to indicate the measured quantity, and a statement of uncertainty.[1,3,4] To determine the composition of unknown samples, measurements often require prior calibration, except for classical methods like gravimetry or titrimetry and absolute instrumental techniques such as coulometry, time-of-flight mass spectrometry (TOF-MS), or isotope ratio mass spectrometry (RMS). Constructing an analytical calibration curve requires adjusting the instrumental range with specific quantities and inputting the concentration of the analyte being measured. Efforts should be made to minimize the uncertainty associated with each measurement, even for techniques that rely solely on injecting a fixed sample volume. Calibration standards for analytical chemistry are typically prepared based on mass fraction rather than volume, as density can vary depending on the dilution solvent. This Letter discusses samples that have already been homogenized in the liquid state and emphasizes the importance of expressing results accurately with appropriate units.

Standardized Units of Measurement: from foundation to actual days

Using a standardized system of units is widely recognized as a valuable tool for effective communication in civil, academic, philosophical, and economic contexts. Expressing scientific data clearly and concisely is essential to ensure comprehension, regardless of the time, region, or country in which the value/unit is

presented and interpreted.[5] The International Bureau of Weights and Measures (BIPM) was established in 1875 for the development of unit standardization protocols, promoting consistency in scientific reports. Since then, advances have allowed for even more precise metrics, culminating in the establishment of the seven base quantities/units by the 14th General Conference on Weights and Measures (GCWM) in 1972. These units include the meter for length, the kilogram for mass, the second for time, the ampere for electric current, the Kelvin for thermodynamic temperature, the candela for luminous intensity, and the mole for the amount of substance.

The seven fundamental units of the International System of Units (SI) are insufficient to describe all the events associated with the properties of matter phenomena. When these units are combined, either the same or different, they generate derived units. For example, average velocity (v) is defined as the position variation (meter) per time of the event (second), generating the unit $m\ s^{-1}$. Volume (V) is the combination of three spatial dimensions (m), generating the unit m^3. In some cases, the combining of units results in the creation of derived units with unique names. The SI system currently defines 22 units with notable names, such as the Joule (J), defined as $kg\ m^2\ s^{-2}$; the Watt (W), defined as $J\ s^{-1}$; and the Newton (N), defined as $kg\ m\ s^{-2}$.

Furthermore, the metric system is not static and undergoes variations due to new ways of understanding matter, technological advances, or universal constants. For instance, in 2018, the SI unit for mass was redefined because the physical artifact representing the kilogram "lost weight" over 120 years. Thus, the definition of the seven base units is no longer tied to physical artifacts but rather on the fundamental constants of nature. This Letter will focus on the mole and its derivative units, as they are central to expressing data and results in analytical chemistry.

Historically, the mole was defined as the number of atoms in exactly 12 g of carbon-12. However, on May 20, 2019 (World Metrology Day), the GCWM redefined the mole as exactly $6.02214076 \times 10^{23}$ elementary entities, as recommended by the International Union of Pure and Applied Chemistry (IUPAC):

> "One mole (mol) contains exactly $6.02214076 \times 10^{23}$ elementary entities. This number is the fixed numerical value of the Avogadro constant, N_A, when expressed in the unit mol^{-1} and is called the Avogadro number. The amount of substance, symbol n, of a system is a measure of the number of specified elementary entities."[6,7]

In this sense, the mole (symbol: mol) is the unit for the amount of substance:

> "When the mole is used, the elementary entities must be specified and any be atoms, molecules, ions, electrons, other particles, or specified groups of such particles."[7]

This alteration in the expression of quantities of matter enhances the precision and dependability of measurements. Furthermore, the mole can be directly compared between elements, regardless of their isotopic ratio. While some chemists may require time to adjust to the new scale, the modification should result in more accurate and consistent analytical science.

Chemists typically use molarity (M) to express concentration, which SI defines as the amount of substance (in moles, n) per unit volume (in cubic meter, m^3). Another term, molality, is less commonly used by analytical chemists to express concentration. Molality is defined as the amount of solute entities divided by the mass of the solvent, and according to SI, the formal unit is $mol\ kg^{-1}$. Figure 1 shows the correlation between the quantity of matter and mass and how to express concentration using molarity and molality.
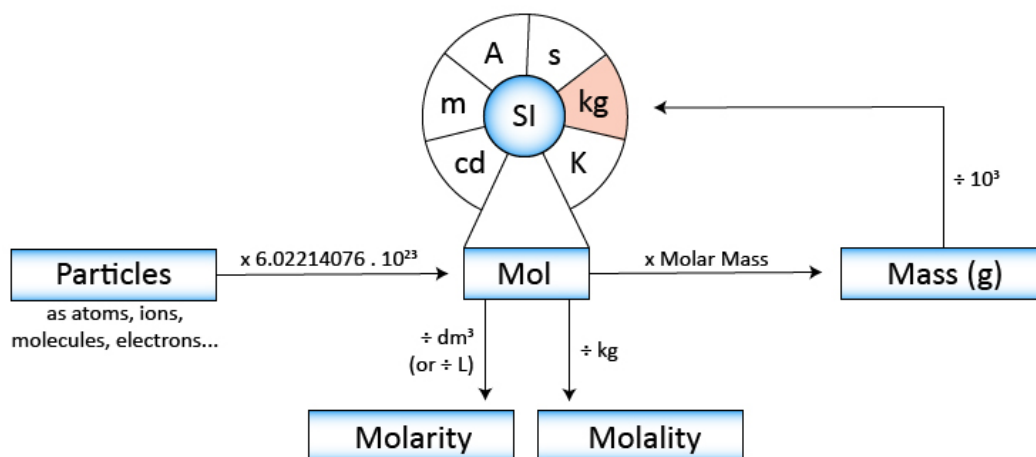
Figure 1. SI units and the centrality of the mole are used to obtain concentrations expressed
as molarity or molality.

Common (but unofficial) units

Uniformity in scientific communication is maintained using SI units. However, many units derived
from the SI system are dimensionless when analyzing and determining concentrations. For instance, the
relationship between the mass of an analyte (in kg) and the mass of a sample (also in kg) is expressed
by the unit $kg\ kg^{-1}$, which is dimensionless (i.e., equivalent to 1). Similarly, the ratio of moles of product
to moles of reagent is represented by $mol\ mol^{-1}$, which is also dimensionless. Unofficial units based on
ppm, ppb, ppt, etc., are often used, with descriptors based on decimal orders to simplify concentration
expression.

Although descriptors such as % ("one part percent", $1:10^2$), ppm ("one part per million", $1:10^6$), ppb ("one
part per billion", $1:10^9$), and ppt ("one part per trillion", $1:10^{12}$) are widely used in laboratories and other
areas of chemistry to express low concentrations of substances in solutions, their use is not recommended.
These descriptors are not official units and can lead to misinterpretations, especially for non-experts.
Analytical chemists must report the results and data concisely, clearly, and reliably. For this purpose, they
must adequately equip the informal unit with the correct expression.

Table I displays the relationship between quantities evaluated using official SI units, standard units,
and their variations, along with their identification in the form of descriptors. Terms such as "ppm" and
"ppb" can have ambiguities because they do not specify whether they refer to parts per million by mass
or volume. This ambiguity can lead to confusion and errors in interpreting results, especially when dealing
with substances with different densities. Therefore, these terms should not be used whenever possible to
express concentrations, especially in a technical report. In many cases, it is beneficial to convert the units
to a more widely recognized unit, such as $mol\ L^{-1}$ (if fraction, $\mu g\ g^{-1}$, for instance), to facilitate comparisons
between different studies or analyses.

Table I. Official and descriptor units used by analytical chemists to express results

Quantity	SI Unit	Common units	Variations		Descriptors / informal units
		$g\ g^{-1}$ (*)	%	-	-
Mass fraction (ω)	$kg\ kg^{-1}$ (*)	$\mu g\ g^{-1}$	$mg\ kg^{-1}$	$g\ ton^{-1}$	ppm
		$ng\ g^{-1}$	$\mu g\ kg^{-1}$	$mg\ ton^{-1}$	ppb
		$pg\ g^{-1}$	$ng\ kg^{-1}$	$\mu g\ ton^{-1}$	ppt

(continued on next page)

Table I. Official and descriptor units used by analytical chemists to express results (continued)

Quantity	SI Unit	Common units	Variations			Descriptors / informal units
Volume fraction (φ)	$m^3\,m^{-3}$ (*)	$L\,L^{-1}$ (*)	%	-	-	-
		$mL\,L^{-1}$	$\mu L\,mL^{-1}$	‰ (= 0.1%)	-	-
		$\mu L\,L^{-1}$	$nL\,mL^{-1}$	-		ppm
		$nL\,L^{-1}$	$pL\,mL^{-1}$	-		ppb
Amount f raction (x)	$mol\,mol^{-1}$ (*)	$mmol\,mol^{-1}$	-	-	-	-
		$\mu mol\,mol^{-1}$	-	-	-	-
		$nmol\,mol^{-1}$	-	-	-	-
Mass concentration (γ)	$kg\,m^{-3}$	$g\,L^{-1}$	-	-	-	-
		$mg\,L^{-1}$	$\mu g\,mL^{-1}$	-		ppm
		$\mu g\,L^{-1}$	$ng\,mL^{-1}$	-		ppb
		$ng\,L^{-1}$	$pg\,mL^{-1}$	-		ppt

(*) are dimensionless quantities or quantities with unit one.

Every analytical chemist has the fundamental ability to convert units to express information as required. However, this task can become problematic if the units are not described correctly, as shown in Table I. To illustrate this, we will consider the practical example of preparing 500 mL of 0.01 mol L^{-1} hydrochloric acid from a 37% m m^{-1} stock (with a density of ρ = 1.19 g mL^{-1} at 20 °C). This task may initially seem complex for students, particularly those in the early stages of their education, due to the need to convert the data.

In this example, the percentage represents a dimensionless mass ratio and, by definition, has no unit (equivalent to 1). However, to achieve the desired molar concentration of 0.01 mol L^{-1}, we can calculate the mass of HCl required (0.1823 g) and the volume (0.4140 mL) of the stock solution (at 37% m m^{-1}), as presented in Box I.

Box I. Calculations were conducted to obtain the theoretical volume value for producing a 0.01 mol L^{-1} HCl solution in 500 mL using 37% m/m solution stock

The molar concentration determines the number of moles	$0.01\,\text{mol/L} = \dfrac{n}{0.5\,\text{L}} \rightarrow n = 5 \cdot 10^{-3}\,\text{mol of HCl}$
The mass can be obtained from the number of moles	$n = \dfrac{m}{MM} \rightarrow m = (5 \cdot 10^{-3}\,\text{mol}) \times \left(36.46\,\dfrac{g}{mol}\right) = 0.1823\,\text{g of HCl}$
The total mass of hydrogen chloride in the initial solution	$\rho = \dfrac{m}{v} \rightarrow m_{total} = \dfrac{1.19\,g}{1.00\,mL} \cdot \dfrac{1000\,mL}{1\,L} \cdot 1\,L = 1190\,g$ 37% of 1190 g = 440.3 g of HCl
The volume of the original solution containing the desired mass of acid must be determined	$V = \dfrac{(0.1823\,\text{g of HCl}) \times (1000\,\text{mL})}{(440.3\,\text{g of HCl})} = 0.4140\,\text{mL}$

Table II. Quantities and values were obtained for preparing a 0.01 mol L^{-1} hydrochloric acid solution from a 37 % m m^{-1} stock standard (ρ = 1.19 g mL^{-1}, at 20 °C)

Quantity	Symbol	Definition	Value	Unit
Mass ratio	$\zeta_{i,j}$	$\zeta_{i,j} = m_i/m_j$	$\approx$ 1 : 2742	g g^{-1} (*)
Mass fraction	ω	$\omega = m_i/\sum m_j$	3.65 x 10^{-4}	g g^{-1} (*)
	$\omega_\%$	$\omega_\% = 100\ x\ \omega$	0.04	% (*)
	ω_{ppm}	$\omega = m_i/\sum m_j$	365	µg g^{-1} or ppm (*)
Mass concentration	γ	$\gamma = m_i/V$	0.365	g L^{-1}, kg m^{-3} or g dm^{-3}
Volume ratio	$\psi_{i,j}$	$\psi_{i,j} = V_i/V_j$	$\approx$ 1 : 1207	mL mL^{-1} (*)
Volume fraction	φ	$\varphi = V_i/\sum V_j$	8.29 x 10^{-4}	mL mL^{-1} (*)
	$\varphi_\%$	$\varphi_\% = 100\ x\ \varphi$	0.08	% (*)
	φ_{ppm}	$\varphi = V_i/\sum V_j$	829	µL L^{-1} or ppm (*)
Amount concentration	C	$C = n/V$	0.01	mol L^{-1} or mol dm^{-3}

In the definitions, m is the mass, V is the volume, and n is the amount of components.
(*) are dimensionless quantities or quantities with unit one.

Furthermore, although quantities with volume units ($\psi_{i,j}$, φ, $\varphi_\%$, φ_{ppm}) can theoretically be calculated, their use should be avoided due to variations in thermodynamic quantities. Brown (2008) emphasizes the necessity of using units such as mass concentration (γ) and amount concentration (C) along with temperature and pressure conditions.[1] For all chemistry professionals, this argument is fundamental to training and professional development, as effects such as the contraction and expansion of volumes or changes in the density of liquids are frequent in the field. In the field of quality control, verifying the condition of a product or substance is essential for safety. This verification is linked not only to legal regulations but also to the effectiveness of the commercial product. This includes products intended for direct application to the organism, such as medicines and food, as well as those related to quality and stability, and raw material for other processes.

Box II. Calculations were conducted to obtain the values as they apply to chemistry. The quantities used include both official and unofficial units

Mass ratio ($\zeta_{i,j}$)	$\zeta_{i,j} = \dfrac{0.1823 \text{ g HCl}}{499.8177 \text{ g } H_2O} = 3.647_3 \cdot 10^{-4} \rightarrow \dfrac{1}{3.647_3 \cdot 10^{-4}} = 1:2742$
Mass fraction (ω)	$\omega = \dfrac{0.1823 \text{ g HCl}}{500.00 \text{ g solution}} = 3.646_0 \cdot 10^{-4}$

Box II. Calculations were conducted to obtain the values as they apply to chemistry. The quantities used include both official and unofficial units (continued)

Mass fraction ($\omega_\%$)	$\omega_\% = 100 \cdot (3.646_0 \cdot 10^{-4}) = 0.04\ \%$
Mass fraction (ω_{ppm})	$\omega_{ppm} = \dfrac{0.1823\ \text{g HCl}}{500.00\ \text{g solution}} \cdot \dfrac{10^6\ \mu\text{g HCl}}{1\ \text{g HCl}} = 365\ \mu\text{g g}^{-1}\ (\text{ppm})$
Mass concentration (γ)	$\gamma = \dfrac{0.1823\ \text{g HCl}}{0.500\ \text{L solution}} = 0.365\ \text{g L}^{-1}$
Volume ratio ($\psi_{i,j}$)	$\varphi = \dfrac{0.4140\ \text{mL HCl}}{499.586\ \text{mL H}_2\text{O}} = 8.29 \cdot 10^{-4} \rightarrow \dfrac{1}{8.29 \cdot 10^{-4}} = 1{:}1207$
Volume fraction (φ)	$\varphi_\% = \dfrac{0.4140\ \text{mL HCl}}{499.586\ \text{mL H}_2\text{O}} = 8.29 \cdot 10^{-4}\ \text{mL mL}^{-1}$
Volume fraction ($\varphi_\%$)	$\varphi_\% = 100 \cdot (8.28 \cdot 10^{-4}) = 0.08\ \%$
Volume fraction (φ_{ppm})	$\varphi_{ppm} = \dfrac{0.4140\ \text{mL HCl}}{499.586\ \text{mL H}_2\text{O}} \cdot \dfrac{10^6\ \mu\text{L HCl}}{1\ \text{mL HCl}} = 829\ \mu\text{L L}^{-1}\ (\text{ppm})$
Amount concentration (C)	$C = \dfrac{(0.1823\ \text{g HCl})}{(36.46\ \text{g/mol}) \cdot (0.5\ \text{L})} = 0.01\ \text{mol L}^{-1}$

Using descriptors as units also poses challenges in environmental management analyses. In Brazil, Resolution 420/2009 from the Brazilian Council for the Environment (CONAMA, 2009) sets criteria and values for soil quality based on the presence of chemical substances in order to assess the impact of human activities on the environment.[9] According to this resolution, the reference value for lead (Pb) in the soil is 180 mg kg^{-1}. For instance, if a chemical analyst analyzed soil (with density ρ = 1.4 g mL^{-1}) and obtained a result of 200 ppm, this exceeds the reference value for lead in soil. In this case, since the author omits the unit and presents the answer in the report as a dimensionless descriptor, it can lead to confusion. In this context, if "ppm" corresponds to mg kg^{-1}, the soil would exceed the permitted limit of Pb per kg of soil, indicating anthropogenic activity. Conversely, if "ppm" corresponds to mg L^{-1}, the soil would be within acceptable limits of 143 mg of Pb per kg of soil, signifying no significant human interference. Therefore, the responsibility of a chemical professional extends beyond conducting the analysis and encompasses expressing the results clearly and unambiguously, particularly in sensitive areas such as environmental management.

The provided text briefly discussed the new definition of the mole. Now, the mole is no longer linked to a physical object, the carbon-12 atom, but is defined purely in terms of Avogadro's constant. In addition to molar concentration, other internationally accepted units and quantities are also presented according to the International System of Units (SI). Some of these units require care in their usage, as they can lead to confusion when used jointly, as is the case with ppm, ppb, and ppt. It is crucial to emphasize that the description of the measured quantity must be clear, precise, and without room for ambiguous interpretations. Accurate communication between the chemical analyst and the requester is essential when presenting a measurement result.

REFERENCES

(1) Brown, R. J. C.; Quantities and units in analytical chemistry. *Int. J. Environ. Anal. Chem.* **2008**, *88*, 681-687. https://doi.org/10.1080/03067310801899722

(2) International Union of Pure and Applied Chemistry (IUPAC). Matrix in analysis. *Compendium of Chemical Terminology*, 3rd ed. (the "Gold Book"), 2019. Compiled by McNaught, A. D.; Wilkinson, A. Blackwell Scientific Publications, Oxford (1997). Online version (2019-) created by S. J. Chalk. ISBN 0-9678550-9-8. https://doi.org/10.1351/goldbook.M03758

(3) International Union of Pure and Applied Chemistry (IUPAC). Quantity calculus. *Compendium of Chemical Terminology*, 3rd ed. (the "Gold Book"), 2019. Compiled by McNaught, A. D.; Wilkinson, A. Blackwell Scientific Publications, Oxford (1997). Online version (2019-) created by S. J. Chalk. ISBN 0-9678550-9-8. https://doi.org/10.1351/goldbook.Q04983

(4) Brown, R. J. C. Units and quantities for analytical chemistry (background paper). *Anal. Methods* **2020**, *12*, 5010-5012. https://doi.org/10.1039/D0AY90126A

(5) International Union of Pure and Applied Chemistry (IUPAC). Unit of measurement. *Compendium of Chemical Terminology*, 3rd ed. (the "Gold Book"), 2019. Compiled by McNaught, A. D.; Wilkinson, A. Blackwell Scientific Publications, Oxford (1997). Online version (2019-) created by S. J. Chalk. ISBN 0-9678550-9-8. https://doi.org/10.1351/goldbook.U06561

(6) International Union of Pure and Applied Chemistry (IUPAC). Mole. *Compendium of Chemical Terminology*, 3rd ed. (the "Gold Book"), 2019. Compiled by McNaught, A. D.; Wilkinson, A. Blackwell Scientific Publications, Oxford (1997). Online version (2019-) created by S. J. Chalk. ISBN 0-9678550-9-8. https://doi.org/10.1351/goldbook.M03980

(7) National Institute of Standards and Technology (NIST). SI Units – Amount of Substance. *Office of weights and measures*, 2024. Available at: https://www.nist.gov/pml/owm/si-units-amount-substance [accessed April / 2024].

(8) International Union of Pure and Applied Chemistry (IUPAC). Analyte. *Compendium of Chemical Terminology*, 3rd ed. (the "Gold Book"), **2019**, Compiled by McNaught, A. D.; Wilkinson, A. Blackwell Scientific Publications, Oxford (1997). Online version (2019-) created by S. J. Chalk. ISBN 0-9678550-9-8. https://doi.org/10.1351/goldbook.A00331

(9) Conselho Nacional do Meio Ambiente (CONAMA). Resolução nº 420. *Diário Oficial da União, 249,* 2009/12/30, pp 81-84. Available at: https://cetesb.sp.gov.br/areas-contaminadas/wp-content/uploads/sites/17/2017/09/resolucao-conama-420-2009-gerenciamento-de-acs.pdf [accessed April / 2024].

Maycon Lucas de Oliveira is a Ph.D. candidate in Chemistry at the University of São Paulo (USP). He holds a degree in Chemistry from USP and postgraduate degrees in Environmental Chemistry from UniBF and Environmental Education from Metropolitan College of São Paulo. His research focuses on Analytical Chemistry, particularly in sample preparation methods for elemental determination, as well as the application of spectroanalytical techniques, including Inductively Coupled Plasma Optical Emission Spectrometry (ICP OES), Atomic Absorption Spectrometry (AAS), High-Resolution Continuum Source Atomic Absorption Spectrometry (HR-CS AAS). Additionally, he works on synthesizing and characterizing iron oxide-based nanomaterials and performs in vitro bioaccessibility assays for pulmonary and gastrointestinal systems.

Maria das Graças Andrade Korn is a Full Professor at the Institute of Chemistry of the University of Bahia (UFBA) with a master's degree in chemistry (Inorganic Analytical Chemistry, 1987) from the Pontifical Catholic University of Rio de Janeiro and a doctorate in chemical sciences from the University of São Paulo (USP) (1997). She was Director of the Analytical Chemistry Division of the Brazilian Chemical Society (2014-2016) and is currently a full member of the Bahia Academy of Sciences. In 2023, she was awarded the Simão Mathias Medal by the Brazilian Chemical Society, and in 2024, the Carol Collins Medal by the SBQ/ENQA Analytical Chemistry Division for her contribution and scientific prominence in the field of Analytical Chemistry in Brazil. She has always worked in analytical chemistry, developing studies on molecular and atomic spectroscopic techniques and sample preparation procedures applied to different types of food samples, environments, fuels, and medicines. The main focus of her research has been to obtain reliable chemical information through the development of fast methods with improved detectability that are ecologically friendly and mainly target more complex systems in order to meet society's demand. (CV)

Márcia Andreia Mesquita Silva da Veiga is an Associate Professor in the Department of Chemistry at the Faculty of Philosophy, Sciences, and Letters of Ribeirão Preto, University of São Paulo, Brazil. She has a degree in chemistry (Federal University of Amazonas, 1991), a master's degree in physical chemistry, and a doctorate in analytical chemistry (Federal University of Santa Catarina, 1996 and 2000), with postdoctoral work in analytical chemistry at the Institute of Chemistry, University of São Paulo (2005). She currently leads the research group L.Q.A.I.A. (Laboratory of Applied Instrumentation and Analytical Chemistry) and is Vice President of the Brazilian Society of Forensic Sciences. She works mainly with optical techniques for trace and isotopic analysis. Her current research focus is on sample preparation procedures, the detection, and quantification of nanomaterials and their applications, bioaccessibility assays in foods and soils, the potential of high-resolution graphite furnace molecular absorption spectrometry for elemental and isotopic analysis, micro trace (evidence) analysis and detection for forensic purposes, and new technological approaches to chemistry teaching. (CV)

ARTICLE

Analysis of Methanol and Ethanol Content in Illegal Alcoholic Beverages using Headspace Gas Chromatography: *Case Studies at Rwanda Forensic Institute*

Etienne Ndikumana[1,2]* iD ✉, **Eliphaz Niyonizera**[2] iD, **Justin N. Kabera**[2] iD, **Astha Pandey**[1] iD

[1]*Center of Excellence for Narcotic Drugs and Psychotropic Substances and School of Forensic Science, National Forensic Sciences University, Sector 9, Gandhinagar, 382007, Gujarat, India*

[2]*Chemistry Division, Rwanda Forensic Institute, KN 8 Ave, Gasabo-Kacyiru, P.O Box: 979 Kigali-Rwanda*
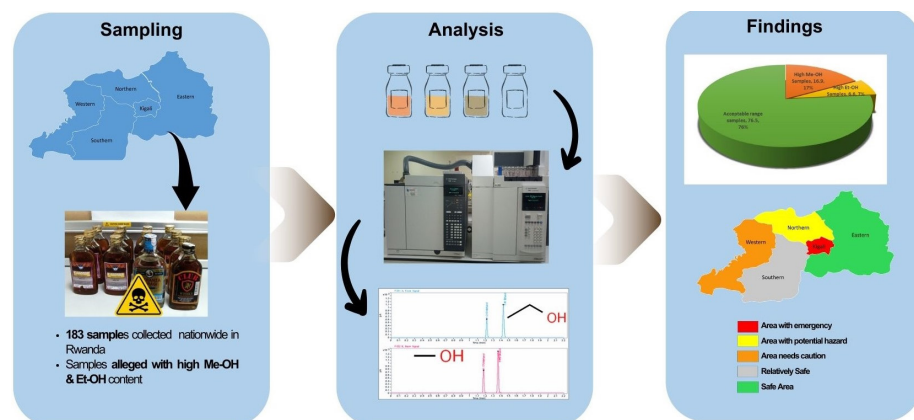
Illegal alcoholic production in Rwanda has become a critical social concern due to its widespread prevalence and associated health risks, stemming from the inexpensive distillation process employed by illicit producers. This often results in the unintentional production of toxic methanol instead of safe ethyl alcohol, presenting a substantial hazard in the context of illegal alcohol production. Methanol, when consumed, transforms into toxic formic acid in the body, causing severe health complications by disrupting mitochondrial respiration. Between 2021 and 2022, 183 forensic cases related to methanol and ethanol poisoning were collected nationwide and examined at the Rwanda Forensic Institute (RFI). Utilizing Headspace Gas Chromatography, the study aimed to quantitatively assess the extent of the problem and compare results to Rwanda's allowable limits for methanol and ethanol in alcoholic beverages. The analysis demonstrated a significant variation in ethanol content (3.8% to 98.9% v v^{-1}) and methanol levels (32% to 58.3% v v^{-1}), with 6.6% of samples exceeding the methanol limit (0.5% v v^{-1}) and 16.9% surpassing the ethanol limit (45% v v^{-1}). The City of Kigali emerged as the primary contributor to non-compliance, notably associated with specific brands like K'bamba, African Buffalo, Merry Cane, Royal Castle, and unbranded alcoholic beverages. Importantly, none of the samples tested positive for both methanol and ethanol simultaneously, emphasizing the urgency of monitoring and regulating Rwanda's alcoholic beverages market to ensure compliance with acceptable methanol and ethanol levels and safeguard public health.

INTRODUCTION

Alcohols, characterised by the presence of a hydroxyl (-OH) group, are a group of hydrocarbons with the potential for toxicity when consumed excessively, leading to intoxication and organ damage. Among the clinically significant toxic alcohols, methanol and ethylene glycol stand out.[1] With historical use in preserving fluids in ancient Egypt, methanol was first identified in 1661 when it was distilled from boxwood and termed the spirit of the box. Later, in 1834, Dumas and Peligot determined its molecular makeup, coining the term, "methylene" from Greek roots meaning "wood wine." Industrial manufacturing of methanol and its derivatives began in 1923.[2]

Illicit alcoholic beverages, which are often produced using industrial methylated spirits and local fermentation processes, can pose risks due to their potentially high levels of methanol.[3] Factors influencing methanol production in fermented alcoholic beverages included raw material characteristics, sterilisation temperatures, pectin content, and pectin methyl esterase (PME) activity,[4,5] with microbes also contributing to methanol production.[6,7]

Although methanol by itself is not very harmful, the hepatic alcohol dehydrogenase (ADH) in the liver breaks it down into formaldehyde, which is then transformed into toxic formic acid in the body. This highly toxic compound can cause serious health problems by interfering with mitochondrial respiration.[8-11] In the production of fruit spirits, the degradation of pectic substances by naturally occurring enzymes like PME leads to significant methanol formation, with the concentration varying based on fruit type and enzyme-substrate interaction.[8] Methanol is rapidly absorbed through various routes and is distributed in tissues with higher lipid or water content, primarily in the eyes, muscles, blood, gastrointestinal tract, liver, and cerebrospinal fluid.[12] Its metabolism mainly occurs in the liver by alcohol dehydrogenase, leading to the production of toxic metabolites.[13,14]

Exposure to methanol can result in symptoms such as headache, vertigo, fatigue, nausea, vomiting, blurred vision, permanent blindness, and even death due to limited detoxification capacity for formic acid.[1,15,16] Methanol is rapidly absorbed with close to 100% bioavailability and a distribution similar to total body water.[17,18]

Ethanol inhibits methanol metabolism by competing for alcohol dehydrogenase, and a blood ethanol level above 100 mg dL^{-1} effectively halts methanol catabolism, leading to its persistence in the body.[19] If ethanol and methanol are ingested together, methanol remains in the body until most of the ethanol is metabolized.[19] However, detecting and quantifying methanol and ethanol accurately in alcoholic beverages suspected of containing excessive amounts is essential in criminal investigation and community safety.

Based on 183 forensic cases that Rwanda Forensic Institute received from 2021 and 2022, with a focus on methanol and ethanol poisoning cases, the study aimed to shed light on the extent of methanol and ethanol toxicity, identifying the source and prevalence of methanol contamination in illicit alcoholic beverages in Rwanda. This was done by using the Headspace Gas Chromatography Flame Ionization Detector (HS-GC-FID). The study findings can guide public health initiatives, law enforcement operations, and educational campaigns aimed at lowering the production and consumption of illicit alcoholic beverages and promoting safer alternatives.

MATERIALS AND METHODS
Reagents and samples

Every substance utilized in this study met the stringent criteria for analytical gas chromatography reagent quality. We acquired certified reference material (CRM) for ethanol and methanol (100 mg dL-1 in water, Cerilliant®, Germany). The Milli-Q water filtration system (Merck Millipore) provided the ultra-pure water. We procured high-purity (5.5 purity) helium, hydrogen, and dried air gases suitable for GC from Gas Labs Limited (Nairobi, Kenya).

A total of 183 samples of illegal alcoholic beverages were collected from various parts of the country, including the City of Kigali (comprising 80 samples), the northern province (consisting of 61 samples), the southern province (with 22 samples), the western province (accounting for 11 samples), and the eastern province (including 9 samples).

Based on their original labels, these samples were divided into different brands, including K'bamba with 22 samples, Muriture with 17 samples, African Buffalo with 14 samples, African Gin with 11 samples, Rabiant with 11 samples, Royal Castle with 9 samples, Merry Cane with 4 samples, and unbranded alcoholic samples with a total of 95 samples. The collection of these samples spanned the years 2021 to 2022 in response to suspected incidents of methanol poisoning, which tragically resulted in 15 fatalities and a multitude of other severe health complications including permanent blindness. The distilled alcoholic samples were maintained at a constant room temperature (RT), whereas the fermented alcoholic samples were carefully stored under refrigerated conditions to ensure the prevention of any further changes or fluctuations in the ethanol and methanol content within the samples.

Rwanda Investigation Bureau (RIB) collected and transported these samples to the laboratory for forensic examination. Every collected sample was properly packed, labelled, and with a unique identification number. To uphold ethical considerations, the identities of the shops and manufacturing factory owners, from which these samples were collected, were kept confidential throughout the study.

Preparation of calibration standards

The analytical standards solutions for methanol and ethanol were prepared using the gravimetric-volumetric approach. We used a process where the analytes were progressively added to the deionized water to prevent the analytes' evaporation.

Each standard was separately added to a 10 mL volumetric flask after being carefully weighted, and then diluted using ultra-pure water to the calibration point. The flasks were promptly sealed, gently inverted and homogenized several times until the standards were evenly distributed throughout the solution. Additionally, a 6.0 mL amount of standard mixture was transferred into a 20 mL headspace vial and sealed using headspace crimp aluminium caps equipped with PTFE silicon septum. This sealing was done immediately, followed by the subsequent analysis using HS-GC-FID. It is worth noting that calibration standards were always freshly prepared for this purpose. A calibration curve, consisting of six data points 0.01 g%, 0.05 g%, 0.1 g%, 0.2 g%, 0.5 g%, and 1 g% (w v^{-1}), for both methanol and ethanol, was generated by plotting the concentrations of the analytes standards against their respective responses (peak areas), as illustrated in Figure 2.

Preparation of sample solutions

Using ultra-pure water, sample solutions were generated using various dilution factors (1:100 for distilled alcoholic samples and 1:25 for fermented alcoholic samples). To obtain the distilled samples, 100 µL of the sample was taken out and placed in a 10 mL volumetric flask that was then filled to the meniscus with ultra-pure water. While 400 µL of the sample was drawn and put into a 10 mL flask of the same type, and then topped off to the meniscus, in the case of fermented samples. A 6.0 mL quantity of each type of sample was taken, put into a 20 mL headspace vial, and sealed with headspace crimp aluminium caps that had PTFE silicon septum. This sealing was completed quickly, and then the instrument analysis came next.

Instrumentation

All measurements were made with Gas Chromatography (GC)-Flame Ionization Detector (FID) (Agilent Technologies Inc., Model 7890B GC) equipped with Headspace (HS) sampler (Agilent Technologies Inc., model 7697A HS). Headspace vial (20 mL) and Headspace Crimp Aluminium caps, PTFE/Silicon septum (Agilent Technologies Inc., US) were used to prepare sample solutions. OpenLab ChemStation, an instrument software, was employed to analyse the data.

Table I. HS-GC-FID conditions

GC-FID conditions	
Carrier gas	Helium, 4 mL min^{-1}
Detector	FID1 & FID2, 300 ºC
Detector gas	Hydrogen 25 mL min^{-1}; Air 300 mL min^{-1}; Nitrogen 10 mL min^{-1}
Injector	Split/split less type; 250 ºC; Split 25:1; split flow 100 mL min^{-1}; inlet pressure 17.382 psi; Septum purge flow 3 mL min^{-1}
Chromatographic column	DB-ALC1 (Agilent Technologies Inc., 123-9134); 20 ºC – 260 ºC (280 ºC), 30 m * 320 µm * 1.8 µm; In: Front SS inlet He; Out: Front Detector FID; Flow rate 4 mL min^{-1}; Pressure flow 17.382 psi DB-ALC2 (Agilent Technologies Inc., 123-9234); 20 ºC – 260 ºC (280 ºC), 30 m * 320 µm * 1.2 µm; In: Front SS inlet He; Out: Back Detector FID; Flow rate 4 mL min^{-1}; Pressure flow 17.382 psi
Temperature program	Set point (initial): 60 ºC; hold time 2.2 min; Post run: 60 ºC
Headspace sampler parameters	
Oven temperature (ºC)	60
Loop temperature (ºC)	70
Transfer line temperature (ºC)	80
Transfer line type	Fused Silica
Transfer line diameter (mm)	0.53
Vial equilibration (min)	5
Vial pressurisation gas	Nitrogen
Loop size (mL)	1
Vial standby flow (mL min^{-1})	20
Sample amount (mL)	6
Injection duration (min)	0.5
GC cycle time (min)	0.4
Vial size (mL)	20
Vial shaking	Level 1, 18 shakes min^{-1}
Fill pressure (psi)	15
Extraction mode	single
Post injection purge	100 mL min^{-1} for 1 min

Validation parameters

The analysis was performed using a method that had already been developed and validated in the laboratory settings, following established standard guidelines for routine analysis.[20]

The chromatographic profiles of both methanol and ethanol appeared to be satisfactory, as depicted in Figure 1.
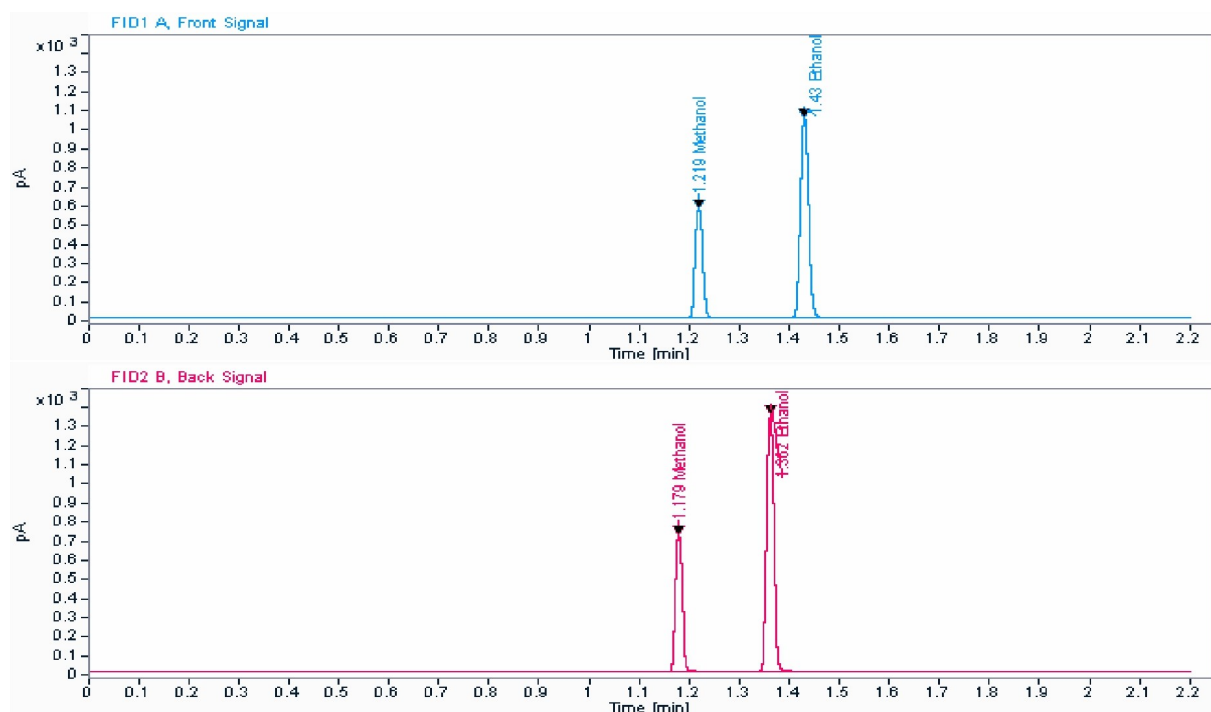
Figure 1. Chromatograms of ethanol and methanol at 0.5 g% using two detectors (FID1 A & FID2 B).

Calibration Model and Carryover

Calibration standards were set up, covering a range of concentrations from 0.01 g% to 1 g% w v^{-1}) for both methanol and ethanol in standard aqueous solutions. Six calibration points achieved a significant correlation (R^2) of 0.997 for methanol and 0.998 for ethanol, indicating a linear connection between the calibration curves. The method used a linear regression model for calibration as shown in Figure 2.

Following each calibrator, an examination of the blank samples was conducted to assess the carryover at different concentrations. It was observed that within the concentration range of 0.01 g% to 1 g%, no carryover was detected in any of the blank samples that followed the calibrators, for ethanol and methanol.
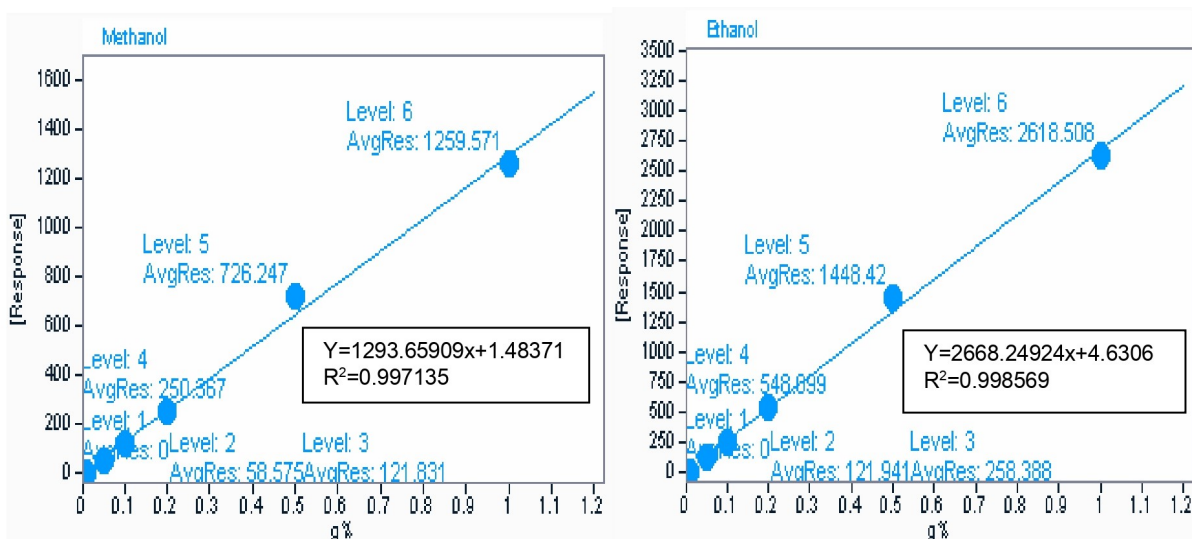
Figure 2. Calibration curves for methanol and ethanol utilising the HS-GC-FID.

Determination of quantification and detection limits

The lower limit of quantification (LOQ) for both analytes was 0.03 g% (w v^{-1}) (signal-to-noise=10), whereas the lower limit of detection (LOD) was 0.01 g% (w v^{-1}) (signal-to-noise=3), as shown in Table II.

Precision and accuracy

Precision was evaluated by conducting analyses in triplicate of three quality control samples (QC) with concentrations of 0.05 g% (low QC), 0.5 g% (medium QC), and 0.8 g% (high QC) for all analytes over five days, along with a freshly prepared calibration curve. The coefficients of variation (% CV) for methanol were determined to be 10.1%, 6.5%, and 5.0%, respectively. Accuracy was also assessed, resulting in values of 114%, 92%, and 100.8% for the low, medium, and high-control concentration samples, respectively. For ethanol, the coefficients of variation (% CV) were determined to be 8.2%, 5.6%, and 3.4%, respectively. Accuracy was also assessed, resulting in values of 105%, 96.8%, and 100.2% for the low, medium, and high-concentration control samples, respectively as indicated in Table II.

Table II. Method validation parameters and calculated values

Analyte	Interference	Linear Range (g%) and R^2	Linear regression equation	Limits (g%)		Carryover	Overall Accuracy (%CV)			Overall Precision (%RSD)		
				LOD	LOQ		Low QC (0.05)	Med. QC (0.5)	High QC (0.8)	Low QC (0.05)	Med. QC (0.5)	High QC (0.8)
Me-OH	None	0.01-1 0.997	Y=1293.65909x+1.48371	0.01	0.03	None	114	92	100.8	10.1	6.5	5.0
Et-OH	None	0.01-1 0.998	Y=2668.24924x+ 4.63046	0.01	0.03	None	105	96.8	100.2	8.2	5.6	3.4

Interference studies

In the interference studies, the method consisted of analysing spiked control samples to assess the potential interference caused by a variety of substances, including acetic acid, ethyl acetate, acetone, propanol, isobutanol, butanol, acetaldehyde, and an array of other volatile compounds that could be present in alcohol beverages. After these spiked samples were analysed, no interference peaks attributable to methanol and ethanol were seen during the retention time (t$_R$).

RESULTS AND DISCUSSION
Analytical results

The quantification of methanol and ethanol in samples being analysed was established using peak areas as a fundamental measurement parameter.[21] In the process of quantitatively analysing analytes, a linear regression model was employed. As the concentration of the analyte increased, the analysis response (peak area) also increased in a linear manner.[22,23]

Every country sets safety guidelines that determine the allowable percentage of alcohol by volume (ABV) for the production and sale of alcoholic beverages.[19,24] In Rwanda, the permissible limits for methanol and ethanol are less than 0.5% and 45% (v v^{-1}), respectively, in alcoholic beverage production and sale.[25]

The measurements of ethanol and methanol concentration in each sample were first calculated in mass percentage (g% w v^{-1}) during analysis, and the results were subsequently converted into alcohol by volume (ABV) or volume percentage (% v v^{-1}).

This observation underscored the significance of ensuring that alcoholic beverages adhere to safety regulations to safeguard public health and legal compliance. Table III offers a comprehensive illustration of the levels of methanol and ethanol detected and quantified in the samples. It is important to note that the ethanol content showed substantial variation, ranging from 3.8% to 98.9% (v v^{-1}) in the samples containing ethanol, and between 32% and 58.3% (v v^{-1}) for the samples in which methanol was detected. The figures marked in red denote instances where the concentrations of methanol or ethanol exceeded the acceptable limits defined by Rwanda's Ministry of Health, leading to legal proceedings.

Table III. Methanol and ethanol concentrations (% v v^{-1}) in analysed samples (2021-2022) and sample collection details, with red-highlighted values indicating levels exceeding Rwanda Ministry of Health limits and subsequent legal consequences

Case No.	Sample Brand	Me-OH(%vv^1)	Et-OH(%vv^{-1})	Collection Area	Case No.	Sample Brand	Me-OH (%vv^{-1})	Et-OH (%vv^{-1})	Collection Area
1	Unbranded	ND	37.1	North	29	Unbranded	ND	43	North
2	Unbranded	ND	36.9	North	30	African Gin	ND	37	North
3	Unbranded	ND	30.8	North	31	African Gin	ND	42.8	North
4	Unbranded	ND	32.8	North	32	African Gin	ND	34.2	North
5	Unbranded	ND	28	North	33	Unbranded	ND	43.4	North
6	Unbranded	ND	30.4	North	34	Unbranded	ND	29.7	North
7	Unbranded	ND	31.9	North	35	Unbranded	ND	37.3	North
8	Unbranded	ND	29.6	North	36	African gin	ND	50	North
9	Unbranded	ND	21.8	North	37	Unbranded	ND	50.7	North
10	Unbranded	ND	23.4	North	38	Unbranded	ND	44.8	North
11	Unbranded	ND	30.3	North	39	Unbranded	ND	39.6	North
12	Unbranded	ND	35.6	North	40	Unbranded	ND	40	North
13	Unbranded	ND	40	North	41	Unbranded	ND	43.6	North
14	Unbranded	ND	43	North	42	Unbranded	ND	21	North
15	Unbranded	ND	47.8	North	43	Unbranded	ND	48.6	North
16	Unbranded	ND	38.9	North	44	Unbranded	ND	43.7	North
17	Unbranded	ND	35.6	North	45	Unbranded	ND	46.7	North
18	Unbranded	ND	38.9	North	46	Muriture	ND	12.5	North
19	Unbranded	ND	39.4	North	47	Unbranded	ND	47.6	North
20	Unbranded	ND	37.1	North	48	Unbranded	ND	41.9	North
21	Unbranded	ND	38	North	49	Unbranded	ND	39.6	North
22	Unbranded	ND	39.7	North	50	Unbranded	ND	47.2	North
23	Unbranded	ND	37.4	North	51	Unbranded	ND	41.6	North
24	Unbranded	ND	44.4	North	52	Unbranded	ND	43.3	North
25	Muriture	ND	4.9	North	53	Unbranded	ND	44.1	North
26	Unbranded	ND	44.1	North	54	Unbranded	ND	44.8	North
27	Unbranded	ND	46.9	North	55	Unbranded	ND	13.5	North
28	Unbranded	ND	49.4	North	56	Unbranded	ND	41.2	North

Table III. Methanol and ethanol concentrations (% v v^{-1}) in analysed samples (2021-2022) and sample collection details, with red-highlighted values indicating levels exceeding Rwanda Ministry of Health limits and subsequent legal consequences (continuation)

Case No.	Sample Brand	Me-OH(%vv^1)	Et-OH(%vv^{-1})	Collection Area	Case No.	Sample Brand	Me-OH (%vv^{-1})	Et-OH (%vv^{-1})	Collection Area
57	Unbranded	ND	32.3	North	85	Royal castle	ND	47.7	Kigali
58	Unbranded	ND	44.6	North	86	Royal castle	ND	50.1	Kigali
59	Muriture	ND	6	Kigali	87	African buffalo	ND	49.6	Kigali
60	Muriture	ND	4	Kigali	88	African buffalo	ND	47.1	Kigali
61	Muriture	ND	6.8	Kigali	89	African buffalo	ND	47.5	Kigali
62	Muriture	ND	4.9	Kigali	90	African buffalo	ND	48.6	Kigali
63	Muriture	ND	8.2	Kigali	91	African buffalo	42.6	ND	Kigali
64	Muriture	ND	5.6	Kigali	92	African buffalo	44.3	ND	Kigali
65	K'bamba	37	ND	Kigali	93	Royal castle	ND	44.2	Kigali
66	K'bamba	45	ND	Kigali	94	African buffalo	ND	39.7	Kigali
67	K'bamba	36	ND	Kigali	95	Royal castle	ND	39.6	Kigali
68	K'bamba	ND	34	Kigali	96	Rabiant	ND	46.5	Kigali
68	K'bamba	ND	38	Kigali	97	Royal castle	ND	43.2	Kigali
70	K'bamba	ND	30	Kigali	98	Royal Castle	ND	45.2	Kigali
71	Unbranded	ND	27.2	North	99	African buffalo	ND	39.9	Kigali
72	Unbranded	ND	36.9	North	100	African Gin	ND	39.8	Kigali
73	Unbranded	ND	39.6	North	101	K'bamba	ND	50.3	Kigali
74	Unbranded	ND	40.8	North	102	African Gin	ND	31.4	Kigali
75	Unbranded	ND	36.7	North	103	Merry cane	ND	33.2	Kigali
76	K'Bamba	ND	47.9	North	104	African Gin	ND	41.7	Kigali
77	African buffalo	ND	41	Kigali	105	K'bamba	33.7	ND	Kigali
78	K'bamba	ND	43	Kigali	106	K'bamba	ND	36	Kigali
79	Unbranded	ND	12	Kigali	107	K'bamba	ND	32	Kigali
80	African buffalo	40.9	ND	Kigali	108	K'bamba	32	ND	Kigali
81	African buffalo	ND	45	Kigali	109	K'bamba	35	ND	Kigali
82	African buffalo	ND	47.5	Kigali	110	K'bamba	ND	60	Kigali
83	African buffalo	ND	47.4	Kigali	111	K'bamba	ND	32	Kigali
84	African buffalo	ND	49.7	Kigali	112	K'bamba	ND	31.9	Kigali

Table III. Methanol and ethanol concentrations (% v v⁻¹) in analysed samples (2021-2022) and sample collection details, with red-highlighted values indicating levels exceeding Rwanda Ministry of Health limits and subsequent legal consequences (continuation)

Case No.	Sample Brand	Me-OH(%vv¹)	Et-OH(%vv⁻¹)	Collection Area	Case No.	Sample Brand	Me-OH (%vv⁻¹)	Et-OH (%vv⁻¹)	Collection Area
113	K'bamba	ND	42.3	Kigali	141	Muriture	ND	6.2	Kigali
114	K'bamba	ND	41.7	Kigali	142	Unbranded	58.3	ND	Kigali
115	K'bamba	ND	34.6	Kigali	143	Merry cane	42.1	ND	Kigali
116	K'bamba	ND	39.8	Kigali	144	Merry cane	37.5	ND	Kigali
117	K'bamba	ND	38.1	Kigali	145	Merry cane	ND	35.7	Kigali
118	Rabiant	ND	41.6	Kigali	146	Muriture	ND	7.5	Kigali
119	Rabiant	ND	40.7	Kigali	147	Muriture	ND	7.8	Kigali
120	Rabiant	ND	38.5	Kigali	148	Unbranded	ND	98.9	Kigali
121	Rabiant	ND	39.6	Kigali	149	African Gin	ND	33.3	Kigali
122	Rabiant	ND	39.1	Kigali	150	African Gin	ND	40.8	Kigali
123	Rabiant	ND	37.7	Kigali	151	Rabiant	ND	37.5	Kigali
124	Rabiant	ND	43.2	Kigali	152	Rabiant	ND	41	Kigali
125	Rabiant	ND	38.1	Kigali	153	Unbranded	ND	49.8	Kigali
126	Unbranded	ND	43.8	Kigali	154	Unbranded	ND	52.6	Kigali
127	African Gin	ND	34	Kigali	155	Unbranded	ND	29.8	West
128	Unbranded	ND	29.8	South	156	Unbranded	ND	45.4	West
129	Unbranded	ND	32.5	South	157	Unbranded	ND	45.9	West
130	Unbranded	ND	29.8	South	158	Unbranded	ND	36.3	West
131	Muriture	ND	7.8	South	159	Unbranded	ND	44	West
132	Unbranded	ND	34.7	South	160	Unbranded	ND	34.9	West
133	Unbranded	ND	35	South	165	Unbranded	ND	40	South
134	Unbranded	ND	23.5	South	166	Unbranded	ND	41.2	South
135	Unbranded	ND	24.1	South	167	Unbranded	ND	96.8	South
136	Muriture	ND	9.1	South	168	African Gin	ND	28.3	South
137	Unbranded	ND	15.1	South	169	Unbranded	ND	13	South
138	Unbranded	ND	40	South	170	Unbranded	ND	11	South
139	Muriture	ND	3.8	South	171	Unbranded	ND	32.5	South
140	Unbranded	ND	39.6	South	172	Unbranded	ND	41.2	West

(continues on the next page)

Table III. Methanol and ethanol concentrations (% v v^{-1}) in analysed samples (2021-2022) and sample collection details, with red-highlighted values indicating levels exceeding Rwanda Ministry of Health limits and subsequent legal consequences (continuation)

Case No.	Sample Brand	Me-OH(%vv^1)	Et-OH(%vv^{-1})	Collection Area	Case No.	Sample Brand	Me-OH (%vv^{-1})	Et-OH (%vv^{-1})	Collection Area
173	Unbranded	ND	90.2	West	179	Unbranded	ND	33.7	East
174	Unbranded	ND	33.6	West	180	African gin	ND	39	East
175	Unbranded	ND	16.7	West	181	Muriture	ND	8	East
176	Unbranded	ND	30.9	West	182	Muriture	ND	8.4	East
177	African Gin	ND	43.9	East	183	Unbranded	ND	42.7	East
178	African Gin	ND	43.5	East					

^{1}ND: Not Detected. ^{2}Me-OH: Methanol. ^{3}Et-OH: Ethanol.

Table IV. Analysing ethanol and methanol levels in samples: A comprehensive breakdown by collection area, brand, and sample count

Collection Area	Samples per Collection Area	Brand or Source	Samples per Brand	Samples with high Me-OH content (>0.5% vv^{-1}) per brand	Samples with high Et-OH content (>45% vv^{-1}) per brand	Samples with high Me-OH content (>0.5% vv^{-1}) per area	Samples with high Et-OH content (>45% vv^{-1}) per area	Samples with high Me-OH content >0.5% vv^{-1} (% of total samples collected)	Samples with high Et-OH content >45% vv^{-1} (% of total samples collected)
City of Kigali	80	Unbranded	6	1	3				
		K'bamba	21	6	1				
		Muriture	9	0	0	12	16	6.5	8.7
		African Buffalo	14	3	8				
		African Gin	6	0	0				
		Rabiant	11	0	1				
		Royal Castle	9	0	3				
		Merry Cane	4	2	0				
Northern Province	61	Unbranded	57	0	9				
		K'bamba	1	0	1				
		Muriture	2	0	0	0	11	0	6.0
		African Buffalo	0	0	0				
		African Gin	1	0	1				
		Rabiant	0	0	0				
		Royal Castle	0	0	0				
		Merry Cane	0	0	0				

Table IV. Analysing ethanol and methanol levels in samples: A comprehensive breakdown by collection area, brand, and sample count (continuation)

Collection Area	Samples per Collection Area	Brand or Source	Samples per Brand	Samples with high Me-OH content (>0.5% vv^{-1}) per brand	Samples with high Et-OH content (>45% vv^{-1}) per brand	Samples with high Me-OH content (>0.5% vv^{-1}) per area	Samples with high Et-OH content (>45% vv^{-1}) per area	Samples with high Me-OH content >0.5% vv^{-1} (% of total samples collected)	Samples with high Et-OH content >45% vv^{-1} (% of total samples collected)
Southern Province	22	Unbranded	17	0	1				
		K'bamba	0	0	0				
		Muriture	4	0	0	0	1	0	0.5
		African Buffalo	0	0	0				
		African Gin	1	0	0				
		Rabiant	0	0	0				
		Royal Castle	0	0	0				
		Merry Cane	0	0	0				
Western Province	11	Unbranded	11	0	3				
		K'bamba	0	0	0				
		Muriture	0	0	0	0	3	0	1.6
		African Buffalo	0	0	0				
		African Gin	0	0	0				
		Rabiant	0	0	0				
		Royal Castle	0	0	0				
		Merry Cane	0	0	0				
Eastern Province	9	Unbranded	4	0	0				
		K'bamba	0	0	0				
		Muriture	2	0	0	0	0	0	0
		African Buffalo	0	0	0				
		African Gin	3	0	0				
		Rabiant	0	0	0				
		Royal Castle	0	0	0				
		Merry Cane	0	0	0				

Discussion

A total of 183 samples of illicit alcoholic beverages were collected from different regions across the country. The collection comprised 80 samples from the City of Kigali, 61 from the northern province, 22 from the southern province, 11 from the western province, and 9 from the eastern province. These samples were further classified into various brands based on their original labelling, including K'bamba (22 samples), Muriture (17 samples), African Buffalo (14 samples), African Gin (11 samples), Royal Castle (9 samples), Merry Cane (4 samples), and unbranded alcoholic beverages (95 samples).

The study used a Headspace gas chromatography method to analyse methanol and ethanol levels in samples, resulting in strong correlation coefficients (R^2) of 0.997 for methanol and 0.998 for ethanol. The method showed low imprecision, with %RSD values not exceeding 10.1%. The accuracy ranged between 92% and 114%, indicating consistent results across concentration levels. The calibration ranged from 0.01 g% to 1 g% (w v^{-1}), allowing precise quantification. The study adhered to Rwanda's Ministry of Health guidelines, ensuring acceptable levels of methanol and ethanol in alcoholic beverages do not exceed 0.5% and 45% (v v^{-1}), respectively.

In a comprehensive analysis of various provinces and the City of Kigali, we observed remarkable differences in the content of methanol and ethanol in tested samples. In the city of Kigali, which had a sample size of 80 (43.7%), it was found that 15% of these samples, exceeded the permissible limit of 0.5% (v v^{-1}) for methanol. A breakdown of these samples revealed varying percentages from different sources or brands, with 7.5% from K'bamba, 3.75% from African Buffalo, 2.5% from Merry Cane, and 1.25% from unbranded samples. Moreover, 20% of the Kigali samples surpassed the allowed limit of 45% (v v^{-1}) for ethanol, with 10% from African Buffalo, 3.75% from Royal Castle, 3.75% from unbranded sources, 1.25% from K'bamba, and 1.25% from Rabiant.

Turning our attention to the Northern province with 61 samples (33.3%), we observed that all samples adhered to the acceptable limit for methanol levels, indicating a high level of compliance. However, when examining ethanol levels, we found that 18% of the samples (11 out of 61) exceeded the allowable limit. Among these samples, 82% were from unbranded samples, 9% were from K'bamba, and another 9% from African Gin.

In the Southern province, where 22 samples (12%) of total samples were collected, a positive trend was observed, with 100% of the samples meeting the acceptable limit for methanol levels. However, in the case of ethanol, only 4.5% of the samples (1 out of 22), specifically from the African Buffalo brand, exceeded the permitted limit. In the western province, which had 11 (6%) of tested samples, all samples (100%) adhered to the acceptable limit for methanol levels, indicating strong compliance. However, when considering ethanol levels, we found that 27.2% of the samples (3 out of 11), all sourced from unbranded samples, exceeded the allowable limit of ethanol. Lastly, in the eastern province with 9 (4.9%) of tested samples, a perfect compliance rate of 100% was observed for both methanol and ethanol levels, indicating a strong adherence to the acceptable limits for methanol and ethanol.

The study findings also revealed that unbranded alcoholic beverages constituted a significant proportion of the samples collected, accounting for 51.9% out of 183. Meanwhile, K'bamba made up 12%, Muriture 10.3%, African Buffalo 7.6%, African Gin 6%, Rabiant 6%, Royal Castle 4.9%, and Merry Cane 2.1% of the sampled beverages. Notably, the majority of unbranded samples, specifically 48.6% of total collected samples, were collected from provinces outside the city of Kigali, the capital. This suggested that most people in rural regions consume home-brewed and locally-made alcoholic beverages due to their affordability in terms of production and consumption.

Out of 183 samples collected from different parts of Rwanda, including the City of Kigali, in response to suspected cases of methanol poisoning, about 6.6% of the samples (12 out of 183) had methanol levels higher than the permissible limit of 0.5% (v v^{-1}). It is noteworthy that the city of Kigali was the only location for all 12 of these positive samples. The percentage of samples in the same pool that had ethanol levels higher than the allowable limit of 45% (v v^{-1}) was about 16.9% (31 out of 183). Of these 31 samples, about 51.6% came from Kigali, approximately 35.5% from the Northern province, approximately 9.7% from the

Western province, and approximately 3.2% from the Southern province. Significantly, no samples from the Eastern province had ethanol and/or methanol over the allowed limit. Particularly, none of these samples tested positive for both methanol and ethanol simultaneously.

CONCLUSIONS

The study examined 183 samples of illicit alcoholic beverages from various parts in Rwanda, applying a precise Headspace Gas Chromatography method to determine methanol and ethanol levels. The results revealed significant variations in compliance with Rwanda's regulatory limits across different provinces. It is significant to highlight that samples containing ethanol ranged from: 3.8% to 98.9% (v v^{-1}) for ethanol-containing samples and 32% to 58.3% (v v^{-1}) for the samples that had methanol identified.

The City of Kigali exhibited notable non-compliance, with 15% of the samples exceeding the acceptable methanol limit and 20% surpassing the ethanol limit. These issues were attributed to specific brands or sources, including K'bamba, African Buffalo, Merry Cane, Royal Castle, and unbranded alcoholic samples or alcoholic beverages produced locally.

The Northern province showed strong compliance with methanol levels but had 18% of samples exceeding the ethanol limit, primarily from unbranded samples. The Southern province had a perfect compliance rate for methanol but saw a minimal non-compliance rate of 4.5% for ethanol from the African Buffalo brand. The Western province had complete compliance with methanol levels, but 27.7% of samples exceeded the ethanol limit, all from unbranded alcoholic samples. The Eastern province exhibited perfect compliance for both methanol and ethanol.

Overall, approximately 6.6% of the samples had excessive methanol levels, and roughly 16.9% exceeded the ethanol limit. The City of Kigali was the main contributor to non-compliance in both categories. Importantly, no samples tested positive for both methanol and ethanol simultaneously. These findings underscored the importance of monitoring and regulating the alcoholic beverages market in Rwanda to ensure compliance with acceptable methanol and ethanol levels and protect public health.

Conflicts of interest

The authors declare that there is no conflict of interest regarding financial or potential sources of bias such as affiliations, funding sources and financial or management relationships which may constitute a conflict of interest.

Acknowledgments

REFERENCES

(1) Nelson, L. S.; Howland, M. A.; Lewin, N. A.; Smith, S. W.; Goldfrank, L. R.; Hoffman, R. S. *Goldfrank's Toxicologic Emergencies,* 11th ed. McGraw Hill/Medical, New York City, USA, 2019.
(2) Aguayo, E. H. *Garriot's Medicolegal Aspects of Alcohol*, 5th ed. James C. Garriott, Ed. Lawyers & Judges Publishing Co., Inc., 2017.
(3) Yayci, N.; Ağritmiş, H.; Turla, A.; Koç, S. Fatalities Due to Methyl Alcohol Intoxication in Turkey: An 8-Year Study. *Forensic Sci. Int.* **2003**, *131* (1), 36–41. https://doi.org/10.1016/S0379-0738(02)00376-6
(4) Frenkel, C.; Peters, J. S.; Tieman, D. M.; Tiznado, M. E.; Handa, A. K. Pectin Methylesterase Regulates Methanol and Ethanol Accumulation in Ripening Tomato (*Lycopersicon esculentum*) Fruit. *J. Biol. Chem.* **1998**, *273* (8), 4293–4295. https://doi.org/10.1074/jbc.273.8.4293

(5)   Micheli, F. Pectin Methylesterases: Cell Wall Enzymes with Important Roles in Plant Physiology. *Trends Plant Sci.* **2001**, *6* (9), 414–419. https://doi.org/10.1016/S1360-1385(01)02045-3

(6)   Bindler, F.; Voges, E.; Laugel, P. The Problem of Methanol Concentration Admissible in Distilled Fruit Spirits. *Food Addit. Contam.* **1988**, *5* (3), 343–351. https://doi.org/10.1080/02652038809373713

(7)   Chaiyavat, C.; Supakan, J.; Chakkrapong, K.; SartjinPeerajan; Sasithorn, S.; Lalida, S. Factors Affecting Methanol Content of Fermented Plant Beverage Containing Morinda Citrifolia. *Afr. J. Biotechnol.* **2013**, *12* (27), 4356–4363. https://doi.org/10.5897/AJB10.1377

(8)   Lamiable, D.; Hoizey, G.; Marty, H.; Vistelle, R. Intoxication aiguë au méthanol. *Revue Française des Laboratoires* **2000**, *2000* (323), 31–34. https://doi.org/10.1016/S0338-9898(00)80265-6

(9)   Liesivuori, J.; Savolainen, A. H. Methanol and Formic Acid Toxicity: Biochemical Mechanisms. *Basic Clin. Pharmacol. Toxicol.* **1991**, *69* (3), 157–163. https://doi.org/10.1111/j.1600-0773.1991.tb01290.x

(10)   The American Academy of Clinical Toxicology Ad Hoc Committee on the Treatment Guidelines for Methanol Poisoning. Barceloux, D. G.; Bond, G. R.; Krenzelok, E. P.; Cooper, H.; Vale, J. A. American Academy of Clinical Toxicology Practice Guidelines on the Treatment of Methanol Poisoning. *Journal of Toxicology: Clinical Toxicology* **2002**, *40* (4), 415–446. https://doi.org/10.1081/CLT-120006745

(11)   Zocca, F.; Lomolino, G.; Curioni, A.; Spettoli, P.; Lante, A. Detection of Pectinmethylesterase Activity in Presence of Methanol during Grape Pomace Storage. *Food Chem.* **2007**, *102* (1), 59–65. https://doi.org/10.1016/j.foodchem.2006.01.061

(12)   Mesri, M.; Behzadnia, M. J.; Nikpoor, M.; Ghazvini, A. Cerebral Methanol Intoxication: A Case Report with Literature Review. *Canadian Journal of Medicine* **2022**, *3* (4), 195–201. https://doi.org/10.33844/cjm.2022.60611

(13)   Kruse, J. A. Methanol and Ethylene Glycol Intoxication. *Crit. Care Clin.* **2012**, *28* (4), 661–711. https://doi.org/10.1016/j.ccc.2012.07.002

(14)   Brunton, L.; Chabner, B. A.; Knollmann, B. C. (Eds.) *Goodman and Gilman's The Pharmacological Basis of Therapeutics*, 12th ed. McGraw Hill / Medical, California, USA, 2011.

(15)   Kruse, J. A. Methanol Poisoning. *Intensive Care Med.* **1992**, *18* (7), 391–397. https://doi.org/10.1007/BF01694340

(16)   Tian, M.; He, H.; Liu, Y.; Li, R.; Zhu, B.; Cao, Z. Fatal Methanol Poisoning with Different Clinical and Autopsy Findings: Case Report and Literature Review. *Leg. Med.* **2022**, *54*, 101995. https://doi.org/10.1016/j.legalmed.2021.101995

(17)   Jones, A. W.; Sternebring, B. Kinetics of Ethanol and Methanol in Alcoholics during Detoxification. *Alcohol and Alcoholism* **1992**. https://doi.org/10.1093/oxfordjournals.alcalc.a045315

(18)   Medinsky, M. A.; Dorman, D. C. Recent Developments in Methanol Toxicity. *Toxicology Letters* **1995**, *82–83*, 707–711. https://doi.org/10.1016/0378-4274(95)03515-X

(19)   Paine, A. J.; Dayan, A. D. Defining a Tolerable Concentration of Methanol in Alcoholic Drinks. *Hum. Exp. Toxicol.* **2001**, *20* (11), 563–568. https://doi.org/10.1191/096032701718620864

(20)   International Council for Harmonisation (ICH). Bioanalytical Method Validation and Study Sample Analysis M10. *ICH Harmonised Guideline: Geneva, Switzerland* **2022.**

(21)   Berkkan, A.; Ulutas, O. K. Analytical Performance and Validation of Headspace-Gas Chromatography-Flame Ionization Detector (HS-GC-FID) Method for Alcohol Content and Evaluation of Efficiency and Possible Toxicity of Hand Sanitizers at the Time of Pandemic. *Rev. Roum. Chim.* **2021**, *66* (6), 547–556. https://doi.org/10.33224/rrch.2021.66.6.07

(22)   Cheng, W. L.; Markus, C.; Lim, C. Y.; Tan, R. Z.; Sethi, S. K.; Loh, T. P. Calibration Practices in Clinical Mass Spectrometry: Review and Recommendations. *Ann. Lab. Med.* **2023**, *43* (1), 5–18. https://doi.org/10.3343/alm.2023.43.1.5

(23)   Tan, A.; Awaiye, K.; Jose, B.; Joshi, P.; Trabelsi, F. Comparison of Different Linear Calibration Approaches for LC–MS Bioanalysis. *J. Chromatogr. B* **2012**, *911*, 192–202. https://doi.org/10.1016/j.jchromb.2012.11.008

(24) Pohanka, M. Toxicology and the Biological Role of Methanol and Ethanol: Current View. *Biomed. Pap.* **2016**, *160* (1), 54–63. https://doi.org/10.5507/bp.2015.023

(25) Ministry of Health. Law Governing Narcotic Drugs, Psychotropic Substances and Precursors in Rwanda, 2012. Available at: https://rwandalii.org/akn/rw/act/law/2012/3/eng@2012-04-09 (accessed April, 2023).

ARTICLE

Sensitive Voltammetric Detection of Acetaminophen on CuONPs-MWCNTs Modified Glassy Carbon Electrode with Enhancement Effect of Anionic Surfactant

Rajesh N. Hegde[1]* (ID) ✉, P. Vishwanatha[1] (ID), Sharanappa T. Nandibewoor[2] (ID)

[1]*Department PG Studies and Research in Chemistry, Sri Dharmasthala Manjunatheshwara College, Ujire-574 240, Karnataka, India*

[2]*K L E Technological University, Hubballi-580 031, Karnataka, India*
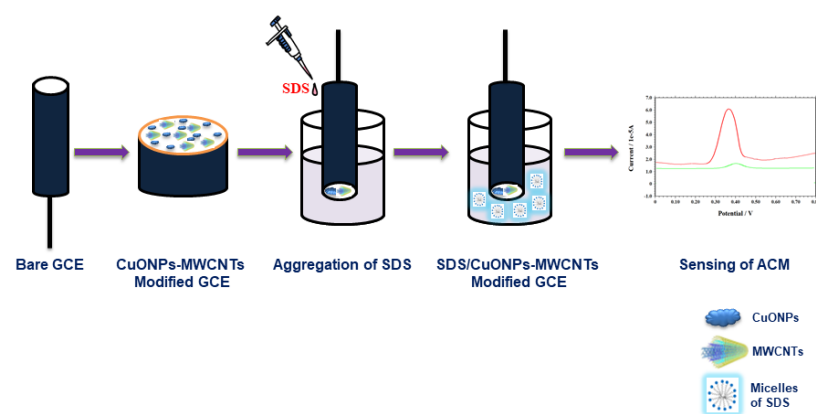
In the present work, a voltammetric method using differential pulse voltammetric technique was developed for the assessment of antipyretic and analgesic drug, acetaminophen. The CuO nanoparticles were prepared and characterized. A glassy carbon electrode (GCE) fabricated with the suspension of CuO nanoparticles (CuONPs) and multi-walled carbon nanotubes (MWCNTs) were used. The modified electrode showed improved anodic peak current by introducing an anionic surfactant sodium dodecyl sulphate in phosphate buffer solution. The effect of the pH of the supporting electrolyte, the amount of nanoparticle suspension and the surfactant concentration was studied at a physiological pH of 7.4. Using differential pulse voltammetry, the fabricated electrode showed linear dynamic range from 9 to 160 nM of acetaminophen concentration. From the calibration plot, the computed detection limit was 5.06 nM and quantification limit was 16.88 nM. The developed method was tested for its reproducibility and assay during a day and intraday as well. The developed process was fruitfully applied to detect acetaminophen in pediatric oral suspensions administered to infants.

Keywords: voltammetry, acetaminophen, surfactant, nanoparticles, sensor

INTRODUCTION

Acetaminophen (ACM), is the most widely studied pharmacological and hepatotoxic drug used by billions of people globally as an antipyretic and analgesic therapeutic drug. It is believed to be safe when

administered in lower doses and it relieves moderate to severe pain and is being used to treat fever. ACM administered to healthy adults is metabolized in the liver and excreted in the urine.[1] Of the administered dose, only about 1-4% is released as pure ACM and most is converted to conjugated forms such as paracetamol glucuronide; about 47-60% is released as paracetamol sulfate and about 25-35% is excreted from the human body. At higher dosage, ACM proved to be deadly for humans and also causes disturbance of heart and mind. The extended and too much use of ACM may lead to toxic metabolite amassing and this can cause failure of kidney and liver or even death. Therefore, it becomes very essential to develop an analytical technique to analyze ACM in various samples.

To date, there are many analytical methods used to analyze and quantify various drug molecules either in real samples or pharmaceutical samples. Among the methods developed, spectroscopic, chromatographic, titrimetric and electrochemical methods are widely used.[2-7] Among all these methods, the electrochemical methods have been strongly developed in recent years because they are cost effective, reliable, require less time for analysis, very simple with good selectivity and high sensitivity. These methods also fall in sustainable analytical methods because of no or less solvent usage. The electrodes based on carbon materials are being employed widely in electrochemical analysis, since they have broad potential window, brilliant electrical conductivity, very little background current, more surface area for reaction, chemically and electrochemically inert, highly stable and very much cost effective.[8-10] High sensitivity and excellent selectivity were achieved by employing modified electrodes using various types of modifiers, especially with the nano-dimensional materials, either carbon based nano-materials or metal based nano-materials or even nano-composites.[11,12]

The surface active substances, i.e., the surfactants are playing vital role in the development of electrochemical sensors in recent years. Surfactants can enhance the electrochemical process which is occurring at the electrode there by excelling the sensitivity of the fabricated electrode via adsorption at interfaces or aggregation into supramolecular structure. In recent days, the surfactants were used to enhance the sensitivity of the methods.[13,14] The SDS is also been used widely to improve the detection and quantification limits of the methods developed.[15,16]

To date, ACM was one of the drug molecules which was extensively studied and detected using various modified electrodes with very low detection limits in different formulations. There was a report on paracetamol sensing using graphite flakes.[17] MWCNTs decorated silver nanoparticles were used to sense ACM with good detection limit and recovery.[18] There was an attempt to study electrochemical kinetics of ACM and its detection on a carbon paste electrode, even though this is economical, but it was bit difficult to produce same surface area using carbon paste electrode.[19] Simultaneous detection of ACM and caffeine was reported using bare graphite electrode, but this lacks in sensitivity.[20] A polyglycine modified GCE was used to detect ACM in syrup with good sensitivity and selectivity.[21] A screen printed carbon electrode was used successfully for the assessment of ACM, acetylsalicylic acid, caffeine simultaneously with good selectivity.[22] An sensor for ACM detection was developed using guanine modified electro, but which is lacking in selectivity and sensitivity.[23] A nanomaterial-poly composite electrode was fabricated for ACM detection in biological fluids with excellent detection limit and sensitive.[24] There was an attempt to recover graphene oxide from Zn-C battery waste to construct a sensor for detection of ACM.[25] The recovery procedure was not so convincing and limit of detection reported was on higher side. ACM and ciprofloxacin were detected simultaneously on a sub-microparticle modified electrode with good linearity range.[26] There was an attempt to develop an organometallic complex encapsulated in nanozeolite electrode.[27] The modified electrode shown excellent electrocatalytic activity for the detection of ACM and ascorbic acid together with good linear range and detection limit. A pencil graphite electrode modified with polymer and gold nanoparticles was constructed.[28] They reported simultaneous assessment of ACM, propyphenazone, and caffeine with good linear range for ACM. A natural zeolite and graphene oxide were used to fabricate carbon paste electrode for the enhanced detection of ACM.[29] The DPV technique used to quantify ACM with excellent linearity range and limit of detection. The square wave voltammetric technique was used to detect ACM using 3D graphene platform.[30] Metal organic framework are now receiving great attention

because of their versatility. ACM was detected using NiCo-MOF with a fair detection limit.[31] Eventhough, there are excellent reports for the detection of ACM, there is need to introduce new electrodes in the field of electro-analytical chemistry and to develop a better method for the sensing of ACM. Therefore, in this work, the CuONPs-MWCNTs modified electrode was fabricated and the signal of oxidation in PBS of physiological pH was significantly enhanced by introducing SDS into the solution. All the parameters were optimized using DPV and the developed method was fruitfully applied to detect ACM in syrups which were administered to infants.

MATERIALS AND METHOD

Chemicals

Multi Walled Carbon Nanotubes (MWCNTs; O.D. × L of 7-15 nm × 0.5-10 μm), ACM, Triton X-100, cetyl trimethyl ammonium bromide (CTAB), sodium dodecyl sulphate (SDS), and $K_3Fe(CN)_6$ were purchased from Sigma-Aldrich. The other chemicals, methanol, NaH_2PO_4, Na_2HPO_4, and acetonitrile were purchased from Rankem Chemicals. To prepare the phosphate buffer solution (PBS), double distilled water was employed. The pH of PBS was varied from 5.4 to 8.0 by employing various volumes of dibasic and monobasic sodium phosphate stock solution. The stock solution of ACM was prepared in methanol. The pediatric oral suspensions produced by different companies and available locally were collected. Calpol (100 mg mL^{-1}) by Enzyme Pharmaceuticals, Gujarat; Akmol-25 (250 mg mL^{-1}) by Akiez Remedies, Varanasi; Dolopar (125 mg mL^{-1}) by Micro Labs Ltd and Wellpar (125 mg / 5 mL) by Wellona Pharma were purchased from local pharmacy. For stock solution preparation, exact volume was measured from syrup bottles and dissolved initially in methanol and diluted with distilled water. To get sufficient concentration to carryout analysis, required volume of PBS was used to dilute the above stock solution.

Instruments

Voltammetric measurements were carried out on a CH Instruments electrochemical analyzer 660E, attached with a conventional three-electrode cell. The three-electrode cell consisting of a bare glassy carbon electrode with a diameter of 2 mm (modified and unmodified) as working electrode, a Pt wire was used as the counter electrode and an Ag/AgCl (3 M KCl) as reference electrode, respectively. All the potentials recorded in this report were specified against the Ag/AgCl electrode. An alumina powder 0.05 μm was used to polish the surface of working electrode and was cleaned ultrasonically. Then, to characterize the prepared CuO nanoparticles, scanning electron microscope with model specification of SEM XL 30 ESEM with EDAX was used.

Preparation and characterization of nanoparticles of CuO

The nanoparticles of CuO were synthesized as reported elsewhere.[32] By mixing vigorously 0.5 M Na_2CO_3 solution and 0.5 M $CuSO_4$ solution at about 80 ºC, the precursor was prepared. This results in basic copper sulphate precipitate, which was filtered immediately and washed to remove the ion traces with doubly distilled water. Then, it was filtered and mass was left for drying in air for 8 hours. The precursor was thermally decomposed in a muffle furnace for a period of 4 hours at 800 ºC which results in the production of nanoparticles of CuO. Then, the SEM image of the prepared nanoparticles was recorded after calcinations and is as shown in Figure 1.
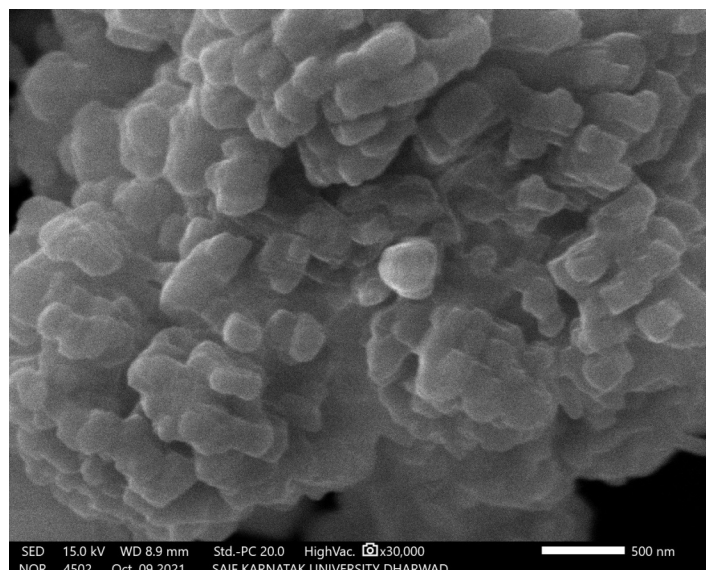
Figure 1. Scanning electron microscopic image of CuO nanoparticles.

Analytical procedure

By breaking up 2 mg each of MWCNTs and CuONPs in acetonitrile (10 mL), the CuONPs-MWCNTs stable suspension was prepared by ultrasonication. The working electrode was polished carefully with the slurry of 0.05 µm alumina powder using the polishing cloth, and then washed with methanol and water in an ultrasonic bath, respectively. Thus, cleaned working electrode was drop-coated with 5 µL of the black suspension of CuONPs- MWCNTs every time and dried in air.

The CuONPs-MWCNTs fabricated GCE was first activated in PBS of pH 7.4 by cyclic voltammetric measurements from 0.0 to 0.8 V until we get stable segments of cyclic voltammograms with a scan rate of 0.05 V s^{-1} for 5 cycles. After that, electrodes (all three) were transferred to second cell of PBS with pH 7.4, which contains accurate amounts of ACM and SDS. With an increment of 0.04 V, amplitude of 0.05 V, pulse width of 0.05 s, sample width of 0.0167 s and pulse period of 0.5 s, the differential pulse voltammogram was recorded between 0 and 0.8 V. All the experiments were performed at 25 ºC in presence of atmospheric oxygen.

RESULTS AND DISCUSSION

Response of modified electrode with potassium ferricyanide

A 1.0 mM solution of $K_3Fe(CN)_6$ in 0.1 M KCl was used to record CVs at CuONPs-MWCNT modified GCE at various scan rates. For the reversible electrode process, the Randles-Sevcik equation (Equation 1) was used to calculate effective surface area of unmodified and modified electrode.

$$Ip = (2.69 \times 10^5) \, n^{3/2}AD^{1/2} \, Co \, v^{1/2} \qquad \text{Equation 1}$$

where Ip is the anodic or cathodic peak current, n is the number of electrons involved, A is the electrode surface area, D is diffusion coefficient, v is the scan rate, and Co is the concentration of $K_3Fe(CN)_6$

For 0.1 M KCl electrolyte with 1.0 mM solution of $K_3Fe(CN)_6$, the n and D values are 1 and 7.6 x 10^{-6} cm^{2}s^{-1}. By slope of the plot of Ip v/s $v^{1/2}$, the active surface areas obtained are 0.1462 cm^2 for modified GCE and 0.03925 cm^2 for bare GCE. From these values, it was concluded that active surface area has become significantly increased after fabrication. Therefore, it was concluded that modification of electrode showed electrocatalytic nature.

Response of ACM

The DPV was recorded for 100 nM ACM with 10 µM of SDS and without SDS on CuONPs-MWCNTs/ GCE. Without SDS, the oxidation peak at about 0.41 V was slightly weaker (Figure 2 (a)) compared to the peak in the presence of SDS at about 0.38 V, with significant enhancement in peak current and negative shift in peak potential (Figure 2(b)). It was well known that SDS can form micelles by self-assembly, which contains hydrophobic tail forming the core and hydrophilic head facing the outer surface. The introduction of SDS into the solution effectively reduces the interface between the electrode and ACM. This reduction in the interface is clear from the enhancement in the peak current as indicated in Figure 2 (b). The added SDS is facilitating the electro-oxidation process there by allowing the analyte to reach the electrode surface and take part in the redox reaction more conveniently by reducing the interaction between the electrode surface and the ACM.[33,34]
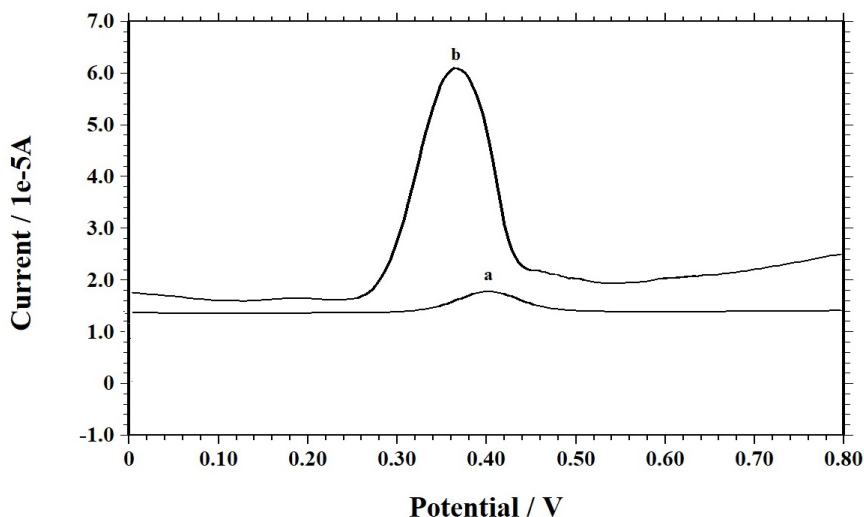
Figure 2. Differential pulse voltammogram of 100 nM ACM at pH 7.4 in 0.1 M PBS on CuONPs-MWCNTs modified GCE (b) with 10 µM of SDS and (a) without SDS.

Effect of quantity of CuONPs-MWCNTs suspension and pH

The effect of the amount of CuONPs-MWCNTs suspension on the anodic peak was investigated. Highest oxidation peak current was obtained when 15 µL of suspension was employed for drop coating. The peak current increased significantly with increasing the amount of the suspension till 15 µL and afterwards, peak current decreased gradually and remain almost constant for higher concentrations of the suspension (Figure 3). This was owing to the fact that at higher quantity, the film is thicker and this results in reduced conductivity, which results in decreased oxidation current. Therefore, 15 µL of suspension was utilized for further studies. The effect of pH was investigated from 8.0 to 5.8 using PBS, since pH of the supporting electrolyte plays key role in the reactions which take place at the electrode. The investigation indicated that, the oxidation potential was shifted to lesser values with increase in pH of the reaction medium. There was no significant variation in peak current, but physiological pH was employed for further studies.
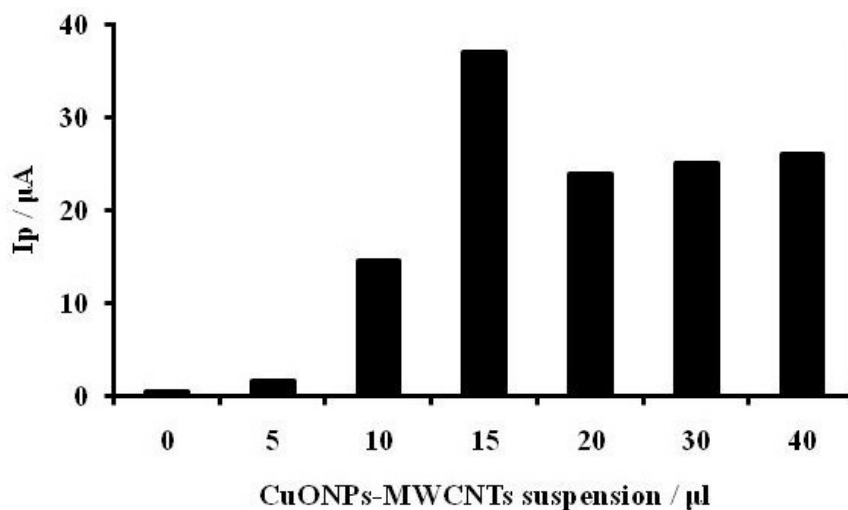
Figure 3. Graph of variation of volume of CuONPs-MWCNTs suspension against peak current.

Effect of surfactants

The influence of different types of surfactants has been tested for this title reaction. It was found that, in presence of neutral surfactant Triton X-100 there was no change in peak current and peak potential. However, in the presence of the cationic surfactant CTAB, the oxidation peak was poorly defined. Even though, an anodic peak was present in the company of all surfactants. However, the added SDS was effectively promoting the electro-oxidation of ACM at the electrode. The effect of concentration of SDS on oxidation reaction was examined. The peak current increased sharply up to 10 µM of SDS (Figure 4).
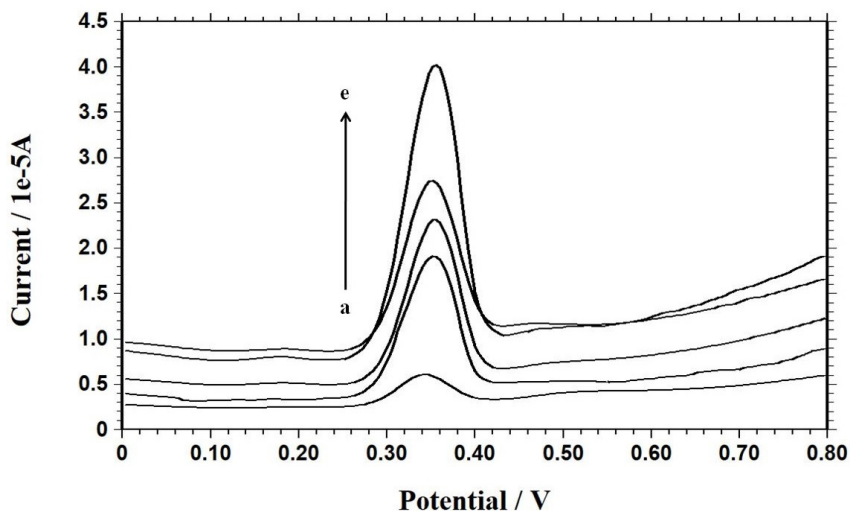
Figure 4. Differential pulse voltammograms of 100 nM ACM on CuONPs-MWCNTs modified GCE with (a) 0.0, (b) 2.5, (c) 5.0, (d) 7.5 and (e) 10 µM of SDS at pH 7.4 in PBS.

Afterwards, the peak current decreased gradually as shown in Figure 5. This may be due to the formation of thick aggregates of SDS at the electrode, which are blocking the surface for the reaction. Hence, 10 µM of SDS was employed for the further studies.
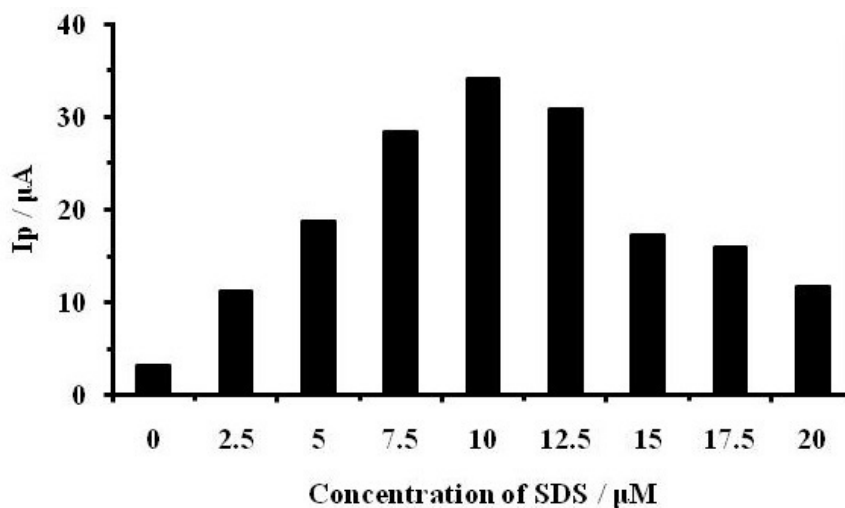
Figure 5. The plot of variation of peak current with concentration of SDS.

Calibration curve

To develop a voltammetric method for the estimation of ACM, DPV was used since the peaks are sharper and well defined using pulse techniques with lower background current. Using PBS as supporting electrolyte at physiological pH, voltammograms were recorded with increasing amount of ACM. The oxidation peak current rose linearly from 9.0 to 160 nM of ACM as shown in Figure 6. The calibration plot was constructed (Inset Figure 6.) which yields the equation Ip = 0.22 C + 3.58; R^2 = 0.996 (C is in nM). It was also observed that, variation from linearity for the higher quantity of ACM, due to the adsorption of analyte or its product after electro-oxidation on the surface of electrode. Using the equations, 3s/m and 10s/m, the detection limit and quantification limits were computed. The obtained detection limit and quantification limit are 5.06 nM and 16.88 nM respectively. These acquired outcomes were matched up with previously reported values and were tabulated in Table I.
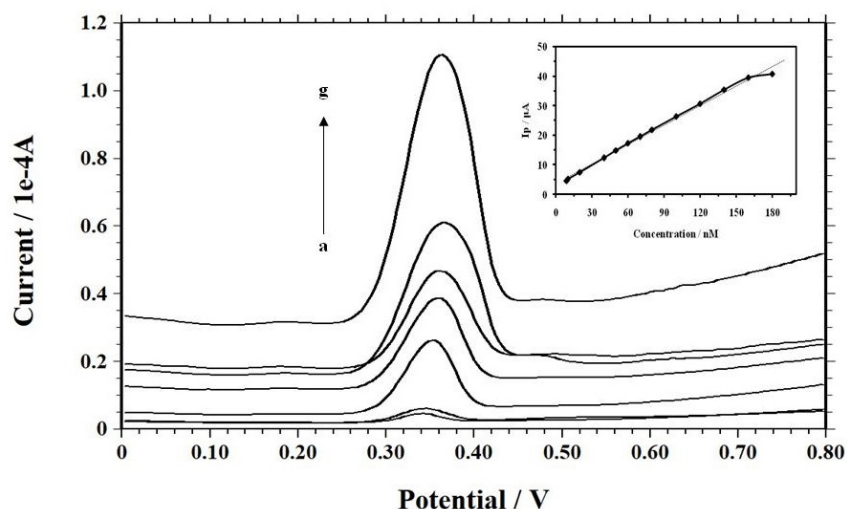
Figure 6. Differential pulse voltammograms with increasing quantities of ACM from (a) 9, (b) 20, (c) 40, (d) 60, (e) 80, (f) 120, and (g) 160 nM at SDS/ CuONPs-MWCNTs modified GCE in PBS. Inset: Plot of peak current *Vs* concentration of ACM.

Table I. Comparison of analytical parameters at various electrodes

Electrode	Method	LDR (µM)	LOD (µM)	Ref.
ePAD	DPV	1-60	0.20	17
AgNPs@HOOC-MWCNT@SPCE	SWV	0.5-1000	0.24	18
Stv-CPE	DPV	0.6-100	0.20	19
BGE	DPV	5-150	0.20	20
Polyglycine-GCE	DPV	0.5-75	0.03	21
SPCE	SWV	—	1.2	22
Guanine-GCE	DPV	0.005-10	0.90	23
MWCNT/GO/Poly(Thr)/GCE	DPV	3-140	0.16	24
ERGO-GCE	DPV	—	0.14	25
C-HAP-GCE	DPV	0.01-1310	0.14	26
NiCoSalenA/CPE	DPV	1.71-32.5	0.51	27
AuNPs/P(L-cyst)/PGE	DPV	0.023-90	—	28
GO/NiZ/CPE	DPV	0.026-0.78	0.007	29
3D/LSG	SWV	0.005-1	—	30
NiCo-MOF/CCE	DPV	5.0-400	1.0	31
SDS/CuONPs-MWCNTs/GCE	DPV	0.009-0.16	0.005	This work

ePAD - Electrochemical paper based analytical device; AgNPs – Silver nanoparticles; MWCNT – Multi walled carbon nanotubes; SPCE – Screen printed carbon electrode; Stv-Stevensite; CPE- Carbon paste electrode; BGE – Bare graphite electrode; GCE – Glassy carbon electrode; GO – Graphene oxide; ERGO – Elctrochemically reduced graphene oxide; HAP – Hydroxyapatite; NiCoSalenA - Nickel-Cobalt Salen nanozeolite; PGE – Pencil graphite electrode; NiZ – Nickel ion zeolite; LSG – Laser scribed graphene; CCE- Carbon cloth electrode ; SDS – Sodium dodecyl sulphate; LDR – Linear dynamic range; LOD – Limit of detection; DPV – Differential pulse voltammetry; SWV – Square wave voltammetry.

Reproducibility study

To study the reproducibility of the fabricated electrode, voltrammograms were recorded with 100 nM ACM at the fabricated electrode, which was re-modified each time for every few hours during a day. The relative standard deviation (RSD) of 2.02% was found for anodic current with 15 measurements and the modified electrode can be used thrice within 5% error. The reproducibility of results between days was analogous to that of within a day at constant temperature. However, the oxidation product was strongly adsorbing on to the electrode and hence the electrode has to be fabricated all over again after each run.

Intra-day and Inter-day assay

To substantiate the accuracy and precision of the above developed process, the assay of ACM was carried out during inter-day and intra-day. This was carried out at various amounts of ACM, i.e., at 10, 80 and 150 nM. Using DPV, voltammograms were recorded one time during a day (n = 6) for five successive days for the inter-day analysis and under alike state at the identical amounts of ACM (n = 6) for five times during a day to compute assay in a day.

During a day assay, the accuracy values obtained were ±1.20%, ±0.43%, and ±0.75% for low, medium and high concentrations levels with recovery values of 101.20%, 99.56% and 100.75%, respectively (Table II). For inter-day assay, the accuracy values of ±0.60%, ±0.53% and ±0.58% were got with recovery values of 99.40%, 100.53% and 99.42% for low, medium and high quantity of ACM, respectively. The average precision values obtained were in the range of 4.67% to 10.24% (Table II). The precision and accuracy values computed were within ±15%, and are hence within tolerable limits.[35]

Table II. Statistics obtained for ACM assay during a day and inter-day

Quantity (nM)	Estimated quantity (nM)	Recovery (%)	Accuracy (%)	Precision (%RSD)
Intra-day				
10	10.12±0.42	101.20	±1.20	6.13
80	79.65±0.64	99.56	±0.43	9.75
150	151.1±.32	100.7	±0.75	5.32
Inter-day				
10	9.94±0.21	99.40	±0.60	10.24
80	80.43±0.17	100.5	±0.53	4.67
150	149.1±0.35	99.42	±0.58	8.74

Assessment of ACM in oral suspensions

By following the identical conditions described above, the assessment of the analyte was carried out. The stock solution was diluted with doubly distilled water so that ACM concentration fall in LDR and introduced into the cell containing accurate quantities of PBS of pH 7.4 and SDS. DPV measurements were recorded and standard addition method was used to compute the concentration of ACM in syrup samples as shown in Figure 7. The computed results were as shown in Table III. It was found that, ACM concentrations obtained by the present method were matching with the labeled claim.
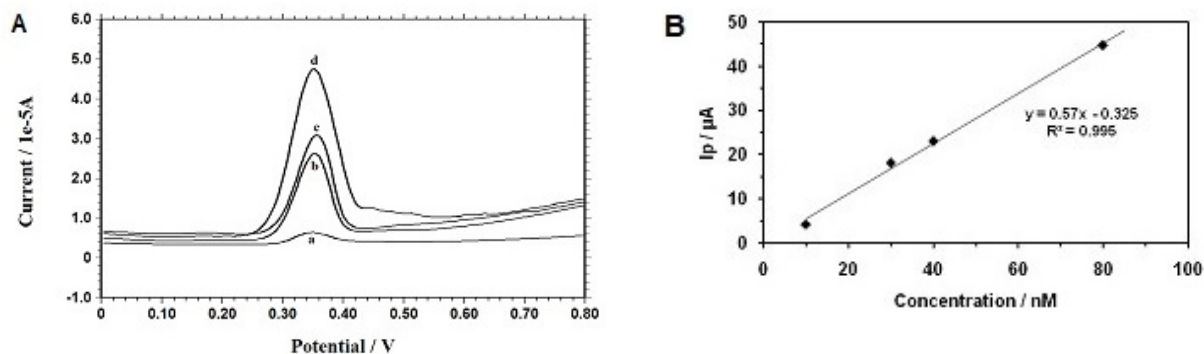
Figure 7. (A) Differential pulse voltammograms for (a) 10 nM ACM, (b) 30, (c) 40, and (d) 80 nM ACM in Calpol syrup at SDS/ CuONPs-MWCNTs modified GCE in PBS; (B) Calibration graph for standard addition method.

Table III. Results computed for ACM assay in syrup samples

	Calpol[a]	Akmol-25[a]	Dolopar[a]	Wellpar[a]
Labeled claim (mg)	100	250	125	125
Amount found (mg)[b]	98.94	249.8	123.8	124.2
Added (nM)	80	80	80	80
Found (nM)	79.02	79.32	78.73	78.82
Recovered (%)[b]	98.77	99.15	98.41	98.53

[a]Name of syrups
[b]Mean of five experiments

CONCLUSIONS

In the present effort, a glassy carbon electrode was fabricated with the suspension of CuO nanoparticles and multi walled carbon nanotubes for electro-oxidation and detection of ACM with the aid of anionic surfactant sodium dodecyl sulphate in PBS. This fabrication introduced a new electrode in the field of electro-analytical chemistry. The fabricated GCE proved the electro-catalytic nature for electro-oxidation of ACM, as indicated in anodic peak current enhancement. This modified electrode showed higher sensitivity, lower detection limit and good recovery values at pH 7.4. The ACM present in various syrup samples were detected using the developed method productively. More efforts are needed to fabricate novel electrodes to detect ACM in real time with good stability.

Conflicts of interest

Authors declare no conflicts of interest.

Acknowledgements

REFERENCES

(1)   van der Marel, C. D.; Anderson, B. J.; van Lingen, R. A. Paracetamol and metabolite pharmacokinetics in infants. *Eur. J. Clin. Pharmacol.* **2003**, *59*, 243-251. https://doi.org/10.1007/s00228-003-0608-0

(2)   Siddiqui, M. R.; Othman, Z. A.; Rahman, N. Analytical techniques in pharmaceutical analysis: A review. *Arab. J. Chem.* **2017**, *10*, S1409-S1421. https://doi.org/10.1016/j.arabjc.2013.04.016

(3)   Sharma, S.; Singh, N.; Ankalgi, A. D. Modern trends in analytical techniques for method development and validation of pharmaceuticals: A Review. *J. Drug Deliv. Ther.* **2021**, *11*, 121-130. https://doi.org/10.22270/jddt.v11i1-s.4515

(4)   Chavan, A.; Gandhimathi, R. Modern analytical tools for the determination of the active pharmaceutical ingredients: a review. *Int. J. Pharm. Sci. Res.* **2022,** *13*, 61-69. http://dx.doi.org/10.13040/IJPSR.0975-8232.13(1).61-69

(5)   Ahmed, S.; Islam, M. S.; Ullah, B. A review article on pharmaceutical analysis of pharmaceutical industry according to pharmacopoeias. *Orient. J. Chem.* **2020**, *36*, 1-10. http://dx.doi.org/10.13005/ojc/360101

(6)   Majidian, M.; Ozcelikay, G.; Cetinkaya, A. Nanomaterial-based electrochemical sensing platform for the determination of Olaparib. *Electrochim. Acta* **2023**, *449*, 142198. https://doi.org/10.1016/j.electacta.2023.142198

(7)   Davani, B. Common methods in pharmaceutical analysis. In: Davani, B. (Ed.), *Pharmaceutical Analysis for Small Molecules*, 1st edition. John Wiley & Sons, Inc. 2017. Chapter 3, p 37.

(8)   Michalkiewicz, S.; Skorupa, A.; Jakubczyk, M. Carbon materials in electroanalysis of preservatives: A Review. *Materials* **2021**, *14*, 7630. https://doi.org/10.3390/ma14247630

(9)   Wang, J. *Analytical Electrochemistry*, 2nd edition. Wiley-VCH, New York, USA. 2000.

(10)   Hegde, R. N.; Vishwanatha, P.; Nandibewoor, S. T. Voltammetric assessment of 8-Oxoguanine at a nano-structured carbon materials based modified glassy carbon electrode. *Braz. J. Anal. Chem.* **2022,** *9*, 84-93. http://dx.doi.org/10.30744/brjac.2179-3425.AR-20-2022

(11)   Qian, L.; Durairaj, S.; Prins, S. Nanomaterial-based electrochemical sensors and biosensors for the detection of pharmaceutical compounds. *Biosens. Bioelectron.* **2021**, *175*, 112836. https://doi.org/10.1016/j.bios.2020.112836

(12)   Pushpanjali, P. A.; Manjunatha, J. G.; Hareesha, N. An overview of recent developments of carbon-based sensors for the analysis of drug molecules. *J. Electrochem. Sci. Eng.* **2021**, *11*, 161-177. https://doi.org/10.5599/jese.999

(13)   Zhang, M.; Ma, M.; Miao, Z. Coal-based activated carbon functionalized with anionic and cationic surfactants for asymmetric capacitive deionization of nitrate. *Colloids Surf., A* **2023,** *663*, 131054. https://doi.org/10.1016/j.colsurfa.2023.131054

(14)   Önal, G. Investigation of the electrochemical properties of vinblastine on boron-doped diamond electrode treated with anodic pre-treatment in anionic surfactant medium. *Diam. Relat. Mater*. **2023**, *133*, 109699. https://doi.org/10.1016/j.diamond.2023.109699

(15)   Nabil, A.; Hendawy, H. A. M.; Abdel-Salam, R. A green voltammetric determination of molnupiravir using a disposable screen-printed reduced graphene oxide electrode: application for pharmaceutical dosage and biological fluid forms. *Chemosensors* **2023,** *11,* 471. https://doi.org/10.3390/chemosensors11090471

(16)   Sawkar, R. R.; Patil, V. B.; Tuwar, S. M. Electrochemical oxidation of Atorvastatin using graphene oxide and surfactant-based sensor. *Mater. Today. Proc.* **2023**, *74*, 267-273. https://doi.org/10.1016/j.matpr.2022.08.192

(17)   Oliveira, L. C.; Rocha, D. S.; Silva-Neto, H. A. Polyester resin and graphite flakes: turning conductive ink to a voltammetric sensor for paracetamol sensing. *Microchim. Acta* **2023**, *190*, 324. https://doi.org/10.1007/s00604-023-05914-9

(18)   Weheabby, S.; Wu, Z.; Al-Hamry, A. Paracetamol detection in environmental and pharmaceutical samples using multi-walled carbon nanotubes decorated with silver nanoparticles. *Microchem. J.* **2023**, *193*, 109192. https://doi.org/10.1016/j.microc.2023.109192

(19)   Gharous, M.; Bounab, L.; Pereira, F. J. Electrochemical kinetics and detection of paracetamol by stevensite-modified carbon paste electrode in biological fluids and pharmaceutical formulations. *Int. J. Mol. Sci.* **2023**, *24*, 11269. https://doi.org/10.3390/ijms241411269

(20)   Stoytcheva, M.; Zlatev, R.; Velkova, Z. The validity of using bare graphite electrode for the voltammetric determination of paracetamol and caffeine. *Int. J. Electrochem. Sci.* **2023**, *18*, 100120. https://doi.org/10.1016/j.ijoes.2023.100120

(21)   İslamoğlu, N.; Mülazımoğlu, I. E.; Mülazımoğlu, A. D. Sensitive and selective determination of paracetamol in antipyretic children's syrup with a polyglycine modified glassy carbon electrode. *Anal. Methods* **2023**, *15*, 4149-4158. https://doi.org/10.1039/D3AY00789H

(22)   Cortés, K.; Triviño, J. J.; Arancibia, V. Simultaneous voltammetric determination of acetylsalicylic acid, caffeine and paracetamol in pharmaceutical formulations using screen-printed carbon electrode. *Electroanalysis* **2023**, *35*, e202200484. https://doi.org/10.1002/elan.202200484

(23)   Islamoglu, N.; Mulazımoglu, A. D. Use of guanine-modified glassy carbon electrode as an electrochemical sensor for the determination of paracetamol. *Bangladesh J. Pharmacol.* **2023**, *18*, 97-104. https://doi.org/10.3329/bjp.v18i3.66459

(24) Prasad, G. V.; Vinothkumar, V.; Jang, S. J. Multi-walled carbon nanotube/graphene oxide/ poly(threonine) composite electrode for boosting electrochemical detection of paracetamol in biological samples. *Microchem. J.* **2023**, *184*, 108205. https://doi.org/10.1016/j.microc.2022.108205

(25) Silva, R. M.; Sperandio, G. H.; da Silva, A. D. Electrochemically reduced graphene oxide films from Zn-C battery waste for the electrochemical determination of paracetamol and hydroquinone. *Microchim. Acta* **2023**, *190*, 273. https://doi.org/10.1007/s00604-023-05858-0

(26) Anitta, S.; Sekar, C. Voltammetric determination of paracetamol and ciprofloxacin in the presence of vitamin C using cuttlefish bone-derived hydroxyapatite sub-microparticles as electrode material. *Results Chem.* **2023**, *5*, 100816. https://doi.org/10.1016/j.rechem.2023.100816

(27) Masihpour, N.; Hassaninejad-Darzi, S. K.; Sarvary, A. Nickel-Cobalt Salen organometallic complexes encapsulated in mesoporous NaA nanozeolite for electrocatalytic quantification of ascorbic acid and paracetamol. *J. Inorg. Organomet. Polym.* **2023**, *33*, 2661-2680. https://doi.org/10.1007/s10904-023-02708-7

(28) Urçuk, A.; Yıldız, C.; Bayraktepe, D. E. Electrochemical sensor for simultaneous determination of paracetamol, propyphenazone, and caffeine – Electrodes based on poly(L-cystine)/gold nanoparticles plating on pencil graphite. *Microchem. J.* **2023**, *193*, 109079. https://doi.org/10.1016/j.microc.2023.109079

(29) Porada, R.; Wenninger, N.; Bernhart, C. Targeted modification of the carbon paste electrode by natural zeolite and graphene oxide for the enhanced analysis of paracetamol. *Microchem. J.* **2023**, *187*, 108455. https://doi.org/10.1016/j.microc.2023.108455

(30) Berni, A.; Lahcen, A. A.; Amine, A. Electrochemical sensing of paracetamol using 3D porous laser scribed graphene platform. *Electroanalysis* **2023**, *35*, e202200137. https://doi.org/10.1002/elan.202200137

(31) Liu, X. L.; Guo, J. W.; Wang, Y. W. A flexible electrochemical sensor for paracetamol based on porous honeycomb-like NiCo-MOF nanosheets. *Rare. Met.* **2023**, *42*, 3311-3317. https://doi.org/10.1007/s12598-023-02349-2

(32) Darezereshki, E.; Bakhtiari, F. A novel technique to synthesis of tenorite (CuO) nanoparticles from low concentration $CuSO_4$ solution. *J. Metall. Sect. B Metall.* **2011,** *47*, 73-78. http://dx.doi.org/10.2298/JMMB1101073D

(33) Fekry, A. M.; Shehata, M.; Azab, S. M. Voltammetric detection of caffeine in pharmacological and beverages samples based on simple nano- Co (II, III) oxide modified carbon paste electrode in aqueous and micellar media. *Sens. Actuators B Chem.* **2023**, *302*, 127172. https://doi.org/10.1016/j.snb.2019.127172

(34) Boltia, S. A.; Kandeel, N. H.; Hegazy, M. A. Analytical eco-scale determination of vortioxetine using advanced electrochemical platform for screen-printed disposable multiwalled carbon nanotube electrode in the presence of an anionic surfactant. *New J. Chem.* **2023**, *47*, 11015-11029. https://doi.org/10.1039/D3NJ00993A

(35) Food and Drug Administration (FDA) *Bioanalytical method validation: guidance for industry*, 2018. https://www.fda.gov/files/drugs/published/Bioanalytical-Method-Validation-Guidance-for-Industry.pdf (accessed Jan. 2024).

BrJAC

ARTICLE

Optimizing Distillation Techniques for Isotopic Determinations in Beverages

Susiane Leonardelli[1,2]* ⍟ ✉, **Júlia Panozzo**[1,2] ⍟, **Júlia Daneluz**[1] ⍟, **Letícia Leonardelli**[1] ⍟,
Gilberto João Cargnel[1] ⍟, **Regina Vanderlinde**[1] ⍟

[1]*Universidade de Caxias do Sul, Instituto de Biotecnologia. Rua Francisco Getúlio Vargas, 1130, 95070-560
Caxias do Sul, RS, Brazil*

[2]*Laboratório de Referência Enológica Evanir da Silva (LAREN/SEAPI). Avenida da Vindima, 1855, 95084-470,
Caxias do Sul, RS, Brazil*
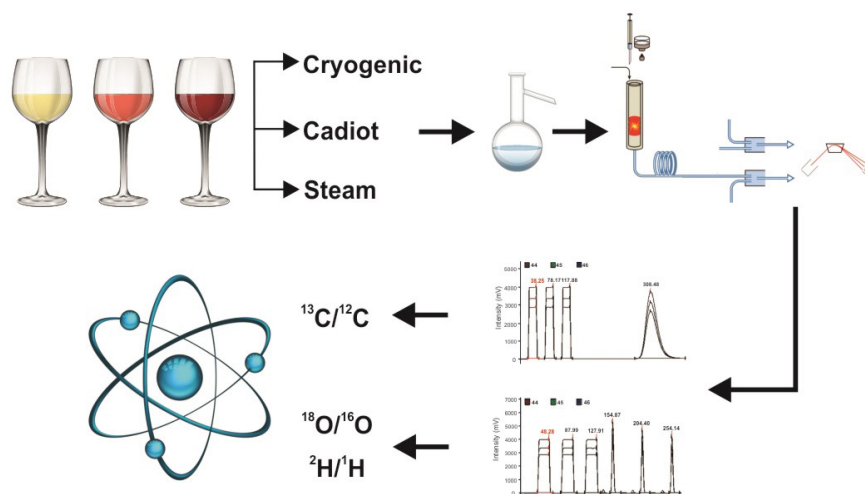
Isotopic analysis offers insights into the authenticity, tracing origin, and detecting adulteration in beverages, with applications in various legal contexts. This research addresses challenges in the distillation process to identify the optimal method for preparing samples for isotopic determinations. This study aimed to compare three distillation systems: cryogenic, Cadiot column and steam for carbon, hydrogen and oxygen determinations in ethanol. Furthermore, to explore the benefits of cryogenic method in beverage distillation and to perform the method validation. Additionally, to evaluate the efficiency of the steam distillation for carbon isotopic determination. The ethanol obtained through cryogenic distillation exhibited $\delta^{13}C$ ranging from -29.54 to -24.60‰, slightly lower than those observed in the Cadiot column (-29.12 to -24.64‰). However, trueness analysis revealed comparable results for both methods, supported by satisfactory Z-score and relative error. The outcomes for hydrogen and oxygen exhibited considerable disparities with significant differences. The results of $\delta^{13}C$ found by steam distillation and cryogenic were similar and the mean difference found between the systems was 0.05‰ and the relative error was 0.20%. The study further explored the advantages of cryogenic distillation in ethanol extraction, demonstrating its efficiency for carbon determinations with notable benefits in terms of time and volume required for extraction. Steam distillation proved feasible for carbon determinations, showing similar results to cryogenic distillation. These findings not only present options for laboratories but also highlight the efficiency of cryogenic distillation in ethanol extraction, offering practical applications for isotopic analysis.

Keywords: beverages, stable isotope, cryogenic distillation, Cadiot column, steam distillation

INTRODUCTION

The capability to discern the origin of chemical substances has established isotopes as an indispensable tool in several disciplines, particularly in forensic science.[1] Regulation and food information to the consumers in the labels are an obligation. The label must include compulsory information following the legislation and can be added optional information. Nonetheless, sometimes the label is correct but the product is adulterated, in this case we have to look for techniques and compounds to control tampering. The major compounds of the alcoholic beverages to control adulteration are ethanol and water.[2]

The origin of alcoholic beverages can be traced back to antiquity, and they have been part of the human culture for many centuries. Over the years, the elaboration oh these beverages have grown significantly with different types of products and development of scientific fundamentals process and legislation.[3] These beverages have parameters that must be performed according to specific legislation, but adulteration is frequent.[4,5]

Considering to work with the ethanol molecules with the purpose to determine stable isotopes to control adulteration, the first step of the preparation is the sample purification, which in beverages are done by distillation. This technique is a robust yet challenging separation with some critical points that comes with drawbacks, such as the interference in the volatile compounds, as well as considerations related to high cost and time constraints.[6,7]

The challenge in the distillation process using high temperatures arise from the formation of an azeotrope, in which is a mix of ethanol and water. The main factor is due to ethanol has a boiling point of 78 °C, while the azeotrope begins to form at 0.2 °C above, for this type of distillation using temperature the critical point is to control the collection of the distillate to avoid contamination. In addition, certain methods for isotopic determination require careful to avoid isotopic fractionation in the distillation process.[8]

In the industry there are various systems available for the recovery and extraction of ethanol from liquid solutions. Techniques using membrane permeation, vacuum stripping, gas stripping, solvent extraction, adsorption, steam distillation and several hybrid methods.[9] The method using Cadiot column is the one internationally recommended for this purpose. However, the official method from International Organisation of Vine and Wine specifies that all the technique available can be used since it meets the specifications and avoids isotopic fractionation.[10]

Considering the established distillation systems, the cryogenic method has been employed for more than six decades, mainly to recover and refine ethylene and propylene from olefin plants.[11] It is a process of separation of mixture, using simple distillation, at high pressure and low temperature. It is used, for example, in the separation of carbon dioxide, where the gas is cooled up to the desublimation temperature and subsequent to the isolation of solid carbon dioxide.[11] This cryogenic method with vacuum is also regarded to a standard method for water extraction in plant tissues for isotope determinations.[12]

The official method recommended for isotopic determinations in beverages in the international compendium takes at least five hours for the extraction[13] and needs substantial expense, so to study and compare other extraction methods is important to improve the sample preparation for the isotopic determinations. Thus, the objective of this research was to evaluate the use of cryogenic, Cadiot column and steam distillation systems for isotopic determinations to provide laboratories with more options. It was also aimed to explore the advantages of cryogenic distillation and validate the parameters. And finally, to compare the efficiency of the steam and cryogenic distillation for carbon isotopic determination.

MATERIAL AND METHODS
Samples

A comprehensive study was conducted on a set of 22 samples harvested in the mountain region of Brazil in 2019, resulting in 76 isotopes determinations aimed at comparing the three distillation systems. The effectiveness of cryogenic distillation for stable carbon isotope ^{13}C was specifically scrutinized in relation to the Cadiot column method, consisting for evaluation seventeen samples: five white and six red wines; four distillates from apple, orange, persimmon and watermelon; as well as one distillate of rice and one of sweet potato.

For the evaluation of hydrogen ^{2}H and oxygen ^{18}O, two white and three red wines were prepared with ethanol extraction conducted through both cryogenic and Cadiot methods. Furthermore, a comparative study involving steam and cryogenic distillation encompassed the preparation and determination of 10 wine samples analysed in triplicate.

Sample preparation
Cryogenic distillation system (CDS)

The CDS setup employed in this research comprised a sealed system regulated by a mechanical device and containing collectors in the end of the extraction line. Figure 1 illustrated the method, which the equipment consists of a diffuser pump, a mechanical pump, a glass tube of 1 m, two liquid nitrogen traps (number 5 and 6) and an extraction line demonstrated for A (Vidropin, São Paulo, Brazil).
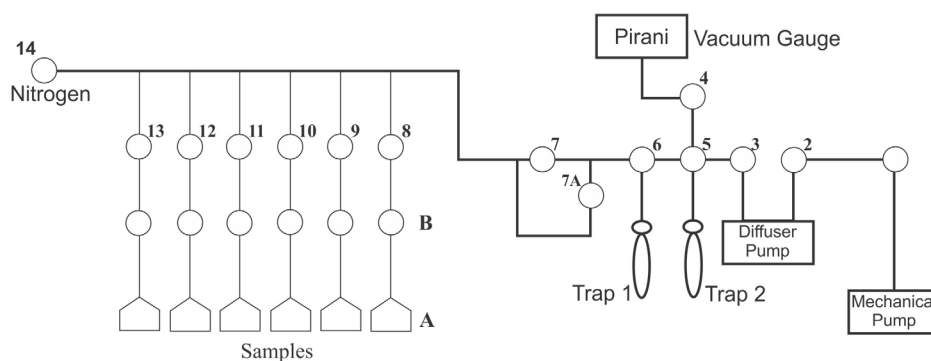
Figure 1. Cryogenic system (CDS) for ethanol distillation.

A volume of 0.0015 L of the sample was placed into a 0.035 L flask, connected to manifold in the end of the extraction line (8 to 13). The liquid was trapped in a vial of 9 mL and immediately cooled, in temperature at -196 ºC and pressure at one Pa. The complete procedure spanned one hour, remaining the distillation for 20 minutes. The ethanol in the samples was vaporizes and gathered in a liquid nitrogen cold trap on side B. After the extraction were completed, the collected analyte was thawed for subsequent analysis.[13,14]

Cadiot column system (CCS)

The distillation process using a Cadiot column (Eurofins Analytics France, Nantes, France) was conducted at the Uruguay National Wine Institute (INAVI) in accordance with the community methods for the analysis of wines in the European Union.[14] Around 0.3 L of the sample were introduced inside a volumetric flask (0.5 L) and heated within the extraction system. The liquid after distillation was trapped in a pre-calibrated erlenmeyer flask (0.12 L), the temperature in the distillation ranging from 78 to 78.2 ºC and lasted approximately 5 h. The round-bottom flask is placed in the heating mantle connected to the extractor and water for the condenser is provided.

Steam distillation system (SDS)

Steam distillation is a method to determine the volume of the alcohol in wine by densimetry using hydrostatic balance. The distillation procedure followed in accordance to the International Compendium of Wine and Musts Analysis.[10] It was measured out 0.1 L of wine sample with a graduated flask between 15 and 25 ºC. The flask was rinsed three times with distilled water and transferred to the distillation tube. Then, 8 mL of the suspension of calcium hydroxide 2 M and antifoam agent were added to the tube and it started the distillation. The distillate was collected in another flask.

Determination of $^{13}C/^{12}C$

The determination of the carbon isotope ratio ($^{13}C/^{12}C$) of ethanol followed the international methodology OIV-MA-AS312-06.[10] The ethanol extracted from sample by distillation was carried out by on-line analysis using an elemental analyser (Flash EA 1112, Thermo Scientific, Bremen, Germany) with an autosampler (AS 1310), coupled to a Delta Plus XL through a Conflo III (Thermo Scientific, Bremen, Germany). The sample of ethanol was injected into a combustion reactor at 900 ºC, all the carbon of the sample was oxidized, passed through a chromatographic column at 45 °C to separated CO_2 from other gas generated and then goes to an isotopic ratio mass spectrometer by a helium flow at 100 mL min^{-1}.

Sample volume was set up by the mass to charge ratio (*m/z*) signal 44 at 3 Volts. Analysing the intensity, it was found that sample volume of 1 µL was employed for ethanol extracted using CDS, while a volume of 0.2 µL was used with the CCS. The analytical error remained below 0.05‰ and the samples were analysed in triplicate. The results were calibrated on the V-PDB scale (Vienna Pee Dee Belemnite) in per mil (‰) against the international reference material Sucrose (NIST 8542, $\delta^{13}C$ value of -10.45‰) and the values were expressed in $\delta^{13}C$.

Performance of the extraction method for carbon using CDS

Linearity was assessed through the repeated analysis of various enrichment levels. Experiments involve the addition of ethanol from sugar cane to a wine sample at concentrations 0, 1, 10, 30, 50, 70, 90, 99 and 100%. The ethanol was extracted from each enriched sample using the CDS, and the analysis were performed in seven replicates.

The accuracy was performed through recovery tests conducted at high, medium, and low analyte concentrations, following the evaluating criteria outlined in the Codex Alimentarius.[15] The precision was gauged through both repeatability and reproducibility assessments in accordance with the Laboratory Guide to Method Validation and Related Topics.[16] The robustness was evaluated doing small intentionally changes in the method, it was considered change in volume and time, the data were statistically evaluated.

Determination of $^2H/^1H$ and $^{18}O/^{16}O$

Oxygen ($^{18}O/^{16}O$) and hydrogen ($^2H/^1H$) determinations were carried out using a high temperature conversion elemental analyser connected to an isotopic ratio mass spectrometer (Delta V Advantage) through a Conflo IV (Thermo Scientific, Bremen, Germany). The pyrolysis process took place in a ceramic tube with glassy carbon at 1450 ºC, under a continuous flow of helium at 1.5 bar to generated H_2. Prior to entering into the mass spectrometer, a 1.4 m molecular sieve chromatographic column at 80 ºC was employed to separate H_2 from CO. Sample injection was facilitated by an autosampler (AS 3000).

The isotopic composition is expressed in delta notation, expressed as δ^2H and $\delta^{18}O$, with reference to a primary standard VSMOW (Vienna Standard Mean Ocean Water) with value of 0‰. The analytical error for hydrogen and oxygen remained below to 2‰ and 0.4‰, respectively.

Statistical analysis

All statistical tests were performed using SPSS software, version 26.0 (Chicago, Illinois, USA). To assess the normality of the data the Kolmogorov Smirnov was employed. Data were analysed by ANOVA at 5% significance level.

RESULTS AND DISCUSSION
CDS and CCS distillation for carbon $\delta^{13}C$

The ethanol obtained through distillation using CCS and CDS did not show a statistically significant difference. The $\delta^{13}C$ values can be observed in Figure 2.
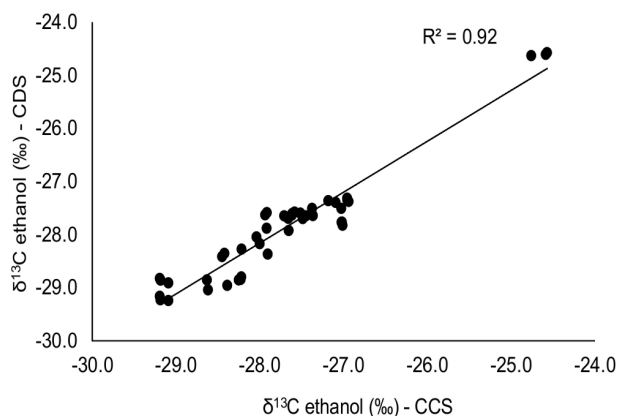
Figure 2. The relationship between $\delta^{13}C$ values of ethanol extracted by CCS (x-axis – Cadiot Column System) and CDS (y-axis – Cryogenic Destilation System) in different beverages.

The $\delta^{13}C$ exhibited a slight variation between the distillations employed to obtain the ethanol. The mean difference identified was 0.14‰, a variance smaller than the findings reported by Rossmann et al.[17] In their study, the authors employed equal method for extraction in two laboratories and they concluded that the variations in $\delta^{13}C$ were attributed to the nature of the material investigated and not exceed the calibration impact.

CDS extraction in general yielded $\delta^{13}C$ values lower than those obtained with CCS. Discrepancies between the systems were also noted in previous studies.[18] In those studies, the researchers noticed a gradual increase in the carbon with 1.2‰ of effect and concluded that there is an influence of the plates, reflux and equilibrium liquid-vapor fractionation.[21] In our investigation, the greatest effect identified was 0.81‰, significantly lower than 1.2‰ as reported in the preview study.

Results reported by Baudler et al.[19] similarly exhibited more negatives values when employing the CCS. Their study involved comparing two extraction systems concerning the starting material, revealing that the distillation process occurs with an inverse vapor pressure isotopic effect, leading to a decrease in $\delta^{13}C$ values.

The mean difference among values is deemed acceptable and falls below the reproducibility limit (R) outlined in the official method for carbon isotopic determination by the OIV. Where for alcohol, the official method sets a reproducibility limit of 0.87‰, while for white wines, it is 0.76‰ and for red wines, it is 0.64‰.[5]

The evaluation of the accuracy of the CDS equipment was conducted and quantitatively calculated. This value concerning $\delta^{13}C$ related to CCS, yielding a mean difference between the systems of 0.57‰ and Z-score of 0.83‰. The outcomes were deemed acceptable, given that the absolute of Z is below 2. This indicated that the $\delta^{13}C$ obtained from the sample distillate through CDS methods are equivalent to those obtained by CCS.

The main benefits of the CDS equipment are concern to the short period to complete the distillation and the sample volume used. Distillation by CCS with 8 columns took approximately 5 h, whereas distillation by the CDS with 6 traps required only one hour. The CDS demonstrated superior speed compared to the CCS, streamlining ethanol extraction for subsequent analysis.

Furthermore, the volume needed for the ethanol extraction in CDS equipment is just 0.0015 L, significantly less than CCS, which varies based on the ethanol percentage in the beverages. Beverages with alcohol exceeding 10%, 0.3 L was required, while samples with alcohol content below 10% needed 0.4 L. Assessing the volume requirements between the distillation methods, CCS necessitates 200 times more sample volume than CDS. Consideration of volume is crucial, especially when dealing with limited availability or expensive and rare samples.

Performance of the CDS for carbon determination δ¹³C

Giving the applicability of CDS to prepare samples for carbon determinations, the method showed satisfactory parameters for the purpose. The dataset showed a great linear range, characterized by a high determination coefficient (R^2) of 0.99. The working range, being linear and directly proportional to the concentrations, proves well suited for the intended purpose. Moreover, the method demonstrated accurate results for carbon isotope parameters, meeting the standards set by Codex Alimentarius, with a recovery rate of 99%, within the set range of 98% to 102%.[15]

Precision as indicated by repeatability and reproducibility showed values of 0.21‰ and 0.30‰, respectively. Yielded results closely aligned with previous studies on wine and fruit juices that employed similar methods.[12,20]

Another crucial aspect to consider is the robustness, which entails intentionally modifying some parameters and examining the impact on the results. The robustness is shown in Table I.

Table I. Robustness considering variations in volume and time

Parameter	Condition	δ¹³C (‰) Mean ± SD
Volume (mL)	1.0	-29.27ᵃ ± 0.08
	1.5	-29.27ᵃ ± 0.05
	2.0	-29.30ᵃ ± 0.04
Time (min)	10	-29.31ᵃ ± 0.06
	15	-29.27ᵃᵇ ± 0.08
	20	-29.25ᵃᵇ ± 0.06
	25	-29.29ᵃᵇ ± 0.05
	30	-29.24ᵇ ± 0.11

Means followed by different letters in the column differ significantly by ANOVA followed by Tukey test at 5% of significance.

The robustness of the CDS was affirmed as the analysed parameters exhibited no statistically meaningful distinctions concerning δ¹³C values. Unique contrast was found for 10 and 30 minutes. Therefore, it is fundamental to adhere and regulate the recommended extraction time of 20 minutes.

CDS and CCS for hydrogen δ²H and oxygen δ¹⁸O

There is also a continuous interest in hydrogen and oxygen characterization for beverages, with a major focus on wines. Influences of the distillation on the δ²H values can be observed in Figure 3.
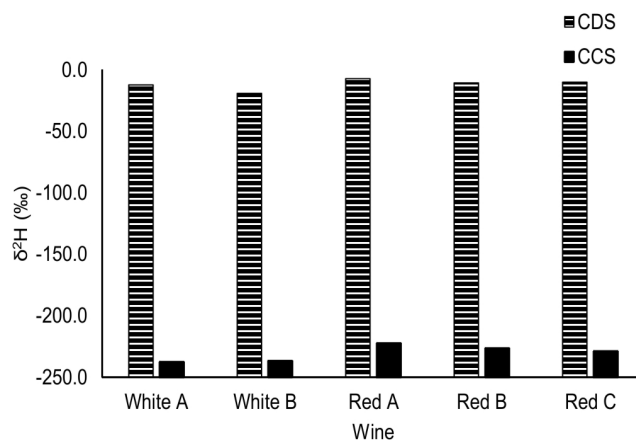
Figure 3. δ^2H values of ethanol distillate by CDS and CCS in wine.

A substantial difference was observed for δ^2H, with distillation using CCS resulting in a notable decrease in δ^2H. Conversely, for $\delta^{18}O$, there was an increase in the values obtained through the CCS, as shown in Figure 4.
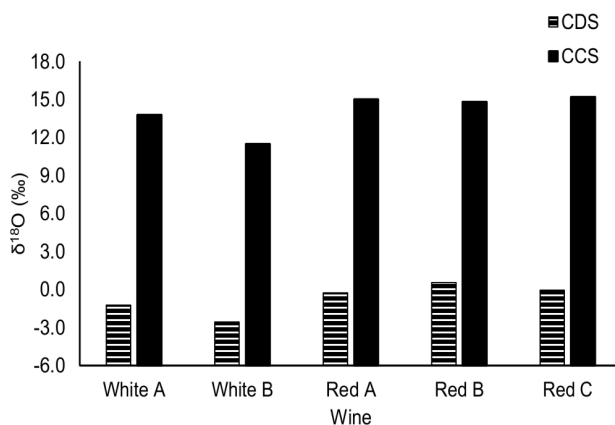
Figure 4. $\delta^{18}O$ values of ethanol distillate by CDS and CCS in wine.

These effects can be attributed to the mixing of water and ethanol, as the CDS does not completely isolate all of the water in the beverage, and water remains in the extracted ethanol after distillation. The values obtained through the CDS closely resembled values found in the atmospheric water reported in previous studies,[21] varying between -146.0 to -11.5‰ for δ^2H and -19.9 to - 2.25‰ for $\delta^{18}O$, as well as values in Germany varying between -170‰ and +18‰ for δ^2H and -24‰ to +2‰ for $\delta^{18}O$.[22] These authors explained that water values are variable due to latitude, altitude and are strongly influenced by seasonal temperatures.

Considering the results above, CDS proved to be ineffective for δ^2H and $\delta^{18}O$ due to water influence on the ethanol extracted. In order to address this limitation, it is crucial to reevaluate the equipment, incorporating steps to capture the water and reduce its impact in this specific application.

CDS and SDS for carbon $\delta^{13}C$

Steam distillation (SDS) is a widely employed method for gauging the alcoholic strength in wine. This technique involves the determination of percentage of ethanol through densimetry using a hydrostatic balance. It is a prevalent system in laboratories for determining alcohol percentage in beverages, forming

a routine aspect of laboratory procedures. Employing this distillate for additional analysis, such as isotopic determinations, offers a practical means of streamlining laboratory process.

The carbon isotopic composition ($\delta^{13}C$) of ethanol extracted from wines through both CDS and SDS is presented in Table II.

Table II. $\delta^{13}C$ values of ethanol extracted by CDS and SDS

CDS (‰)	SDS (‰)	Relative error (%)
-22.88 ± 0.09	-22.87 ± 0.05	-0.04
-22.48 ± 0.18	-22.64 ± 0.09	0.69
-22.25 ± 0.08	-22.13 ± 0.04	-0.51
-21.85 ±0.12	-22.00 ± 0.12	0.67
-22.61 ± 0.11	-23.66 ± 0.15	4.44
-22.27 ± 0.11	-22.74 ± 0.13	2.09
-22.76 ± 0.14	-22.37 ± 0.03	-1.73
-23.11 ± 0.12	-22.72 ± 0.13	-1.72
-23.46 ± 0.17	-23.20 ± 0.13	-1.11
-24.27 ± 0.08	-23.08 ± 0.16	-0.82

ANOVA, significance level of 5%.

The $\delta^{13}C$ values of the ethanol samples exhibited no significance differences between the two systems under consideration. The mean difference observed between the systems was 0.05‰, with a mean relative error of 0.20‰, both falling within the previously established range deemed as low and satisfactory for carbon determination in this study. As a result, the SDS exhibited $\delta^{13}C$ values similar to those of the CDS, demonstrating its effectiveness in distilling wines for carbon isotope determinations.

This research has effectively met its objective by comparing the distillation systems for isotopic determination. It has not only fulfilled its goal but also presented choices for laboratories to consider in the ethanol extraction for isotopic determination.

CONCLUSION

In conclusion, this study successfully achieved its objective comparing cryogenic, Cadiot column, and steam distillation systems for isotopic determinations. The research not only provided additional options for laboratories but also explored the benefits of cryogenic distillation in ethanol extraction revealing that cryogenic is efficient for carbon isotopic determination, yielding comparable results to the official method. Furthermore, cryogenic demonstrated a significant advantage in terms of time and volume required. On the other hand, cryogenic proves unsuitable for hydrogen and oxygen analyses due to substantial water interference in the extracted ethanol.

The steam distillation system produced carbon isotope values comparable to those obtained through the cryogenic method. These results underscore feasibility of using steam distillation for $\delta^{13}C$ in beverages. These findings provide valuable insights to the field of isotopic determinations.

Conflicts of interest

The authors declare that there are no conflicts of interest.

REFERENCES

(1) Matos, M. P. V; Jackson, G. P. Isotope Ratio Mass Spectrometry in Forensic Science Applications. *Forensic Chem*. **2019**, *13*, 100154, 1-75. https://doi.org/10.1016/j.forc.2019.100154

(2) Coldea, T. E.; Mudura, E.; Socaciu, C. Advances in Distilled Beverages Authenticity and Quality Testing. In: Stauffer, M. (Ed.) *Ideas and Applications Toward Sample Preparation for Food and Beverage Analysis*. InechOpen, 2017, Chapter 6, p 182. https://doi.org/10.5772/intechopen.72041

(3) Núñez-Caraballo, A.; García-García, J. D.; Ilyina, A.; Flores-Gallegos, A. C.; Michelena-Álvarez, L. G.; Rodrígues-Cutiño, G.; Martínez-Hernández, J. L.; Aguilar, C. N. Alcoholic Beverages: Current Situation and Generalities of Anthropological Interest. In: Grumezescu, A. M.; Holban, A. M. (Eds). *Processing and Sustainability of Beverages*. Woodhead Publishing, 2019. Vol. 2: The Science of Beverages, pp 37-72. https://doi.org/10.1016/B978-0-12-815259-1.00002-1

(4) Neto, A. G. C.; Costa, M. M. A.; Schuler, M. S. V.; Azevedo, E. P. P. Study of The Main Types of Beverages Adulteration Seized in Recife City. *Braz. J. Forensic Sci*. **2016**, *5* (2), 133-145. https://doi.org/10.17063/bjfs5(2)y2016133

(5) International Standard for the Labelling of Wines. OIV publications, 2022, Paris, France. Available at: https://www.oiv.int/public/medias/8175/en-oiv-wine-labelling-standard-2022.pdf (accessed Dec. 2023).

(6) Hattoi, R.; Yamada, K.; Hasegawa, K.; Ishikawa, Y.; Ito, Y.; Sakamoto, Y.; Yoshida, N. An improved method for the measurement of the isotope ratio of ethanol in various samples, including alcoholic and non-alcoholic beverages. *Rapid Commun. Mass Spectrom.* **2008,** *22* (21), 3410-3414. https://doi.org/10.1002/rcm.3753

(7) Onuki, S.; Koziel, J. A.; Leeuwen, J. V.; Jenks, W. S.; Grewell, D. A.; Lingshuang, C. Ethanol production, purification, and analysis techniques: a review. *Annual International Meeting - American Society of Agricultural and Biological Engineers* **2008**. https://doi.org/10.13031/2013.25186

(8) Kumar, S.; Singh, N.; Prasad, R. Anhydrous ethanol: a renewable source of energy. *Renew. Sust. Energ. Rev*. **2010**, *14* (7), 1830-1844. https://doi.org/10.1016/j.rser.2010.03.015

(9) Offeman, R. D.; Stephenson, S. K.; Franqui, D.; Cline, J. L.; Robertson, G. H.; Orts, W. J. Extraction of ethanol with higher alcohol solvents and their toxicity to yeast. *Sep. Purif. Technol*. **2008**, *63* (2), 444-451. https://doi.org/10.1016/j.seppur.2008.06.005

(10) Compendium of international methods of wine and must analysis. OIV publications, 2022, Paris, France. Available at: https://www.oiv.int (accessed Dec. 2023).

(11) Llewellyn, P. L.; Rodrigues-Reinoso, F.; Rouqerol, J.; Seaton, N. (Eds). *Characterization of Porous Solids VII: Proceedings of the 7th International Symposium on the Characterization of Porous Solids* (COPS-VII), Aix-en-Provence, France. Elsevier, 2006, Vol. 160, 1-734.

(12) Muhammad, A. H.; Nadeem, F.; Tariq, R.; Rashid, A. *Renewable and Alternative Energy Resources. Renew and Alternative Energy Resources*. Academic Press, 2022. https://doi.org/10.1016/C2018-0-03161-8

(13) Camin, F.; Simoni, M.; Hermann, A.; Thomas, F.; Perini, M. Validation of the 2H-SNIF NMR and IRMS Methods for Vinegar and Vinegar Analysis: An International Collaborative Study. *Molecules* **2020**, *25* (2932), 1-11. https://doi.org/10.3390/molecules25122932

(14) Commission Regulation (EEC) No 2676/90 of 17 September 1990. Official Journal L 272, **1990**, pp 1-192. Available at: https://www.fao.org/faolex/results/details/en/c/LEX-FAOC036018/ (accessed Dec. 2023).

(15) FAO/WHO. Codex Alimentarius Commission Procedural Manual. Food and Agriculture Organization of the United Natios and World Health Organization. **2018** (26th ed.), Rome, Italy. Available at: www.codexalimentarius.org. (acessed Dec. 2023).

(16) Magnusson, B.; Örnemark, U. *Eurachem Guide: The Fitness for Purpose of Analytical Methods – A Laboratory Guide to Method Validation and Related Topics*. **2014**, 2nd ed. ISBN 978-91-87461-59-0. Available at: https://www.eurachem.org/images/stories/Guides/pdf/MV_guide_2nd_ed_EN.pdf (acessed Dec. 2023).

(17) Rossmann, A.; Schmidt, H. L.; Reniero, F.; Versini, G.; Moussa, I.; Merle, M. H. Z. Stable carbon isotope content in ethanol of EC data bank wines from Italy, France and German. *Z. Lebensm. Unters. Forsch*. **1996**, *203*, 293-301. https://doi.org/10.1007/BF01192881

(18) Moussa, I.; Naulet, N.; Martin, M. L.; Martin, G. J. A Site-Specific and Multieiement Approach to the Determination of Liquid-Vapor Isotope Fractionation Parameters. The Case of Alcohols. *J. Phys. Chem*. **1990,** *94*, 8303-8309. https://doi.org/10.1021/j100384a056

(19) Baudler, R.; Adam, L.; Rossmann, A.; Versini, G.; Engel, K.-H. Influence of the distillation step on the ratio stable isotopes of ethanol in cherry brandies. *J. Agric. Food Chem.* **2006,** *54* (3), 864-869. https://doi.org/10.1021/jf052043a

(20) Thomas, F.; Jamin, E. ^{2}H NMR and ^{13}C-IRMS analyses of acetic acid from vinegar, ^{18}O-IRMS analysis of water in vinegar: International collaborative study report. *Anal. Chim. Acta* **2009**, *649* (1), 98-105. https://doi.org/10.1016/j.aca.2009.07.014

(21) Boschetti, T.; Cifuentes, J.; Iacumin, P.; Selmo, E. Local meteoric water line of Northern Chile (18° S-30° S): An application of error-in-variables regression to the oxygen and hydrogen stable isotope ratio of precipitation. *Water* **2019**, *11* (4), 791. https://doi.org/10.3390/w11040791

(22) Stumpp, C.; Klaus, J.; Stichler, W. Analysis of long-term stable isotopic composition in German precipitation. *J. Hydrol*. **2014,** *517*, 351-361. https://doi.org/10.1016/j.jhydrol.2014.05.034

BrJAC

ARTICLE

Evidence of Increase in the Oxidative Stress in C57BL Mice Subjected to Daily Diacetyl Treatment: Oxidative Stress in Mice Subjected to Diacetyl Treatment

Letícia Dias Lima Jedlicka[1] [iD], **Danilo Santos Souza[2]** [iD], **Danielle Zildeana Sousa Furtado[3,4]** [iD], **Lucas Ximenes Araújo[5,6]** [iD], **Emanuel Carrilho[5,6]** [iD], **Nilson Antonio Assunção[7]*** [iD] [✉]

[1]Instituto de Estudos em Saúde e Biológicas, Universidade Federal do Sul e Sudeste do Pará, UNIFESSPA, Campus III, Marabá, PA, Brazil

[2]Departamento de Agroindustria do Sertão, Universidade Federal de Sergipe, Rodovia Engenheiro Jorge Neto, km 3, Silos, 49680-000, Nossa Senhora da Glória, SE, Brazil

[3]Escola Paulista de Medicina, Universidade Federal de São Paulo, UNIFESP, Rua Botucatu, 740, Vila Clementino, 04023-062, São Paulo, SP, Brazil

[4]Faculdade de Tecnologia de Teresina, Rua Rio Grande do Norte, 790, Pirajá, Teresina, 64003-420, PI, Brazil

[5]Instituto de Química de São Carlos, Universidade de São Paulo, Avenida Trabalhador Sancarlense, Parque Arnold Schimidt, 13566-590, São Carlos, SP, Brazil

[6]Instituto Nacional de Ciência e Tecnologia em Bioanálise, INCTBio, Campinas, SP, Brazil

[7]Departamento de Química, Instituto de Ciências Ambientais, Químicas e Farmacêuticas, Universidade Federal de São Paulo, Rua Prof. Artur Riedel, 275, Jd. Eldorado, 09972-270, Diadema, SP, Brazil
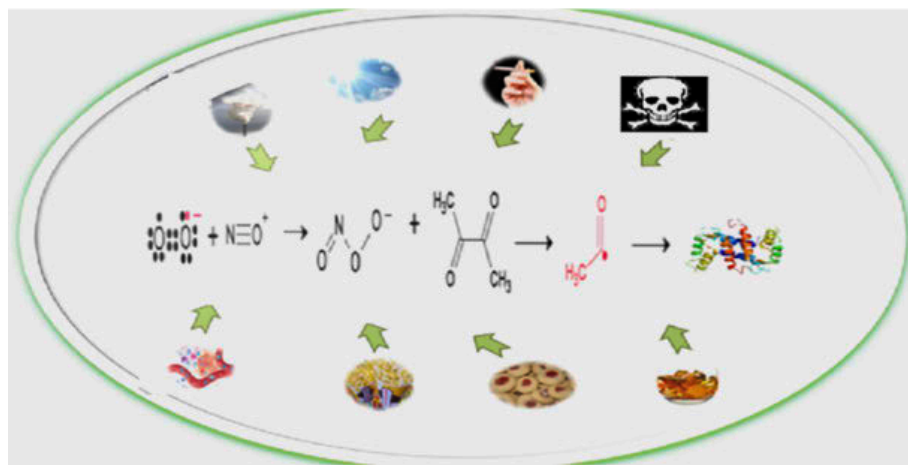
The food industry commonly utilizes diacetyl as a flavoring agent. However, concerns have recently emerged regarding its potential to cause adverse health effects, especially in individuals with frequent exposure. In this study, our objective was to assess the impacts of diacetyl on male mice by exposing them to diacetyl through drinking water for 15 days, thereby simulating the consumption of diacetyl-containing products. Our study focused on crucial parameters associated with dicarbonyl stress, specifically evaluating methylglyoxal, glutathione synthetase, and glutathione levels in liver tissue using LC-MS. We also analyzed changes in concentrations of plasmatic proteins. Our findings indicated a decrease in

methylglyoxal levels despite increased carbonyl compounds and the glutathione / glutathione synthetase ratio, implying significant alterations in the proteomic profile due to diacetyl consumption. Subsequent analysis identified nineteen differentially expressed proteins, with fifteen suppressed proteins in both groups exposed to diacetyl. Gene ontology analysis revealed that these proteins play roles in various biological responses and metabolic processes, underscoring the potential health risks associated with daily diacetyl consumption. This study emphasizes the necessity for further research and consideration of diacetyl's potential adverse health effects, mainly when used as a flavoring agent in food products.

Keywords: methylglyoxal, glutathione, proteomic, carbonyl stress, diacetyl

INTRODUCTION

Diacetyl is an α-dicarbonyl compound present in a variety of foods such as latkes (potato pancakes), wine, beer, cake, microwave popcorn, and biscuits.[1–6] It may be naturally present in these foods[7] or be added for the purpose of enhancing or improving the taste and/or aroma.[6,8,9] This compound is also found in conventional cigarettes and has recently been employed in the formulation of electronic cigarettes.[10,11]

Previous *in vitro* studies conducted by our group have demonstrated that diacetyl reacts with peroxynitrite, which is an endogenous substance whose production is increased in stress situations.[11–15] In the present study, the formation of a high concentration of acetyl radicals was demonstrated *in vitro* through a nucleophilic addition reaction of peroxynitrite with 2,3-butanedione in phosphate buffer (pH 7.2).

Previously we shown, by the addition of L-histidine or 2'-deoxyguanosine to the reaction medium, that acetyl radicals generated from the reaction between 2,3-butanedione and peroxynitrite promote the acetylation of proteins and nitrogenous bases.[12,14] Another *in vitro* study by our group also proved the production of acetyl radicals and the formation of acetylated products via magnetic resonance and mass spectrometry data, which was due to covalent bonds between the acetyl radicals and amino acids, peptides, and proteins.[11–15] *In vivo* studies have also been performed in Wistar rats and C57BL mice demonstrating that the daily intake of diacetyl causes significant changes in the protein, including increased protein acetylation.[16,17] The increase in acetyl radicals contributes to the redox imbalance of the organism; one of the defense mechanisms is the increased production and consumption of antioxidant substances by the body,[18] such as glutathione.[19,20] Another study, *in vivo*, of our group showed that diacetyl intake is capable to modify plasmatic metabolic profile in mices C57/Bl, this study also demonstrated that there were responses between males and females who ingested daily diacetyl, can lead to a predisposition to different diseases depending on the sexes and also leave to metabolic alterations.[17]

Methylglyoxal (MGO) is α-dicarbonyl compound present in cells and is an important precursor of free radicals, as well as being an intermediate in cellular metabolism under normal and pathological conditions.[21,22] Three metabolic routes of MGO formation in mammals are known; one suggests the formation of MGO from phosphate trioses, and another, from ketone bodies. These two routes account for 90% of the MGO formed in the body. A third route leads to the formation of MGO from glycine and threonine, with the previous formation of amino acids.[23] The increased in MGO production can lead to the formation of carbonyl stress revealed that carbonyl stress by chronic exposure to MGO is associated altered GSH/GSSG redox potential.[24] In addition, the reactions involved in the formation of carbonyl species are related with increase the formation of reactive oxygen species (ROS). It can lead to increase in oxidative stress and consequent structural and functional damage to macromolecules such as proteins.[25] And the proteins play an important role in most processes biological, they are repatriated by various biological and molecular functions like, for example: catalysis, transport, connection to substances, function signaling, hormonal, among others. Mass spectrometry is used in most studies in proteomics, being responsible for most of protein identification.[26]

MATERIALS AND METHODS
Reagents and standards
Trichloroacetic acid P.A (TCA) (Merck, Germany), trifluoroacetic acid (TFA) chromatographic grade, acetonitrile MS grade (Sigma-Aldrich, Germany), and formic acid HPLC grade (Sigma-Aldrich, Germany) were used. For quantitation: glutathione (GSH), methylglyoxal, tryptophan, o-phenylene diamine (DB) and oxidized glutathione (GSSG) (Sigma-Aldrich, Germany). Diacetyl, heparin, and acid trifluoroacetic were purchased from Sigma Aldrich (MO, USA). Bradford reagent, Dithiothreitol (DTT) and iodoacetamide (IAA) were purchased from Biorad, USA and trypsin from Promega, USA.

Mouse model development
All procedures used in the present study were performed in accordance with the guidelines established by the Brazilian College of Animal Experimentation (COBEA) and were approved by the Ethical Committee of the School of Medicine of the Federal University of São Paulo (UNIFESP); protocol No. 975911013/16.

Ten- to twelve-week-old male C57BL mice were distributed into three groups, each consisting of six animals. These mice were chosen exclusively as males to avoid the hormonal variability present during the females' estrous cycle, which can affect the accuracy of the data collected.[27] The animals were housed in cages under controlled conditions with 50−70% humidity, a temperature range of 19-26 °C, and a 12-hour light/12-hour dark cycle and were fed *ad libitum.* The mice received two different doses of diacetyl, based on the reference study by Colley et al., for 15 weeks.[28] The treatment groups were as follows: a control group that received only drinking water; a group that received 200 mg (diacetyl) per kg (animal weight) per day in the drinking water; and a group that received 300 mg kg^{-1} day^{-1} in the drinking water. Following 15 weeks of treatment, the animals were anesthetised with CO_2 and sacrificed. The livers were removed and stored at -80 °C until use. The blood was collected in a tube with heparin that was centrifuged, and the plasma was collected and stored -80 °C freezer.

GSH and GSSG analysis
GSH and GSSG extraction was performed based on the methodology described by Mika *et. al*[22] with some adaptations. Firstly, an aliquot of approximately 50 mg hepatic tissue was placed in a microfuge tube, and a 1:4 (v/v) solution of trichloroacetic acid (10%) was added, followed by immediately homogenization using a vortex for 1 min. The solution was subsequently centrifuged at 10,000 x g for 10 min at 4 °C, and the supernatant was collected and diluted (1:200) with the mobile phase (0.1% formic acid−H_2O) prior to HPLC.

For both glutathione and methylglyoxal analysis, liquid chromatography (LC) was operated using a UFLC XR (Shimadzu, Japan) automatic injector equipment, coupled to a mass spectrometer with a linear ion trap analyzer and electrospray (ESI) ionization source (Amazon model; Bruker, Germany). Separation of the analytes occurred on a C18 reversed-phase analytical column (100 mm x 3 mm, 2.5 μm) (Shim-Pack XR ODS-II). A C18, 4.6 x 12.5 mm guard column (Eclipse XDB-C18 4-Pack, Zorbax-Agilent Technologies, USA) was coupled to the methylglyoxal determination system.

The mobile phase was composed by water and 0.1% formic acid (Phase A) and ACN and 0.1% formic acid (Phase B). A volume of 5 μL sample was injected, and the gradient started with 1% solvent B, increasing to 3% over 2.5 min, 30% over 3 min, and 35% over 40 min. A decrease to 30% and 1% occurred over 7 and 9 min, respectively, and was maintained for an additional 6 minutes for stabilization. The flow was maintained constant at 0.2 mL min^{-1} and the column temperature at 40 °C. The ions [M + 1] of GSH and GSSG generated from the ESI were analyzed in IT ultra scan mode, the masses were 308.1 *m/z* and 613 *m/z*, respectively. The parameters established were ESI voltage, 4500 V; nebulizer pressure, 1.2 bar; gas flow, 6.0 L min^{-1}; temperature of the source, 180 °C; and scanning range, 110−700 *m/z*. The Supplementary material (Table S1-S2) present the results for the parameters evaluated during the validation of the method for the separation and quantitation of GSH and GSSG.

Methylglyoxal analysis

Preparation of the samples for methylglyoxal analysis was performed using tissue based on the protocol described by Rabbani and Xue.[29] Approximately 50 mg hepatic tissue was homogenized in 10 µL TCA saline (4% + 0.9% NaCl) using a vortex at 6 °C for 10 seconds, followed by the addition of 80 µL H_2O (Milli-Q). Subsequently, 5 µL tryptophan standard (13C13 and 15N) (400 nM) was added. Following further vortex, the mixture was centrifuged (1000 x g, 4 ºC) for 10 min, and 35 µL supernatant was transferred to the inserts.

The methylglyoxal derivatization process was carried out by the addition of 5 µL sodium azide (3% w/v) and 10 µL DB derivatization reagent (0.5 nM) to the insert, to a final volume of 50 µL. The mixture was incubated for four hours in the dark at room temperature. After the incubation period, the extract was subjected to liquid chromatography mass spectrometry (LC-MS) analysis with a total injection of 50 µL to determine the derivatization product (2-methylquinoxaline − 2MQ).

The conditions for the separation of methylglyoxal were as described by Rabbani and Thornalley, 2014,[23] using mobile phase A, containing 0.1% (v/v) TFA in water, and mobile phase B containing 0.1% (v/v) TFA with 50% (v/v) water and HPLC grade acetonitrile. The samples were maintained at 4 ºC in the autosampler. A volume of 50 µL sample was injected, and a flow of 0.2 mL min^{-1} 0% mobile phase A was started and maintained for 0.5 min. Subsequently, a linear gradient of 0 to 100% phase B was started over 10 min, which was maintained for 5 min and reduced to the initial 0% phase B at 16 min. These conditions were maintained for a further 15 min to achieve rebalancing and column washing. Thus, a 31-min chromatographic run was performed. The internal tryptophan and 2MQ (2-methylquinoxaline-2MQ) standards were ionized by the ESI in positive mode [M + 1] and monitored in ultra scan mode on the ion trap in the range of 100−300 *m/z*. The ions 207.2 *m/z* and 145.2 *m/z* for labeled tryptophan (1C13 and N15) and 2MQ, respectively, were extracted. The other conditions of the mass spectrometer were set at: ESI voltage, 4500 V; temperature of the source, 180 °C; end plate offset voltage, 500 V, gas pressure, 1.2 bar; and gas flow, 6.0 L min^{-1}. The summary of the of the analysis of variance (ANOVA) of the linear model used in the quantification of methylglyoxal is described in supplementary material (Table S3).

The quantification of methylglyoxal was carried out using a significantly linear calibration curve ($p<0.05$) with no lack of fit. The concentration range of the 2-MQ standard used was from 2.0 to 20.0 pmol L^{-1}, with points executed in triplicate, and the peak areas were obtained after chromatogram integration. For quantification in liver samples, tryptophan was used as an internal standard (IS) with a fixed concentration of 8 pmol L^{-1} to be subtracted from the total amount measured in the samples.

Proteic Carbonyl Analysis

Carbonyl determination compounds was carried out according to the method described by Levine and collaborators with some minor adjustments as follow above.[30] The carbonyl groups analyzed in the plasma samples were first derivatized with 2,4-dinitrophenylhydrazone (DNP) by reaction with 2,4-dinitrophenylhydrazine (DNPH), in the presence of 2.5 M HCl. The samples were incubated in the dark, at room temperature, for 1 hour, shaking the tubes every 15 minutes. Then, a 20% solution of TCA was added to the test and white tubes. Both tubes were incubated on ice for 10 minutes and centrifuged at 12000 rpm for 10 min at 4 ºC, the supernatant was discarded, and the pellet was washed with 10% TCA solution. The pellet was washed four more times, with a 1:1 solution of ethanol and ethyl acetate. The pellets were resuspended in 6.0 M guanidine solution and incubated at 37 °C for 10 minutes. The samples were quickly centrifuged with a spin, analyzed by spectrophotometry and the results were expressed in nanomoles of carbonyl per milligram of protein.

Protein Analysis

The total protein concentration in plasma was determined by the Bradford method.[31] Than, 50 µg of protein from plasma were digested separately, first were added Rapid Digest (PN: 186001861. Waters, USA) reduced with DTT (Biorad, USA) and alkylated with iodoacetamide (Biorad, USA). Trypsin

(Promega, USA) was added at a ratio of 1:100 enzyme: protein, and the reaction was stopped by adding TFA (Sigma Aldrich). The sample was dried by Speed Vacuum concentrators to reduce the volume to approximately 50 µL, was added 30 µL 0.5% TFA. The digested samples were filtered with a PVDF 0.22 µm syringe filter (PN SLGV033RS; Millipore Millex-GV, Ireland) the sample was stored at 4 °C until mass spectrometry analysis.

Three replicates of digested plasma samples were analyzed by mass spectrometry in SYNAPT G2 HDMS (Waters, USA) coupled Nano-Acquity HPLC (Waters, USA) equipped with a binary pump, autosampler, and a thermostatically controlled column compartment. In Nano-LC utilize a C18 reversed phase column Acquity UPLC Nano-CSH with dimensions 130 x 200 mm, 75 µm particle size of 1.7 µM (PN: 186 007 072; Waters, USA) and a trap nano-column Acquity BEH C18 130 µM with dimensions 180 x 20 mm, 5 µm particle size (BP: 186 003 682; Waters, US). The column temperature was maintained at 40 °C. Samples were separated using a mobile phase gradient composed of (A) formic acid/H_2O (1:1000) and (B) Formic acid/ACN (1:1000) and an elution gradient 7-35% B over 90 min. The flow rate was set 275 nL min^{-1} and the injection volume was 5 µL. The acquisitions were performed using the SYNAPT G2 mass spectrometer (Waters, USA) equipped with an ESI. The mass spectrometer was operated in positive mode at 3.0 kV, desolvation temperature 70 °C, the drying gas (N_2) at a flow rate of 4 L min^{-1}. All acquisition transactions were controlled by MassLynx software version 4.1 (Waters, USA) for analysis MS/MS method was used data-independent acquisition (DIA) and CID fragmentation with argon gas. Mass spectra were collected between 50 and 1600 *m/z* and total time of 1.25 s scan. The calibration was performed with [Glu-1]-fibrinopeptide b-500 fmol µl^{-1} (PN: 700 004 729; Waters, USA) and flow of 500 nL min^{-1} acquired for 1 s every 60 s. The low collision energy was 4 eV and the high-energy collision ranged 17-60 eV.

Bioinformatic analysis

Data files were processed by ProteinLynx Global Service (PGLS) (version 3, Waters, Milford, MA, USA) with limits for low scores, high energy, and intensity of 50 and 750 and 1200, respectively, resolution of the time of flight (TOF) and width of automatic peaks *m/z* from calibrant. The searches against the database were performed with sequences of *mus musculus* from Uniprot.[32] The following parameters were adopted: cysteine carbamidomethylation as fixed modification and lysine acetylation, histidine, arginine, methionine oxidation as variable modifications, and one missed cleavage and automatic precursor and fragment error tolerance. The limits used for identification were minimum one fragment by peptide, five fragments of protein, two fragments of peptide and maximal false positive rate of 5%, as estimated by simultaneous search with a reverse database.

Label free quantification

We preceded the Label-free quantification based on DIA workflows from PGLS. We use the protein top 3 Matched Peptide Intensity Sum (TOP 3), this parameter is calculated automatic by PGLS. And corresponding to the mean of the three highest peptides areas measured for each protein. Then, we divided the sum of all observed TOP 3 peptide intensities by the number of all observable peptides; this ratio provides a measure to approximate absolute protein concentration.[33,34]

Orthologs Analysis

We subject Orthologs to Gene Ontology (GO) term analysis-based PANTHER classification online tools.[35] This analysis was performed for determining the functions of proteins differentially expressed in group treated with diacetyl from control group. For this search we used the Uniprot IDs with *mus muscullus* genome.[36]

Such database was chosen as the reference database for the output report on biological process, and molecular function information.[32] For classification of pathways with these proteins we use the panther database.[35] These analyses were performed to get the profile of this proteins differentially expressed in group treated with diacetyl from control group.

Statistical analysis

The statistical analysis was based on statistical methods for comparing data through hypothesis testing ANOVA was applied followed by Tukey's test ($p \leq 0.05$) *a post hoc* test used to determine the significant differences between group means in an analysis of variance setting using GraphPad Prism (version 5.00 for Windows, GraphPad Software, San Diego California USA) to analyze the proteins concentration screening.

Additionally, principal component analysis (PCA) was applied to identify trends or similarities between samples as well as any correlation between variables, using the web toll Clustvies.[32,37]

RESULTS AND DISCUSSION

Quantitation of GSH and hepatic reduced glutathione (GSSG) in mouse liver

The results for the determined concentrations of GSH and GSSH in the livers of mice subjected to diacetyl in the diet are shown in Table I. It can be observed that the GSH content in mouse liver was higher than that of GSSH under all treatment conditions with the addition of diacetyl radicals as compared with mice that received no diacetyl in the diet. In this case, the GSH content was similar to the control, although there was a numerical difference with respect to the GSSG content (1.68 ± 0.57 and 1.03 ± 0.43 μg_{GSH} mg_{liver}^{-1} for GSH and GSSG, respectively). These results can be justified by the fact that livers from different mice were analyzed, which have different metabolisms despite being standardized under the same genetic and environmental conditions. This likely increased the variability of the data, and consequently increased the standard deviations, minimizing the statistical difference between the data.

Table I. Concentrations of GSH and GSSG in the livers of mice subjected to a diet containing diacetyl

Treatment	GSH (μg_{GSH} mg_{liver}^{-1})	GSSG (μg_{GSSG} mg_{liver}^{-1})
Control	1.68 ± 0.57^{aB}*	1.03 ± 0.43^{aA}
200 mg	2.48 ± 0.61^{aA}	0.73 ± 0.22^{bA}
300 mg	2.02 ± 0.41^{aAB}	0.71 ± 0.26^{bA}

*Means followed by the same lowercase letter in the row and the same upper case in the column do not represent a significant difference at $p \leq 0.05$, according to Tukey's test.

It can also be seen from Table I, that the GSH content was increased in the livers of mice subjected to a diet containing diacetyl radicals (200 and 300 mg), rising from 1.68 μg_{GSH} mg_{liver}^{-1} for the control to 2.48 and 2.02 μg_{GSH} mg_{liver}^{-1} for treatment with 200 and 300 mg, respectively. On the other hand, the GSSG content was reduced in the livers of mice submitted to a diet containing diacetyl. Livers of mice that received no diacetyl in the diet contained approximately 1.03 ± 0.43 μg_{GSH} mg_{liver}^{-1}, whereas the livers of mice that received the dietary radical had a content of 0.73 and 0.71 μg_{GSH} mg_{liver}^{-1} for 200 and 300 mg treatment, respectively. Similar to the GSH concentration in mouse liver, the different diacetyl radical concentrations studied (200 and 300 mg) in the diet were insufficient to cause significant differences between them. It was only possible to observe significant differences when the data were compared with those of the control mice.

The results for the ratio between GSH and GSSG are shown in Figure 1A. It is noteworthy that there was a significant difference between the data obtained from the mice treated with the dietary diacetyl radicals and those obtained from the control mice. The GSH/GSSG ratio for the control group remained at approximately 1.60, and that for the groups treated with 200 and 300 mg diacetyl was approximately 2.4 and 3.9, respectively. Although these groups differed from the control, there was no significant difference between the two groups, as can be observed in Figure 1A.

Figure 1B shows the MGO levels in liver tissue, it can be observed that incorporation of diacetyl (200 and 300 mg) into the diet significantly reduced the content of MGO present in mouse liver ($p \leq 0.05$) as compared with the livers of the control mice that received no diacetyl in the diet. The livers of the mice in the control group had a mean MGO content of approximately 13.65 ± 3.33 $pmol_{MGO}$ mg_{liver}^{-1}, whereas those in the groups that received 200 and 300 mg diacetyl in the diet presented concentrations of approximately 9.27 ± 2.4 and 9.4 ± 2.4 $pmol_{MGO}$ mg_{liver}^{-1}, respectively. Therefore, the results show that treatment with diacetyl at these concentrations was insufficient to differentiate among the groups in relation to the MGO content in the liver, maintaining a significant equality ($p \leq 0.05$).
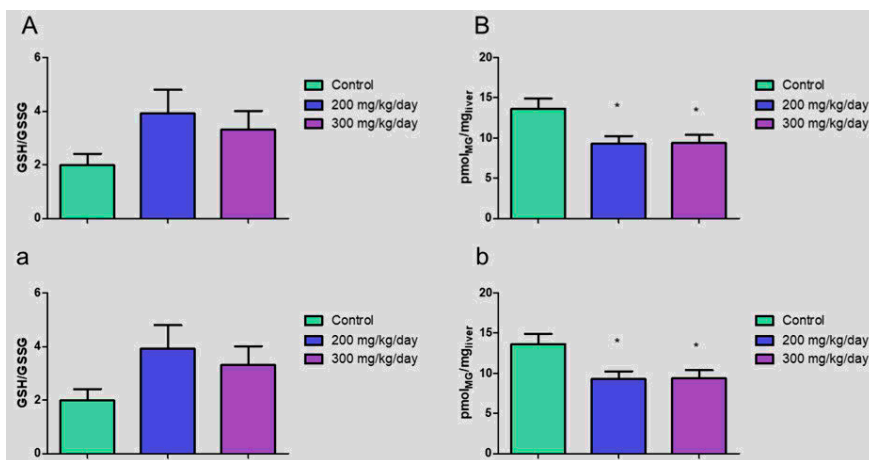
Figure 1. (A) Ratio of GSH/GSSG content determined in the livers of mice subject ted to daily intake of diacetyl. (B) MGO content determined in the livers of mice subjected to daily intake of diacetyl. *Significative difference from control group.

Carbonyl Stress analysis

The rise in the carbonyl species is a strong indicator to oxidative stress is increased, in this work we show this rise in carbonyl species in plasma from mouse treated with diacetyl. Also, we show when animals consumption more diacetyl the increased in carbonyl species is higher. (Figure 2)
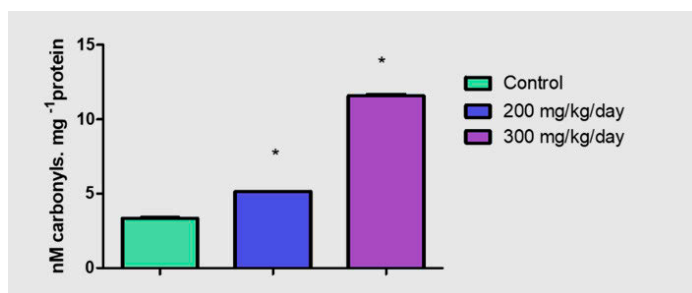
Figure 2. Carbonyl stress in plasma of mice subjected to daily intake of diacetyl. *Significative difference from control group.

PCA analyses and Heatmap from GSH, GSSG, MGO ant Carbonyl Stress

To ensure a cleaner and more coherent visualization of the data, PCA was conducted using average values due to the use of isogenic mice, which are genetically identical, and because the studies involved pooling samples from each group. This methodological choice aimed to minimize variability and present a more representative overview of the underlying patterns, reducing the potential for artifacts. The heatmap

(Figure 3a) displays the differences in substance levels, showing the separation between the control and diacetyl-treated groups. The rows are centered, and unit variance scaling is applied to the rows. Both rows and columns are clustered using correlation distance and average linkage, resulting in five rows and three columns. Despite the use of averages, the reliability and accuracy of the results were not compromised. The PCA analyses (Figure 3b) demonstrated that have significative difference and separation between the control group and the groups treated with 200 and 300 mg kg^{-1} day^{-1} of diacetyl. This analysis shows a perfect separation PC1 81% and PC2 19% totalizing 100%. Unit variance scaling is applied to rows; SVD with imputation is used to calculate principal components. X and Y axis show principal component 1 and principal component 2 that explain 81% and 19% of the total variance. The data preprocessing is available in the supplementary material (Tables S4-S6).
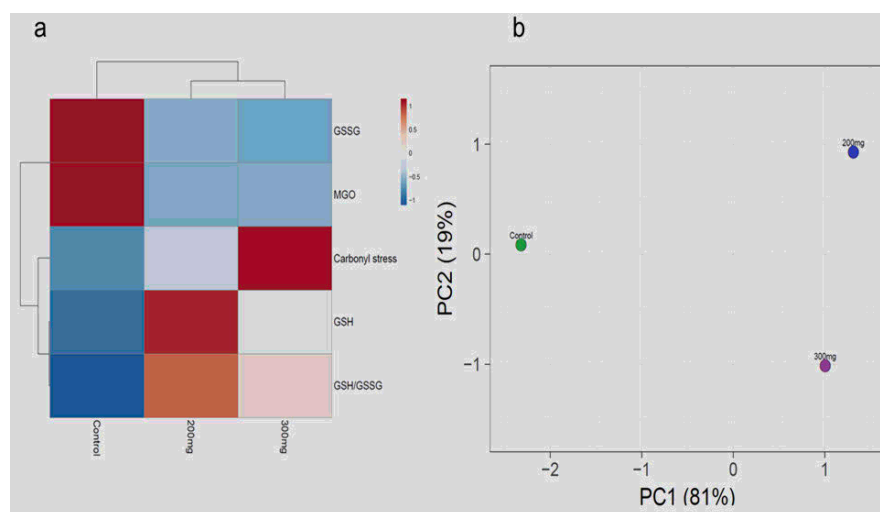
Figure 3. (a) Heatmap analyses from GSH, GSSG, MGO in liver tissue and Carbonyl Stress (carbonyl compounds in plasma); (b) PCA analyses from GSH, GSSG, MGO ant Carbonyl Stress; *(dot green corresponding to control group, dot blue corresponding to group treated with 200 mg kg^{-1} day^{-1} of diacetyl and dot purple corresponding to group treated with 300 mg kg^{-1} day^{-1} of diacetyl).

Proteomic Analysis

The proteomics analysis in plasma from groups control (in supplementary material Table S7) and treated with 200 (Table S8) and 300 mg kg^{-1} day^{-1} (Table S9) show differences between the control and treated groups. As showed in Table II, two proteins (A2M and Albu) that are less expressed in treated groups. We also, identified four proteins (IDHC, KLKB1, KV6AB and PHLD) that are identified only in control group, and identified some proteins that are not identified in the group that received 300 mg kg^{-1} day^{-1} of diacetyl (APOC3, B2MG, CBG, CBPN, CFAH, CPN2, FETUA, FETUB, HEP2, LUM and MBL2).

Table II. Relative quantification (%) of plasmatic proteins differentially expressed identified in control group and groups treated with 100, 200 and 300 mg kg^{-1} day^{-1} of 2,3-butanedione

Protein Acess	Protein key	Control (fmol)	200 mg kg^{-1} day^{-1} (fmol)	Compare to control group	300 mg kg^{-1} day^{-1} (fmol)	Compare to control group
A2M	162	9.135 ± 1.525*	8.41 ± 2.0*	↔	3.67 ± 2.11*	↓
ALBU	846	21.878 ± 2.793*	20.96 ± 3.4	↔	12.061 ± 2.600*	↓
A1AT4	151	N/F	3.674 ± 0.26	↑	2.187 ± 1.543	↑

(continued on next page)

Table II. Relative quantification (%) of plasmatic proteins differentially expressed identified in control group and groups treated with 100, 200 and 300 mg kg $^{-1}$ day^{-1} of 2,3-butanedione (continued)

Protein Acess	Protein key	Control (fmol)	200 mg kg $^{-1}$ day^{-1} (fmol)	Compare to control group	300 mg kg $^{-1}$ day^{-1} (fmol)	Compare to control group
HA10	9187	N/F	0.152 ± 0.115	↑	0,404 ± 0.08	↑
IDHC	9991	0.113 ± 0.095	N/F	——	N/F	——
KLKB1	11379	0.118 ± 0.005	N/F	——	N/F	——
KV6AB	11609	0.046 ± 0.034	N/F	——	N/F	——
PHLD	16194	0,079 ± 0.020	N/F	——	N/F	——
APOC3	1273	0.043 ± 0.018	0.034 ± 0.027	↔	N/F	——
B2MG	1899	0.223 ± 0.103	0.221 ± 0.178	↔	N/F	——
CBG	2878	0.251 ± 0.054	0.241 ± 0.052	↔	N/F	——
CBPN	2931	0.059 ± 0.025	0.062 ± 0.014	↔	N/F	——
CFAH	3735	0.433 ± 0.110	0.327 ± 0.053	↔	N/F	——
CPN2	4710	0.114 ± 0.048	0.100 ± 0.042	↔	N/F	——
FETUA	7642	0.680 ± 0.132	0.991 ± 0.413	↔	N/F	——
FETUB	7643	0.320 ± 0.090	0.313 ± 0.086	↔	N/F	——
HEP2	9394	0.096 ± 0.020	0.095 ± 0.019	↔	N/F	——
LUM	12289	0.073 ± 0.008	0.085 ± 0.012	↔	N/F	——
MBL2	12678	0.140 ± 0.041	0.112 ± 0.052	↔	N/F	——

Mean ± SEM (N=3), ↑ increase comparing to control group or expressed only in treated group, ↓ decrease comparing to control group, ↔ no difference from control group, * significant difference between the proteins (lines) in the different groups (columns). ANOVA TWO ways *post hoc* test Bonferroni * P > < 0.0001.

The proteins differentially expressed in treaded groups belongs to different class (Figure 4a), including defense/immunity protein (PC00090), extracellular matrix protein (PC00102), protein-binding activity modulator (PC00095), transfer/carrier protein (PC00219), metabolite interconversion enzyme (PC00262), protein modifying enzyme (PC00260) and transmembrane signal receptor (PC00197). The Figure 4b shows that proteins are involved in three molecular functions indicated by panther dB as binding (GO:0005488), catalytic activity (GO:0003824) and molecular function regulator (GO:0098772). Already the biological process (Figure 4c) that proteins participates are biological regulation (GO:0065007), cellular component organization or biogenesis (GO:0071840), cellular process (GO:0009987), immune system process (GO:0002376), response to stimulus (GO:0050896), developmental process (GO:0032502), growth (GO:0040007), localization (GO:0051179), metabolic process (GO:0008152) and multicellular organismal process (GO:0032501). Furthermore, these proteins differentially expressed in treated groups are involved into three important pathways Blood coagulation (P00011), T cell activation (P00053) and Gonadotropin-releasing hormone receptor pathway (P06664) according to panther database analysis.[35]
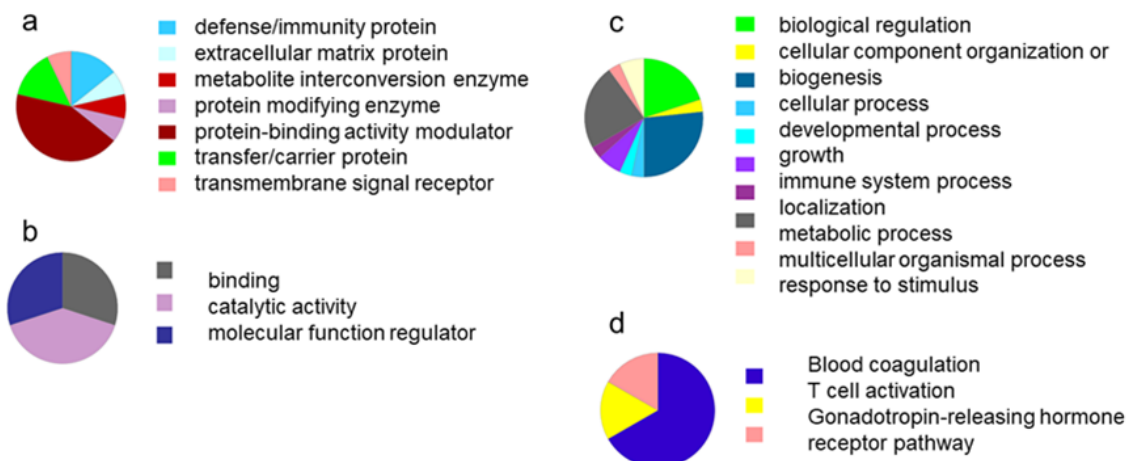
Figure 4. Go analysis from proteins with differential expression in groups treated with diacetyl: (a) Protein Class, (b) Metabolical process, (c) Biological process and (d) Pathways.

Discussion

The different diacetyl radical concentrations (200 and 300 mg) in the diet were insufficient to cause significant differences in GSH between the two groups; however, when the data were compared with those of the control mice, an increase in GSH was observed (Table I). Regarding the ratio between GSH and GSSG (Figure 1A), it is noteworthy that there was a significant difference between the data obtained in mice treated with the dietary diacetyl radicals and those obtained in mice in the control group. The GSH/GSSG ratio for the control group remained at approximately 1.60, and the ratio for the groups treated with 200 and 300 mg diacetyl was approximately 2.4 and 3.9, respectively. GSH is involved in many biological processes, such as detoxification of xenobiotics, and is important in animal tissues to help prevent injuries caused by reactive oxygen species such as free radicals and peroxides. Most of the glutathione in cells is in the form of GSH, but when cells suffer oxidative stress, the GSSG form accumulates, increasing the ratio of GSSG to GSH. An increased ratio of GSH/GSSG is an indication of oxidative stress.[38–40]

Similarities were noted between the 200 and 300 mg treatment samples, which is the result of lower concentrations of MGO (Figure 1B). In general, the control samples had great variation in the concentrations of MGO, which can be explained by the metabolic individuality of each animal studied. The decrease in MGO levels may be related to the increase in the GSH/GSSG ratio, suggesting that MGO may have been consumed or detoxified. Schmitz *et. al* have previously shown that there is a relationship between the methylglyoxal levels and the GSH/GSSG ratio.[41] Indeed, liver is the main responsible tissue for detoxification of MGO and glyoxal.[42,43] This liver detoxification ability may explain the decreased levels of MGO in the liver of animals from groups treated with diacetyl compared to the liver of animals from control group. Another condition that corroborates for MGO decrease is besides it being a very reactive compound the MGO has a largely renal excretion, and this mechanism can prevent the toxicity of MGO.[43] Intracellular MGO has been proven to be detoxified by the glyoxalase system. However, the details of this mechanisms for detoxification of MGO have not yet been fully elucidated.[43,44] The increase in carbonyl compounds (Figure 2) reflects a situation of dicarbonyl stress, that can modify function and structure of biomolecules, increasing the ROS (reactive oxygen species) and consequently the oxidative stress.[44] This unbalance of ROS and carbonyl compounds can lead an increase in protein changes and contributing to cell and tissue dysfunction.[23–25,29] This rise in carbonyl compounds reinforce our hypothesis that diacetyl intake cooperates to rise the oxidative stress and can lead to protein modifications. Besides, when dicarbonyl concentrations get rise, also increase the potential for protein and cell dysfunction leading to the organisms developed a disease or impaired health.[29]

As expected, we can see in figure 3a, through the heatmap, the clear separation of the control group from the two groups treated with diacetyl. There is some expressive difference between groups as show in figure 3b, seasonable we can differentiate perfectly of three groups, so when we add PC1 and PC2 we get 100% separation. This result expressed by the figures 3a and 3b shows that diacetyl intake in both dosages (200 and 300 mg kg^{-1} day^{-1}) cause changes in the metabolism of this animals causing harm to health.

The animals treated with diacetyl also suffered changes in the protein plasmatic profile (Table II), we observe the decrease in albumin. This protein (Alb) is the most abundant protein in the plasma and perform important role to transport of substances in organism. Moreover, the albumin is related with indirect detoxification of extracellular MGO, because this way MGO can cross the cell membrane and be detoxified by glyoxalase system.[43,44] Besides MGO has fast and strong MG scavenging effect of albumin[43] and this scavenging effect can modify this protein and thus not allow or hinder its identification. Beyond albumin we observed the protein A2M that presented quantitative decrease in treated group with 300 mg kg^{-1} day^{-1} of diacetyl. The protein (A2M) is an antiprotease involved in the blood coagulation and the low expression of this protein contributing to the allergic inflammatory response[45,46] and had a significant negative correlation with age.[47] Already the proteins A1AT4 and HA10 were upregulated, the A1AT4 is a serine proteinase inhibitor that are involved in proteolytic processes regulation including fibrinolysis and inflammation.[48,49] The protein HA10 as describe in uniport is involved in the presentation of foreign antigens to the immune system and as Li *et. al,*[50] A1AT4 contribute to the augmented activation of T lymphocytes. How we show in Figure 4 this modification in proteins promotes changes in some metabolic and biologic process as well promotes alterations in important pathways especially the T-cell activation and blood coagulation consequently leads to break of homeostasis and may induce disease development.

CONCLUSIONS

These works suggest that the consumption of diacetyl is harmful and capable of promoting changes in the redox balance. Once, diacetyl intake decreases levels of MGO in liver tissue and increase carbonyl species in plasma moreover promoted alteration in proteomic plasmatic profile in mice and consequently in the metabolic profile. The data indicate that carbonyl stress can represent an important mechanism to alteration the protein profile probably caused by diacetyl intake.

The results from here open a gap to be explored in future research on the likely detoxification of MGO when high concentrations of diacetyl have been ingested.

Conflicts of interest

The authors declare that there is no conflict of interest in the preparation of this article.

REFERENCES

(1) Papetti, A.; Mascherpa, D.; Gazzani, G. Free α-dicarbonyl compounds in coffee, barley coffee and soy sauce and effects of *in vitro* digestion. *Food Chem.* **2014**, *164*, 259-265. https://doi.org/10.1016/j.foodchem.2014.05.022

(2) Cavalcanti, Z. R.; Filho, A. P. L. A.; Pereira, C. A. C.; Coletta, E. N. A. M. Bronchiolitis associated with exposure to artificial butter flavoring in workers at a cookie factory in Brazil. *Jornal Brasileiro de Pneumologia* **2012**, *38* (3). https://doi.org/10.1590/S1806-37132012000300016

(3) Bartowsky, E. J.; Henschke, P. A. The "buttery" attribute of wine - diacetyl - desirability, spoilage and beyond. *Int. J. Food Microbiol.* **2004**, *96* (3), 235-252. https://doi.org/10.1016/j.ijfoodmicro.2004.05.013

(4) Bortoleto, G. G.; Gomes, W. P. C.; Ushimura, L. C.; Bonança, R. A.; Novello, E. H. Evaluation of the profile of volatile organic compounds in industrial and craft beers. *J. Microbiol., Biotechnol. Food Sci.* **2022**, *12* (2), e5532. https://doi.org/10.55251/jmbfs.5532

(5) Gaffney, S. H.; Abelmann, A.; Pierce, J. S.; Glynn, M. E.; Henshaw, J. L.; McCarthy, L. A.; Lotter, J. T.; Liong, M.; Finley, B. L. Naturally occurring diacetyl and 2,3-pentanedione concentrations associated with roasting and grinding unflavored coffee beans in a commercial setting. *Toxico. Rep.* **2015**, *2*, 1171-1181. https://doi.org/10.1016/j.toxrep.2015.08.003

(6) National Center for Biotechnology Information. *PubChem Compound Summary for CID 650, 2,3-Butanedione.* https://pubchem.ncbi.nlm.nih.gov/compound/2_3-butanedione [accessed: February, 2024].

(7) Rincon-Delgadillo, M. I.; Lopez-Hernandez, A.; Wijaya, I.; Rankin, S. A. Diacetyl levels and volatile profiles of commercial starter distillates and selected dairy foods. *J. Dairy Sci.* **2012**, *95* (3), 1128-1139. https://doi.org/10.3168/jds.2011-4834

(8) Shibamoto, T. Diacetyl: Occurrence, Analysis, and Toxicity. *J. Agric. Food Chem.* **2014**, *62* (18), 4048-4053. https://doi.org/10.1021/jf500615u

(9) Allen, J. G.; Flanigan, S. S.; LeBlanc, M.; Vallarino, J.; MacNaughton, P.; Stewart, J. H.; Christiani, D. C. Flavoring Chemicals in E-Cigarettes: Diacetyl, 2,3-Pentanedione, and Acetoin in a Sample of 51 Products, Including Fruit-, Candy-, and Cocktail-Flavored E-Cigarettes. *Environ. Health Perspect.* **2016**, *124* (6), 733-739. https://doi.org/10.1289/ehp.1510185

(10) Pierce, J. S.; Abelmann, A.; Spicer, L. J.; Adams, R. E.; Finley, B. L. Diacetyl and 2,3-pentanedione exposures associated with cigarette smoking: implications for risk assessment of food and flavoring workers. *Crit. Rev. Toxicol.* **2014**, *44* (5), 420-435. https://doi.org/10.3109/10408444.2014.882292

(11) Alves, A. N. L.; Jedlicka, L. D. L.; Massari, J.; Juliano, M. A.; Bechara, E. J. H.; Assunção, N. A. Electrospray Ionization Mass Spectrometry Applied to Study the Radical Acetylation of Amino Acids, Peptides and Proteins. *J. Braz. Chem. Soc.* **2013**, *24* (12), 1983-1990. https://doi.org/10.5935/0103-5053.20130248

(12) Massari, J.; Fujiy, D. E.; Dutra, F.; Vaz, S. M.; Costa, A. C. O.; Micke, G. A.; Tavares, M. F. M.; Tokikawa, R.; Assunção, N. A.; Bechara, E. J. H. Radical Acetylation of 2′-Deoxyguanosine and L-Histidine Coupled to the Reaction of Diacetyl with Peroxynitrite in Aerated Medium. *Chem. Res. Toxicol.* **2008**, *21* (4), 879-887. https://doi.org/10.1021/tx7002799

(13) Massari, J.; Tokikawa, R.; Medinas, D. B.; Angeli, J. P. F.; Di Mascio, P.; Assunção, N. A.; Bechara, E. J. H. Generation of Singlet Oxygen by the Glyoxal-Peroxynitrite System. *J. Am. Chem. Soc.* **2011**, *133* (51), 20761-20768. https://doi.org/10.1021/ja2051414

(14) Massari, J.; Tokikawa, R.; Zanolli, L.; Tavares, M. F. M.; Assunção, N. A.; Bechara, E. J. H. Acetyl Radical Production by the Methylglyoxal-Peroxynitrite System: A Possible Route for l-Lysine Acetylation. *Chem. Res. Toxicol.* **2010**, *23* (11), 1762-1770. https://doi.org/10.1021/tx1002244

(15) Tokikawa, R.; Loffredo, C.; Uemi, M.; Machini, M. T.; Bechara, E. J. H. Radical Acylation of L-Lysine Derivatives and L-Lysine-Containing Peptides by Peroxynitrite-Treated Diacetyl and Methylglyoxal. *Free Radic. Res.* **2014**, *48* (3), 357-370. https://doi.org/10.3109/10715762.2013.871386

(16) Jedlicka, L. D. L.; Guterres, S. B.; Balbino, A. M.; Neto, G. B.; Landgraf, R. G.; Fernandes, L.; Carrilho, E.; Bechara, E. J. H.; Assuncao, N. A. Increased Chemical Acetylation of Peptides and Proteins in Rats after Daily Ingestion of Diacetyl Analyzed by Nano-LC-MS/MS. *PeerJ* 6:e4688 **2018**. https://doi.org/10.7717/peerj.4688

(17) Jedlicka, L. D. L.; Silva, J. D. C.; Balbino, A. M.; Neto, G. B.; Furtado, D. Z. S.; Silva, H. D. T. Da; Cavalcanti, F. D. B. C.; Van Der Heijden, K. M.; Penatti, C. A. A.; Bechara, E. J. H.; Assunção, N. A. Effects of Diacetyl Flavoring Exposure in Mice Metabolism. *Biomed Res. Int.* **2018**, *2018*, Article ID 9875319. https://doi.org/10.1155/2018/9875319

(18) Espinosa-Diez, C.; Miguel, V.; Mennerich, D.; Kietzmann, T.; Sánchez-Pérez, P.; Cadenas, S.; Lamas, S. Antioxidant Responses and Cellular Adjustments to Oxidative Stress. *Redox Biology* **2015**, *6*, 183-197. https://doi.org/10.1016/j.redox.2015.07.008

(19) Schafer, F. Q.; Buettner, G. R. Redox Environment of the Cell as Viewed through the Redox State of the Glutathione Disulfide/Glutathione Couple. *Free Radical Biol. Med*. **2001**, *30* (11), 1191-1212. https://doi.org/10.1016/S0891-5849(01)00480-4

(20) Silva, M. S.; Gomes, R. A.; Ferreira, A. E. N.; Freire, A. P.; Cordeiro, C. The glyoxalase pathway: the first hundred years... and beyond. *Biochem. J*. **2013**, *453* (1), 1-15. https://doi.org/10.1042/BJ20121743

(21) Dutra, F.; Bechara, E. J. H. Bioquímica e Ação Citotóxica de Alfa-Aminocetonas Endógenas. *Quim. Nova* **2005**, *28* (3). https://doi.org/10.1590/s0100-40422005000300021

(22) Mika, D.; Guruvayoorappan, C. Experimental study on anti-tumor and anti-inflammatory effect of *Thespesia populnea* phytochemical extract in mice models. *Immunopharmacol. Immunotoxicol.* **2013**, *35* (1), 157-163. https://doi.org/10.3109/08923973.2012.735237

(23) Rabbani, N.; Thornalley, P. J. Measurement of Methylglyoxal by Stable Isotopic Dilution Analysis LC-MS/MS with Corroborative Prediction in Physiological Samples. *Nat. Protoc.* **2014**, *9* (8), 1969-1979. https://doi.org/10.1038/nprot.2014.129

(24) Tatone, C.; Heizenrieder, T.; Di Emidio, G.; Treffon, P.; Amicarelli, F.; Seidel, T.; Eichenlaub-Ritter, U. Evidence that carbonyl stress by methylglyoxal exposure induces DNA damage and spindle aberrations, affects mitochondrial integrity in mammalian oocytes and contributes to oocyte ageing. *Hum. Reprod.* **2011**, *26* (7), 1843-1859. https://doi.org/10.1093/humrep/der140

(25) Donato, L.; Scimone, C.; Alibrandi, S.; Nicocia, G.; Rinaldi, C.; Sidoti, A.; D'Angelo, R. Discovery of *GLO1* New Related Genes and Pathways by RNA-Seq on A2E-Stressed Retinal Epithelial Cells Could Improve Knowledge on Retinitis Pigmentosa. *Antioxidants* **2020**, *9* (5), 416. https://doi.org/10.3390/antiox9050416

(26) Lovric, J. *Introducing Proteomics: From Concepts to Sample Separation, Mass Spectrometry and Data Analysis*. John Wiley & Sons, 2011.

(27) Zucker, I. The Mixed Legacy of the Rat Estrous Cycle. *Biol. Sex. Differ.* **2023**, *14*, Article number: 55. https://doi.org/10.1186/s13293-023-00542-7

(28) Colley, J.; Gaunt, I. F.; Lansdown, A. B. G.; Grasso, P.; Gangolli, S. D. Acute and short-term toxicity of diacetyl in rats. *Food Cosmet. Toxicol.* **1969**, *7*, 571-580. https://doi.org/10.1016/s0015-6264(69)80460-8

(29) Rabbani, N.; Xue, M.; Thornalley, P. J. Dicarbonyls and glyoxalase in disease mechanisms and clinical therapeutics. *Glycoconj. J.* **2016**, *33*, 513-525. https://doi.org/10.1007/s10719-016-9705-z

(30) Levine, R. L.; Garland, D.; Oliver, C. N.; Amici, A.; Climent, I.; Lenz, A. G.; Ahn, B. W.; Shaltiel, S.; Stadtman, E. R. Determination of carbonyl content in oxidatively modified proteins. *Methods Enzymol.* **1990**, *186*, 464-478. https://doi.org/10.1016/0076-6879(90)86141-H

(31) Bradford, M. M. A Rapid and sensitive method for the quantitation of microgram quantities of protein utilizing the principle of protein-dye binding. *Anal. Biochem.* **1976**, *72* (1–2), 248-254. https://doi.org/10.1016/0003-2697(76)90527-3

(32) The UniProt Consortium. UniProt: The Universal Protein Knowledgebase in 2023. *Nucleic Acids Res.* **2023**, *51* (D1), D523-D531. https://doi.org/10.1093/nar/gkac1052

(33) Bantscheff, M.; Lemeer, S.; Savitski, M. M.; Kuster, B. Quantitative Mass Spectrometry in Proteomics: Critical Review Update from 2007 to the Present. *Anal. Bioanal. Chem.* **2012**, *404*, 939-965. https://doi.org/10.1007/s00216-012-6203-4

(34) Silva, J. C.; Gorenstein, M. V.; Li, G. Z.; Vissers, J. P. C.; Geromanos, S. J. Absolute Quantification of Proteins by LCMSE: A Virtue of Parallel MS Acquisition. *Mol. Cell. Proteomics* **2006**, *5* (1), 144-156. https://doi.org/10.1074/mcp.M500230-MCP200

(35) Thomas, P. D.; Ebert, D.; Muruganujan, A.; Mushayahama, T.; Albou, L. P.; Mi, H. PANTHER: Making genome-scale phylogenetics accessible to all. *Protein Sci*. **2022**, *31* (1), 8-22. https://doi.org/10.1002/pro.4218

(36) The UniProt Consortium. *Taxonomy - Mus musculus*. https://www.uniprot.org/taxonomy/10090

(37) Metsalu, T.; Vilo, J. ClustVis: a web tool for visualizing clustering of multivariate data using Principal Component Analysis and heatmap. *Nucleic Acids Res.* **2015**, *43* (W1), W566-W570. https://doi.org/10.1093/nar/gkv468

(38) Forman, H. J.; Zhang, H.; Rinna, A. Glutathione: Overview of its protective roles, measurement, and biosynthesis. *Mol. Aspects Med.* **2009**, *30* (1-2), 1-12. https://doi.org/10.1016/j.mam.2008.08.006.

(39) Julius, M.; Lang, C. A.; Gleiberman, L.; Harburg, E.; Difranceisco, W.; Schork, A. Glutathione and morbidity in a community-based sample of elderly. *J. Clin. Epidemiol.* **1994**, *47* (9), 1021-1026. https://doi.org/10.1016/0895-4356(94)90117-1

(40) Streck, E. L.; De Prá, S. D. T.; Ferro, P. R.; Carvalho-Silva, M.; Gomes, L. M.; Agostini, J. F.; Damiani, A.; Andrade, V. M.; Schuck, P. F.; Ferreira, G. C.; Scaini, G. Role of antioxidant treatment on DNA and lipid damage in the brain of rats subjected to a chemically induced chronic model of tyrosinemia type II. *Mol. Cell. Biochem.* **2017**, *435*, 207-214. https://doi.org/10.1007/s11010-017-3070-5

(41) Schmitz, A. E.; de Souza, L. F.; dos Santos, B.; Maher, P.; Lopes, F. M.; Londero, G. F.; Klamt, F.; Dafre, A. L. Methylglyoxal-Induced Protection Response and Toxicity: Role of Glutathione Reductase and Thioredoxin Systems. *Neurotox. Res.* **2017**, *32*, 340-350. https://doi.org/10.1007/s12640-017-9738-5

(42) Shangari, N.; Depeint, F.; Furrer, R.; Bruce, W. R.; Popovic, M.; Zheng, F.; O'Brien, P. J. A thermolyzed diet increases oxidative stress, plasma α-aldehydes and colonic inflammation in the rat. *Chem.-Biol. Interact.* **2007**, *169* (2), 100-109. https://doi.org/10.1016/j.cbi.2007.05.009

(43) Zunkel, K.; Simm, A.; Bartling, B. Long-Term Intake of the Reactive Metabolite Methylglyoxal Is Not Toxic in Mice. *Chem. Toxicol.* **2020**, *141*, 111333. https://doi.org/10.1016/j.fct.2020.111333

(44) Kalapos, M. P. Where does plasma methylglyoxal originate from? *Diabetes Res. Clin. Pract.* **2013**, *99* (3), 260-271. https://doi.org/10.1016/j.diabres.2012.11.003

(45) Chen, X.; Xie, Z. H.; Lv, Y. X.; Tang, Q. P.; Zhang, H.; Zhang, J. Y.; Wu, B.; Jiang, W. H. A Proteomics Analysis Reveals That A2M Might Be Regulated by STAT3 in Persistent Allergic Rhinitis. *Clin. Exp. Allergy* **2016**, *46* (6), 813-824. https://doi.org/10.1111/cea.12711

(46) Barbosa, J. H. P.; Souza, I. T.; Santana, A. E. G.; Goulart, M. O. F. A determinação dos produtos avançados de glicação (AGEs) e de lipoxidação (ALEs) em alimentos e em sistemas biológicos: Avanços, Desafios e Perspectivas. *Quim. Nova* **2016**, *39* (5), 608-620. http://dx.doi.org/10.5935/0100-4042.20160048

(47) Rugsarash, W.; Tungtrongchitr, R.; Petmitr, S.; Phonrat, B.; Pongpaew, P.; Harnroongroj, T.; Tungtrongchitr, A. The genetic association between alpha-2-macroglobulin (A2M) gene deletion polymorphism and low serum A2M concentration in overweight/obese Thais. *Nutr. Neurosci.* **2006**, *9* (1–2), 93-98. https://doi.org/10.1080/10284150600771777

(48) Barbour, K. W.; Goodwin, R. L.; Guillonneau, F.; Wang, Y.; Baumann, H.; Berger, F. G. Functional Diversification during Evolution of the Murine A1-Proteinase Inhibitor Family: Role of the Hypervariable Reactive Center Loop. *Mol. Biol. Evol.* **2002**, *19* (5), 718-727. https://doi.org/10.1093/oxfordjournals.molbev.a004130

(49) Wright, H. T. The Structural Puzzle of How Serpin Serine Proteinase Inhibitors Work. *BioEssays* **1996**, *18* (6). https://doi.org/10.1002/bies.950180607

(50) Li, D. A.; He, Y.; Guo, Y. J.; Wang, F.; Song, S. X.; Wang, Y.; Yang, F.; He, X. W.; Sun, S. H. Comparative Proteomics Analysis to Annexin B1 DNA and Protein Vaccination in Mice. *Vaccine* **2007**, *25* (5), 932-938. https://doi.org/10.1016/j.vaccine.2006.08.042

SUPPLEMENTARY MATERIAL

Table S1. Parameters for validation of the separation method of GSH and GSSG

Compounds	LOD (nmol L^{-1})	LOQ (nmol L^{-1})	Linearity (nmol L^{-1})	Equation	r^2	Lack of fit ($p<0,05$)
GSH	0.16	0.40	79.52 - 2544.79	y = 34100.78+1396.1x	0.995	0.754
GSSG	0.07	0.27	79.78 - 618.33	y = -56696.30+4599.7x	0.995	0.191

Table S2. Instrumental accuracy of the GSH and GSSG separation in standards and sample along with recovery values for the extraction method

Precision	Type	Levels*	GSH	GSSG
Intra-day (%, n=10)	Standard	N1	10.32	11.23
		N2	3.25	7.87
		N3	2.57	4.56
	Sample	N1	13.15	11.67
		N2	11.82	9.25
		N3	8.33	10.78
Intra-day (%, n=5)	Standard	N1	11.85	11.90
		N2	5.08	10.51
		N3	2.44	9.66
	Sample	N1	11.58	13.12
		N2	9.67	11.37
		N3	8.48	9.98
Recovery (%, mean ± DP, n = 4)[c]		N1	98.69±8.95	97.94±5.67
		N2	101.11±6.38	101.13±4.73
		N3	100.48±4.35	100.47±8.53

*Concentration of standards: N1: 79 nmol L^{-1} of GSH; 79 nmol L^{-1} of GSSG; N2: 1204 nmol L^{-1} of GSH; 349 nmol L^{-1} of GSSG; N3: 2544 nmol L^{-1} of GSH; 618 nmol L^{-1} GSSG.

Table S3. Summary of the ANOVA of the linear model used in the quantification of methylglyoxal

Source of Variance	QS	d.f.	MS	Regression		Lack of fit	
				MS$_R$/MS$_r$	F$_{1,14,95\%}$	MS$_{Lad}$/MS$_{Pe}$	F$_{4,12,95\%}$
Regression	2.23x10^{12}	1	2.23x10^{12}	3408.01	4.60	0.862	3.26
Lack of fit	2.25x10^9	4	5.64x10^8				
Pure Error	7.85x10^9	12	6.54x10^8				
QS$_{Total}$	2.24x10^{12}	17					

QS: quadratic sum; d.f.: degrees of freedom; MS$_R$: regression mean square, MS$_r$: residue mean.

Table S4. Variance explained by principal components (3 components)

	PC1	PC2	PC3
Individual	0.81	0.19	0.00
Cumulative	0.81	1.00	1.00

Table S5. Principal components (3 data points in rows, 3 components in columns)

	PC1	PC2	PC3
Control	-2.32	-0.09	0.00
200 mg	1.31	-0.93	-0.00
300 mg	1.00	1.02	0.00

Table S6. Component loadings (5 dimensions in rows, 3 components in columns)

	PC1	PC2	PC3
GSH	0.43	-0.52	0.25
GSSG	-0.49	-0.13	0.85
GSH/GSSG	0.48	-0.23	0.20
MGO	-0.50	-0.05	-0.23
Carbonyl stress	0.30	0.81	0.34

Table S7. Identified proteins in control group (three technical replicates)

Replicate number	Protein Description	Protein Matched Products	Protein matched Peptides	Protein seq Cover (%)
1	Serum albumin OS=Mus musculus GN=Alb PE=1 SV=3	769	58	65.46
1	Apolipoprotein A-I OS=Mus musculus GN=Apoa1 PE=1 SV=2	194	18	38.26
1	Hemoglobin subunit alpha OS=Mus musculus GN=Hba PE=1 SV=2	70	6	52.82
1	Serotransferrin OS=Mus musculus GN=Tf PE=1 SV=1	541	50	54.52
1	Serine protease inhibitor A3K OS=Mus musculus GN=Serpina3k PE=1 SV=2	238	18	31.58
1	Alpha-2-macroglobulin OS=Mus musculus GN=A2m PE=1 SV=3	699	62	33.71
1	Alpha-1-antitrypsin 1-5 OS=Mus musculus GN=Serpina1e PE=1 SV=1	144	16	34.87
1	Alpha-1-antitrypsin 1-4 OS=Mus musculus GN=Serpina1d PE=2 SV=1	236	24	42.37
1	Carboxylesterase 1C OS=Mus musculus GN=Ces1c PE=1 SV=4	170	18	33.57
1	Alpha-1-antitrypsin 1-3 OS=Mus musculus GN=Serpina1c PE=1 SV=2	201	20	43.2

Table S7. Identified proteins in control group (three technical replicates) (continued)

Replicate number	Protein Description	Protein Matched Products	Protein matched Peptides	Protein seq Cover (%)
1	Alpha-1-antitrypsin 1-1 OS=Mus musculus GN=Serpina1a PE=1 SV=4	201	20	43.1
1	Alpha-1-antitrypsin 1-2 OS=Mus musculus GN=Serpina1b PE=1 SV=2	191	17	36.08
1	Serine protease inhibitor A3M OS=Mus musculus GN=Serpina3m PE=1 SV=2	92	9	16.27
1	Hemoglobin subunit beta-1 OS=Mus musculus GN=Hbb-b1 PE=1 SV=2	39	6	47.62
1	Hemopexin OS=Mus musculus GN=Hpx PE=1 SV=2	140	18	50.22
1	Kininogen-1 OS=Mus musculus GN=Kng1 PE=1 SV=1	100	13	29.05
1	Enolase 1 OS=Saccharomyces cerevisiae (st	119	16	43.48
1	Isoform 3 of Kininogen-1 OS=Mus musculus GN=Kng1	94	12	36.25
1	Isoform LMW of Kininogen-1 OS=Mus musculus GN=Kng1	94	12	40.28
1	Hemoglobin subunit beta-2 OS=Mus musculus GN=Hbb-b2 PE=1 SV=2	28	4	23.81
1	Complement C3 OS=Mus musculus GN=C3 PE=1 SV=3	248	37	25.62
1	Hemoglobin subunit epsilon-Y2 OS=Mus musculus GN=Hbb-y PE=1 SV=2	19	2	6.8
1	Murinoglobulin-1 OS=Mus musculus GN=Mug1 PE=1 SV=3	234	28	19.44
1	Apolipoprotein A-II OS=Mus musculus GN=Apoa2 PE=1 SV=2	40	5	53.92
1	Carboxylesterase 1D OS=Mus musculus GN=Ces1d PE=1 SV=1	34	4	9.2
1	Serine protease inhibitor A3G OS=Mus musculus GN=Serpina3g PE=2 SV=2	37	8	21.82
1	Serine protease inhibitor A3C OS=Mus musculus GN=Serpina3c PE=2 SV=1	33	5	6.47
1	Serine protease inhibitor A3N OS=Mus musculus GN=Serpina3n PE=1 SV=1	33	5	6.46
1	Serine protease inhibitor A3F OS=Mus musculus GN=Serpina3f PE=1 SV=3	34	6	16.18
1	Beta-2-glycoprotein 1 OS=Mus musculus GN=Apoh PE=1 SV=1	60	11	31.59
1	Alpha-2-HS-glycoprotein OS=Mus musculus GN=Ahsg PE=1 SV=1	44	6	26.67
1	Liver carboxylesterase 1 OS=Mus musculus GN=Ces1 PE=2 SV=1	23	2	4.07
1	Ig heavy chain V region AC38 205.12 OS=Mus musculus PE=1 SV=1	11	1	16.1
1	Ig heavy chain V region J558 OS=Mus musculus PE=1 SV=1	11	1	16.24
1	Ig heavy chain V region MOPC 104E OS=Mus musculus PE=1 SV=1	11	1	16.24
1	Murinoglobulin-2 OS=Mus musculus GN=Mug2 PE=2 SV=2	146	18	10.96
1	Apolipoprotein A-IV OS=Mus musculus GN=Apoa4 PE=1 SV=3	60	11	27.34

Table S7. Identified proteins in control group (three technical replicates) (continued)

Replicate number	Protein Description	Protein Matched Products	Protein matched Peptides	Protein seq Cover (%)
1	Isoform 2 of Ig mu chain C region OS=Mus musculus GN=Ighm	80	12	28.21
1	Ig mu chain C region OS=Mus musculus GN=Ighm PE=1 SV=2	80	12	29.52
1	Ig kappa chain V-III region MOPC 70 OS=Mus musculus PE=1 SV=1	18	2	30.63
1	Ig kappa chain V-III region PC 7132 OS=Mus musculus PE=1 SV=1	18	2	30.36
1	Ig kappa chain V-III region 50S10.1 OS=Mus musculus PE=1 SV=1	18	2	30.63
1	Ig kappa chain V-III region PC 2880/PC 1229 OS=Mus musculus PE=1 SV=1	18	2	30.63
1	Vitamin D-binding protein OS=Mus musculus GN=Gc PE=1 SV=2	98	16	30.67
1	Ig kappa chain V-III region PC 6684 OS=Mus musculus PE=1 SV=1	14	1	16.22
1	Ig kappa chain V-III region PC 7769 OS=Mus musculus PE=1 SV=1	14	1	16.22
1	Ig kappa chain V-III region PC 7175 OS=Mus musculus PE=1 SV=1	14	1	16.22
1	Ig kappa chain V-III region PC 2485/PC 4039 OS=Mus musculus PE=1 SV=1	14	1	16.22
1	Ig kappa chain V-III region PC 7940 OS=Mus musculus PE=1 SV=1	14	1	16.22
1	Ig kappa chain V-III region PC 7183 OS=Mus musculus PE=1 SV=1	14	1	16.22
1	Ig kappa chain V-III region PC 7210 OS=Mus musculus PE=1 SV=1	14	1	16.36
1	Ig kappa chain V-III region PC 6308 OS=Mus musculus PE=1 SV=1	14	1	16.22
1	Ig kappa chain V-III region PC 7043 OS=Mus musculus PE=1 SV=1	14	1	16.22
1	Ig kappa chain V-III region CBPC 101 OS=Mus musculus PE=1 SV=1	14	1	16.22
1	Ig kappa chain V-III region PC 3741/TEPC 111 OS=Mus musculus PE=1 SV=1	14	1	16.22
1	Ig kappa chain V-III region TEPC 124 OS=Mus musculus PE=1 SV=1	14	1	16.07
1	Ig kappa chain V-III region PC 2413 OS=Mus musculus PE=1 SV=1	14	1	16.22
1	Clusterin OS=Mus musculus GN=Clu PE=1 SV=1	52	9	26.34
1	Isoform Short of Complement C3 OS=Mus musculus GN=C3	39	7	15.14
1	Apolipoprotein E OS=Mus musculus GN=Apoe PE=1 SV=2	29	5	18.97
1	Complement factor B OS=Mus musculus GN=Cfb PE=1 SV=2	75	12	15.24
1	Fibrinogen alpha chain OS=Mus musculus GN=Fga PE=2 SV=1	61	14	25.73
1	Isoform 2 of Fibrinogen alpha chain OS=Mus musculus GN=Fga	60	13	32.68
1	Corticosteroid-binding globulin OS=Mus musculus GN=Serpina6 PE=1 SV=1	23	4	9.07
1	Ceruloplasmin OS=Mus musculus GN=Cp PE=1 SV=2	109	17	21.39

(continued on next page)

Table S7. Identified proteins in control group (three technical replicates) (continued)

Replicate number	Protein Description	Protein Matched Products	Protein matched Peptides	Protein seq Cover (%)
1	Serum paraoxonase/arylesterase 1 OS=Mus musculus GN=Pon1 PE=1 SV=2	14	3	15.21
1	Beta-2-microglobulin OS=Mus musculus GN=B2m PE=1 SV=2	9	2	14.29
1	Alpha-2-antiplasmin OS=Mus musculus GN=Serpinf2 PE=1 SV=1	35	6	10.59
1	Histidine-rich glycoprotein OS=Mus musculus GN=Hrg PE=1 SV=2	43	10	18.48
1	Fibrinogen gamma chain OS=Mus musculus GN=Fgg PE=1 SV=1	36	7	14.45
1	Complement factor H OS=Mus musculus GN=Cfh PE=1 SV=2	57	11	15.4
1	Plasminogen OS=Mus musculus GN=Plg PE=1 SV=3	72	14	15.52
1	Isoform 2 of Ig gamma-2B chain C region OS=Mus musculus GN=Igh-3	20	5	13.43
1	Ig gamma-2B chain C region OS=Mus musculus GN=Igh-3 PE=1 SV=3	20	5	11.14
1	Mannose-binding protein C OS=Mus musculus GN=Mbl2 PE=2 SV=2	14	2	11.89
1	Prothrombin OS=Mus musculus GN=F2 PE=1 SV=1	38	7	14.72
1	Plasma protease C1 inhibitor OS=Mus musculus GN=Serping1 PE=1 SV=3	28	5	16.67
1	Gelsolin OS=Mus musculus GN=Gsn PE=1 SV=3	52	10	13.08
1	Isoform 2 of Gelsolin OS=Mus musculus GN=Gsn	48	9	13
1	Leucine zipper protein 2 OS=Mus musculus GN=Luzp2 PE=2 SV=1	25	7	33.04
1	Apolipoprotein C-III OS=Mus musculus GN=Apoc3 PE=1 SV=2	3	1	19.19
1	Reversed Sequence 25008	5	1	4.76
1	Lactotransferrin OS=Mus musculus GN=Ltf PE=2 SV=4	16	5	9.05
1	Antithrombin-III OS=Mus musculus GN=Serpinc1 PE=1 SV=1	61	13	28.17
1	Alpha-2-macroglobulin-P OS=Mus musculus GN=A2mp PE=2 SV=2	36	12	8.89
1	Inter-alpha-trypsin inhibitor heavy chain H2 OS=Mus musculus GN=Itih2 PE=1 SV=1	53	9	11.63
1	Heparin cofactor 2 OS=Mus musculus GN=Serpind1 PE=1 SV=1	18	5	11.09
1	Carboxypeptidase N subunit 2 OS=Mus musculus GN=Cpn2 PE=1 SV=2	17	3	5.3
1	Reversed Sequence 12561	14	3	13.39
1	Fibrinogen beta chain OS=Mus musculus GN=Fgb PE=2 SV=1	48	10	25.16
1	Succinate dehydrogenase [ubiquinone] cytochrome b small subunit_ mitochondrial OS=Mus musculus GN=Sdhd PE=2 SV=2	9	2	15.09
1	Reversed Sequence 25034	13	4	15.73
1	Isoform 2 of Alpha-(1_3)-fucosyltransferase 10 OS=Mus musculus GN=Fut10	15	4	17.89

Table S7. Identified proteins in control group (three technical replicates) (continued)

Replicate number	Protein Description	Protein Matched Products	Protein matched Peptides	Protein seq Cover (%)
1	Alpha-(1_3)-fucosyltransferase 10 OS=Mus musculus GN=Fut10 PE=2 SV=1	16	5	19.33
1	Fetuin-B OS=Mus musculus GN=Fetub PE=1 SV=1	14	2	4.9
1	Reversed Sequence 1705	16	4	43.15
1	Transthyretin OS=Mus musculus GN=Ttr PE=1 SV=1	10	2	19.05
1	Complement component C9 OS=Mus musculus GN=C9 PE=1 SV=2	18	6	11.5
1	Ig alpha chain C region OS=Mus musculus PE=1 SV=1	9	1	4.36
1	Isocitrate dehydrogenase [NADP] cytoplasmic OS=Mus musculus GN=Idh1 PE=1 SV=2	17	3	7.25
1	Isoform 3 of Afamin OS=Mus musculus GN=Afm	17	8	15.06
1	Afamin OS=Mus musculus GN=Afm PE=1 SV=2	17	8	15.13
1	Plasma kallikrein OS=Mus musculus GN=Klkb1 PE=1 SV=2	24	7	13.48
1	Zinc-alpha-2-glycoprotein OS=Mus musculus GN=Azgp1 PE=1 SV=2	12	4	12.05
1	Phosphatidylinositol-glycan-specific phospholipase D OS=Mus musculus GN=Gpld1 PE=1 SV=1	38	8	10.63
1	Isoform 4 of DENN domain-containing protein 1B OS=Mus musculus GN=Dennd1b	6	2	9.22
1	Isoform 2 of DENN domain-containing protein 1B OS=Mus musculus GN=Dennd1b	8	3	8.54
1	Proline-rich transmembrane protein 4 OS=Mus musculus GN=Prrt4 PE=2 SV=3	8	2	2.88
2	Serum albumin OS=Mus musculus GN=Alb PE=1 SV=3	793	65	70.23
2	Apolipoprotein A-I OS=Mus musculus GN=Apoa1 PE=1 SV=2	192	19	37.12
2	Serine protease inhibitor A3K OS=Mus musculus GN=Serpina3k PE=1 SV=2	213	16	31.34
2	Alpha-2-macroglobulin OS=Mus musculus GN=A2m PE=1 SV=3	698	63	37.53
2	Hemoglobin subunit alpha OS=Mus musculus GN=Hba PE=1 SV=2	69	5	54.23
2	Alpha-1-antitrypsin 1-4 OS=Mus musculus GN=Serpina1d PE=2 SV=1	215	20	41.16
2	Serotransferrin OS=Mus musculus GN=Tf PE=1 SV=1	549	51	55.81
2	Alpha-1-antitrypsin 1-3 OS=Mus musculus GN=Serpina1c PE=1 SV=2	187	17	39.08
2	Alpha-1-antitrypsin 1-1 OS=Mus musculus GN=Serpina1a PE=1 SV=4	187	17	38.98
2	Alpha-1-antitrypsin 1-2 OS=Mus musculus GN=Serpina1b PE=1 SV=2	198	17	38.98
2	Serine protease inhibitor A3M OS=Mus musculus GN=Serpina3m PE=1 SV=2	96	9	16.27

Table S7. Identified proteins in control group (three technical replicates) (continued)

Replicate number	Protein Description	Protein Matched Products	Protein matched Peptides	Protein seq Cover (%)
2	Alpha-1-antitrypsin 1-5 OS=Mus musculus GN=Serpina1e PE=1 SV=1	125	13	34.87
2	Hemoglobin subunit beta-1 OS=Mus musculus GN=Hbb-b1 PE=1 SV=2	61	8	73.47
2	Hemoglobin subunit beta-2 OS=Mus musculus GN=Hbb-b2 PE=1 SV=2	41	4	21.77
2	Carboxylesterase 1C OS=Mus musculus GN=Ces1c PE=1 SV=4	168	17	34.84
2	Enolase 1 OS=Saccharomyces cerevisiae (st	132	18	45.77
2	Complement C3 OS=Mus musculus GN=C3 PE=1 SV=3	234	36	23.99
2	Hemoglobin subunit epsilon-Y2 OS=Mus musculus GN=Hbb-y PE=1 SV=2	21	2	6.8
2	Hemopexin OS=Mus musculus GN=Hpx PE=1 SV=2	171	23	59.13
2	Beta-2-glycoprotein 1 OS=Mus musculus GN=Apoh PE=1 SV=1	57	10	37.68
2	Murinoglobulin-1 OS=Mus musculus GN=Mug1 PE=1 SV=3	232	29	20.05
2	Kininogen-1 OS=Mus musculus GN=Kng1 PE=1 SV=1	87	13	24.81
2	Isoform 3 of Kininogen-1 OS=Mus musculus GN=Kng1	80	12	30.42
2	Isoform LMW of Kininogen-1 OS=Mus musculus GN=Kng1	80	12	33.8
2	Alpha-2-HS-glycoprotein OS=Mus musculus GN=Ahsg PE=1 SV=1	47	6	29.57
2	Carboxylesterase 1D OS=Mus musculus GN=Ces1d PE=1 SV=1	44	6	11.15
2	Apolipoprotein A-II OS=Mus musculus GN=Apoa2 PE=1 SV=2	31	3	14.71
2	Murinoglobulin-2 OS=Mus musculus GN=Mug2 PE=2 SV=2	157	19	11.72
2	Apolipoprotein A-IV OS=Mus musculus GN=Apoa4 PE=1 SV=3	65	13	36.71
2	Liver carboxylesterase 1 OS=Mus musculus GN=Ces1 PE=2 SV=1	35	5	10.8
2	Corticosteroid-binding globulin OS=Mus musculus GN=Serpina6 PE=1 SV=1	23	5	17.38
2	Isoform 2 of Ig mu chain C region OS=Mus musculus GN=Ighm	73	11	25.05
2	Ig mu chain C region OS=Mus musculus GN=Ighm PE=1 SV=2	73	11	26.21
2	Serine protease inhibitor A3N OS=Mus musculus GN=Serpina3n PE=1 SV=1	55	8	17.46
2	Serine protease inhibitor A3C OS=Mus musculus GN=Serpina3c PE=2 SV=1	43	5	6.47
2	Serine protease inhibitor A3G OS=Mus musculus GN=Serpina3g PE=2 SV=2	43	5	6.14
2	Apolipoprotein E OS=Mus musculus GN=Apoe PE=1 SV=2	30	4	16.4
2	Serine protease inhibitor A3F OS=Mus musculus GN=Serpina3f PE=1 SV=3	38	4	5.84
2	Isoform Short of Complement C3 OS=Mus musculus GN=C3	51	7	16.82

Table S7. Identified proteins in control group (three technical replicates) (continued)

Replicate number	Protein Description	Protein Matched Products	Protein matched Peptides	Protein seq Cover (%)
2	Isoform 2 of Fibrinogen alpha chain OS=Mus musculus GN=Fga	64	13	27.29
2	Fibrinogen alpha chain OS=Mus musculus GN=Fga PE=2 SV=1	64	13	19.26
2	Beta-2-microglobulin OS=Mus musculus GN=B2m PE=1 SV=2	11	2	7.56
2	Ceruloplasmin OS=Mus musculus GN=Cp PE=1 SV=2	125	21	29.88
2	Complement factor B OS=Mus musculus GN=Cfb PE=1 SV=2	77	13	19.97
2	Ig heavy chain V region AC38 205.12 OS=Mus musculus PE=1 SV=1	9	2	16.1
2	Ig heavy chain V region J558 OS=Mus musculus PE=1 SV=1	9	2	16.24
2	Ig heavy chain V region MOPC 104E OS=Mus musculus PE=1 SV=1	9	2	16.24
2	Histidine-rich glycoprotein OS=Mus musculus GN=Hrg PE=1 SV=2	51	9	16.57
2	Clusterin OS=Mus musculus GN=Clu PE=1 SV=1	52	10	20.98
2	Ig kappa chain V-III region MOPC 70 OS=Mus musculus PE=1 SV=1	17	2	30.63
2	Ig kappa chain V-III region PC 7132 OS=Mus musculus PE=1 SV=1	17	2	30.36
2	Ig kappa chain V-III region 50S10.1 OS=Mus musculus PE=1 SV=1	17	2	30.63
2	Ig kappa chain V-III region PC 2880/PC 1229 OS=Mus musculus PE=1 SV=1	17	2	30.63
2	Serum paraoxonase/arylesterase 1 OS=Mus musculus GN=Pon1 PE=1 SV=2	23	5	21.13
2	Vitamin D-binding protein OS=Mus musculus GN=Gc PE=1 SV=2	70	11	22.9
2	Apolipoprotein C-III OS=Mus musculus GN=Apoc3 PE=1 SV=2	9	2	38.38
2	Ig kappa chain V-III region PC 6684 OS=Mus musculus PE=1 SV=1	11	1	16.22
2	Ig kappa chain V-III region PC 7769 OS=Mus musculus PE=1 SV=1	11	1	16.22
2	Ig kappa chain V-III region PC 7175 OS=Mus musculus PE=1 SV=1	11	1	16.22
2	Ig kappa chain V-III region PC 2485/PC 4039 OS=Mus musculus PE=1 SV=1	11	1	16.22
2	Ig kappa chain V-III region PC 7940 OS=Mus musculus PE=1 SV=1	11	1	16.22
2	Ig kappa chain V-III region PC 7183 OS=Mus musculus PE=1 SV=1	11	1	16.22
2	Ig kappa chain V-III region PC 7210 OS=Mus musculus PE=1 SV=1	11	1	16.36
2	Ig kappa chain V-III region PC 6308 OS=Mus musculus PE=1 SV=1	11	1	16.22
2	Ig kappa chain V-III region PC 7043 OS=Mus musculus PE=1 SV=1	11	1	16.22
2	Ig kappa chain V-III region CBPC 101 OS=Mus musculus PE=1 SV=1	11	1	16.22
2	Ig kappa chain V-III region PC 3741/TEPC 111 OS=Mus musculus PE=1 SV=1	11	1	16.22

Table S7. Identified proteins in control group (three technical replicates) (continued)

Replicate number	Protein Description	Protein Matched Products	Protein matched Peptides	Protein seq Cover (%)
2	Ig kappa chain V-III region TEPC 124 OS=Mus musculus PE=1 SV=1	11	1	16.07
2	Ig kappa chain V-III region PC 2413 OS=Mus musculus PE=1 SV=1	11	1	16.22
2	Fibrinogen gamma chain OS=Mus musculus GN=Fgg PE=1 SV=1	46	12	28.44
2	Fibrinogen beta chain OS=Mus musculus GN=Fgb PE=2 SV=1	60	11	23.28
2	Mannose-binding protein C OS=Mus musculus GN=Mbl2 PE=2 SV=2	18	3	15.98
2	Inter-alpha-trypsin inhibitor heavy chain H2 OS=Mus musculus GN=Itih2 PE=1 SV=1	62	12	12.16
2	Isoform 2 of Ig gamma-2B chain C region OS=Mus musculus GN=Igh-3	13	4	12.84
2	Ig gamma-2B chain C region OS=Mus musculus GN=Igh-3 PE=1 SV=3	13	4	10.64
2	Complement component C8 gamma chain OS=Mus musculus GN=C8g PE=1 SV=1	19	3	17.33
2	Fetuin-B OS=Mus musculus GN=Fetub PE=1 SV=1	15	3	9.54
2	Plasminogen OS=Mus musculus GN=Plg PE=1 SV=3	46	10	12.68
2	Antithrombin-III OS=Mus musculus GN=Serpinc1 PE=1 SV=1	48	9	23.23
2	Gelsolin OS=Mus musculus GN=Gsn PE=1 SV=3	64	17	23.33
2	Isoform 2 of Gelsolin OS=Mus musculus GN=Gsn	61	16	23.94
2	Plasma protease C1 inhibitor OS=Mus musculus GN=Serping1 PE=1 SV=3	36	7	24.21
2	Ig kappa chain V-VI region NQ2-6.1 OS=Mus musculus PE=2 SV=1	6	1	14.81
2	Alpha-2-macroglobulin-P OS=Mus musculus GN=A2mp PE=2 SV=2	26	5	4.14
2	Prothrombin OS=Mus musculus GN=F2 PE=1 SV=1	45	12	22.65
2	Alpha-2-antiplasmin OS=Mus musculus GN=Serpinf2 PE=1 SV=1	33	9	21.59
2	Carboxypeptidase N catalytic chain OS=Mus musculus GN=Cpn1 PE=2 SV=1	15	5	15.97
2	Reversed Sequence 25008	10	2	14.63
2	Complement factor H OS=Mus musculus GN=Cfh PE=1 SV=2	51	11	11.35
2	Lumican OS=Mus musculus GN=Lum PE=1 SV=2	8	3	11.24
2	Isoform 2 of Interleukin-1 receptor accessory protein OS=Mus musculus GN=Il1rap	8	2	5.28
2	Interleukin-1 receptor accessory protein OS=Mus musculus GN=Il1rap PE=1 SV=1	8	2	3.33
2	PRKR-interacting protein 1 OS=Mus musculus GN=Prkrip1 PE=1 SV=2	8	2	10.22
2	Carboxypeptidase N subunit 2 OS=Mus musculus GN=Cpn2 PE=1 SV=2	22	5	7.13

Table S7. Identified proteins in control group (three technical replicates) (continued)

Replicate number	Protein Description	Protein Matched Products	Protein matched Peptides	Protein seq Cover (%)
2	Heparin cofactor 2 OS=Mus musculus GN=Serpind1 PE=1 SV=1	12	3	6.07
2	Ras association domain-containing protein 1 OS=Mus musculus GN=Rassf1 PE=2 SV=1	15	5	18.24
2	Isoform 3 of Afamin OS=Mus musculus GN=Afm	40	11	23.73
2	Afamin OS=Mus musculus GN=Afm PE=1 SV=2	40	11	23.85
2	Inter alpha-trypsin inhibitor_ heavy chain 4 OS=Mus musculus GN=Itih4 PE=1 SV=2	35	10	12.21
2	Isoform 2 of Inter alpha-trypsin inhibitor_ heavy chain 4 OS=Mus musculus GN=Itih4	31	9	11.18
2	Zinc-alpha-2-glycoprotein OS=Mus musculus GN=Azgp1 PE=1 SV=2	9	4	7.49
2	Isoform 2 of Afamin OS=Mus musculus GN=Afm	34	8	26.05
2	Inter-alpha-trypsin inhibitor heavy chain H1 OS=Mus musculus GN=Itih1 PE=1 SV=2	27	8	12.57
2	Ig gamma-2A chain C region secreted form OS=Mus musculus PE=1 SV=1	8	4	8.36
2	Protein AMBP OS=Mus musculus GN=Ambp PE=2 SV=2	9	2	9.17
2	Reversed Sequence 22519	5	1	12.57
2	Alpha-enolase OS=Mus musculus GN=Eno1 PE=1 SV=3	10	1	1.38
2	Reversed Sequence 9051	7	2	11.93
2	Reversed Sequence 12908	15	2	5.53
3	Serum albumin OS=Mus musculus GN=Alb PE=1 SV=3	791	64	66.45
3	Apolipoprotein A-I OS=Mus musculus GN=Apoa1 PE=1 SV=2	244	21	46.21
3	Serotransferrin OS=Mus musculus GN=Tf PE=1 SV=1	619	52	51.51
3	Serine protease inhibitor A3K OS=Mus musculus GN=Serpina3k PE=1 SV=2	219	17	33.49
3	Hemoglobin subunit alpha OS=Mus musculus GN=Hba PE=1 SV=2	73	6	55.63
3	Alpha-1-antitrypsin 1-4 OS=Mus musculus GN=Serpina1d PE=2 SV=1	247	21	39.71
3	Alpha-2-macroglobulin OS=Mus musculus GN=A2m PE=1 SV=3	704	58	35.59
3	Alpha-1-antitrypsin 1-2 OS=Mus musculus GN=Serpina1b PE=1 SV=2	225	18	37.77
3	Alpha-1-antitrypsin 1-3 OS=Mus musculus GN=Serpina1c PE=1 SV=2	218	19	39.56
3	Alpha-1-antitrypsin 1-1 OS=Mus musculus GN=Serpina1a PE=1 SV=4	218	19	39.47
3	Alpha-1-antitrypsin 1-5 OS=Mus musculus GN=Serpina1e PE=1 SV=1	140	13	33.41
3	Hemoglobin subunit beta-1 OS=Mus musculus GN=Hbb-b1 PE=1 SV=2	53	7	49.66

Table S7. Identified proteins in control group (three technical replicates) (continued)

Replicate number	Protein Description	Protein Matched Products	Protein matched Peptides	Protein seq Cover (%)
3	Serine protease inhibitor A3M OS=Mus musculus GN=Serpina3m PE=1 SV=2	89	7	16.03
3	Enolase 1 OS=Saccharomyces cerevisiae (st	125	14	29.29
3	Carboxylesterase 1C OS=Mus musculus GN=Ces1c PE=1 SV=4	164	17	32.31
3	Hemoglobin subunit beta-2 OS=Mus musculus GN=Hbb-b2 PE=1 SV=2	35	3	15.65
3	Alpha-2-HS-glycoprotein OS=Mus musculus GN=Ahsg PE=1 SV=1	48	4	22.61
3	Hemopexin OS=Mus musculus GN=Hpx PE=1 SV=2	156	21	44.78
3	Complement C3 OS=Mus musculus GN=C3 PE=1 SV=3	303	43	28.2
3	Murinoglobulin-1 OS=Mus musculus GN=Mug1 PE=1 SV=3	300	37	27.03
3	Apolipoprotein A-II OS=Mus musculus GN=Apoa2 PE=1 SV=2	36	3	34.31
3	Beta-2-glycoprotein 1 OS=Mus musculus GN=Apoh PE=1 SV=1	80	12	44.35
3	Hemoglobin subunit epsilon-Y2 OS=Mus musculus GN=Hbb-y PE=1 SV=2	18	2	6.8
3	Kininogen-1 OS=Mus musculus GN=Kng1 PE=1 SV=1	107	16	32.83
3	Isoform 3 of Kininogen-1 OS=Mus musculus GN=Kng1	99	15	41.46
3	Isoform LMW of Kininogen-1 OS=Mus musculus GN=Kng1	90	14	43.29
3	Apolipoprotein A-IV OS=Mus musculus GN=Apoa4 PE=1 SV=3	67	13	31.9
3	Murinoglobulin-2 OS=Mus musculus GN=Mug2 PE=2 SV=2	193	21	10.96
3	Corticosteroid-binding globulin OS=Mus musculus GN=Serpina6 PE=1 SV=1	44	6	16.37
3	Clusterin OS=Mus musculus GN=Clu PE=1 SV=1	72	14	41.07
3	Isoform 2 of Ig mu chain C region OS=Mus musculus GN=Ighm	78	11	25.47
3	Ig mu chain C region OS=Mus musculus GN=Ighm PE=1 SV=2	78	11	26.65
3	Ig kappa chain V-III region MOPC 70 OS=Mus musculus PE=1 SV=1	17	2	30.63
3	Ig kappa chain V-III region PC 7132 OS=Mus musculus PE=1 SV=1	17	2	30.36
3	Ig kappa chain V-III region 50S10.1 OS=Mus musculus PE=1 SV=1	17	2	30.63
3	Ig kappa chain V-III region PC 2880/PC 1229 OS=Mus musculus PE=1 SV=1	17	2	30.63
3	Antithrombin-III OS=Mus musculus GN=Serpinc1 PE=1 SV=1	64	11	21.08
3	Carboxylesterase 1D OS=Mus musculus GN=Ces1d PE=1 SV=1	44	4	9.2
3	Serine protease inhibitor A3F OS=Mus musculus GN=Serpina3f PE=1 SV=3	33	4	9.44
3	Ig kappa chain V-III region PC 6684 OS=Mus musculus PE=1 SV=1	11	1	16.22
3	Ig kappa chain V-III region PC 7769 OS=Mus musculus PE=1 SV=1	11	1	16.22

Table S7. Identified proteins in control group (three technical replicates) (continued)

Replicate number	Protein Description	Protein Matched Products	Protein matched Peptides	Protein seq Cover (%)
3	Ig kappa chain V-III region PC 7175 OS=Mus musculus PE=1 SV=1	11	1	16.22
3	Ig kappa chain V-III region PC 2485/PC 4039 OS=Mus musculus PE=1 SV=1	11	1	16.22
3	Ig kappa chain V-III region PC 7940 OS=Mus musculus PE=1 SV=1	11	1	16.22
3	Ig kappa chain V-III region PC 7183 OS=Mus musculus PE=1 SV=1	11	1	16.22
3	Ig kappa chain V-III region PC 7210 OS=Mus musculus PE=1 SV=1	11	1	16.36
3	Ig kappa chain V-III region PC 6308 OS=Mus musculus PE=1 SV=1	11	1	16.22
3	Ig kappa chain V-III region PC 7043 OS=Mus musculus PE=1 SV=1	11	1	16.22
3	Ig kappa chain V-III region CBPC 101 OS=Mus musculus PE=1 SV=1	11	1	16.22
3	Ig kappa chain V-III region PC 3741/TEPC 111 OS=Mus musculus PE=1 SV=1	11	1	16.22
3	Ig kappa chain V-III region TEPC 124 OS=Mus musculus PE=1 SV=1	11	1	16.07
3	Ig kappa chain V-III region PC 2413 OS=Mus musculus PE=1 SV=1	11	1	16.22
3	Serine protease inhibitor A3C OS=Mus musculus GN=Serpina3c PE=2 SV=1	30	3	6.24
3	Serine protease inhibitor A3N OS=Mus musculus GN=Serpina3n PE=1 SV=1	30	3	6.22
3	Serine protease inhibitor A3G OS=Mus musculus GN=Serpina3g PE=2 SV=2	30	3	5.91
3	Isoform Short of Complement C3 OS=Mus musculus GN=C3	69	9	21.87
3	Fibrinogen gamma chain OS=Mus musculus GN=Fgg PE=1 SV=1	71	11	28.67
3	Apolipoprotein E OS=Mus musculus GN=Apoe PE=1 SV=2	35	7	30.23
3	Ig heavy chain V region MOPC 104E OS=Mus musculus PE=1 SV=1	15	3	44.44
3	Mannose-binding protein C OS=Mus musculus GN=Mbl2 PE=2 SV=2	24	3	15.98
3	Ig heavy chain V region AC38 205.12 OS=Mus musculus PE=1 SV=1	13	2	27.97
3	Ig heavy chain V region J558 OS=Mus musculus PE=1 SV=1	13	2	28.21
3	Histidine-rich glycoprotein OS=Mus musculus GN=Hrg PE=1 SV=2	56	11	18.48
3	Serum paraoxonase/arylesterase 1 OS=Mus musculus GN=Pon1 PE=1 SV=2	16	2	8.45
3	Liver carboxylesterase 1 OS=Mus musculus GN=Ces1 PE=2 SV=1	27	2	2.83
3	Isoform 2 of Fibrinogen alpha chain OS=Mus musculus GN=Fga	71	13	31.42
3	Fibrinogen alpha chain OS=Mus musculus GN=Fga PE=2 SV=1	74	14	24.08
3	Apolipoprotein C-III OS=Mus musculus GN=Apoc3 PE=1 SV=2	6	1	19.19

Table S7. Identified proteins in control group (three technical replicates) (continued)

Replicate number	Protein Description	Protein Matched Products	Protein matched Peptides	Protein seq Cover (%)
3	Vitamin D-binding protein OS=Mus musculus GN=Gc PE=1 SV=2	96	13	25.21
3	Fibrinogen beta chain OS=Mus musculus GN=Fgb PE=2 SV=1	67	13	30.35
3	Alpha-2-antiplasmin OS=Mus musculus GN=Serpinf2 PE=1 SV=1	57	9	21.38
3	Prothrombin OS=Mus musculus GN=F2 PE=1 SV=1	87	15	31.88
3	Ceruloplasmin OS=Mus musculus GN=Cp PE=1 SV=2	92	12	14.89
3	Complement factor B OS=Mus musculus GN=Cfb PE=1 SV=2	89	16	26.02
3	Inter-alpha-trypsin inhibitor heavy chain H2 OS=Mus musculus GN=Itih2 PE=1 SV=1	69	10	13.53
3	Fetuin-B OS=Mus musculus GN=Fetub PE=1 SV=1	32	6	20.1
3	Beta-2-microglobulin OS=Mus musculus GN=B2m PE=1 SV=2	7	1	7.56
3	Protein AMBP OS=Mus musculus GN=Ambp PE=2 SV=2	16	3	13.75
3	Isoform 2 of Ig gamma-2B chain C region OS=Mus musculus GN=Igh-3	15	3	16.72
3	Ig gamma-2B chain C region OS=Mus musculus GN=Igh-3 PE=1 SV=3	15	3	13.86
3	Plasminogen OS=Mus musculus GN=Plg PE=1 SV=3	78	18	22.17
3	Plasma protease C1 inhibitor OS=Mus musculus GN=Serping1 PE=1 SV=3	26	5	13.69
3	Gelsolin OS=Mus musculus GN=Gsn PE=1 SV=3	54	12	15.77
3	Complement factor H OS=Mus musculus GN=Cfh PE=1 SV=2	68	17	23.26
3	Isoform 2 of Gelsolin OS=Mus musculus GN=Gsn	51	11	15.87
3	Ig kappa chain V-VI region NQ2-6.1 OS=Mus musculus PE=2 SV=1	6	1	14.81
3	Major urinary proteins 11 and 8 (Fragment) OS=Mus musculus GN=Mup8 PE=2 SV=1	19	4	27.15
3	Major urinary protein 6 OS=Mus musculus GN=Mup6 PE=1 SV=2	19	4	22.78
3	Major urinary protein 17 OS=Mus musculus GN=Mup17 PE=2 SV=2	16	3	22.78
3	Carboxypeptidase N subunit 2 OS=Mus musculus GN=Cpn2 PE=1 SV=2	28	6	10.6
3	Lumican OS=Mus musculus GN=Lum PE=1 SV=2	22	5	13.61
3	Epidermal growth factor receptor OS=Mus musculus GN=Egfr PE=1 SV=1	31	6	5.12
3	Alpha-2-macroglobulin-P OS=Mus musculus GN=A2mp PE=2 SV=2	24	7	5.97
3	Glutathione peroxidase 3 OS=Mus musculus GN=Gpx3 PE=2 SV=2	6	2	10.18
3	Isoform 3 of Afamin OS=Mus musculus GN=Afm	33	9	22.42
3	Afamin OS=Mus musculus GN=Afm PE=1 SV=2	33	9	22.53

Table S7. Identified proteins in control group (three technical replicates) (continued)

Replicate number	Protein Description	Protein Matched Products	Protein matched Peptides	Protein seq Cover (%)
3	Keratin_ type II cytoskeletal 75 OS=Mus musculus GN=Krt75 PE=1 SV=1	10	1	2.18
3	Keratin_ type II cytoskeletal 6A OS=Mus musculus GN=Krt6a PE=1 SV=3	15	2	3.98
3	Keratin_ type II cytoskeletal 6B OS=Mus musculus GN=Krt6b PE=1 SV=3	10	1	2.14
3	Keratin_ type II cytoskeletal 5 OS=Mus musculus GN=Krt5 PE=1 SV=1	24	4	8.28
3	Heparin cofactor 2 OS=Mus musculus GN=Serpind1 PE=1 SV=1	18	6	15.27
3	Carboxypeptidase N catalytic chain OS=Mus musculus GN=Cpn1 PE=2 SV=1	15	5	19.04
3	Major urinary protein 2 OS=Mus musculus GN=Mup2 PE=1 SV=1	12	3	16.11
3	Major urinary protein 1 OS=Mus musculus GN=Mup1 PE=1 SV=1	12	3	16.11
3	Phosphatidylinositol-glycan-specific phospholipase D OS=Mus musculus GN=Gpld1 PE=1 SV=1	30	6	8.6
3	Isoform 2 of Afamin OS=Mus musculus GN=Afm	30	6	20
3	Plasma kallikrein OS=Mus musculus GN=Klkb1 PE=1 SV=2	33	12	20.85
3	Isoform 2 of Inter alpha-trypsin inhibitor_ heavy chain 4 OS=Mus musculus GN=Itih4	51	12	15.95
3	Inter alpha-trypsin inhibitor_ heavy chain 4 OS=Mus musculus GN=Itih4 PE=1 SV=2	51	12	15.29
3	Angiotensinogen OS=Mus musculus GN=Agt PE=1 SV=1	11	2	4.61
3	Isocitrate dehydrogenase [NADP] cytoplasmic OS=Mus musculus GN=Idh1 PE=1 SV=2	12	2	5.56
3	Ig kappa chain V-II region 26-10 OS=Mus musculus PE=1 SV=1	7	1	11.5
3	Complement C5 OS=Mus musculus GN=C5 PE=1 SV=2	52	14	8.63
3	Isoform 2 of Interleukin-1 receptor accessory protein OS=Mus musculus GN=Il1rap	15	5	11.11
3	Interleukin-1 receptor accessory protein OS=Mus musculus GN=Il1rap PE=1 SV=1	15	6	10
3	Complement component C9 OS=Mus musculus GN=C9 PE=1 SV=2	26	9	18.61
3	Complement C1q subcomponent subunit B OS=Mus musculus GN=C1qb PE=1 SV=2	9	3	15.42
3	Carboxylesterase 1E OS=Mus musculus GN=Ces1e PE=1 SV=1	10	1	1.25
3	Proline-rich transmembrane protein 4 OS=Mus musculus GN=Prrt4 PE=2 SV=3	8	2	2.99
3	Isoform 5 of Cation channel sperm-associated protein subunit gamma 1 OS=Mus musculus GN=Catsperg1	5	2	2.23
3	Isoform 3 of Cation channel sperm-associated protein subunit gamma 1 OS=Mus musculus GN=Catsperg1	5	2	1

Table S7. Identified proteins in control group (three technical replicates) (continued)

Replicate number	Protein Description	Protein Matched Products	Protein matched Peptides	Protein seq Cover (%)
3	Isoform 2 of Cation channel sperm-associated protein subunit gamma 1 OS=Mus musculus GN=Catsperg1	5	2	0.73
3	Cation channel sperm-associated protein subunit gamma 1 OS=Mus musculus GN=Catsperg1 PE=2 SV=1	5	2	0.7
3	Cation channel sperm-associated protein subunit gamma 2 OS=Mus musculus GN=Catsperg2 PE=1 SV=1	4	1	0.7
3	Isoform 6 of Cation channel sperm-associated protein subunit gamma 1 OS=Mus musculus GN=Catsperg1	4	1	4.17
3	Isoform 4 of Cation channel sperm-associated protein subunit gamma 1 OS=Mus musculus GN=Catsperg1	4	1	3.7
3	Reversed Sequence 15288	2	1	8.97
3	Isoform 3 of DnaJ homolog subfamily A member 3_ mitochondrial OS=Mus musculus GN=Dnaja3	6	2	6.99
3	DnaJ homolog subfamily A member 3_ mitochondrial OS=Mus musculus GN=Dnaja3 PE=1 SV=1	6	2	6.25
3	H-2 class I histocompatibility antigen_ Q10 alpha chain OS=Mus musculus GN=H2-Q10 PE=1 SV=3	12	2	7.69
3	Isoform 5 of Actin-binding LIM protein 1 OS=Mus musculus GN=Ablim1	17	4	19.4
3	Toll/interleukin-1 receptor domain-containing adapter protein OS=Mus musculus GN=Tirap PE=1 SV=1	5	2	7.47
3	Isoform 2 of Protein Z-dependent protease inhibitor OS=Mus musculus GN=Serpina10	10	3	4.31
3	Protein Z-dependent protease inhibitor OS=Mus musculus GN=Serpina10 PE=1 SV=1	10	3	3.79
3	Inter-alpha-trypsin inhibitor heavy chain H1 OS=Mus musculus GN=Itih1 PE=1 SV=2	26	6	7.28
3	Reversed Sequence 12561	10	2	4.39
3	Reversed Sequence 21325	7	2	16.73
3	Reversed Sequence 11292	16	4	12.07
3	Isoform 3 of Uncharacterized protein C1orf112 homolog OS=Mus musculus	12	5	4.14
3	Isoform 2 of Uncharacterized protein C1orf112 homolog OS=Mus musculus	12	5	3.78
3	Uncharacterized protein C1orf112 homolog OS=Mus musculus PE=2 SV=2	12	5	3.88
3	Transcription elongation factor A protein-like 1 OS=Mus musculus GN=Tceal1 PE=2 SV=1	5	1	7.27
3	Reversed Sequence 1868	3	1	8.45

Table S8. Identified proteins in group treated with 200 mg kg^{-1} day^{-1} of diacetyl (three technical replicates)

Replicate number	Protein description	Protein Matched Products	Protein Matched Peptides	Protein seqCover (%)
1	Apolipoprotein A-I OS=Mus musculus GN=Apoa1 PE=1 SV=2	153	14	54.55
1	Serum albumin OS=Mus musculus GN=Alb PE=1 SV=3	477	43	56.58
1	Hemoglobin subunit alpha OS=Mus musculus GN=Hba PE=1 SV=2	83	8	55.63
1	Hemoglobin subunit beta-1 OS=Mus musculus GN=Hbb-b1 PE=1 SV=2	56	7	59.18
1	Alpha-1-antitrypsin 1-4 OS=Mus musculus GN=Serpina1d PE=2 SV=1	181	19	46.49
1	Serotransferrin OS=Mus musculus GN=Tf PE=1 SV=1	379	44	47.06
1	Serine protease inhibitor A3K OS=Mus musculus GN=Serpina3k PE=1 SV=2	141	13	37.56
1	Hemoglobin subunit beta-2 OS=Mus musculus GN=Hbb-b2 PE=1 SV=2	35	5	35.37
1	Alpha-1-antitrypsin 1-5 OS=Mus musculus GN=Serpina1e PE=1 SV=1	111	12	32.45
1	Alpha-1-antitrypsin 1-2 OS=Mus musculus GN=Serpina1b PE=1 SV=2	161	18	44.55
1	Alpha-2-macroglobulin OS=Mus musculus GN=A2m PE=1 SV=3	364	37	29.1
1	Alpha-1-antitrypsin 1-3 OS=Mus musculus GN=Serpina1c PE=1 SV=2	151	19	44.66
1	Alpha-1-antitrypsin 1-1 OS=Mus musculus GN=Serpina1a PE=1 SV=4	151	19	44.55
1	Apolipoprotein A-IV OS=Mus musculus GN=Apoa4 PE=1 SV=3	81	11	36.71
1	Hemoglobin subunit epsilon-Y2 OS=Mus musculus GN=Hbb-y PE=1 SV=2	11	1	6.8
1	Enolase 1 OS=Saccharomyces cerevisiae (st	124	15	41.88
1	Serine protease inhibitor A3M OS=Mus musculus GN=Serpina3m PE=1 SV=2	55	7	15.55
1	Apolipoprotein A-II OS=Mus musculus GN=Apoa2 PE=1 SV=2	28	2	14.71
1	Carboxylesterase 1C OS=Mus musculus GN=Ces1c PE=1 SV=4	79	13	31.59
1	Apolipoprotein E OS=Mus musculus GN=Apoe PE=1 SV=2	30	5	16.08
1	Murinoglobulin-1 OS=Mus musculus GN=Mug1 PE=1 SV=3	158	25	18.83
1	Complement C3 OS=Mus musculus GN=C3 PE=1 SV=3	124	23	19.18
1	Transthyretin OS=Mus musculus GN=Ttr PE=1 SV=1	34	5	46.26

(continued on next page)

Table S8. Identified proteins in group treated with 200 mg kg^{-1} day^{-1} of diacetyl (three technical replicates) (cont.)

Replicate number	Protein description	Protein Matched Products	Protein Matched Peptides	Protein seqCover (%)
1	Isoform 2 of Fibrinogen alpha chain OS=Mus musculus GN=Fga	64	12	26.03
1	Fibrinogen alpha chain OS=Mus musculus GN=Fga PE=2 SV=1	64	12	18.38
1	Serine protease inhibitor A3G OS=Mus musculus GN=Serpina3g PE=2 SV=2	36	7	15.45
1	Serine protease inhibitor A3C OS=Mus musculus GN=Serpina3c PE=2 SV=1	33	4	6.47
1	Serine protease inhibitor A3N OS=Mus musculus GN=Serpina3n PE=1 SV=1	33	4	6.46
1	Serine protease inhibitor A3F OS=Mus musculus GN=Serpina3f PE=1 SV=3	34	7	16.85
1	Alpha-2-HS-glycoprotein OS=Mus musculus GN=Ahsg PE=1 SV=1	24	1	6.09
1	Kininogen-1 OS=Mus musculus GN=Kng1 PE=1 SV=1	67	11	23.45
1	Clusterin OS=Mus musculus GN=Clu PE=1 SV=1	40	6	14.51
1	Isoform 3 of Kininogen-1 OS=Mus musculus GN=Kng1	58	9	25.63
1	Carboxylesterase 1D OS=Mus musculus GN=Ces1d PE=1 SV=1	25	4	9.91
1	Antithrombin-III OS=Mus musculus GN=Serpinc1 PE=1 SV=1	65	17	42.58
1	Murinoglobulin-2 OS=Mus musculus GN=Mug2 PE=2 SV=2	88	13	9.3
1	Isoform LMW of Kininogen-1 OS=Mus musculus GN=Kng1	48	8	25.69
1	Major urinary proteins 11 and 8 (Fragment) OS=Mus musculus GN=Mup8 PE=2 SV=1	7	3	27.81
1	Major urinary protein 1 OS=Mus musculus GN=Mup1 PE=1 SV=1	7	3	23.33
1	Major urinary protein 17 OS=Mus musculus GN=Mup17 PE=2 SV=2	7	3	23.33
1	Major urinary protein 6 OS=Mus musculus GN=Mup6 PE=1 SV=2	7	3	23.33
1	Major urinary protein 2 OS=Mus musculus GN=Mup2 PE=1 SV=1	6	2	14.44
1	Hemopexin OS=Mus musculus GN=Hpx PE=1 SV=2	47	9	31.96
1	Vitamin D-binding protein OS=Mus musculus GN=Gc PE=1 SV=2	59	9	13.45
1	Major urinary protein 5 OS=Mus musculus GN=Mup5 PE=2 SV=1	5	1	6.11
1	Liver carboxylesterase 1 OS=Mus musculus GN=Ces1 PE=2 SV=1	11	1	1.59

Table S8. Identified proteins in group treated with 200 mg kg^{-1} day^{-1} of diacetyl (three technical replicates) (cont.)

Replicate number	Protein description	Protein Matched Products	Protein Matched Peptides	Protein seqCover (%)
1	Isoform Short of Complement C3 OS=Mus musculus GN=C3	15	4	9.72
1	Ig heavy chain V region AC38 205.12 OS=Mus musculus PE=1 SV=1	5	1	16.1
1	Ig heavy chain V region J558 OS=Mus musculus PE=1 SV=1	5	1	16.24
1	Ig heavy chain V region MOPC 104E OS=Mus musculus PE=1 SV=1	5	1	16.24
1	Zinc-alpha-2-glycoprotein OS=Mus musculus GN=Azgp1 PE=1 SV=2	7	3	7.82
1	Histidine-rich glycoprotein OS=Mus musculus GN=Hrg PE=1 SV=2	29	5	11.24
1	Alpha-2-antiplasmin OS=Mus musculus GN=Serpinf2 PE=1 SV=1	14	5	14.26
1	Gelsolin OS=Mus musculus GN=Gsn PE=1 SV=3	54	10	16.28
1	Isoform 2 of Gelsolin OS=Mus musculus GN=Gsn	52	9	16.42
1	Serum paraoxonase/arylesterase 1 OS=Mus musculus GN=Pon1 PE=1 SV=2	8	3	12.96
1	Beta-2-glycoprotein 1 OS=Mus musculus GN=Apoh PE=1 SV=1	35	8	35.94
1	Isoform 2 of Ig mu chain C region OS=Mus musculus GN=Ighm	31	7	17.26
1	Ig mu chain C region OS=Mus musculus GN=Ighm PE=1 SV=2	31	7	18.06
1	Ig kappa chain V-III region PC 6684 OS=Mus musculus PE=1 SV=1	4	1	16.22
1	Ig kappa chain V-III region PC 7769 OS=Mus musculus PE=1 SV=1	4	1	16.22
1	Ig kappa chain V-III region PC 7175 OS=Mus musculus PE=1 SV=1	4	1	16.22
1	Ig kappa chain V-III region PC 2485/PC 4039 OS=Mus musculus PE=1 SV=1	4	1	16.22
1	Ig kappa chain V-III region PC 7940 OS=Mus musculus PE=1 SV=1	4	1	16.22
1	Ig kappa chain V-III region PC 7183 OS=Mus musculus PE=1 SV=1	4	1	16.22
1	Ig kappa chain V-III region PC 7210 OS=Mus musculus PE=1 SV=1	4	1	16.36
1	Ig kappa chain V-III region PC 6308 OS=Mus musculus PE=1 SV=1	4	1	16.22
1	Ig kappa chain V-III region PC 7043 OS=Mus musculus PE=1 SV=1	4	1	16.22

Table S8. Identified proteins in group treated with 200 mg kg^{-1} day^{-1} of diacetyl (three technical replicates) (cont.)

Replicate number	Protein description	Protein Matched Products	Protein Matched Peptides	Protein seqCover (%)
1	Ig kappa chain V-III region CBPC 101 OS=Mus musculus PE=1 SV=1	4	1	16.22
1	Ig kappa chain V-III region PC 3741/TEPC 111 OS=Mus musculus PE=1 SV=1	4	1	16.22
1	Ig kappa chain V-III region TEPC 124 OS=Mus musculus PE=1 SV=1	4	1	16.07
1	Ig kappa chain V-III region MOPC 70 OS=Mus musculus PE=1 SV=1	4	1	16.22
1	Ig kappa chain V-III region PC 7132 OS=Mus musculus PE=1 SV=1	4	1	16.07
1	Ig kappa chain V-III region PC 2413 OS=Mus musculus PE=1 SV=1	4	1	16.22
1	Ig kappa chain V-III region 50S10.1 OS=Mus musculus PE=1 SV=1	4	1	16.22
1	Ig kappa chain V-III region PC 2880/PC 1229 OS=Mus musculus PE=1 SV=1	4	1	16.22
1	Fibrinogen beta chain OS=Mus musculus GN=Fgb PE=2 SV=1	43	10	24.53
1	Fetuin-B OS=Mus musculus GN=Fetub PE=1 SV=1	13	5	15.98
1	Plasminogen OS=Mus musculus GN=Plg PE=1 SV=3	52	11	15.15
1	Prothrombin OS=Mus musculus GN=F2 PE=1 SV=1	36	11	19.09
1	Complement factor B OS=Mus musculus GN=Cfb PE=1 SV=2	36	10	14.32
1	Ceruloplasmin OS=Mus musculus GN=Cp PE=1 SV=2	58	15	18.38
1	Complement component C9 OS=Mus musculus GN=C9 PE=1 SV=2	14	5	9.49
1	Isoform 2 of Complement factor D OS=Mus musculus GN=Cfd	12	2	13.95
1	Complement factor D OS=Mus musculus GN=Cfd PE=1 SV=1	12	2	13.9
1	Reversed Sequence 5196	11	2	20.12
1	Inter-alpha-trypsin inhibitor heavy chain H2 OS=Mus musculus GN=Itih2 PE=1 SV=1	37	10	11.21
1	Corticosteroid-binding globulin OS=Mus musculus GN=Serpina6 PE=1 SV=1	12	6	12.59
1	Lumican OS=Mus musculus GN=Lum PE=1 SV=2	11	6	17.46
1	Reversed Sequence 9591	46	15	31.82
1	Plasma protease C1 inhibitor OS=Mus musculus GN=Serping1 PE=1 SV=3	19	3	10.32

Table S8. Identified proteins in group treated with 200 mg kg⁻¹ day⁻¹ of diacetyl (three technical replicates) (cont.)

Replicate number	Protein description	Protein Matched Products	Protein Matched Peptides	Protein seqCover (%)
1	Carboxypeptidase N catalytic chain OS=Mus musculus GN=Cpn1 PE=2 SV=1	12	6	18.82
1	Isoform D of Tumor necrosis factor receptor superfamily member 18 OS=Mus musculus GN=Tnfrsf18	5	1	12.12
1	Isoform C of Tumor necrosis factor receptor superfamily member 18 OS=Mus musculus GN=Tnfrsf18	5	1	7.21
1	Isoform B of Tumor necrosis factor receptor superfamily member 18 OS=Mus musculus GN=Tnfrsf18	5	1	5.44
1	Tumor necrosis factor receptor superfamily member 18 OS=Mus musculus GN=Tnfrsf18 PE=1 SV=1	5	1	7.02
1	Isoform 2 of Ig gamma-2B chain C region OS=Mus musculus GN=Igh-3	8	3	4.78
1	Ig gamma-2B chain C region OS=Mus musculus GN=Igh-3 PE=1 SV=3	8	3	3.96
1	Reversed Sequence 147	8	2	14.29
1	Myelin protein zero-like protein 1 OS=Mus musculus GN=Mpzl1 PE=1 SV=1	7	4	25.93
1	U3 small nucleolar RNA-associated protein 14 homolog A OS=Mus musculus GN=Utp14a PE=1 SV=1	17	5	13.17
1	AP-3 complex subunit mu-1 OS=Mus musculus GN=Ap3m1 PE=1 SV=1	4	1	3.59
1	H-2 class I histocompatibility antigen_ Q10 alpha chain OS=Mus musculus GN=H2-Q10 PE=1 SV=3	6	1	4.62
1	Heparin cofactor 2 OS=Mus musculus GN=Serpind1 PE=1 SV=1	12	5	7.95
1	Isoform 2 of Myelin protein zero-like protein 1 OS=Mus musculus GN=Mpzl1	4	2	23.67
1	Isoform Gamma of Prostaglandin E2 receptor EP3 subtype OS=Mus musculus GN=Ptger3	6	2	10.71
1	Isoform Beta of Prostaglandin E2 receptor EP3 subtype OS=Mus musculus GN=Ptger3	6	2	10.8
1	Prostaglandin E2 receptor EP3 subtype OS=Mus musculus GN=Ptger3 PE=1 SV=1	6	2	10.68
1	Alpha-2-macroglobulin-P OS=Mus musculus GN=A2mp PE=2 SV=2	19	8	8.62
1	Inter alpha-trypsin inhibitor_ heavy chain 4 OS=Mus musculus GN=Itih4 PE=1 SV=2	25	10	7.86
1	Isoform 2 of Inter alpha-trypsin inhibitor_ heavy chain 4 OS=Mus musculus GN=Itih4	25	9	8.19
1	Proline-rich transmembrane protein 4 OS=Mus musculus GN=Prrt4 PE=2 SV=3	5	2	2.33
1	Reversed Sequence 10110	8	3	8.58

Table S8. Identified proteins in group treated with 200 mg kg^{-1} day^{-1} of diacetyl (three technical replicates) (cont.)

Replicate number	Protein description	Protein Matched Products	Protein Matched Peptides	Protein seqCover (%)
1	Isoform 3 of Protein CASC4 OS=Mus musculus GN=Casc4	14	4	8.38
1	Isoform 2 of Protein CASC4 OS=Mus musculus GN=Casc4	14	4	7.21
1	Protein CASC4 OS=Mus musculus GN=Casc4 PE=2 SV=1	14	4	6.67
1	Biotin--protein ligase OS=Mus musculus GN=Hlcs PE=2 SV=1	6	3	5.54
1	Isoform 4 of Coiled-coil domain-containing protein 33 OS=Mus musculus GN=Ccdc33	6	3	5.75
1	Isoform 3 of Coiled-coil domain-containing protein 33 OS=Mus musculus GN=Ccdc33	6	3	5.75
1	Coiled-coil domain-containing protein 33 OS=Mus musculus GN=Ccdc33 PE=2 SV=2	6	3	4.26
1	Isoform 4 of Interleukin-1 receptor-associated kinase-like 2 OS=Mus musculus GN=Irak2	11	5	10.23
1	Isoform 2 of Interleukin-1 receptor-associated kinase-like 2 OS=Mus musculus GN=Irak2	11	5	8.54
1	Interleukin-1 receptor-associated kinase-like 2 OS=Mus musculus GN=Irak2 PE=2 SV=2	11	5	7.88
1	FERM_ RhoGEF and pleckstrin domain-containing protein 2 OS=Mus musculus GN=Farp2 PE=1 SV=2	16	9	6.76
1	Fibronectin OS=Mus musculus GN=Fn1 PE=1 SV=4	47	19	9.04
1	tRNA-dihydrouridine(16/17) synthase [NAD(P)(+)]-like OS=Mus musculus GN=Dus1l PE=2 SV=1	6	2	7.79
1	Angiotensinogen OS=Mus musculus GN=Agt PE=1 SV=1	11	3	4.61
1	Zinc finger protein 474 OS=Mus musculus GN=Znf474 PE=2 SV=2	3	2	6.34
1	Complement factor H OS=Mus musculus GN=Cfh PE=1 SV=2	20	8	10.05
1	Isoform 5 of Coiled-coil domain-containing protein 33 OS=Mus musculus GN=Ccdc33	1	1	19.08
1	Short-chain specific acyl-CoA dehydrogenase_ mitochondrial OS=Mus musculus GN=Acads PE=1 SV=2	7	2	10.92
1	Spermatogenesis-associated protein 24 OS=Mus musculus GN=Spata24 PE=1 SV=1	6	2	11.71
1	Proteasome subunit beta type-8 OS=Mus musculus GN=Psmb8 PE=1 SV=2	16	6	28.62
1	Opticin OS=Mus musculus GN=Optc PE=2 SV=2	3	1	14.94
1	Fibrinogen gamma chain OS=Mus musculus GN=Fgg PE=1 SV=1	23	6	23.17
1	Isoform 2 of Serine racemase OS=Mus musculus GN=Srr	9	3	14.65
1	Serine racemase OS=Mus musculus GN=Srr PE=1 SV=1	9	3	13.57

Table S8. Identified proteins in group treated with 200 mg kg^{-1} day^{-1} of diacetyl (three technical replicates) (cont.)

Replicate number	Protein description	Protein Matched Products	Protein Matched Peptides	Protein seqCover (%)
1	Protein unc-119 homolog A OS=Mus musculus GN=Unc119 PE=1 SV=1	6	1	7.5
1	FERM_ RhoGEF and pleckstrin domain-containing protein 1 OS=Mus musculus GN=Farp1 PE=1 SV=1	15	8	2.96
1	Deoxyribonuclease-2-beta OS=Mus musculus GN=Dnase2b PE=2 SV=1	9	3	12.99
1	Isoform 2 of E3 ubiquitin-protein ligase SH3RF1 OS=Mus musculus GN=Sh3rf1	17	6	8.93
1	E3 ubiquitin-protein ligase SH3RF1 OS=Mus musculus GN=Sh3rf1 PE=1 SV=2	17	6	8.63
1	DnaJ homolog subfamily C member 14 OS=Mus musculus GN=Dnajc14 PE=2 SV=2	12	3	2.84
1	Nascent polypeptide-associated complex subunit alpha_ muscle-specific form OS=Mus musculus GN=Naca PE=1 SV=2	13	7	2.74
1	E3 ubiquitin-protein ligase SHPRH OS=Mus musculus GN=Shprh PE=1 SV=1	5	1	0.24
1	Reversed Sequence 48	10	3	14.12
1	Isoform 4 of E3 ubiquitin-protein ligase SH3RF1 OS=Mus musculus GN=Sh3rf1	14	5	14.96
1	Isoform 3 of E3 ubiquitin-protein ligase SH3RF1 OS=Mus musculus GN=Sh3rf1	14	5	6.88
1	Reversed Sequence 24017	15	4	7.8
1	Protein virilizer homolog OS=Mus musculus GN=Kiaa1429 PE=1 SV=1	8	3	0.39
1	Carboxyl-terminal PDZ ligand of neuronal nitric oxide synthase protein OS=Mus musculus GN=Nos1ap PE=1 SV=3	11	6	11.93
1	Nascent polypeptide-associated complex subunit alpha OS=Mus musculus GN=Naca PE=1 SV=1	2	1	6.98
2	Apolipoprotein A-I OS=Mus musculus GN=Apoa1 PE=1 SV=2	178	18	30
2	Hemoglobin subunit alpha OS=Mus musculus GN=Hba PE=1 SV=2	92	9	59.09
2	Serum albumin OS=Mus musculus GN=Alb PE=1 SV=3	421	40	80.28
2	Serine protease inhibitor A3K OS=Mus musculus GN=Serpina3k PE=1 SV=2	161	13	58.55
2	Hemoglobin subunit beta-1 OS=Mus musculus GN=Hbb-b1 PE=1 SV=2	59	7	30.86
2	Hemoglobin subunit beta-2 OS=Mus musculus GN=Hbb-b2 PE=1 SV=2	37	4	53.74
2	Serotransferrin OS=Mus musculus GN=Tf PE=1 SV=1	329	38	29.93

Table S8. Identified proteins in group treated with 200 mg kg^{-1} day^{-1} of diacetyl (three technical replicates) (cont.)

Replicate number	Protein description	Protein Matched Products	Protein Matched Peptides	Protein seqCover (%)
2	Alpha-1-antitrypsin 1-5 OS=Mus musculus GN=Serpina1e PE=1 SV=1	100	11	42.9
2	Alpha-2-macroglobulin OS=Mus musculus GN=A2m PE=1 SV=3	359	37	21.31
2	Hemoglobin subunit epsilon-Y2 OS=Mus musculus GN=Hbb-y PE=1 SV=2	14	1	31.24
2	Alpha-1-antitrypsin 1-2 OS=Mus musculus GN=Serpina1b PE=1 SV=2	154	14	6.8
2	Alpha-1-antitrypsin 1-4 OS=Mus musculus GN=Serpina1d PE=2 SV=1	154	15	32.93
2	Enolase 1 OS=Saccharomyces cerevisiae (st	150	18	34.38
2	Serine protease inhibitor A3M OS=Mus musculus GN=Serpina3m PE=1 SV=2	76	7	47.14
2	Alpha-1-antitrypsin 1-3 OS=Mus musculus GN=Serpina1c PE=1 SV=2	143	13	11.96
2	Alpha-1-antitrypsin 1-1 OS=Mus musculus GN=Serpina1a PE=1 SV=4	143	13	25.97
2	Apolipoprotein A-IV OS=Mus musculus GN=Apoa4 PE=1 SV=3	90	14	25.91
2	Carboxylesterase 1C OS=Mus musculus GN=Ces1c PE=1 SV=4	105	18	46.08
2	Apolipoprotein A-II OS=Mus musculus GN=Apoa2 PE=1 SV=2	17	1	40.43
2	Murinoglobulin-1 OS=Mus musculus GN=Mug1 PE=1 SV=3	131	17	9.8
2	Serine protease inhibitor A3G OS=Mus musculus GN=Serpina3g PE=2 SV=2	41	6	12.94
2	Serine protease inhibitor A3C OS=Mus musculus GN=Serpina3c PE=2 SV=1	35	4	12.05
2	Serine protease inhibitor A3N OS=Mus musculus GN=Serpina3n PE=1 SV=1	35	4	6.47
2	Kininogen-1 OS=Mus musculus GN=Kng1 PE=1 SV=1	82	14	6.46
2	Serine protease inhibitor A3F OS=Mus musculus GN=Serpina3f PE=1 SV=3	35	6	31.01
2	Complement C3 OS=Mus musculus GN=C3 PE=1 SV=3	152	24	14.83
2	Isoform 3 of Kininogen-1 OS=Mus musculus GN=Kng1	66	10	16.36
2	Isoform LMW of Kininogen-1 OS=Mus musculus GN=Kng1	59	9	30.63
2	Apolipoprotein E OS=Mus musculus GN=Apoe PE=1 SV=2	39	8	31.25
2	Transthyretin OS=Mus musculus GN=Ttr PE=1 SV=1	36	5	28.94
2	Isoform 2 of Fibrinogen alpha chain OS=Mus musculus GN=Fga	64	17	46.26

Table S8. Identified proteins in group treated with 200 mg kg⁻¹ day⁻¹ of diacetyl (three technical replicates) (cont.)

Replicate number	Protein description	Protein Matched Products	Protein Matched Peptides	Protein seqCover (%)
2	Fibrinogen alpha chain OS=Mus musculus GN=Fga PE=2 SV=1	64	17	36.62
2	Hemopexin OS=Mus musculus GN=Hpx PE=1 SV=2	64	13	25.86
2	Carboxylesterase 1D OS=Mus musculus GN=Ces1d PE=1 SV=1	23	3	27.61
2	Alpha-2-HS-glycoprotein OS=Mus musculus GN=Ahsg PE=1 SV=1	21	2	5.31
2	Liver carboxylesterase 1 OS=Mus musculus GN=Ces1 PE=2 SV=1	16	2	11.01
2	Clusterin OS=Mus musculus GN=Clu PE=1 SV=1	40	9	2.83
2	Vitamin D-binding protein OS=Mus musculus GN=Gc PE=1 SV=2	60	9	36.16
2	Ceruloplasmin OS=Mus musculus GN=Cp PE=1 SV=2	74	16	17.44
2	Cytochrome b-c1 complex subunit 9 OS=Mus musculus GN=Uqcr10 PE=1 SV=1	5	1	24.41
2	Complement factor B OS=Mus musculus GN=Cfb PE=1 SV=2	54	12	26.56
2	Murinoglobulin-2 OS=Mus musculus GN=Mug2 PE=2 SV=2	76	12	19.32
2	Antithrombin-III OS=Mus musculus GN=Serpinc1 PE=1 SV=1	46	11	8.34
2	Isoform 2 of Ig gamma-2B chain C region OS=Mus musculus GN=Igh-3	15	2	30.32
2	Ig gamma-2B chain C region OS=Mus musculus GN=Igh-3 PE=1 SV=3	15	2	7.16
2	Plasma protease C1 inhibitor OS=Mus musculus GN=Serping1 PE=1 SV=3	20	4	5.94
2	Ig heavy chain V region AC38 205.12 OS=Mus musculus PE=1 SV=1	5	1	12.3
2	Ig heavy chain V region J558 OS=Mus musculus PE=1 SV=1	5	1	16.1
2	Ig heavy chain V region MOPC 104E OS=Mus musculus PE=1 SV=1	5	1	16.24
2	Alpha-2-antiplasmin OS=Mus musculus GN=Serpinf2 PE=1 SV=1	22	6	16.24
2	Isoform 2 of Complement factor D OS=Mus musculus GN=Cfd	5	1	13.44
2	Complement factor D OS=Mus musculus GN=Cfd PE=1 SV=1	5	1	8.14
2	Beta-2-glycoprotein 1 OS=Mus musculus GN=Apoh PE=1 SV=1	25	6	8.11
2	Fetuin-B OS=Mus musculus GN=Fetub PE=1 SV=1	20	4	24.64

(continued on next page)

Table S8. Identified proteins in group treated with 200 mg kg^{-1} day^{-1} of diacetyl (three technical replicates) (cont.)

Replicate number	Protein description	Protein Matched Products	Protein Matched Peptides	Protein seqCover (%)
2	Coiled-coil domain-containing protein 160 OS=Mus musculus GN=Ccdc160 PE=2 SV=1	22	5	19.85
2	Isoform Short of Complement C3 OS=Mus musculus GN=C3	16	4	23.53
2	Gelsolin OS=Mus musculus GN=Gsn PE=1 SV=3	53	11	9.35
2	Isoform 2 of Gelsolin OS=Mus musculus GN=Gsn	51	10	18.46
2	Fibrinogen beta chain OS=Mus musculus GN=Fgb PE=2 SV=1	53	13	18.74
2	Inter-alpha-trypsin inhibitor heavy chain H2 OS=Mus musculus GN=Itih2 PE=1 SV=1	43	9	28.27
2	Prothrombin OS=Mus musculus GN=F2 PE=1 SV=1	38	8	13.64
2	Plasminogen OS=Mus musculus GN=Plg PE=1 SV=3	45	12	13.59
2	Histidine-rich glycoprotein OS=Mus musculus GN=Hrg PE=1 SV=2	28	7	11.08
2	Reversed Sequence 25102	15	2	12.38
2	Reversed Sequence 15087	4	2	8.83
2	Isoform Gamma of Prostaglandin E2 receptor EP3 subtype OS=Mus musculus GN=Ptger3	6	2	35.71
2	Isoform Beta of Prostaglandin E2 receptor EP3 subtype OS=Mus musculus GN=Ptger3	6	2	3.85
2	Prostaglandin E2 receptor EP3 subtype OS=Mus musculus GN=Ptger3 PE=1 SV=1	6	2	3.88
2	Isoform 2 of Ig mu chain C region OS=Mus musculus GN=Ighm	32	7	3.84
2	Ig mu chain C region OS=Mus musculus GN=Ighm PE=1 SV=2	32	7	15.37
2	Zinc-alpha-2-glycoprotein OS=Mus musculus GN=Azgp1 PE=1 SV=2	11	3	16.08
2	Apolipoprotein C-III OS=Mus musculus GN=Apoc3 PE=1 SV=2	4	1	13.68
2	THO complex subunit 7 homolog OS=Mus musculus GN=Thoc7 PE=1 SV=2	11	2	19.19
2	Ankyrin repeat domain-containing protein 49 OS=Mus musculus GN=Ankrd49 PE=2 SV=1	6	1	11.27
2	Claudin-5 OS=Mus musculus GN=Cldn5 PE=1 SV=2	5	1	8.4
2	Alpha-2-macroglobulin-P OS=Mus musculus GN=A2mp PE=2 SV=2	18	7	7.8
2	Ig kappa chain V-III region PC 6684 OS=Mus musculus PE=1 SV=1	4	1	7.6

Table S8. Identified proteins in group treated with 200 mg kg⁻¹ day⁻¹ of diacetyl (three technical replicates) (cont.)

Replicate number	Protein description	Protein Matched Products	Protein Matched Peptides	Protein seqCover (%)
2	Ig kappa chain V-III region PC 7769 OS=Mus musculus PE=1 SV=1	4	1	16.22
2	Ig kappa chain V-III region PC 7175 OS=Mus musculus PE=1 SV=1	4	1	16.22
2	Ig kappa chain V-III region PC 2485/PC 4039 OS=Mus musculus PE=1 SV=1	4	1	16.22
2	Ig kappa chain V-III region PC 7940 OS=Mus musculus PE=1 SV=1	4	1	16.22
2	Ig kappa chain V-III region PC 7183 OS=Mus musculus PE=1 SV=1	4	1	16.22
2	Ig kappa chain V-III region PC 7210 OS=Mus musculus PE=1 SV=1	4	1	16.22
2	Ig kappa chain V-III region PC 6308 OS=Mus musculus PE=1 SV=1	4	1	16.36
2	Ig kappa chain V-III region PC 7043 OS=Mus musculus PE=1 SV=1	4	1	16.22
2	Ig kappa chain V-III region CBPC 101 OS=Mus musculus PE=1 SV=1	4	1	16.22
2	Ig kappa chain V-III region PC 3741/TEPC 111 OS=Mus musculus PE=1 SV=1	4	1	16.22
2	Ig kappa chain V-III region TEPC 124 OS=Mus musculus PE=1 SV=1	4	1	16.22
2	Ig kappa chain V-III region MOPC 70 OS=Mus musculus PE=1 SV=1	4	1	16.07
2	Ig kappa chain V-III region PC 7132 OS=Mus musculus PE=1 SV=1	4	1	16.22
2	Ig kappa chain V-III region PC 2413 OS=Mus musculus PE=1 SV=1	4	1	16.07
2	Ig kappa chain V-III region 50S10.1 OS=Mus musculus PE=1 SV=1	4	1	16.22
2	Ig kappa chain V-III region PC 2880/PC 1229 OS=Mus musculus PE=1 SV=1	4	1	16.22
2	RNA-directed RNA polymerase L OS=Lymphocytic choriomeningitis virus (strain Armstrong) GN=L PE=1 SV=1	28	11	16.22
2	Inter-alpha-trypsin inhibitor heavy chain H1 OS=Mus musculus GN=Itih1 PE=1 SV=2	29	10	2.67
2	Guanine nucleotide exchange factor VAV2 OS=Mus musculus GN=Vav2 PE=1 SV=1	14	4	15.1
2	Isoform 2 of THO complex subunit 7 homolog OS=Mus musculus GN=Thoc7	7	1	2.88
2	Complement factor H OS=Mus musculus GN=Cfh PE=1 SV=2	31	9	5.84

Table S8. Identified proteins in group treated with 200 mg kg^{-1} day^{-1} of diacetyl (three technical replicates) (cont.)

Replicate number	Protein description	Protein Matched Products	Protein Matched Peptides	Protein seqCover (%)
2	Isoform STEP38 of Tyrosine-protein phosphatase non-receptor type 5 OS=Mus musculus GN=Ptpn5	12	4	8.51
2	Tyrosine-protein phosphatase non-receptor type 5 OS=Mus musculus GN=Ptpn5 PE=2 SV=2	12	4	15.03
2	Reversed Sequence 8126	19	4	9.61
2	Alpha-(1_3)-fucosyltransferase 10 OS=Mus musculus GN=Fut10 PE=2 SV=1	9	4	13.16
2	Isoform 2 of Alpha-(1_3)-fucosyltransferase 10 OS=Mus musculus GN=Fut10	7	2	13.93
2	Isoform 3 of Monocarboxylate transporter 5 OS=Mus musculus GN=Slc16a4	4	1	11.93
2	Isoform 2 of Monocarboxylate transporter 5 OS=Mus musculus GN=Slc16a4	4	1	14.17
2	Monocarboxylate transporter 5 OS=Mus musculus GN=Slc16a4 PE=2 SV=1	4	1	10.9
2	Isoform 2 of Inter alpha-trypsin inhibitor_ heavy chain 4 OS=Mus musculus GN=Itih4	30	10	10.2
2	Inter alpha-trypsin inhibitor_ heavy chain 4 OS=Mus musculus GN=Itih4 PE=1 SV=2	30	10	10.74
2	Serum paraoxonase/arylesterase 1 OS=Mus musculus GN=Pon1 PE=1 SV=2	5	3	10.3
2	Coagulation factor X OS=Mus musculus GN=F10 PE=1 SV=1	10	4	6.48
2	Noelin OS=Mus musculus GN=Olfm1 PE=1 SV=1	18	7	3.53
2	Corticosteroid-binding globulin OS=Mus musculus GN=Serpina6 PE=1 SV=1	10	5	6.6
2	Reversed Sequence 1667	21	5	11.59
3	Apolipoprotein A-I OS=Mus musculus GN=Apoa1 PE=1 SV=2	145	15	52.65
3	Serum albumin OS=Mus musculus GN=Alb PE=1 SV=3	419	40	58.55
3	Serine protease inhibitor A3K OS=Mus musculus GN=Serpina3k PE=1 SV=2	149	12	33.97
3	Hemoglobin subunit beta-1 OS=Mus musculus GN=Hbb-b1 PE=1 SV=2	46	6	53.74
3	Hemoglobin subunit alpha OS=Mus musculus GN=Hba PE=1 SV=2	110	11	81.69
3	Hemoglobin subunit beta-2 OS=Mus musculus GN=Hbb-b2 PE=1 SV=2	29	4	29.93
3	Alpha-2-macroglobulin OS=Mus musculus GN=A2m PE=1 SV=3	379	40	31.37
3	Serotransferrin OS=Mus musculus GN=Tf PE=1 SV=1	341	40	37.59

Table S8. Identified proteins in group treated with 200 mg kg⁻¹ day⁻¹ of diacetyl (three technical replicates) (cont.)

Replicate number	Protein description	Protein Matched Products	Protein Matched Peptides	Protein seqCover (%)
3	Hemoglobin subunit epsilon-Y2 OS=Mus musculus GN=Hbb-y PE=1 SV=2	14	1	6.8
3	Alpha-1-antitrypsin 1-5 OS=Mus musculus GN=Serpina1e PE=1 SV=1	95	10	21.07
3	Alpha-1-antitrypsin 1-4 OS=Mus musculus GN=Serpina1d PE=2 SV=1	143	15	30.99
3	Enolase 1 OS=Saccharomyces cerevisiae (st	118	16	39.82
3	Serine protease inhibitor A3M OS=Mus musculus GN=Serpina3m PE=1 SV=2	69	6	11.96
3	Alpha-1-antitrypsin 1-2 OS=Mus musculus GN=Serpina1b PE=1 SV=2	124	13	28.81
3	Apolipoprotein A-IV OS=Mus musculus GN=Apoa4 PE=1 SV=3	85	13	39.24
3	Alpha-1-antitrypsin 1-3 OS=Mus musculus GN=Serpina1c PE=1 SV=2	128	13	25.97
3	Alpha-1-antitrypsin 1-1 OS=Mus musculus GN=Serpina1a PE=1 SV=4	128	13	25.91
3	Carboxylesterase 1C OS=Mus musculus GN=Ces1c PE=1 SV=4	103	16	37.91
3	Apolipoprotein A-II OS=Mus musculus GN=Apoa2 PE=1 SV=2	30	1	9.8
3	Serine protease inhibitor A3G OS=Mus musculus GN=Serpina3g PE=2 SV=2	36	6	15.45
3	Serine protease inhibitor A3C OS=Mus musculus GN=Serpina3c PE=2 SV=1	28	3	6.47
3	Serine protease inhibitor A3N OS=Mus musculus GN=Serpina3n PE=1 SV=1	28	3	6.46
3	Serine protease inhibitor A3F OS=Mus musculus GN=Serpina3f PE=1 SV=3	33	5	15.73
3	Murinoglobulin-1 OS=Mus musculus GN=Mug1 PE=1 SV=3	134	22	19.51
3	Apolipoprotein E OS=Mus musculus GN=Apoe PE=1 SV=2	25	4	16.4
3	Kininogen-1 OS=Mus musculus GN=Kng1 PE=1 SV=1	55	9	20.12
3	Isoform 3 of Kininogen-1 OS=Mus musculus GN=Kng1	46	7	21.04
3	Isoform LMW of Kininogen-1 OS=Mus musculus GN=Kng1	46	7	23.38
3	Complement C3 OS=Mus musculus GN=C3 PE=1 SV=3	135	26	20.69
3	Antithrombin-III OS=Mus musculus GN=Serpinc1 PE=1 SV=1	60	14	31.83
3	Clusterin OS=Mus musculus GN=Clu PE=1 SV=1	31	6	20.98
3	Isoform 2 of Fibrinogen alpha chain OS=Mus musculus GN=Fga	65	10	26.93

Table S8. Identified proteins in group treated with 200 mg kg⁻¹ day⁻¹ of diacetyl (three technical replicates) (cont.)

Replicate number	Protein description	Protein Matched Products	Protein Matched Peptides	Protein seqCover (%)
3	Fibrinogen alpha chain OS=Mus musculus GN=Fga PE=2 SV=1	65	10	19.01
3	Hemopexin OS=Mus musculus GN=Hpx PE=1 SV=2	40	9	21.96
3	Reversed Sequence 17913	8	2	44.44
3	Vitamin D-binding protein OS=Mus musculus GN=Gc PE=1 SV=2	59	10	23.95
3	Transthyretin OS=Mus musculus GN=Ttr PE=1 SV=1	29	5	46.26
3	Zinc-alpha-2-glycoprotein OS=Mus musculus GN=Azgp1 PE=1 SV=2	5	2	8.79
3	Ceruloplasmin OS=Mus musculus GN=Cp PE=1 SV=2	62	16	21.02
3	Carboxylesterase 1D OS=Mus musculus GN=Ces1d PE=1 SV=1	20	5	10.62
3	Apolipoprotein C-III OS=Mus musculus GN=Apoc3 PE=1 SV=2	7	2	38.38
3	Murinoglobulin-2 OS=Mus musculus GN=Mug2 PE=2 SV=2	77	12	8.27
3	Gelsolin OS=Mus musculus GN=Gsn PE=1 SV=3	45	9	17.05
3	Isoform 2 of Gelsolin OS=Mus musculus GN=Gsn	41	7	15.73
3	Beta-2-glycoprotein 1 OS=Mus musculus GN=Apoh PE=1 SV=1	30	7	22.32
3	Isoform Short of Complement C3 OS=Mus musculus GN=C3	18	5	16.64
3	Fetuin-B OS=Mus musculus GN=Fetub PE=1 SV=1	21	4	19.33
3	Inter-alpha-trypsin inhibitor heavy chain H2 OS=Mus musculus GN=Itih2 PE=1 SV=1	57	9	11.42
3	Serum paraoxonase/arylesterase 1 OS=Mus musculus GN=Pon1 PE=1 SV=2	8	2	8.45
3	Complement factor B OS=Mus musculus GN=Cfb PE=1 SV=2	38	10	14.06
3	Isoform 2 of Ig gamma-2B chain C region OS=Mus musculus GN=Igh-3	14	2	7.16
3	Ig gamma-2B chain C region OS=Mus musculus GN=Igh-3 PE=1 SV=3	14	2	5.94
3	Liver carboxylesterase 1 OS=Mus musculus GN=Ces1 PE=2 SV=1	10	2	2.48
3	Alpha-2-antiplasmin OS=Mus musculus GN=Serpinf2 PE=1 SV=1	24	7	16.29
3	Immunoglobulin J chain OS=Mus musculus GN=Igj PE=2 SV=4	7	5	22.64
3	Prothrombin OS=Mus musculus GN=F2 PE=1 SV=1	23	6	8.09

Table S8. Identified proteins in group treated with 200 mg kg⁻¹ day⁻¹ of diacetyl (three technical replicates) (cont.)

Replicate number	Protein description	Protein Matched Products	Protein Matched Peptides	Protein seqCover (%)
3	Histidine-rich glycoprotein OS=Mus musculus GN=Hrg PE=1 SV=2	27	7	15.81
3	Reversed Sequence 21346	3	1	18.18
3	Alpha-2-macroglobulin-P OS=Mus musculus GN=A2mp PE=2 SV=2	35	9	7.33
3	Fibrinogen beta chain OS=Mus musculus GN=Fgb PE=2 SV=1	26	7	15.38
3	Isoform 2 of Ig mu chain C region OS=Mus musculus GN=Ighm	16	5	14.11
3	Ig mu chain C region OS=Mus musculus GN=Ighm PE=1 SV=2	16	5	14.76
3	Carboxypeptidase N catalytic chain OS=Mus musculus GN=Cpn1 PE=2 SV=1	15	5	13.57
3	Major urinary protein 20 OS=Mus musculus GN=Mup20 PE=1 SV=1	9	3	12.15

Table S9. Identified proteins in group treated with 300 mg kg⁻¹ day⁻¹ of diacetyl (three technical replicates)

Replicate number	Protein Description	Protein Matched Products	Protein matched Peptides	Protein seqCover (%)
1	Serum albumin OS=Mus musculus GN=Alb PE=1 SV=3	628	47	67.27
1	Alpha-1-antitrypsin 1-2 OS=Mus musculus GN=Serpina1b PE=1 SV=2	207	13	24.46
1	Hemoglobin subunit alpha OS=Mus musculus GN=Hba PE=1 SV=2	114	9	83.10
1	Serine protease inhibitor A3K OS=Mus musculus GN=Serpina3k PE=1 SV=2	214	16	39.23
1	Serotransferrin OS=Mus musculus GN=Tf PE=1 SV=1	595	45	60.98
1	Alpha-1-antitrypsin 1-4 OS=Mus musculus GN=Serpina1d PE=2 SV=1	193	15	35.35
1	Apolipoprotein A-I OS=Mus musculus GN=Apoa1 PE=1 SV=2	246	21	45.45
1	Hemoglobin subunit beta-1 OS=Mus musculus GN=Hbb-b1 PE=1 SV=2	99	8	59.18
1	Alpha-1-antitrypsin 1-3 OS=Mus musculus GN=Serpina1c PE=1 SV=2	162	12	25.24
1	Alpha-1-antitrypsin 1-1 OS=Mus musculus GN=Serpina1a PE=1 SV=4	162	12	25.18
1	Serine protease inhibitor A3M OS=Mus musculus GN=Serpina3m PE=1 SV=2	113	7	11.96
1	Alpha-1-antitrypsin 1-5 OS=Mus musculus GN=Serpina1e PE=1 SV=1	157	13	24.94
1	Hemoglobin subunit beta-2 OS=Mus musculus GN=Hbb-b2 PE=1 SV=2	77	6	35.37
1	Alpha-2-macroglobulin OS=Mus musculus GN=A2m PE=1 SV=3	674	52	38.13

Table S9. Identified proteins in group treated with 300 mg kg^{-1} day^{-1} of diacetyl (three technical replicates) (cont.)

Replicate number	Protein Description	Protein Matched Products	Protein matched Peptides	Protein seqCover (%)
1	Apolipoprotein A-IV OS=Mus musculus GN=Apoa4 PE=1 SV=3	192	24	64.05
1	Hemopexin OS=Mus musculus GN=Hpx PE=1 SV=2	227	26	57.83
1	Isoform 3 of Kininogen-1 OS=Mus musculus GN=Kng1	162	16	44.79
1	Kininogen-1 OS=Mus musculus GN=Kng1 PE=1 SV=1	166	17	36.31
1	Isoform LMW of Kininogen-1 OS=Mus musculus GN=Kng1	152	15	46.99
1	Carboxylesterase 1C OS=Mus musculus GN=Ces1c PE=1 SV=4	172	16	27.44
1	Alpha-2-HS-glycoprotein OS=Mus musculus GN=Ahsg PE=1 SV=1	97	7	26.96
1	Beta-2-glycoprotein 1 OS=Mus musculus GN=Apoh PE=1 SV=1	99	15	48.12
1	Murinoglobulin-1 OS=Mus musculus GN=Mug1 PE=1 SV=3	384	41	34.82
1	Complement C3 OS=Mus musculus GN=C3 PE=1 SV=3	403	56	40.41
1	Hemoglobin subunit epsilon-Y2 OS=Mus musculus GN=Hbb-y PE=1 SV=2	22	1	6.80
1	Isoform 2 of Fibrinogen alpha chain OS=Mus musculus GN=Fga	122	15	37.34
1	Fibrinogen alpha chain OS=Mus musculus GN=Fga PE=2 SV=1	126	16	33.46
1	Fibrinogen gamma chain OS=Mus musculus GN=Fgg PE=1 SV=1	110	14	37.16
1	Apolipoprotein E OS=Mus musculus GN=Apoe PE=1 SV=2	89	12	39.23
1	Serine protease inhibitor A3N OS=Mus musculus GN=Serpina3n PE=1 SV=1	72	10	24.16
1	Serine protease inhibitor A3G OS=Mus musculus GN=Serpina3g PE=2 SV=2	62	6	10.23
1	Serine protease inhibitor A3C OS=Mus musculus GN=Serpina3c PE=2 SV=1	55	6	8.39
1	Major urinary proteins 11 and 8 (Fragment) OS=Mus musculus GN=Mup8 PE=1 SV=1	45	6	51.66
1	Major urinary protein 17 OS=Mus musculus GN=Mup17 PE=2 SV=2	45	6	43.33
1	Major urinary protein 6 OS=Mus musculus GN=Mup6 PE=1 SV=2	45	6	43.33
1	Murinoglobulin-2 OS=Mus musculus GN=Mug2 PE=2 SV=2	187	20	16.47
1	Fibrinogen beta chain OS=Mus musculus GN=Fgb PE=2 SV=1	160	19	40.54
1	Haptoglobin OS=Mus musculus GN=Hp PE=1 SV=1	83	13	40.35
1	Vitamin D-binding protein OS=Mus musculus GN=Gc PE=1 SV=2	138	18	42.02
1	Ig mu chain C region OS=Mus musculus GN=Ighm PE=1 SV=2	71	8	24.67
1	Isoform 2 of Ig mu chain C region OS=Mus musculus GN=Ighm	70	7	18.95
1	Serine protease inhibitor A3F OS=Mus musculus GN=Serpina3f PE=1 SV=3	51	6	13.48

Table S9. Identified proteins in group treated with 300 mg kg^{-1} day^{-1} of diacetyl (three technical replicates) (cont.)

Replicate number	Protein Description	Protein Matched Products	Protein matched Peptides	Protein seqCover (%)
1	Antithrombin-III OS=Mus musculus GN=Serpinc1 PE=1 SV=1	133	17	32.26
1	Major urinary protein 2 OS=Mus musculus GN=Mup2 PE=1 SV=1	35	5	36.67
1	Major urinary protein 1 OS=Mus musculus GN=Mup1 PE=1 SV=1	35	5	36.67
1	Alpha-2-antiplasmin OS=Mus musculus GN=Serpinf2 PE=1 SV=1	63	11	20.16
1	Gelsolin OS=Mus musculus GN=Gsn PE=1 SV=3	140	17	30.13
1	Isoform 2 of Gelsolin OS=Mus musculus GN=Gsn	135	16	31.19
1	Isoform Short of Complement C3 OS=Mus musculus GN=C3	76	15	35.14
1	Plasminogen OS=Mus musculus GN=Plg PE=1 SV=3	168	33	51.23
1	Clusterin OS=Mus musculus GN=Clu PE=1 SV=1	62	10	28.35
1	Apolipoprotein C-III OS=Mus musculus GN=Apoc3 PE=1 SV=2	21	2	27.27
1	Prothrombin OS=Mus musculus GN=F2 PE=1 SV=1	113	17	25.40
1	Fetuin-B OS=Mus musculus GN=Fetub PE=1 SV=1	56	7	25.26
1	Histidine-rich glycoprotein OS=Mus musculus GN=Hrg PE=1 SV=2	69	10	24.95
1	Ig gamma-2A chain C region secreted form OS=Mus musculus PE=1 SV=1	30	3	11.94
1	Plasma protease C1 inhibitor OS=Mus musculus GN=Serping1 PE=1 SV=3	62	12	24.40
1	H-2 class I histocompatibility antigen_ Q10 alpha chain OS=Mus musculus GN=H2-Q10 PE=1 SV=3	37	5	17.85
1	Corticosteroid-binding globulin OS=Mus musculus GN=Serpina6 PE=1 SV=1	28	7	18.89
1	Isoform 2 of Ig gamma-2B chain C region OS=Mus musculus GN=Igh-3	40	7	25.07
1	Ig gamma-2B chain C region OS=Mus musculus GN=Igh-3 PE=1 SV=3	40	7	20.79
1	Carboxylesterase 1D OS=Mus musculus GN=Ces1d PE=1 SV=1	43	5	10.09
1	Ceruloplasmin OS=Mus musculus GN=Cp PE=1 SV=2	129	23	36.19
1	H-2 class I histocompatibility antigen_ Q8 alpha chain OS=Mus musculus GN=H2-Q8 PE=2 SV=1	22	6	27.91
1	H-2 class I histocompatibility antigen_ Q7 alpha chain OS=Mus musculus GN=H2-Q7 PE=1 SV=1	21	5	15.87
1	Isoform 2 of H-2 class I histocompatibility antigen_ alpha chain OS=Mus musculus GN=H2-D1	15	2	7.02
1	H-2 class I histocompatibility antigen_ alpha chain (Fragment) OS=Mus musculus GN=H2-D1 PE=1 SV=1	15	2	6.71
1	H-2 class I histocompatibility antigen_ D-D alpha chain OS=Mus musculus GN=H2-D1 PE=1 SV=1	15	2	5.48
1	H-2 class I histocompatibility antigen_ D-B alpha chain OS=Mus musculus GN=H2-D1 PE=1 SV=2	15	2	5.52

Table S9. Identified proteins in group treated with 300 mg kg^{-1} day^{-1} of diacetyl (three technical replicates) (cont.)

Replicate number	Protein Description	Protein Matched Products	Protein matched Peptides	Protein seqCover (%)
1	Beta-2-microglobulin OS=Mus musculus GN=B2m PE=1 SV=2	17	3	21.01
1	Serum paraoxonase/arylesterase 1 OS=Mus musculus GN=Pon1 PE=1 SV=2	37	5	16.06
1	Ig heavy chain V region AC38 205.12 OS=Mus musculus PE=1 SV=1	14	2	27.97
1	Heparin cofactor 2 OS=Mus musculus GN=Serpind1 PE=1 SV=1	29	6	12.55
1	Vitronectin OS=Mus musculus GN=Vtn PE=1 SV=2	23	5	12.55
1	Inter alpha-trypsin inhibitor_ heavy chain 4 OS=Mus musculus GN=Itih4 PE=1 SV=2	92	18	25.16
1	Retinol-binding protein 4 OS=Mus musculus GN=Rbp4 PE=2 SV=2	15	3	20.90
1	Protein AMBP OS=Mus musculus GN=Ambp PE=2 SV=2	21	4	15.19
1	Epidermal growth factor receptor OS=Mus musculus GN=Egfr PE=1 SV=1	82	18	19.92
1	Glutathione peroxidase 3 OS=Mus musculus GN=Gpx3 PE=2 SV=2	24	7	40.27
1	Inter-alpha-trypsin inhibitor heavy chain H2 OS=Mus musculus GN=Itih2 PE=1 SV=1	70	13	17.76
1	Carboxypeptidase N subunit 2 OS=Mus musculus GN=Cpn2 PE=1 SV=2	53	11	32.18
1	Isoform 2 of Inter alpha-trypsin inhibitor_ heavy chain 4 OS=Mus musculus GN=Itih4	80	17	24.70
1	Complement factor H OS=Mus musculus GN=Cfh PE=1 SV=2	99	24	26.90
1	Liver carboxylesterase 1 OS=Mus musculus GN=Ces1 PE=2 SV=1	21	2	2.83
1	Mannose-binding protein C OS=Mus musculus GN=Mbl2 PE=2 SV=2	20	3	12.70
1	Carboxypeptidase N catalytic chain OS=Mus musculus GN=Cpn1 PE=2 SV=1	12	4	10.72
1	Phosphatidylinositol-glycan-specific phospholipase D OS=Mus musculus GN=Gpld1 PE=1 SV=1	57	13	16.61
1	Complement factor B OS=Mus musculus GN=Cfb PE=1 SV=2	76	17	25.49
1	Isoform 3 of Afamin OS=Mus musculus GN=Afm	42	10	20.79
1	Afamin OS=Mus musculus GN=Afm PE=1 SV=2	42	10	20.89
1	Isoform 2 of Afamin OS=Mus musculus GN=Afm	38	7	16.74
1	Zinc-alpha-2-glycoprotein OS=Mus musculus GN=Azgp1 PE=1 SV=2	36	8	26.38
1	Reversed Sequence 12334	18	4	15.48
1	Carbonic anhydrase 1 OS=Mus musculus GN=Ca1 PE=2 SV=4	9	3	27.59
1	Peroxiredoxin-2 OS=Mus musculus GN=Prdx2 PE=1 SV=3	13	4	34.34
1	Fibronectin OS=Mus musculus GN=Fn1 PE=1 SV=4	115	28	16.51

Table S9. Identified proteins in group treated with 300 mg kg⁻¹ day⁻¹ of diacetyl (three technical replicates) (cont.)

Replicate number	Protein Description	Protein Matched Products	Protein matched Peptides	Protein seqCover (%)
1	Angiotensinogen OS=Mus musculus GN=Agt PE=1 SV=1	21	3	7.34
1	Lumican OS=Mus musculus GN=Lum PE=1 SV=2	24	8	16.86
1	Complement factor D OS=Mus musculus GN=Cfd PE=1 SV=1	9	4	29.34
1	Complement C5 OS=Mus musculus GN=C5 PE=1 SV=2	99	18	12.14
1	Interleukin-1 receptor accessory protein OS=Mus musculus GN=Il1rap PE=1 SV=1	29	8	15.61
1	Isoform 2 of Interleukin-1 receptor accessory protein OS=Mus musculus GN=Il1rap	26	6	18.33
1	Complement component C9 OS=Mus musculus GN=C9 PE=1 SV=2	46	11	16.06
1	Inter-alpha-trypsin inhibitor heavy chain H1 OS=Mus musculus GN=Itih1 PE=1 SV=2	45	12	18.96
1	Major urinary protein 5 OS=Mus musculus GN=Mup5 PE=2 SV=1	14	4	31.67
1	Complement component C8 alpha chain OS=Mus musculus GN=C8a PE=2 SV=1	34	11	23.34
1	Isoform 2 of Ig gamma-3 chain C region OS=Mus musculus	16	5	31.31
1	Ig gamma-3 chain C region OS=Mus musculus PE=1 SV=2	16	5	25.88
1	Alpha-2-macroglobulin-P OS=Mus musculus GN=A2mp PE=2 SV=2	28	12	11.19
1	Coagulation factor X OS=Mus musculus GN=F10 PE=1 SV=1	22	9	19.13
1	Apolipoprotein C-I OS=Mus musculus GN=Apoc1 PE=1 SV=1	8	2	20.45
1	Plasma kallikrein OS=Mus musculus GN=Klkb1 PE=1 SV=2	27	9	14.42
1	Isoform 3 of Sulfhydryl oxidase 1 OS=Mus musculus GN=Qsox1	29	8	9.86
1	Isoform 2 of Sulfhydryl oxidase 1 OS=Mus musculus GN=Qsox1	37	10	17.40
1	Sulfhydryl oxidase 1 OS=Mus musculus GN=Qsox1 PE=1 SV=1	37	10	15.37
1	Complement C4-B OS=Mus musculus GN=C4b PE=1 SV=3	74	21	15.25
1	Isoform 2 of Complement component C8 beta chain OS=Mus musculus GN=C8b	25	9	25.62
1	Complement component C8 beta chain OS=Mus musculus GN=C8b PE=1 SV=1	25	9	22.75
1	Coagulation factor XII OS=Mus musculus GN=F12 PE=2 SV=2	36	11	27.14
1	Inhibitor of carbonic anhydrase OS=Mus musculus GN=Ica PE=1 SV=1	38	15	29.14
1	Reversed Sequence 475	21	7	16.36
1	Insulin-like growth factor-binding protein complex acid labile subunit OS=Mus musculus GN=Igfals PE=2 SV=1	20	4	12.60
1	Immunoglobulin J chain OS=Mus musculus GN=Igj PE=2 SV=4	14	5	30.19

Table S9. Identified proteins in group treated with 300 mg kg⁻¹ day⁻¹ of diacetyl (three technical replicates) (cont.)

Replicate number	Protein Description	Protein Matched Products	Protein matched Peptides	Protein seqCover (%)
1	Inter-alpha-trypsin inhibitor heavy chain H3 OS=Mus musculus GN=Itih3 PE=1 SV=3	38	12	15.86
1	Major urinary protein 20 OS=Mus musculus GN=Mup20 PE=1 SV=1	14	4	29.28
1	Extracellular matrix protein 1 OS=Mus musculus GN=Ecm1 PE=1 SV=2	17	8	15.21
1	Major urinary protein 3 OS=Mus musculus GN=Mup3 PE=1 SV=1	19	4	16.85
1	Apolipoprotein D OS=Mus musculus GN=Apod PE=2 SV=1	6	3	12.70
1	Hepatocyte growth factor activator OS=Mus musculus GN=Hgfac PE=1 SV=1	19	6	14.70
1	Complement factor I OS=Mus musculus GN=Cfi PE=1 SV=3	30	8	9.78
1	Leukemia inhibitory factor receptor OS=Mus musculus GN=Lifr PE=1 SV=1	34	13	12.73
1	Isoform 2 of Leukemia inhibitory factor receptor OS=Mus musculus GN=Lifr	32	12	16.55
1	Reversed Sequence 12002	9	4	20.31
1	Reversed Sequence 15257	25	5	25.73
1	Properdin OS=Mus musculus GN=Cfp PE=2 SV=2	16	7	22.63
1	H-2 class I histocompatibility antigen_ Q9 alpha chain (Fragment) OS=Mus musculus GN=H2-Q9 PE=3 SV=1	11	4	11.50
1	Isoform 2 of Protein Z-dependent protease inhibitor OS=Mus musculus GN=Serpina10	16	6	16.24
1	Protein Z-dependent protease inhibitor OS=Mus musculus GN=Serpina10 PE=1 SV=1	17	7	16.29
1	Isoform Short of Extracellular matrix protein 1 OS=Mus musculus GN=Ecm1	12	6	11.29
1	Pigment epithelium-derived factor OS=Mus musculus GN=Serpinf1 PE=1 SV=2	10	4	12.71
1	H-2 class I histocompatibility antigen_ K-D alpha chain OS=Mus musculus GN=H2-K1 PE=1 SV=1	5	1	2.72
1	Pyrethroid hydrolase Ces2e OS=Mus musculus GN=Ces2e PE=1 SV=1	12	5	8.23
1	Mdm2-binding protein OS=Mus musculus GN=Mtbp PE=1 SV=1	27	8	19.24
1	Reversed Sequence 12416	27	12	13.55
1	Keratin_ type I cuticular Ha5 OS=Mus musculus GN=Krt35 PE=2 SV=1	16	9	33.63
1	Carboxylesterase 1E OS=Mus musculus GN=Ces1e PE=1 SV=1	8	1	1.25
1	Ig gamma-1 chain C region secreted form OS=Mus musculus GN=Ighg1 PE=1 SV=1	11	3	14.51
1	Ig gamma-1 chain C region_ membrane-bound form OS=Mus musculus GN=Ighg1 PE=1 SV=2	11	3	11.96

Table S9. Identified proteins in group treated with 300 mg kg^{-1} day^{-1} of diacetyl (three technical replicates) (cont.)

Replicate number	Protein Description	Protein Matched Products	Protein matched Peptides	Protein seqCover (%)
1	DNA replication licensing factor MCM2 OS=Mus musculus GN=Mcm2 PE=1 SV=3	35	11	16.81
1	WNT1-inducible-signaling pathway protein 3 OS=Mus musculus GN=Wisp3 PE=3 SV=2	12	6	16.95
1	Reversed Sequence 6465	8	6	15.88
1	SUN domain-containing protein 3 OS=Mus musculus GN=Sun3 PE=2 SV=1	6	2	10.31
1	ER membrane protein complex subunit 9 OS=Mus musculus GN=Emc9 PE=2 SV=1	8	3	10.68
1	Glycerophosphodiester phosphodiesterase domain-containing protein 1 OS=Mus musculus GN=Gdpd1 PE=2 SV=1	7	4	14.33
1	Lymphocyte transmembrane adapter 1 OS=Mus musculus GN=Lax1 PE=2 SV=2	13	5	25.06
1	Isoform 2 of N-acetylmuramoyl-L-alanine amidase OS=Mus musculus GN=Pglyrp2	12	4	10.18
1	N-acetylmuramoyl-L-alanine amidase OS=Mus musculus GN=Pglyrp2 PE=1 SV=1	12	4	9.62
1	TATA element modulatory factor OS=Mus musculus GN=Tmf1 PE=1 SV=2	27	11	10.27
1	Reversed Sequence 20212	11	3	17.17
1	Ataxin-1 OS=Mus musculus GN=Atxn1 PE=1 SV=2	14	5	10.75
1	Isoform 3 of N-acetylmuramoyl-L-alanine amidase OS=Mus musculus GN=Pglyrp2	10	3	11.33
1	Reversed Sequence 817	21	11	22.04
1	Isoform 2 of Elongator complex protein 2 OS=Mus musculus GN=Elp2	17	7	12.42
1	Elongator complex protein 2 OS=Mus musculus GN=Elp2 PE=1 SV=1	18	8	11.07
1	Homeobox protein Hox-D9 OS=Mus musculus GN=Hoxd9 PE=2 SV=1	8	2	11.50
1	WD repeat-containing protein 93 OS=Mus musculus GN=Wdr93 PE=2 SV=1	10	3	2.30
1	Rho-related BTB domain-containing protein 1 OS=Mus musculus GN=Rhobtb1 PE=1 SV=2	11	4	11.94
2	Serum albumin OS=Mus musculus GN=Alb PE=1 SV=3	661	53	59.7
2	Apolipoprotein A-I OS=Mus musculus GN=Apoa1 PE=1 SV=2	179	19	34.47
2	Hemoglobin subunit beta-1 OS=Mus musculus GN=Hbb-b1 PE=1 SV=2	83	8	59.18
2	Hemoglobin subunit alpha OS=Mus musculus GN=Hba PE=1 SV=2	94	8	55.63
2	Serotransferrin OS=Mus musculus GN=Tf PE=1 SV=1	509	46	51.22
2	Alpha-2-macroglobulin OS=Mus musculus GN=A2m PE=1 SV=3	568	55	35.79

(continued on next page)

Table S9. Identified proteins in group treated with 300 mg kg^{-1} day^{-1} of diacetyl (three technical replicates) (cont.)

Replicate number	Protein Description	Protein Matched Products	Protein matched Peptides	Protein seqCover (%)
2	Hemoglobin subunit beta-2 OS=Mus musculus GN=Hbb-b2 PE=1 SV=2	66	6	35.37
2	Serine protease inhibitor A3K OS=Mus musculus GN=Serpina3k PE=1 SV=2	174	14	31.1
2	Alpha-1-antitrypsin 1-5 OS=Mus musculus GN=Serpina1e PE=1 SV=1	132	13	32.45
2	Hemoglobin subunit epsilon-Y2 OS=Mus musculus GN=Hbb-y PE=1 SV=2	29	2	6.8
2	Alpha-1-antitrypsin 1-4 OS=Mus musculus GN=Serpina1d PE=2 SV=1	218	22	44.31
2	Alpha-1-antitrypsin 1-3 OS=Mus musculus GN=Serpina1c PE=1 SV=2	197	20	41.02
2	Alpha-1-antitrypsin 1-1 OS=Mus musculus GN=Serpina1a PE=1 SV=4	197	20	40.92
2	Serine protease inhibitor A3M OS=Mus musculus GN=Serpina3m PE=1 SV=2	81	8	16.03
2	Alpha-1-antitrypsin 1-2 OS=Mus musculus GN=Serpina1b PE=1 SV=2	193	18	44.79
2	Enolase 1 OS=Saccharomyces cerevisiae (st	132	18	42.56
2	Complement C3 OS=Mus musculus GN=C3 PE=1 SV=3	211	32	21.35
2	Isoform 3 of Kininogen-1 OS=Mus musculus GN=Kng1	75	9	27.29
2	Kininogen-1 OS=Mus musculus GN=Kng1 PE=1 SV=1	75	9	19.82
2	Isoform LMW of Kininogen-1 OS=Mus musculus GN=Kng1	72	8	27.55
2	Carboxylesterase 1C OS=Mus musculus GN=Ces1c PE=1 SV=4	108	16	40.97
2	Murinoglobulin-1 OS=Mus musculus GN=Mug1 PE=1 SV=3	237	32	25.54
2	Alpha-2-HS-glycoprotein OS=Mus musculus GN=Ahsg PE=1 SV=1	36	3	8.12
2	Apolipoprotein A-IV OS=Mus musculus GN=Apoa4 PE=1 SV=3	61	12	27.34
2	Hemopexin OS=Mus musculus GN=Hpx PE=1 SV=2	101	15	38.04
2	Apolipoprotein E OS=Mus musculus GN=Apoe PE=1 SV=2	39	6	23.15
2	Apolipoprotein A-II OS=Mus musculus GN=Apoa2 PE=1 SV=2	33	3	14.71
2	Isoform 2 of Fibrinogen alpha chain OS=Mus musculus GN=Fga	82	17	39.5
2	Fibrinogen alpha chain OS=Mus musculus GN=Fga PE=2 SV=1	82	17	27.88
2	Murinoglobulin-2 OS=Mus musculus GN=Mug2 PE=2 SV=2	140	19	11.92
2	Beta-2-glycoprotein 1 OS=Mus musculus GN=Apoh PE=1 SV=1	44	10	33.91
2	Alpha-2-antiplasmin OS=Mus musculus GN=Serpinf2 PE=1 SV=1	46	8	17.31
2	Carboxylesterase 1D OS=Mus musculus GN=Ces1d PE=1 SV=1	36	4	10.27
2	Histidine-rich glycoprotein OS=Mus musculus GN=Hrg PE=1 SV=2	38	7	14.67

Table S9. Identified proteins in group treated with 300 mg kg^{-1} day^{-1} of diacetyl (three technical replicates) (cont.)

Replicate number	Protein Description	Protein Matched Products	Protein matched Peptides	Protein seqCover (%)
2	Liver carboxylesterase 1 OS=Mus musculus GN=Ces1 PE=2 SV=1	24	4	11.33
2	Clusterin OS=Mus musculus GN=Clu PE=1 SV=1	54	8	41.96
2	Ig heavy chain V region AC38 205.12 OS=Mus musculus PE=1 SV=1	8	1	16.1
2	Ig heavy chain V region J558 OS=Mus musculus PE=1 SV=1	8	1	16.24
2	Ig heavy chain V region MOPC 104E OS=Mus musculus PE=1 SV=1	8	1	16.24
2	Antithrombin-III OS=Mus musculus GN=Serpinc1 PE=1 SV=1	68	15	34.41
2	Serum paraoxonase/arylesterase 1 OS=Mus musculus GN=Pon1 PE=1 SV=2	16	2	8.45
2	Fibrinogen gamma chain OS=Mus musculus GN=Fgg PE=1 SV=1	38	6	19.04
2	Isoform Short of Complement C3 OS=Mus musculus GN=C3	34	6	14.39
2	Serine protease inhibitor A3C OS=Mus musculus GN=Serpina3c PE=2 SV=1	19	3	3.36
2	Serine protease inhibitor A3N OS=Mus musculus GN=Serpina3n PE=1 SV=1	19	3	3.35
2	Serine protease inhibitor A3G OS=Mus musculus GN=Serpina3g PE=2 SV=2	19	3	3.18
2	Serine protease inhibitor A3F OS=Mus musculus GN=Serpina3f PE=1 SV=3	23	4	10.34
2	Vitamin D-binding protein OS=Mus musculus GN=Gc PE=1 SV=2	50	9	19.33
2	Succinate dehydrogenase [ubiquinone] cytochrome b small subunit_ mitochondrial OS=Mus musculus GN=Sdhd PE=2 SV=2	9	2	15.09
2	Fibrinogen beta chain OS=Mus musculus GN=Fgb PE=2 SV=1	65	14	30.35
2	Isoform 2 of Ig mu chain C region OS=Mus musculus GN=Ighm	74	14	29.47
2	Ig mu chain C region OS=Mus musculus GN=Ighm PE=1 SV=2	74	14	30.84
2	Ceruloplasmin OS=Mus musculus GN=Cp PE=1 SV=2	97	19	23.19
2	Haptoglobin OS=Mus musculus GN=Hp PE=1 SV=1	31	8	22.77
2	Ig kappa chain V-III region PC 6684 OS=Mus musculus PE=1 SV=1	10	1	16.22
2	Ig kappa chain V-III region PC 7769 OS=Mus musculus PE=1 SV=1	10	1	16.22
2	Ig kappa chain V-III region PC 7175 OS=Mus musculus PE=1 SV=1	10	1	16.22
2	Ig kappa chain V-III region PC 2485/PC 4039 OS=Mus musculus PE=1 SV=1	10	1	16.22
2	Ig kappa chain V-III region PC 7940 OS=Mus musculus PE=1 SV=1	10	1	16.22
2	Ig kappa chain V-III region PC 7183 OS=Mus musculus PE=1 SV=1	10	1	16.22
2	Ig kappa chain V-III region PC 7210 OS=Mus musculus PE=1 SV=1	10	1	16.36
2	Ig kappa chain V-III region PC 6308 OS=Mus musculus PE=1 SV=1	10	1	16.22

Table S9. Identified proteins in group treated with 300 mg kg^{-1} day^{-1} of diacetyl (three technical replicates) (cont.)

Replicate number	Protein Description	Protein Matched Products	Protein matched Peptides	Protein seqCover (%)
2	Ig kappa chain V-III region PC 7043 OS=Mus musculus PE=1 SV=1	10	1	16.22
2	Ig kappa chain V-III region CBPC 101 OS=Mus musculus PE=1 SV=1	10	1	16.22
2	Ig kappa chain V-III region PC 3741/TEPC 111 OS=Mus musculus PE=1 SV=1	10	1	16.22
2	Ig kappa chain V-III region TEPC 124 OS=Mus musculus PE=1 SV=1	10	1	16.07
2	Ig kappa chain V-III region MOPC 70 OS=Mus musculus PE=1 SV=1	10	1	16.22
2	Ig kappa chain V-III region PC 7132 OS=Mus musculus PE=1 SV=1	10	1	16.07
2	Ig kappa chain V-III region PC 2413 OS=Mus musculus PE=1 SV=1	10	1	16.22
2	Ig kappa chain V-III region 50S10.1 OS=Mus musculus PE=1 SV=1	10	1	16.22
2	Ig kappa chain V-III region PC 2880/PC 1229 OS=Mus musculus PE=1 SV=1	10	1	16.22
2	Beta-2-microglobulin OS=Mus musculus GN=B2m PE=1 SV=2	13	3	19.33
2	Reversed Sequence 3017	27	4	19.5
2	Alpha-2-macroglobulin-P OS=Mus musculus GN=A2mp PE=2 SV=2	33	11	11.19
2	Complement factor B OS=Mus musculus GN=Cfb PE=1 SV=2	49	13	20.5
2	Regenerating islet-derived protein 3-alpha OS=Mus musculus GN=Reg3a PE=1 SV=1	9	2	27.43
2	Complement component C9 OS=Mus musculus GN=C9 PE=1 SV=2	42	11	20.8
2	Inter-alpha-trypsin inhibitor heavy chain H2 OS=Mus musculus GN=Itih2 PE=1 SV=1	48	13	19.56
2	Prothrombin OS=Mus musculus GN=F2 PE=1 SV=1	41	7	14.56
2	Plasminogen OS=Mus musculus GN=Plg PE=1 SV=3	51	13	26.85
2	Nucleoprotein (Fragment) OS=Sendai virus (strain Harris) GN=N PE=1 SV=1	9	3	33.73
2	Plasma protease C1 inhibitor OS=Mus musculus GN=Serping1 PE=1 SV=3	14	2	5.56
2	Isoform 2 of Ig gamma-2B chain C region OS=Mus musculus GN=Igh-3	16	4	16.12
2	Ig gamma-2B chain C region OS=Mus musculus GN=Igh-3 PE=1 SV=3	16	4	13.37
2	Gelsolin OS=Mus musculus GN=Gsn PE=1 SV=3	48	14	17.95
2	Isoform 2 of Gelsolin OS=Mus musculus GN=Gsn	46	13	18.19
2	Carboxypeptidase N catalytic chain OS=Mus musculus GN=Cpn1 PE=2 SV=1	8	3	8.97
2	Isoform 2 of Interleukin-1 receptor accessory protein OS=Mus musculus GN=Il1rap	15	5	13.89

(continued on next page)

Table S9. Identified proteins in group treated with 300 mg kg⁻¹ day⁻¹ of diacetyl (three technical replicates) (cont.)

Replicate number	Protein Description	Protein Matched Products	Protein matched Peptides	Protein seqCover (%)
2	Interleukin-1 receptor accessory protein OS=Mus musculus GN=Il1rap PE=1 SV=1	15	5	8.77
2	Reversed Sequence 431	15	6	15.55
2	H-2 class I histocompatibility antigen_ Q10 alpha chain OS=Mus musculus GN=H2-Q10 PE=1 SV=3	15	3	12.92
2	RNA-directed RNA polymerase L OS=Lymphocytic choriomeningitis virus (strain Armstrong) GN=L PE=1 SV=1	44	16	9.95
2	Complement factor H OS=Mus musculus GN=Cfh PE=1 SV=2	52	14	15.72
2	Plasma kallikrein OS=Mus musculus GN=Klkb1 PE=1 SV=2	24	7	11.13
2	Isoform 2 of Inter alpha-trypsin inhibitor_ heavy chain 4 OS=Mus musculus GN=Itih4	37	9	9.75
2	Inter alpha-trypsin inhibitor_ heavy chain 4 OS=Mus musculus GN=Itih4 PE=1 SV=2	37	9	9.34
2	Peroxiredoxin-2 OS=Mus musculus GN=Prdx2 PE=1 SV=3	9	2	9.09
2	Angiotensinogen OS=Mus musculus GN=Agt PE=1 SV=1	15	5	17.61
2	Apolipoprotein C-III OS=Mus musculus GN=Apoc3 PE=1 SV=2	4	1	19.19
2	Reversed Sequence 16327	8	4	15.5
2	Glycerophosphodiester phosphodiesterase 1 OS=Mus musculus GN=Gde1 PE=2 SV=1	6	1	3.93
2	M-phase inducer phosphatase 1 OS=Mus musculus GN=Cdc25a PE=2 SV=2	13	5	11.48
2	Reversed Sequence 6339	13	6	20.03
2	Anoctamin-4 OS=Mus musculus GN=Ano4 PE=2 SV=2	17	9	12.04
2	Mannose-binding protein C OS=Mus musculus GN=Mbl2 PE=2 SV=2	9	4	9.43
2	Complement component C8 gamma chain OS=Mus musculus GN=C8g PE=1 SV=1	5	2	10.4
2	Isoform 2 of Plakophilin-4 OS=Mus musculus GN=Pkp4	31	8	4.97
2	Plakophilin-4 OS=Mus musculus GN=Pkp4 PE=1 SV=1	31	8	4.79
2	Isoform 2 of Transcription factor Sp9 OS=Mus musculus GN=Sp9	11	1	4.51
2	Transcription factor Sp9 OS=Mus musculus GN=Sp9 PE=2 SV=1	11	1	4.34
2	Isoform 2 of Complement component C8 beta chain OS=Mus musculus GN=C8b	12	2	5.54
2	Complement component C8 beta chain OS=Mus musculus GN=C8b PE=1 SV=1	12	2	4.92

BrJAC

TECHNICAL NOTE

Optimization of the Hollow Fiber Microextraction conditions for the Determination of Pesticides in Whole Blood by GC-MS

Carolina Schmeiske[1,2] iD, Dayse Fernanda de Souza[1,2] iD, Bruno José Gonçalves da Silva[1]* iD ✉

[1]Departamento de Química, Universidade Federal do Paraná, 81530-000 Curitiba, PR, Brazil

[2]Laboratório de Toxicologia Forense, Polícia Científica do Paraná, 81020-430 Curitiba, PR, Brazil
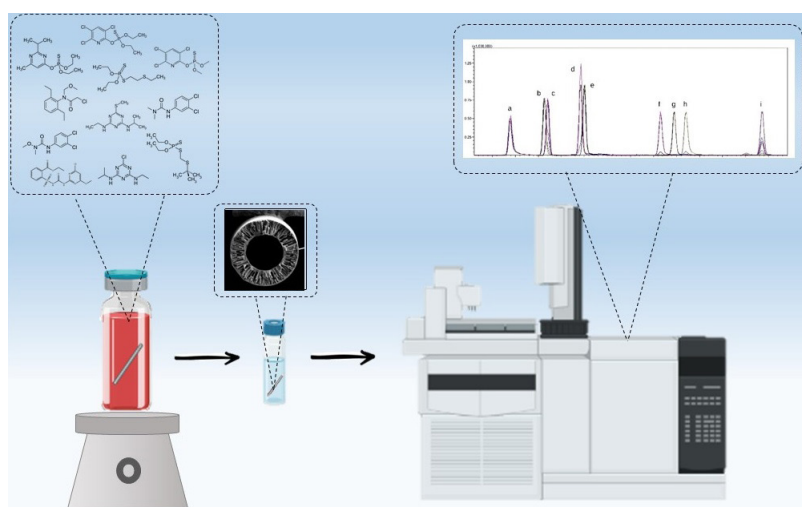
In forensic toxicology, the sample preparation procedure has been a crucial step in the analytical method development. The main objectives of the sample preparation include the extraction and pre-concentration of the analytes and removal of interfering species, such as endogenous compounds in the biological samples. In recent years, microextraction techniques have been generating interest due to their advantages, especially because the solvent volumes employed during the extraction are greatly reduced, contributing to the principles of green chemistry. In this work, a method based on hollow fiber microextraction (HFμE) and gas chromatography coupled to mass spectrometry (GC-MS) was evaluated for determination of pesticides (chlorpyrifos, chlorpyrifos methyl, diazinon, disulfoton, terbufos alachlor, ametryn, and atrazine) in postmortem whole blood samples. The extraction procedure was performed using polypropylene fibers as device and 1-octanol as extraction solvent. The fiber was immersed under magnetic stirring in the donor phase, which consisted of 500 microliters of whole blood and 7.5 milliliters of buffer solution. After the extraction time, the fiber was transferred to a vial containing an organic solvent and the analytes were desorbed by stirring. The extraction procedure was optimized. In the desorption step, desorption solvent, agitation mode, and time were evaluated. Multivariate optimization of pH, agitation speed, and salt addition were also performed, followed by univariate optimization of extraction time. After optimization, the extraction conditions that showed the best response were: pH adjustment to value 6, stirring at 600 rpm for 40 minutes without salt addition. For the desorption step, 1 minute of vortex agitation using ethyl acetate as the desorption solvent was defined as the optimal desorption condition. Under these conditions, the pesticides were successfully extracted from postmortem whole blood samples.

INTRODUCTION

Forensic toxicology is defined as the application of toxicology in a legal context. One of the fields of forensic toxicology is postmortem toxicology, or death investigation toxicology.[1] The aim of postmortem toxicology has been to evaluate if a certain compound was the cause of death, if it somehow contributed to it, or if it caused some subject incapacitation.[2,3]

Among the groups of substances of forensic interest, pesticides stand out in Brazil as the country is one of the largest consumers of these substances in the world.[4,5] A study of the data of deaths by intoxication that occurred in Brazil in the period between 2010 and 2015 showed that pesticides were the main toxic agent envolved.[6]

Several matrices can be used in postmortem toxicological analysis. Between them, blood is the selected matrix for quantitative analysis and correlating the concentrations found with pharmacological and toxic effects.[7,8] Postmortem samples are, usually, more complex than samples collected from living subjects due to processes of autolysis and putrefaction. In postmortem blood, separation of red blood cells from serum is usually not possible, so whole blood must be used. Whole blood samples present a great variety of endogenous compounds, such as fatty acids and cholesterol.[2,9,10] In this context, sample preparation has been a very important step in toxicological analysis to concentrate analytes and eliminate matrix interferents before injection in the chromatographic system.[7,11]

Liquid-liquid extraction (LLE) is a simple procedure still widely used in forensic toxicology. LLE is based on the partitioning of the analytes between the sample and several immiscible organic solvents. Although it is a simple and generally efficient technique, it has disadvantages like the great consumption of toxic solvents.[12,13] Motivated by the green chemistry principles, research in miniaturized techniques of extraction that use a minimal amount of solvent, or no solvent at all, have been developed.[12,14]

The miniaturization of classic LLE led to liquid-phase microextraction techniques.[15] Several microextraction techniques have been applied to the extraction of pesticides from biological samples, as can be seen in Table I.

Table I. Application of microextraction techniques to the extraction of pesticides from biological matrices

Extraction method	Matrix	Analytes	Instrumental	Ref.
VA-DLLME	Blood/stomach content/liver	Dichlorvos	GC-MS	16
	Urine	Triazol herbicides	GC-MS	17
DLLME	Plasma/serum	Organochlorine pesticides	GC-MS/MS	18
	Blood	Organophosphate pesticides	HPLC-UV	19
	Urine	20 pesticides of various classes	LC-MS/MS	20
	Urine	Malathion	HPLC-UV	21
DLLME-SFO	Blood/urine	Pyrethroid insecticides	GC-MS	22
	Plasma/urine	Organophosphate pesticides / Pyrethroid inseticticides	GC-MS	23

Table I. Application of microextraction techniques to the extraction of pesticides from biological matrices (continued)

Extraction method	Matrix	Analytes	Instrumental	Ref.
DI-SPME	Serum	Carbamates / organophospate pesticides	TD-ESI/MS/MS	24
HF-SBME	Plasma	Organophosphate / Organochlorine pesticides	GC-FID	25
SDME	Urine	Tebuconazole, pendimethalin, DDT, DDE	HPLC-UV	26
DSPE-DLLME	Urine	Chlorpyrifos	HPLC-UV	27

VA: vortex-assisted; DLLME: dispersive liquid-liquid microextraction; DI-SPME: direct immersion solid phase microextraction; HF-SBME: hollow-fiber solvent bar microextraction; SFO: solidification of floating organic droplet; SDME: single drop microextraction; DSPE: dispersive solid phase extraction; GC: gas chromatography; MS: mass spectrometry; TD-ESI: thermal desorption-electrospray ionization; FID: flame ionization detector; HPLC: high performance liquid chromatography; UV: ultraviolet detector.

Between microextraction techniques, several methods are based in the use of hollow fibers. The use of hollow fibers began when Pedersen-Bjergaard and Rasmussen introduced them as a support for the organic solvent, creating the *hollow fiber liquid-phase microextraction* (HF-LPME).[28] In this technique, the pores of a hollow hydrophobic membrane are impregnated with the organic solvent, while its interior (called lumen) is filled with the acceptor phase. This acceptor phase may be the same organic solvent used for pore impregnation (two-phase HF-LPME) or an aqueous phase (three-phase HF-LPME). The fiber is then immersed in a vial containing the sample (donor phase) and the analytes are extracted from the donor phase, through the immobilized solvent in the pores, to the acceptor phase, which is subsequently collected.[29,30]

As the fiber acts as a physical barrier between the sample and acceptor phase, preventing macromolecules from reaching the lumen, HF-LPME is the most widely used liquid-phase microextraction technique for the extraction of complex biological fluids. But the technique still has some disadvantages, such as the need of microsyringes to fill the lumen and recover the extract, which limits the number of samples that can be processed simultaneously and requires operator skills. Still, the contact area between the extraction solvent and the sample is limited, since the fiber remains fixed during the process.[31,32]

In order to simplify the extraction process, eliminating manual operations with the use of microsyringes, Ide and Nogueira developed the *hollow fiber microextraction* (HFμE). In HFμE, a hollow fiber segment is impregnated with the extraction solvent, and then immersed in the donor phase under agitation. At the end of extraction time, the fiber is transferred to a vial containing an organic solvent, which is submitted to agitation to perform analytes desorption.[33,34] This technique has been applied to the determination of polycyclic aromatic hydrocarbons and organochlorine pesticides in matrices such as surface water, residual water, soil, tea, fish liver and tomato.

Several factors can be adjusted to optimize the extraction procedure, including the membrane characteristics, extraction solvent, extraction time, pH, temperature, agitation, salt addition.[30,35-37] Extraction time must, ideally, be as short as possible. Extraction recovery increases with time until equilibrium is reached. During method optimization, equilibrium time can be established through Recovery x Time curves.[30,37]

Donor phase pH must be adjusted in a way that, according to pKa, acidic or basic compounds remain non-ionized, increasing their solubility in the organic solvent.[35,37,38] Temperature and agitation of the system can both decrease extraction time as they increase diffusion coefficients and decrease the viscosity. Agitation is commonly performed via magnetic stirring or ultrasonic bath. However, increasing the temperature is avoided since it can cause bubble formation and solvent loss due to evaporation.[30,35-37] Salt addition can

increase extraction efficiency, specially of polar compounds, due to salting out effect, that decreases the solubility of the compounds in the aqueous phase. On the other hand, interaction of the analytes with the ions, as well as increase of the matrix viscosity, can reduce analytes diffusion.[35-37]

In this work, HFµE technique was evaluated and optimized for extraction of eight pesticides (chlorpyrifos, chlorpyrifos methyl, diazinon, disulfoton, terbufos, alachlor, ametryn, atrazine) in postmortem whole blood samples and determination by GC-MS.

MATERIALS AND METHODS

Analytical standards

Analytical standards of diazinon (98,4%), chlorpyrifos (98,4%), ametryn (95,8%), chlorpyrifos methyl (99,8%), atrazine (98,1%), disulfoton (94%), terbufos (98,6%), alachlor (99,5%), and the internal standard etrimfos (62%) were provided by the Laboratory of Forensic Toxicology of Scientific Police of Paraná. Stock solutions were prepared by dissolving the compounds in methanol (Dinâmica) at 1 mg mL^{-1}. Working solutions of the analytes at 100 µg mL^{-1} were prepared by further dilution of the stock solutions right before analysis.

Reagents and chemicals

1-octanol (Sigma-Aldrich) was used as extraction solvent and ethyl acetate (Mallinckrodt), acetone (J.T.Baker) and hexane (Panreac) were tested as desorption solvents. The influence of salt addition in the extraction was evaluated using sodium sulfate (Synth). Phosphate buffer pH 2 and 6 were prepared with phosphoric acid, potassium phosphate monobasic (both Sigma-Aldrich) and potassium phosphate dibasic (Merck). Acetate buffer pH 4 was prepared with acetic acid and sodium hydroxide (both Merck).

Instrumentation and chromatographic conditions

Gas chromatography assays were performed at GCMS2010 Plus coupled to mass spectrometer TQ 8040 (Shimadzu). Data obtained were treated with GCMS Solution software. Separation was carried out at SH-Rtx-5MS 30.0 m x 0.25 mm x 0.25 µm column (Shimadzu). Helium was used as carrier gas at a flow of 1.0 mL min^{-1}. Oven temperature was set at 75 ºC and maintained for 3 min, followed by an increase of 20 ºC min^{-1} until 205 ºC, then 30 ºC min^{-1} until 250 ºC, which was maintained for 4 min. Injection was performed at splitless mode (injection volume: 1 µL) and injector temperature was set at 300 ºC. Mass spectra were obtained at SIM mode. Transfer line and ionization source temperatures were set at 275 ºC and 250 ºC, respectively.

Whole blood samples

The postmortem whole blood samples used were collected in necropsies performed by the Scientific Police of Paraná. These samples were previously analyzed by the Laboratory of Forensic Toxicology of the Scientific Police of Paraná and proved to be free of the analytes subjects of this study. Samples were stored at -20 ºC and brought at room temperature before being handled.

Extraction procedure

For hollow fiber microextraction, polipropylene fibers with 600 µm i.d., 200 µm wall thickness and 0.2 µm pore diameter were used (Q3/2 Accurel, Membrana). Fibers were cut into 1 cm segments and cleaned in acetone under ultrasonic agitation (Easy Elmassonic, Elma), followed by air drying. The fibers were used only for one extraction procedure and then discarded, due to their low cost. For pores impregnation, the fiber segments were dipped at 1-octanol for 20 seconds, then transferred for a 10 mL vial containing the donor phase. The donor phase was composed of whole blood (500 µL), containing the internal standard (etrimfos), and buffer solution (7.5 mL). The system was maintained under magnetic stirring (KMO2 basic, Ika-Werke). After extraction time, the fiber was transferred to an insert vial containing 100 µL of the desorption solvent.

Optimization of the extraction procedure

For the optimization assays, blank whole blood samples spiked with the analytes at 1.0 µg mL^{-1} and internal standard at 0.5 µg mL^{-1} were used. Optimization of the desorption step was performed following a 2² factorial design (Table II). Agitation mode (vortex and ultrasound) and time (1 and 5 minutes) were optimized.

Table II. Factors and levels of desorption optimization

Factor	Level -1	Level +1
Agitation mode	Vortex	Ultrasound
Time (minutes)	1	5

Multivariate optimization of the parameters pH, agitation speed and salt addition were performed following a Box-Behnken design. Factors and levels studied are described in Table III. For pH adjustment, phosphate buffer (pH 2 and 6) and acetate buffer (pH 4) were used. Salt addition was performed with sodium sulfate. At these assays, extraction time was fixed as 30 minutes.

Table III. Factors and levels of the Box-Behnken design for optimization of extraction

Factor	Level -1	Central Point (0)	Level +1
pH	2 (phosphate buffer)	4 (phosphate buffer)	6 (acetate buffer)
Agitation speed (rpm)	600	800	1000
Salt addition (% m/v)	0	2.5	5

After optimization of these parameters, time extraction was optimized by univariate mode (10, 20, 30, 40, 50 and 60 minutes).

RESULTS AND DISCUSSION
Gas chromatography analysis

For GC analysis, etrimfos was used as internal standard. Etrimfos was selected since it has similar properties to the analytes and is banned in Brazil. The chromatogram obtained after the injection of a mix containing the analytes and IS at 1 µg mL^{-1} under the defined conditions can be seen in Figure 1. Information about the retention times obtained for all analytes and internal standard, quantification and confirmation ions selected, as well as some physicochemical properties of the compounds is demonstrated in Table IV.
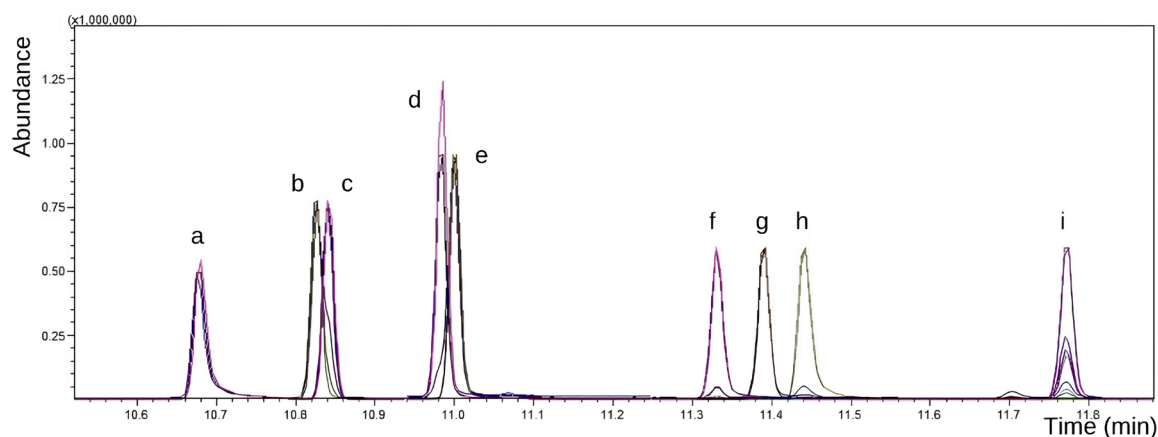
Figure 1. GC-MS chromatogram obtained at SIM mode of a mix containing the analytes and IS at 1 µg mL^{-1}. a: Atrazine; b: Terbufos; c: Diazinon; d: Disulfoton, e: Etrimfos, f: Chlorpyrifos methyl, g: Alachlor, h: Ametryn, i: Chlorpyrifos.

Table IV. Identification parameters and physicochemical properties of the analytes

Compound	Molecular formula	RT (min)	Quantitation ion	Confirmation ions	Molecular weight (g mol^{-1})	pKa	LogP[a]
Atrazine	$C_9H_{11}Cl_3NO_3PS$	10.670	200	215-173	350.6	ND[b]	4.7
Terbufos	$C_7H_7Cl_3NO_3PS$	10.805	231	103-125	322.5	ND[a]	4
Diazinon	$C_{12}H_{21}N_2O_3PS$	10.825	179	137-152	304.35	2,6[b]	3.69
Disulfoton	$C_8H_{19}O_2PS_3$	10.970	88	89-142	274.4	ND[a]	3.95
Chlorpyrifos methyl	$C_9H_{21}O_2PS_3$	11.310	286	288	288.4	ND[a]	4.51
Alachlor	$C_{14}H_{20}ClNO_2$	11.370	160	188-146	269.77	0,62[a]	3.09
Ametryn	$C_9H_{17}N_5S$	11.430	212	227-170	227.33	4,1[b]	2.63
Chlorpyrifos	$C_8H_{14}ClN_5$	11.750	197	199-314	215.68	1,6[a]	2.7
Etrimfos (IS)	$C_{10}H_{17}N_2O_4PS$	10.980	181	292-168	292.29	ND[a]	2.94

References: a[39]; b[40]

As it is possible to see in Table IV, some of the compounds presented very similar retention times, and co-elution was observed between terbufos and diazinon, and between disulfoton and etrimfos. This problem was resolved by selection of monitoring ions for these analytes that weren't present at the mass spectrum of the co-eluted substance.

Selectivity of the chromatographic method was assessed in terms of matrix interferences and interferences from other commonly encountered analytes. To the matrix interferences assay, 10 blank matrix samples from different sources were analyzed by the developed method. A *m/z* ion 227 was detected at ametryn retention time. This ion is the most abundant ion in ametryn mass spectrum, therefore would be chosen as the quantitation ion for this compound. After this study, however, *m/z* 227 was replaced by 212, the second most abundant ion in ametryn mass spectrum. No interference was detected when monitoring the ion 212.

The second selectivity study was performed by injection of a mix containing common medications and drugs of abuse that could be present in real samples (Table V). GC analysis was performed in *full scan* mode and only imipramine and cocaine were detected. Both showed, however, longer retention times than the last eluted analyte. Besides direct injection, this interferences mix was added to a blank matrix at 0.5 mg mL^{-1} concentration, and submitted to the extraction procedure before GC analysis. In this assay, it was possible to verify that the two compounds previously detected (imipramine and cocaine) were not extracted by the developed extraction method.

Table V. Retention time of the analytes and possible interferents studied

Analyte	Retention time (min)
Atrazine	**10.670**
Terbufos	**10.805**
Diazinon	**10.825**
Disulfoton	**10.970**
Etrimfos	**10.980**
Chlorpyrifos methyl	**11.310**
Alachlor	**11.370**
Ametryn	**11.430**
Chlorpyrifos	**11.750**
Etrimfos (IS)	**10.980**
Cocaine	13.356
Imipramine	13.536
Acetylsalicilic acid	ND
Bromazepam	ND
Caffeine	ND
Codeine	ND
Diazepam	ND
Diclofenac	ND
Fluoxetine	ND
Ibuprofen	ND
MDA	ND
MDMA	ND
Nortriptyline	ND
Paracetamol	ND

The bold values represent the retention times of the analytes; ND: not detected.

Optimization of HFµE
Desorption step

Ethyl acetate, acetone and hexane were evaluated as desorption solvents. Duplicate analysis with each solvent was performed following extraction of blank whole blood samples added with the analytes and internal standard. The medium peak area obtained for each analyte showed that most of them showed better response when desorption was performed with ethyl acetate.

Besides the desorption solvent, factors that influence the desorption efficiency include agitation mode and desorption time. These factors were also evaluated using a 2^2 factorial design. In this study, time had more impact on response when ultrasound was applied. Overall, 1 minute vortex desorption was more efficient than 5 minutes ultrasound desorption for all analytes, except for disulfoton. So, desorption was set to be carried out in ethyl acetate, through 1 minute vortex agitation, in order to improve analytical frequency.

Multivariate optimization – pH, agitation speed and salt addition

Optimization of the factors pH, agitation speed and salt addition were performed by multivariate mode. Multivariate optimization allows to visualize interaction effects between the factors, as opposed to univariate optimization.[41] For this purpose, a Box-Behnken design was performed (Table II). Box-Behnken designs are based in 3 levels fractional factorial designs. The study was performed with quintuplicate of central point, resulting in 17 experiments. The data obtained for all analytes were analyzed using the desirability function. The use of desirability allows the evaluation of all the analytes together. The response obtained for each analyte in each assay was converted to a desirability value between 0 and 1, as 0 was defined as 50% of the lowest area obtained for each analyte, and 1 as the highest area plus 50%. The calculated desirability values were submitted to a multiple linear regression and the pareto graph of the effects can be seen at Figure 2.

According to the graph, the only parameter with significant effect, by itself, is pH. As previously mentioned, pH must be adjusted to a value where analytes remain in non-ionized form, according to pKa.[35,37,38] As this study included both acidic and basic compounds, as well as non-ionic, with different values of pKa (Table III), an optimum pH value for all analytes would be impossible. Thus, a compromise condition should be found. The pH effect was positive, that is, higher the pH, higher the extraction efficiency. So, pH 6 was selected as the best pH to perform the extraction.
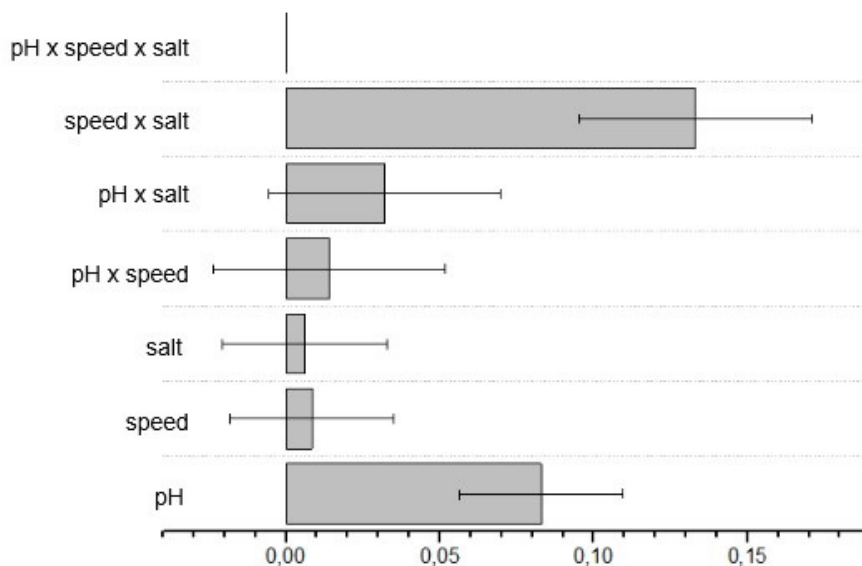
Figure 2. Pareto graph of the extraction effects – pH, agitation speed and salt addition.

Agitation speed was expected to show a positive effect since it improves analytes diffusion. However, no effect was observed, indicating that the lowest speed used was already high enough for this parameter. Salt addition can both increase or decrease extraction efficiency. In this case, no effect was observed for this parameter either.[30,35-37]

Although agitation speed and salt addition, by themselves, showed no effect in extraction efficiency, there's an interaction effect between both, which is also demonstrated by the pareto graph (Figure 2). To evaluate the best condition of these two factors, the response surface was plotted (Figure 3). The response surface shows that higher extraction efficiency is obtained at lower agitation (600 rpm) with no salt addition, or at higher agitation speed (1.000 rpm) and salt addition at 5% m/v concentration. This behavior occurs probably because the salt addition increases the viscosity of the donor phase, which difficult the analytes diffusion. Thus, higher agitation speed is needed to compensate for this negative impact. Between these two conditions of maximum response, the condition with agitation at 600 rpm and no salt addition was selected to minimize reagent consumption.
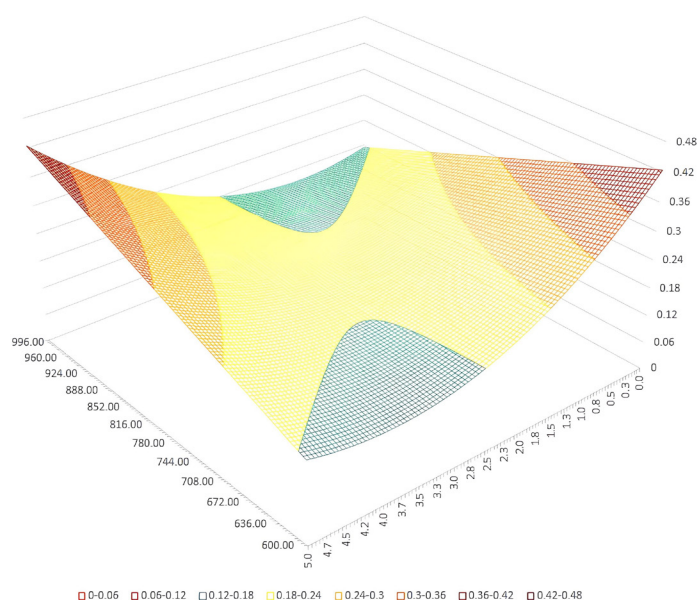
Figure 3. Response surface of the factors stirring speed and salt addition in the extraction.

Extraction time

After multivariate optimization, time univariate optimization was performed. Triplicate assays were performed at 10, 20, 30, 40, 50 and 60 minutes. The response of all analytes increased until 40 minutes of extraction. After this time, most of the compounds reach a plateau, indicating that equilibrium was achieved. Variation in analytes response that occurred after this time were all within the standard deviation. Therefore, 40 min was seen as the optimum time to perform analytes extraction.

CONCLUSION

Hollow fiber microextraction (HFμE) is a simple extraction technique based on other membrane-based extractions, like HF-LPME, but making it easier by eliminating the use of microsyringes and reducing manual steps that requires operator skill. It uses only few microliters of extraction solvent, in alignment with green chemistry techniques. In this work, the potential use of this technique in postmortem forensic toxicology was demonstrated by the optimization of an extraction procedure for the detection of selected pesticides in whole blood samples. Further work includes the validation of the developed method before application in real samples.

Conflicts of interest

The authors declare that they have no known competing financial interests or personal relationships that could have appeared to influence the work reported in this paper.

REFERENCES
(1) Wyman, J. F. Principles and Procedures in Forensic Toxicology. *Clin. Lab. Med.* **2012**, *32* (3), 493–507. https://doi.org/10.1016/j.cll.2012.06.005
(2) Skopp, G. Postmortem Toxicology. *Forensic Sci. Med. Pathol.* **2010**, *6* (4), 314–325. https://doi.org/10.1007/s12024-010-9150-4
(3) Smith, M. P.; Bluth, M. H. Forensic Toxicology: An Introduction. *Clin. Lab. Med.* **2016**, *36* (4), 753–759. https://doi.org/10.1016/j.cll.2016.07.002
(4) Ramos, J. S. A.; Pedroso, T. M. A.; Godoy, F. R.; Batista, R. E.; de Almeida, F. B.; Francelin, C.; Ribeiro, F. L.; Parise, M. R.; de Melo e Silva, D. Multi-Biomarker Responses to Pesticides in an Agricultural Population from Central Brazil. *Sci. Total Environ.* **2021**, *754*. https://doi.org/10.1016/j.scitotenv.2020.141893
(5) de Araújo Nascimento, F.; Alves, A. A.; Nunes, H. F.; Miziara, F.; Parise, M. R.; de Melo e Silva, D. Cultivated Areas and Rural Workers' Behavior Are Responsible for the Increase in Agricultural Intoxications in Brazil? Are These Factors Associated? *Environ. Sci. Pollut. Res.* **2020**, *27* (30), 38064–38071. https://doi.org/10.1007/s11356-020-09988-3
(6) Bochner, R.; Freire, M. M. Analysis of deaths by intoxication that occurred in Brazil from 2010 to 2015 based on the Mortality Information System (SIM). *Ciência & Saúde Coletiva* **2020**, *25* (2), 761-772. https://doi.org/10.1590/1413-81232020252.15452018
(7) Peters, F. T.; Wissenbach, D. K.; Busardo, F. P.; Marchei, E.; Pichini, S. Method Development in Forensic Toxicology. *Curr. Pharm. Des.* **2018**, *23* (36), 5455-5467. https://doi.org/10.2174/1381612823666170622113331
(8) Vincenti, M.; Cavanna, D.; Gerace, E.; Pirro, V.; Petrarulo, M.; Di Corcia, D.; Salomone, A. Fast Screening of 88 Pharmaceutical Drugs and Metabolites in Whole Blood by Ultrahigh-Performance Liquid Chromatography-Tandem Mass Spectrometry. *Anal. Bioanal. Chem.* **2013**, *405* (2–3), 863–879. https://doi.org/10.1007/s00216-012-6403-y
(9) Jones, G. R. Postmortem Toxicology. In: Jickells, S.; Negrusz, A. (Eds). *Clarke's Analytical Forensic Toxicology*. Pharmaceutical Press, London, 2008, pp 191–217.
(10) Skopp, G. Preanalytic Aspects in Postmortem Toxicology. *Forensic Sci. Int.* **2004**, *142* (2–3), 75–100. https://doi.org/10.1016/j.forsciint.2004.02.012
(11) Manousi, N.; Samanidou, V. Green Sample Preparation of Alternative Biosamples in Forensic Toxicology. *Sustain Chem. Pharm.* **2021**, *20*, 100388. https://doi.org/10.1016/j.scp.2021.100388
(12) Campillo, N.; Gavazov, K.; Viñas, P.; Hagarova, I.; Andruch, V. Liquid-Phase Microextraction: Update May 2016 to December 2018. *Appl. Spectrosc. Rev.* **2019**, *55* (4), 307–326. https://doi.org/10.1080/05704928.2019.1604537
(13) Wille, S. M. R.; Lambert, W. E. E. Recent Developments in Extraction Procedures Relevant to Analytical Toxicology. *Anal. Bioanal. Chem.* **2007**, *388* (7), 1381–1391. https://doi.org/10.1007/s00216-007-1294-z
(14) He, Y.; Concheiro-Guisan, M. Microextraction Sample Preparation Techniques in Forensic Analytical Toxicology. *Biomed. Chromatogr.* **2019**, *33* (1), 1–12. https://doi.org/10.1002/bmc.4444
(15) Burato, J. S. S.; Medina, D. A. V.; de Toffoli, A. L.; Maciel, E. V. S.; Lanças, F. M. Recent Advances and Trends in Miniaturized Sample Preparation Techniques. *J. Sep. Sci.* **2020**, *43* (1), 202–225. https://doi.org/10.1002/jssc.201900776

(16) Jain, R.; Jain, B.; Chauhan, V.; Deswal, B.; Kaur, S.; Sharma, S.; A. S. Abourehab, M. Simple Determination of Dichlorvos in Cases of Fatal Intoxication by Gas Chromatography-Mass Spectrometry. *J. Chromatogr. B* **2023**, *1215*. https://doi.org/10.1016/j.jchromb.2022.123582

(17) Machado, S. C.; Souza, B. M.; Marciano, L. P. A.; Pereira, A. F. S.; de Carvalho, D. T.; Martins, I. A Sensitive and Accurate Vortex-Assisted Liquid-Liquid Microextraction-Gas Chromatography-Mass Spectrometry Method for Urinary Triazoles. *J. Chromatogr. A* **2019**, *1586*, 9–17. https://doi.org/10.1016/j.chroma.2018.11.082

(18) Shin, H. Trace-level Analysis of Polychlorinated Biphenyls, Organochlorine Pesticides and Polycyclic Aromatic Hydrocarbons in Human Plasma or Serum by Dispersive Liquid–Liquid Microextraction and Gas Chromatography–Tandem Mass Spectrometry. *Biomed. Chromatogr.* **2022**, *36* (6). https://doi.org/10.1002/bmc.5360

(19) Akramipour, R.; Golpayegani, M. R.; Sedighi, M.; Fattahi, F.; Fattahi, N. Determination of Common Organophosphorus Pesticides in the Blood of Children with Acute Leukaemia Using a Double-Solvent System as a Novel Extractant for Dispersive Liquid-Liquid Microextraction. *RSC Adv.* **2020**, *10* (73), 44736–44742. https://doi.org/10.1039/d0ra09303c

(20) Gallo, V.; Tomai, P.; Gherardi, M.; Fanali, C.; De Gara, L.; D'Orazio, G.; Gentili, A. Dispersive Liquid-Liquid Microextraction Using a Low Transition Temperature Mixture and Liquid Chromatography-Mass Spectrometry Analysis of Pesticides in Urine Samples. *J. Chromatogr. A* **2021**, *1642*. https://doi.org/10.1016/j.chroma.2021.462036

(21) Ramin, M.; Khadem, M.; Omidi, F.; Pourhosein, M.; Golbabaei, F.; Shahtaheri, S. J. *Development of Dispersive Liquid-Liquid Microextraction Procedure for Trace Determination of Malathion Pesticide in Urine Samples. Iran. J. Public Health* **2019**, *48* (10), 1893-1902. https://doi.org/10.18502/ijph.v48i10.3498

(22) Zhu, M.; Niu, Z.; Zhang, W.; Zhang, J.; Wen, Y. The Combination of Two Microextraction Methods Coupled with Gas Chromatography for the Determination of Pyrethroid Insecticides in Multimedia Environmental Samples: Air, Water, Soil, Urine and Blood. *Water and Environ. J.* **2020**, *34* (S1), 503–515. https://doi.org/10.1111/wej.12553

(23) Jouyban, A.; Farajzadeh, M. A.; Mogaddam, M. R. A. Dispersive Liquid–Liquid Microextraction Based on Solidification of Deep Eutectic Solvent Droplets for Analysis of Pesticides in Farmer Urine and Plasma by Gas Chromatography–Mass Spectrometry. *J. Chromatogr. B* **2019**, *1124*, 114–121. https://doi.org/10.1016/j.jchromb.2019.06.004

(24) Su, H.; Lin, H. H.; Su, L. J.; Lin, C. C.; Jiang, Z. H.; Chen, S. J.; Shiea, J.; Lee, C. W. Direct Immersion Solid-Phase Microextraction Combined with Ambient Ionization Tandem Mass Spectrometry to Rapidly Distinguish Pesticides in Serum for Emergency Diagnostics. *J. Food Drug Anal.* **2022**, *30* (1), 26–37. https://doi.org/10.38212/2224-6614.3399

(25) Zuluaga, M.; Yathe-G, L.; Rosero-Moreano, M.; Taborda-Ocampo, G. Multi-Residue Analysis of Pesticides in Blood Plasma Using Hollow Fiber Solvent Bar Microextraction and Gas Chromatography with a Flame Ionization Detector. *Environ. Toxicol. Pharmacol.* **2021**, *82*. https://doi.org/10.1016/j.etap.2020.103556

(26) Mafra, G.; Will, C.; Huelsmann, R.; Merib, J.; Carasek, E. A Proof-of-Concept of Parallel Single-Drop Microextraction for the Rapid and Sensitive Biomonitoring of Pesticides in Urine. *J. Sep. Sci.* **2021**, *44* (9), 1961–1968. https://doi.org/10.1002/jssc.202001157

(27) Ramin, M.; Omidi, F.; Khadem, M.; Shahtaheri, S. J. Combination of Dispersive Solid-Phase Extraction with Dispersive Liquid-Liquid Microextraction Followed by High-Performance Liquid Chromatography for Trace Determination of Chlorpyrifos in Urine Samples. *Int. J. Environ. Anal. Chem.* **2021**, *101* (6), 810–820. https://doi.org/10.1080/03067319.2019.1672670

(28) Pedersen-Bjergaard S.; Rasmussen, K. E. Liquid-Liquid-Liquid Microextraction for Sample Preparation of Biological Fluids Prior to Capillary Electrophoresis. *Anal. Chem.* **1997**, *71* (14), 2650–2656. https://doi.org/10.1021/ac990055n

(29) Esrafili, A.; Baharfar, M.; Tajik, M.; Yamini, Y.; Ghambarian, M. Two-Phase Hollow Fiber Liquid-Phase Microextraction. *TrAC, Trends Anal. Chem.* **2018**, *108*, 314–322. https://doi.org/10.1016/j.trac.2018.09.015

(30) Sharifi, V.; Abbasi, A.; Nosrati, A. Application of Hollow Fiber Liquid Phase Microextraction and Dispersive Liquid-Liquid Microextraction Techniques in Analytical Toxicology. *J. Food Drug. Anal.* **2016**, *24* (2), 264–276. https://doi.org/10.1016/j.jfda.2015.10.004

(31) López-López, J. A.; Mendiguchía, C.; Pinto, J. J.; Moreno, C. Application of Solvent-Bar Micro-Extraction for the Determination of Organic and Inorganic Compounds. *TrAC, Trends Anal. Chem.* **2019**, *110*, 57–65. https://doi.org/10.1016/j.trac.2018.10.034.

(32) Yamini, Y.; Rezazadeh, M.; Seidi, S. Liquid-Phase Microextraction – The Different Principles and Configurations. *TrAC, Trends Anal. Chem.* **2019**, *112*, 264–272. https://doi.org/10.1016/j.trac.2018.06.010

(33) Ide, A. H.; Nogueira, J. M. F. Hollow Fiber Microextraction: A New Hybrid Microextraction Technique for Trace Analysis. *Anal. Bioanal. Chem.* **2018,** *410*, 2911–2920. https://doi.org/10.1007/s00216-018-0971-4

(34) Ide, A. H.; Nogueira, J. M. F. Dual-Hollow Fiber Microextraction (Dual-HFµE) - Application for Monitoring Trace Levels of Organochlorine Pesticides in Real Matrices. *Int. J. Environ. Anal. Chem.* **2019**, *100* (12), 1402–1414. https://doi.org/10.1080/03067319.2019.1655006

(35) Alsharif, A. M. A.; Tan, G. H.; Choo, Y. M.; Lawal, A. Efficiency of Hollow Fiber Liquid-Phase Microextraction Chromatography Methods in the Separation of Organic Compounds: A Review. *J. Chromatogr. Sci.* **2017**, *55* (3), 378–391. https://doi.org/10.1093/chromsci/bmw188

(36) Dmitrienko, S. G.; Apyari, V. V.; Tolmacheva, V. V.; Gorbunova, M. V. Liquid–Liquid Extraction of Organic Compounds into a Single Drop of the Extractant: Overview of Reviews. *J. Anal. Chem.* **2021**, *76* (8), 907–919. https://doi.org/10.1134/S1061934821080049

(37) Pedersen-Bjergaard, S. Microextraction with Supported Liquid Membranes. In: Poole, C. F. (Ed). *Liquid-Phase Extraction, Handbooks in Separation Science*. Elsevier, 2019. Chapter 8, pp 241-263. https://doi.org/10.1016/B978-0-12-816911-7.00008-6

(38) He, Y. Recent Advances in Application of Liquid-Based Micro-Extraction: A Review. *Chem. Pap.* **2014**, *68* (8), 995–1007. https://doi.org/10.2478/s11696-014-0562-6

(39) PPDB: Pesticide Properties Database. https://sitem.herts.ac.uk/aeru/ppdb/en/atoz.htm#T

(40) PubChem Database. https://pubchem.ncbi.nlm.nih.gov

(41) Ferreira, S. L. C.; Bruns, R. E.; Ferreira, H. S.; Matos, G. D.; David, J. M.; Brandão, G. C.; da Silva, E. G. P.; Portugal, L. A.; dos Reis, P. S.; Souza, A. S.; dos Santos, W. N. L. Box-Behnken Design: An Alternative for the Optimization of Analytical Methods. *Anal. Chim. Acta* **2007**, *597* (2), 179–186. https://doi.org/10.1016/j.aca.2007.07.011

BrJAC

Brazilian Journal of Analytical Chemistry Conquers the World

During the 2024 European Symposium on Analytical Spectrometry (ESAS), held from June 24 – 28, 2024 at the University of Warsaw's Biological and Chemical Research Centre, Poland, Prof. Dr. Marco Aurélio Zezzi Arruda, Editor-in-Chief of the Brazilian Journal of Analytical Chemistry (BrJAC), delivered a brief presentation on the progress and achievements the journal has made in recent years.

Prof. Dr. Marco Aurélio Zezzi Arruda, Editor-in-Chief of the Brazilian Journal of Analytical Chemistry (BrJAC), presenting the journal at the 2024 European Symposium on Analytical Spectrometry. Photo: Marco A. Z. Arruda

BrJAC is indexed in Clarivate Analytics' Emerging Source Citation Index (ESCI) with a Journal Impact Factor (JIF) of 1.1 for 2023 and a Journal Citation Index (JCI) of 0.23 for 2023. BrJAC is also indexed in SCOPUS, with a CiteScore of 1.6 for 2023 and a CiteScore Tracker of 2.0 for 2024. In Google Scholar, BrJAC has an h-index of 12 and is included in the CAplus Core Journal Coverage List. The journal is classified in the Qualis/Capes B3 stratum for the period 2017/2020.

The BrJAC is the first Brazilian scientific journal dedicated to all branches of Analytical Chemistry. It was launched on June 18, 2010, in order to fulfill the idealistic vision of a group of researchers to achieve true academic-industrial integration, fostering both innovation and technical-scientific development.

The composition of the BrJAC Editorial Board, which brings together professionals in the Analytical Chemistry field who work in academia, the private sector, and public institutions, reflects the search for academic-industrial integration. Since its inception in 2010, BrJAC has shown an upward trend in scientific quality and worldwide visibility.

To find out more about BrJAC, please visit: www.brjac.com.br

Text written by Lilian Freitas, BrJAC Publisher

BrJAC

FEATURE

XIII Workshop on Sample Preparation

From June 18 to 20, 2024, the city of Piracicaba in the state of São Paulo, Brazil, hosted the 13th edition of the traditional Workshop on Sample Preparation (WPA). The event took place at the Luiz de Queiroz College of Agriculture (ESALQ/USP).

WPA-2024 brought together some of the world's leading experts in sample preparation for elemental analysis and spectrometric techniques. The program included conferences, mini-conferences, roundtables, and poster and flash presentations by congress participants, as well as various practical activities.

The WPA-2024 Organizing Committee consisted of Alex Virgilio from the Center for Nuclear Energy in Agriculture (CENA/USP), Ana Rita Nogueira from the Brazilian Agricultural Research Corporation (Embrapa/CPPSE), Cassiana Nomura from the Institute of Chemistry/USP, and Fábio Rocha from CENA/USP.

On the first day of the event, Prof. Dr. Francisco J. Krug (CENA/USP) was honored in a ceremony attended by Ramon Murray Barnes (University of Massachusetts, Amherst, USA), Helmar Wiltsche (Technical University of Graz, Graz, Austria), Camillo Pirola (Milestone, Italy), Wilson Hernandes (Anacom, Brazil), José Roberto Ferreira (CENA/USP), Érico Marlon Moraes Flores (Federal University of Santa Maria), Márcia Messias da Silva (Federal University of Rio Grande do Sul), and Joaquim Araújo Nóbrega (Federal University of São Carlos), and representative of the Brazilian Journal of Analytical Chemistry (BrJAC).

BrJAC tribute to Prof. Dr. Krug. From left to right: Luciene Campos (BrJAC Advertiser), Prof. Dr. Krug and Prof. Dr. Érico M. M. Flores. Photo WPA

Prof. Krug was the creator of the Workshop on Sample Preparation and also the author of the book "Métodos de preparo de amostras para análise elementar" (Editors: Krug, F.J. and Rocha, F.R.P. Publisher: EDIT-SBQ. ISBN: 978-85-64099-22-7).

Prof. Krug worked as a researcher at CENA/USP between 1975 and 2023, and since 2005 as a full professor at the same institution. He was a level 1A researcher at the National Council for Scientific and Technological Development (CNPq), indicating his high level of seniority and scientific leadership in his field. He has been a full member of the São Paulo State Academy of Sciences (ACIESP) since 2012. Throughout his career, he was honored with several prestigious awards, including the "Paschoal Senise" medal (2012), "Simão Matias" medal (2018), and "Adilson Curtius" medal (2022). Prof. Krug has published more than 200 scientific articles and has supervised 50 postgraduate students.

Opening lecture by Prof. Dr. Krug. Photo: WPA

After the tribute, Prof. Krug delivered a lecture titled, "Reminiscences of the Workshops on Sample Preparation."

Conferences

WPA-2024 featured conferences by Prof. Ramon Barnes (University of Massachusetts, Amherst), Prof. Helmar Wiltsche (Graz University of Technology), Prof. Érico M. M. Flores (Federal University of Santa Maria), Prof. Márcia F. Mesko (Federal University of Pelotas), Prof. Fábio A. Duarte (Federal University of Santa Maria), Prof. Mário H. Gonzalez (São Paulo State University - UNESP), Prof. Leandro W. Hantao (University of Campinas), Prof. Marcia M. Silva (Federal University of Rio Grande do Sul), and Prof. Juliana Naozuka (Federal University of São Paulo).

Conferences held during the event. Photo: WPA

Sponsors' mini-conferences

WPA-2024 also featured mini-conferences held by the event's sponsors. Participants had the opportunity to attend the lectures: "Workflow optimization: Efficient strategies for sample preparation" by Nova Analitica and Milestone; "Direct solid sampling by LIBS/LA-ICP-MS: Avoiding the defeat of sample digestion" by dpUnion; "Microwaves beyond digestion" by Anton Paar; and "Experimental approaches with a focus on experiments involving Single-cell ICP-MS" by PerkinElmer.

About WPA

The Workshop on Sample Preparation (WPA) has been held since 1996, with biannual editions hosted by universities and research centers in different regions of Brazil. In 2024, the WPA celebrated its 28th anniversary. The event has always been attended by leading Brazilian and international experts in sample preparation, who present the latest innovations for preparing complex samples to researchers, academics, and other professionals from sectors such as clinical, food, environmental, steel, and chemical industries.

Participants during one of the practical activities at WPA-2024. Photo: WPA

The WPA aims to provide a forum for discussing advances in the field of sample preparation in order to solve analytical problems. The event traditionally includes both theoretical and practical activities, enabling participants to discuss concepts related to sample preparation and the application of new technologies. Participation in the WPA is limited to 120 participants.

Text written by Lilian Freitas, BrJAC Publisher

Source: **Workshop on Sample Preparation**

BrJAC

SPONSOR REPORT

This section is dedicated for sponsor responsibility articles.

Rapid Qualitative and Quantitative Analysis of Residual Solvents in Food Packaging by Static Headspace coupled to GC-FID/MS

Giulia Riccardino and Cristian Cojocariu / *Thermo Fisher Scientific, Runcorn, UK*

This report was extracted from the Thermo Scientific Application Note 10689

The aim of this report is to demonstrate the qualitative and quantitative performance of the Thermo Scientific™ TriPlus™ 500 Gas Chromatography Headspace Autosampler coupled to a dual-detector GC-FID/MS for the determination of residual solvents in food packaging according to the European Standard EN 13628-1 method [1] and to highlight a highly efficient workflow through extended automation from sampling to data reporting.

Keywords: Residual solvents, flexible food packaging, food safety, valve and loop, headspace-gas chromatography, HS-GC, multiple headspace extraction, MHE, flame ionization detector, FID, mass spectrometer detector, MS, single quadrupole GC-MS, ISQ 7000, TriPlus 500 HS.

INTRODUCTION

Packaging materials are essential for maintaining food integrity and to ensure safe handling, transportation, and storage. Common food packaging materials are polymer-based thin films or paper-based coatings often layered or imprinted on the outside with inks, dyes, and paints intended to address the consumer appeal and convenience. The chemical components of such food packaging (especially from polymers, dyes, and inks) can migrate into the food products, modifying the organoleptic properties and the composition of the food and posing health risks to the consumer. As a consequence, regulatory measures are in place to make sure that food contact materials do not transfer any components to the packed foodstuff in quantities that could affect human health, change the composition, or modify the organoleptic properties of the product [2]. In the United States a migration limit of 50 ppm is applicable for residual solvents and non-volatile food additives [3]. In addition, precise quantification of residual solvents in flexible packaging is also regulated through set methods such as EN 13628-1:2002.

Analysis of volatile impurities in solid polymers is challenging, especially with regard to sampling and extraction techniques. Liquid injections of such samples require dissolution of packaging polymers into a suitable solvent prior to gas chromatography (GC) injection. This can result in high viscosity solutions containing non-volatile, long chain polymers that can potentially contaminate the GC injector ports. This, in turn, will require frequent inlet liner replacement and system maintenance that will increase the cost of analysis.

An alternative to liquid injections is headspace sampling: a fast and simple technique that enables the extraction of volatile and semi-volatile compounds from food packaging samples without the need for time-consuming sample preparation. In particular, static headspace with multiple headspace extraction (MHE) [4] can be used for absolute quantitative analysis of volatiles in solid matrices. This technique is particularly useful when matrix-matched calibration reference materials are not available.

In this study, the quantitative results for residual solvent analysis in food packaging materials, obtained with the TriPlus 500 Headspace (HS) autosampler, are reported. A dual detector FID/MS configuration allowed for the detection, identification (flame ionization detection), and confirmation (mass spectrometry

detection) of unknown impurities. The experiments also focused on assessing method linearity [1] according to EN 13628:1:2002 and precision, as well as the overall quantitative performance of the analytical setup for routine analysis of residual solvents in food packaging.

EXPERIMENTAL

In all experiments, a TriPlus 500 HS autosampler was coupled to a Thermo Scientific™ TRACE™ 1310 Gas Chromatograph equipped with a Thermo Scientific™ Instant Connect Split/Splitless SSL Injector. A Thermo Scientific™ Dual Detector Microfluidics device (P/N 19071030) was used to split 1:1 the carrier gas flow from the analytical column between a Thermo Scientific™ Instant Connect Flame Ionization Detector (FID) and a Thermo Scientific™ ISQ™ 7000 Single Quadrupole GC-MS system.

Chromatographic separation was achieved on a Thermo Scientific™ TraceGOLD™ TG-1MS GC capillary column, 30 m × 0.32 mm × 3.0 µm (P/N 26099-4840). Additional HS-GC-FID/MS conditions are given in Table 1. The GC oven temperature program was optimized to decrease the analysis time and improve sample throughput; all peaks of interest are eluting in <7 minutes with adequate peak chromatographic resolution (Rs > 1). An incubation time of 40 minutes per MHE step was optimized to cover the majority of food packaging material types. According to the EN 13628-1:2002 method, linearity was assessed on n = 4 headspace extraction cycles.

Table 1 (part 1). HS-GC-FID and ISQ 7000 mass spectrometer operating conditions for residual solvent determination

TRACE 1310 GC	
Inlet Module and Mode:	SSL, split
Split Ratio:	20:1
Septum Purge Mode, Flow (mL/min):	Constant, 5
Carrier Gas, Carrier Mode, Pressure (kPa):	He, constant pressure, 110
Oven Temperature Program	
Temperature 1 (°C):	50
Hold Time (min):	1
Temperature 2 (°C):	110
Rate (°C/min):	30
Temperature 2 (°C):	250
Rate 2 (°C/min):	20
FID	
Temperature (°C):	250
Air Flow (mL/min):	350
H2 Flow (mL/min):	35
N2 Flow (mL/min):	40
Acquisition Rate (Hz):	25
ISQ 7000 Single Quadrupole GC-MS system	
Ion Source:	ExtractaBrite
Transfer Line Temp. (°C):	250
Source Temperature (°C):	250
Ionization Mode:	EI
Electron Energy (eV):	70
Acquisition Mode:	Full-scan (*m/z* 25-350)

Table 1 (part 2). HS-GC-FID and ISQ 7000 mass spectrometer operating conditions used for residual solvent determination

TriPlus 500 HS Autosampler Parameters (MHE)	
Incubation Temp. (°C):	120
Incubation Time (min):	40
Vial Shaking:	Medium
Vial Pressurization Mode:	Pressure
Vial Pressure (kPa) (Auxiliary Gas Nitrogen):	55
Vial Pressure Equilibration Time (min):	1
Loop Size (mL):	1
Loop/Sample Path Temp. (°C):	120
Loop Filling Pressure (kPa):	34
Loop Equilibration Time (min):	1
Extraction Cycles:	4
Needle Purge Flow Level:	4
Injection Mode:	MHE
Injection Time (min):	1

Table 1 (part 3). HS-GC-FID and ISQ 7000 mass spectrometer operating conditions for residual solvent determination

TriPlus 500 HS Autosampler Parameters (total vaporization)	
Incubation Temp. (°C):	120
Incubation Time (min):	40
Vial Shaking:	Medium
Vial Pressurization Mode:	Pressure
Vial Pressure (kPa) (Auxiliary Gas Nitrogen):	55
Vial Pressure Equilibration Time (min):	1
Loop Size (mL):	1
Loop/Sample Path Temp. (°C):	120
Loop Filling Pressure (kPa):	34
Loop Equilibration Time (min):	1
Needle Purge Flow Level:	4
Injection Mode:	Standard
Injection Time (min):	1

Data acquisition, processing and reporting

The data was acquired, processed, and reported using the Thermo Scientific™ Chromeleon™ Chromatography Data System (CDS) software, version 7.2. Integrated instrument control ensures full automation from instrument set-up to raw data processing, reporting, and storage. Simplified e-workflows deliver effective data management ensuring ease of use, sample integrity, and traceability. Chromeleon CDS also offers the option to scale up the data handling process in the laboratory from a single workstation to an enterprise environment to further improve productivity [5].

Standard and sample preparation

Two standard mixtures, each containing different residual solvents that can be found in packaging materials (mixture 1 and mixture 2 at 7.14% v/v and 9.09% v/v, respectively), were purchased from Sigma Aldrich® (P/N 48994-U and 48995-U). A volume (1 µL) of each standard solution (corresponding to 71.4 µg and 90.9 µg of mixture 1 and 2, respectively) was spiked into the same 10 mL empty sealed headspace glass vial and used as retention time reference for compound identification as well as for MHE linearity assessment with total vaporization. A complete list of analyzed compounds is reported in Table 2.

Samples of packaged foods (pizza, cookies, bread, salad, and salami) were purchased locally and the packaging (cling film, wraps, and trays) was separated from the food and analyzed following the EN 13628-1:2002 method. A sample surface of 40 cm^2 (2 × 20 cm) was cut, coiled, and sealed into a 10 mL crimp cap headspace vial (vials P/N 10CV, caps P/N 20-MCBC-ST3). As specified in the EN 13628-1:2002 method, the ratio between the sample area (in cm^2) and the vial volume (in mL) was maintained between 3 and 5.

Table 2. Correlation coefficients (R^2) calculated using the full-scan EI traces. *For all compounds in the reference standard R^2 ≥ 0.997. Correlation coefficients for FID data were 1.000 for all components, hence data are not shown.*

MHE Linearity		
Component Name	**RT (min)**	**Correlation Coefficient (R^2)**
Methanol	1.72	0.997
Ethanol	2.11	0.997
Acetone	2.37	0.998
2-Propanol	2.44	0.999
Methyl acetate	2.73	0.999
1-Propanol	2.98	0.998
2-Butanone	3.33	0.999
2-Butanol	3.42	1.000
Ethyl acetate	3.53	0.999
2-Methyl-1-propanol	3.68	0.999
2-Methoxyethanol	3.74	0.997
Tetrahydrofuran	3.80	0.999
Isopropyl acetate	4.04	0.998
1-Methoxy-2-propanol	4.20	0.997
Cyclohexane	4.34	0.998
Propylacetate	4.57	0.999
4-Methyl-2-pentanone	4.89	0.998
Isobutyl acetate	5.22	0.999
Toluene	5.38	0.997
Butyl acetate	5.63	0.999
2-Methoxyethyl acetate	5.74	0.997
2-Etoxyethyl acetate	6.47	0.998
Cyclohexanone	6.66	0.999

RESULTS AND DISCUSSION

MHE linearity assessment according to EN 13628-1:2002 method

A reference solvent standard mix was prepared as described in the standard and sample preparation section and analyzed using the total vaporization technique [4] applying the MHE conditions reported in Table 1. MHE allows the extrapolation of the total content of analytes in a liquid or solid matrix through multiple headspace cycles. The amount of analyte present in the sample is calculated by direct comparison of the peak area responses to external standards previously analyzed in a similar way but without matrix.

MHE linearity was assessed by plotting the natural logarithm of the peak areas in the standard solution versus the number of headspace cycles (n = 4). Chromeleon CDS interactive charts and reprocessing features allowed for fast MHE calibration plots and correlation coefficient calculations without the need of external calculation tools, as shown in Figure 1. For all the investigated compounds, the calculated correlation coefficients (R^2) were 1.000 for FID data and ≥0.997 for EI full-scan MS traces (Table 2). In both cases calculated correlation coefficients met the method requirement ($R^2 \geq 0.98$) confirming an excellent linearity.
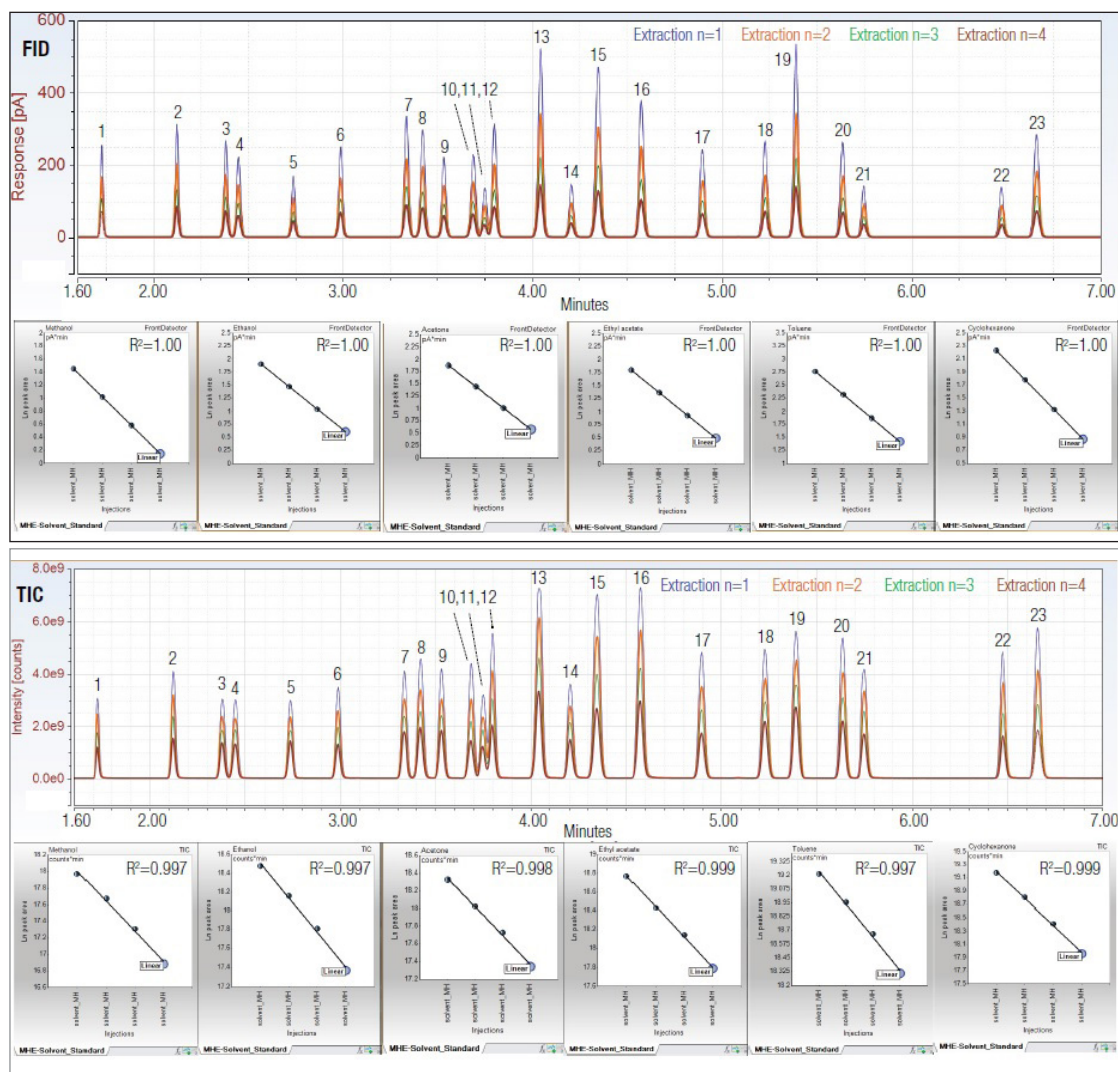
Figure 1. FID and TIC (full-scan, EI at 70 eV) traces for reference standard and corresponding MHE calibration curves for selected compounds (left to right: methanol, ethanol, acetone, ethyl acetate, toluene, and cyclohexanone) as examples. *Calibration curves were obtained by plotting the natural logarithm of peak area responses (total vaporization MHE) versus the corresponding MHE extraction step.*

Quantification of residual solvent in food packaging materials using MHE

The packaging materials were prepared as described and analyzed using the MHE conditions reported in Table 1. The microfluidic device allowed for splitting the gas flow 1:1 to the FID and the ISQ single quadrupole mass spectrometer, ensuring a minimal effect on the retention times (max RT shifts 0.04 min) by choosing either the FID or MS chromatogram as reference. The sample and the standard solution FID chromatograms were compared to verify the presence of known residual solvents. Several residual solvents such methanol (RT = 1.72 min) and ethylacetate (RT = 3.53 min) were detected in the sliced salami lid (D) and plastic tray (E), whereas ethanol (RT = 2.11 min) and acetone (RT = 2.37 min) were present in salad wrap (C) (Figure 3).

Full-scan data were used to putatively confirm the identity of detected solvent impurities, increasing the confidence in compound identification. When searching the mass spectrum of the peak eluting at RT = 1.72 min against NIST17 library, the best library match was acetaldehyde (not included in the standard mixtures) with a SI score of 953 (sliced salami tray:E) and 729 (sliced salami lid:D) (Figure 3). Acetaldehyde is usually present in meat and meat products [6]. Using the same approach, ethanol and acetone in salad wrap (C) and ethyl acetate in sliced salami (lid:D and tray:E) were also putatively confirmed with a SI score of 929, 913, 874, and 950, respectively. These chemicals are actually released by the packaging since they are typically used in solvent-based inks imprinted on the external layer of flexible packages [7]. Additional unknown compounds (*) detected in the samples were confirmed using spectral library comparison against NIST17 library (Figure 2).

Obtaining good ($R^2 \geq 0.98$) MHE linearity is fundamental to achieve accurate quantitation of residual solvents in solid food packaging materials. MHE linearity in the samples was assessed as previously described. The correlation coefficients (R^2) were 0.998 and 0.995 for ethyl acetate in sliced salami (lid and tray, respectively). R^2 for ethanol and acetone in salad wrap were 0.996 and 0.998, respectively (Figure 4).

The concentration (in mg/m^2) of residual solvents detected in the samples was calculated using the FID data applying the formula reported in paragraph 9.2.10.1 of the EN method. No residual solvents were found in the majority of samples. Traces of ethyl acetate were found in the sliced salami wrap (lid: 0.76 mg/m^2, tray: 29 mg/m^2). Ethanol (0.97 mg/m^2) and acetone (1.9 mg/m^2) were also present in salad wrap. All levels were within the safety limits reported for residual solvent and non-volatile food additives [3].

Peaks (A):

1. Methanol	9. Ethyl acetate	17. 4-Methyl-2-pentanone
2. Ethanol	10. 2-Methyl-1-propanol	18. Isobutyl acetate
3. Acetone	11. 2-Methoxyethanol	19. Toluene
4. 2-Propanol	12. Tetrahydrofuran	20. Butyl acetate
5. Methyl acetate	13. Isopropyl acetate	21. 2-Methoxyethyl-acetate
6. 1-Propanol	14. 1-Methoxy-2-propanol	22. 2-Ethoxyethyl acetate
7. 2-Butanone	15. Cyclohexane	23. Cyclohexanone
8. 2-Butanol	16. Propyl acetate	
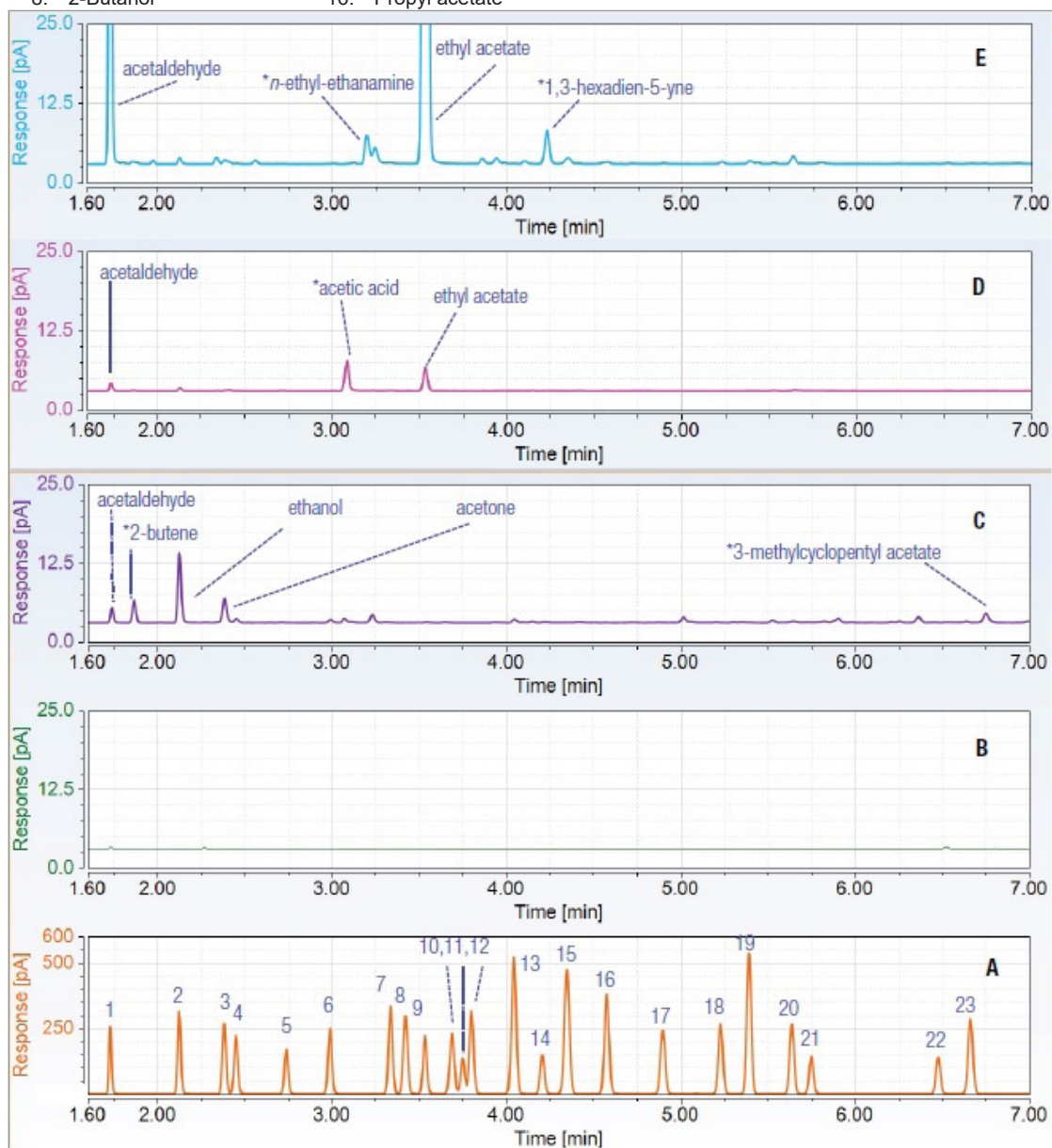
Figure 2. FID chromatograms showing a comparison between the residual solvents in the reference standard solution (A), empty blank vial (B), salad wrap (C), sliced salami wrap: lid (D) and tray (E). *Based solely on retention time comparison, methanol and ethyl acetate were detected in both sliced salami samples (lid:D, tray:E). Ethanol and acetone were found in salad wraps (C). FID signal responses (y-axis) are normalized for the empty vial (B) and samples (C,D,E). Unknown peaks (*) in the samples were confirmed comparing their mass spectra (full-scan, EI traces) against the NIST17 library and are reported as an example. Peaks not annotated were below the integration threshold of 0.04 pA * min.*
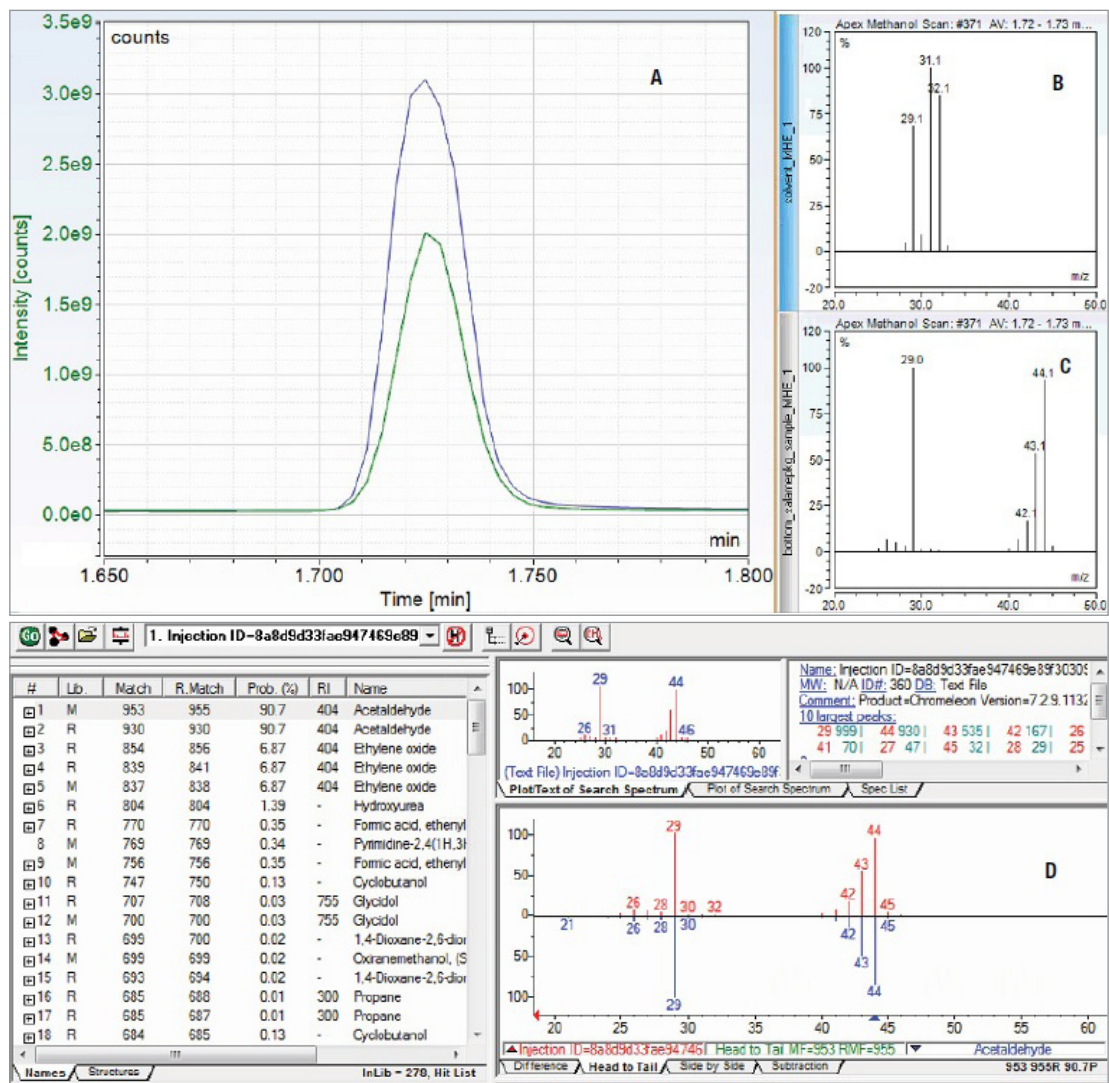
Figure 3. Identification of residual solvent peak eluting at RT=1.72 min in salami tray sample. *Comparison of TIC chromatograms (full-scan, EI at 70 eV) showing retention time comparison of peak eluting at RT=1.72 min in solvent standard (blue) and salami tray (green) (A). Background subtracted EI mass spectra for this peak in solvent standard (B) and in the sliced salami tray (C) did not confirm methanol. NIST library result (D) putatively identified this compound as acetaldehyde with a SI score of 953 and a probability of 91%.*
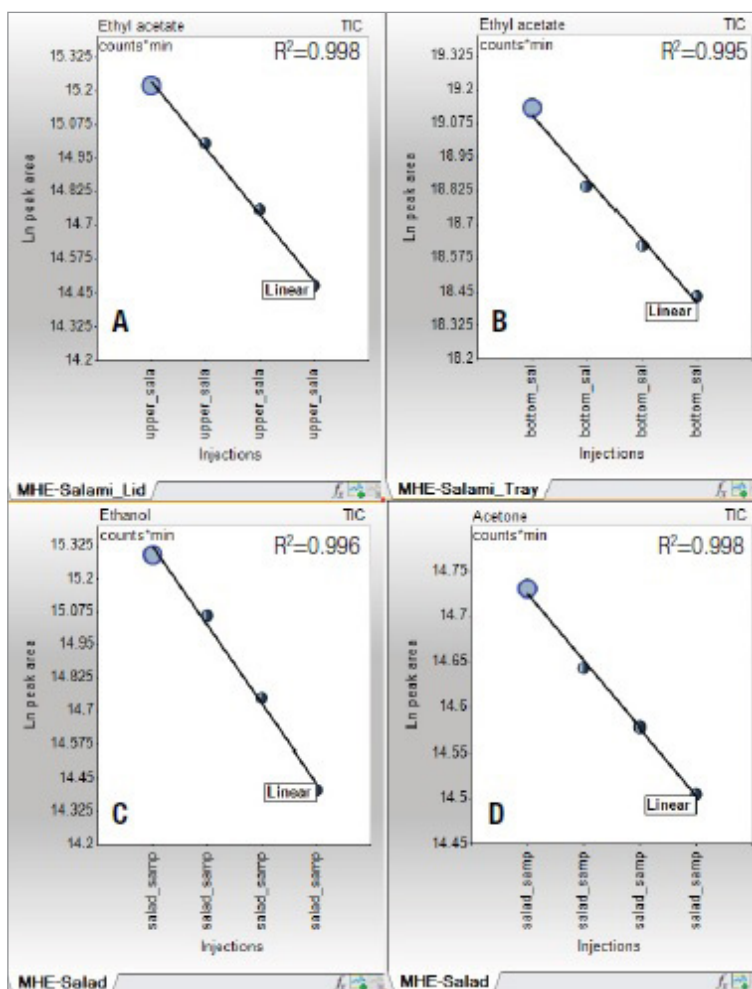
Figure 4. MHE linearity for ethyl acetate in sliced salami lid (A) and sliced salami tray (B), ethanol (C), and acetone (D) in salad wrap. *The resulting correlation coefficients (R^2) were 0.998 and 0.995 for sliced salami (lid and tray, respectively) and 0.996 and 0.998 for ethanol and acetone, respectively, in salad wrap.*

CONCLUSIONS

The results obtained with the TriPlus 500 HS autosampler are compliant with the EN 13628-1:2002 standard method requirements.

- The MHE capability allows for absolute quantitative analysis of residual solvent impurities in solid samples, overcoming the matrix effect and eliminating the need of sample preparation. Using the MHE mode, excellent linearity with correlation coefficient $R^2 \geq 0.995$ was obtained for all analytes in both solvent standard and samples, meeting the minimum required value of $R^2 \geq 0.98$, thus confirming excellent instrument performance for MHE quantitative analysis.

- Traces of residual solvents were found in three of the six analyzed food packaging samples. Acetone and ethanol were detected at 1.9 and 0.97 mg/m^2 in salad wrap samples, respectively, and ethyl acetate was found in sliced salami tray at 29 mg/m^2 and lid at 0.76 mg/m^2. No residual solvents were present in pizza cling film, cookies, and bread wraps.

- The dual detector configuration FID/MS increases the confidence in compound identification, allowing for the detection of possible analyte co-elution, otherwise difficult to assess in the absence of MS data. Moreover, several unknown peaks in the samples have been putatively confirmed (using spectral library match score thresholds of >950 SI) through comparison with NIST17 spectral library.

- The low bleed and superior inertness of the TraceGOLD column allowed for highly reliable results. The high analytical column efficiency allowed for fast GC oven ramp with adequate chromatographic separation (Rs ≥ 1.0) for all the analyzed compounds, reducing analysis time. Moreover, up to 240 sample vials can be accommodated into the trays for unattended 24-hour operation. The automated cycle time optimization allows for continuous sample processing ensuring the overlapping between the MHE cycles of the same sample. The overlapping capability is maintained between the final injection of one sample and the incubation of the next one increasing the sample throughput.

- Chromeleon CDS software ensures data integrity, traceability, and effective data management from instrument control to the final report. The integrated charts and the advanced report capability allowed for easy and integrated MHE data reprocessing, thus eliminating the need for external calculation tools.

Overall, the results obtained show that the TriPlus 500 HS autosampler coupled to the TRACE 1310 GC and the ISQ 7000 single quadrupole GC-MS system represents a robust analytical configuration for routine laboratories delivering outstanding reliability for MHE quantitative analysis of residual solvents in food packaging.

REFERENCES

1. EN 13628-1:2002 Packaging- Flexible Packaging Material – Determination of residual solvents by static headspace gas chromatography – Part 1.; Absolute methods.
2. Food Contact Materials - Regulation (EC) No 1935/2004 – European Implementation Assessment Study, May 2016.
3. Title 21, Code of Federal Regulation, Direct Additive Part, 170.3, Indirect Additive, Part 174–179.
4. Kolb, B., Ettre, I., Static headspace-gas chromatography Theory and Practice, Second Edition Wiley, 2006.
5. Thermo Fisher Scientific, Chromeleon CDS Enterprise – Compliance, Connectivity, Confidence, BR72617-EN0718S.
6. Kosowska, M., Majcher, M.A., Fortuna, T., Volatile compounds in meat and meat products, Food Science and Technology, Campinas, vol. 37 issue 1, Jan-March 2017, 1–7.
7. Packaging Materials - Printing inks for food packaging composition and properties of printing inks, International Life Science Institute ILSI Europe, December 2011.

This Sponsor Report is the responsibility of Thermo Fisher Scientific.

BrJAC

SPONSOR REPORT

This section is dedicated for sponsor responsibility articles.

Unstoppable analysis of pesticides residues in black tea using triple quadrupole GC-MS

Camille Grigsby[1], Carlos Parra[1], Jerry Mueller[1], Katie Banaszewski[1], Giulia Riccardino[2] and Adam Ladak[3]

[1]NOW Foods, Bloomingdale, IL, USA. [2]Thermo Fisher Scientific, Milan, IT. [3]Thermo Fisher Scientific, Hemel Hempstead, UK

This report was extracted from the Thermo Scientific Application Note 000560

Goal: The aim of this application note is to demonstrate the performance of the Thermo Scientific™ TSQ™ 9610 triple quadrupole mass spectrometer coupled to the Thermo Scientific™ TRACE™ 1610 GC for trace level determination of pesticide residues in black tea.

INTRODUCTION

Products of botanical origin, including black tea, have become an increasingly prevalent part of the worldwide health culture with their global market forecast to reach more than $230 billion by 2027. Manufacturers must ensure that these botanicals are safe for consumption, which requires routine/robust trace analysis of pesticide residues. Pesticides are chemicals used for crop protection against a variety of pests such as weeds, fungi, rodents, and insects. Because of their extensive use, pesticides can be found in the air, soil, water, and ultimately in the food chain. Despite their use being highly regulated, misuse of pesticides can lead to unwanted contamination of food and have possible impacts on both human and environmental health.

Laboratories performing the analysis of pesticides in botanical Table 1. GC-MS/MS and autosampler experimental conditions for matrices face numerous challenges. A prominent obstacle to accurate pesticide residue determination is matrix interference. As most botanical ingredients exist in a form of concentrated extracts, smaller sample sizes are needed to overcome heavy matrix interference, in turn requiring highly sensitive instrumentation to detect trace amounts of pesticide residues. Sensitivity is key in this analysis as the regulatory maximum residue levels (MRLs) must be met. The typical global MRL level for pesticides in food is 0.01 mg/kg. High-throughput laboratories must consistently hit the MRL levels in matrix with minimal user intervention on the GC-MS/MS system. Unplanned and prolonged instrument downtime can delay the return of results to the manufacturer of the botanicals. It is therefore essential that the GC-MS/MS produces confident and reliable results over time to ensure consumer safety.

In this study, the suitability of the TSQ 9610 triple quadrupole GC-MS/MS system was assessed for the analysis of more than 200 pesticides in black tea at trace concentrations supplemented with SPE cleanup. The linearity, accuracy, precision, limit of quantitation, and injection reproducibility of 20 selected analytes representative of the different pesticide classes in black tea matrix were demonstrated.

EXPERIMENTAL

Data was acquired with a TSQ 9610 triple quadrupole mass spectrometer equipped with a Thermo Scientific™ NeverVent™ Advanced Electron Ionization (AEI) ion source was coupled to a TRACE 1610 gas chromatograph equipped with a Thermo Scientific™ iConnect™ Split/Splitless (iConnect-SSL) injector and a Thermo Scientific™ AI/AS 1610 liquid autosampler. The NeverVent technology allows for ion source cleaning, filament replacement, and column exchange without breaking instrument vacuum, therefore ensuring minimum downtime to the laboratory workflow. Chromatographic separation was achieved on a Thermo Scientific™ TraceGOLD™ TG-5SILMS analytical column, 30 m × 0.25 mm i.d. × 0.25 µm fused silica capillary, with 10 m SafeGuard, (P/N 26096-1421). The MS/MS method monitored a minimum of three transitions for each compound. Additional method details are in Table 1.

Table 1. GC-MS/MS and autosampler experimental conditions for the analysis of pesticides

Parameter Value	Parameter Value
Injection liner	Thermo Scientific ™ LinerGOLD™ Splitless Liner, Single Taper with Quartz Wool, 4 mm (P/N 453A1925-UI)
GC column	TraceGOLD TG-5SILMS analytical column, 30 m × 0.25 mm i.d. × 0.25 µm fused silica capillary column with 10 m SafeGuard, P/N 26096-1421
Injection volume	1 µL
Injection temperature	260 °C
Splitless time	1 min
Column flow	1.4 mL/min, He
Run time	26.5 min
MS source temperature	320 °C
Emission current	10 µA
Aquistion mode	timed-SRM

Compounds were evaluated using SANTE/12682/2019 (Quality Control and Method Validation Procedures for Pesticide Residues Analysis in Food and Feed[1]) guidelines:

- Compound recovery should be within a mean recovery of 80–120%. If recovery within this range cannot be achieved, correction for recovery is necessary, or an explanation given for why a correction factor was not applied.
- Ion ratios for detected compounds must be within ±30% of the average of matrix-matched calibration standards.
- Detected compounds must have a signal-to-noise ratio (S/N) of at least 3:1.

In this application, difficult-to-analyze compounds, in addition to compounds from different pesticide classes (organophosphates, organochlorides, synthetic pyrethroids, and herbicide methyl esters), are highlighted in the results.

Data acquisition, processing, and reporting

Data were acquired, processed, and reported using the Thermo Scientific™ Chromeleon™ Chromatography Data System (CDS) software, version 7.3. Integrated instrument control ensures full

automation of the analytical workflow combined with an intuitive user interface for data analysis, processing, customizable reporting, and storage in compliance with the Federal Drug Administration Title 21 Code of Federal Regulations Part 11 (Title 21 CFR Part 11). The advanced reprocessing capability of Chromeleon CDS ensures immediate and easy data analysis, offering the possibility to easily flag and check the compliance of the results with the SANTE/12682/2019 criteria.[1]

Sample preparation

Sample preparation involved the addition of water and acetonitrile to a black tea matrix, followed by QuEChERS extraction. Final clean-up was performed with solid-phase extraction using a cartridge consisting of graphitized carbon black (GCB) and primary−secondary amine sorbent (PSA). The resulting extract solutions were concentrated and re-diluted with toluene for a GC-MS/MS analysis.

RESULTS AND DISCUSSION

Chromatography

Black tea is an extremely complex sample, and it is important that the matrix interferences are removed during sample preparation to produce good chromatography and subsequent quantitation of pesticides at the MRLs defined by the regulations. A timed-selected reaction monitoring (t-SRM) acquisition method allowed for simultaneous acquisition of multiple characteristic ions for each pesticide, maintaining high sensitivity and selectivity to discriminate between the target compounds and the matrix, thus ensuring a confident and selective identification of analytes. Figure 1 shows the t-SRM acquisition of pesticides at 5 µg/kg in black tea.

Linearity

The TSQ 9610 NeverVent AEI is equipped with the Thermo Scientific™ XLXR™ detector, which offers an extended dynamic range and longer lifetime compared with its predecessor. In this experiment, linearity was evaluated for select analytes using matrix-matched calibration curves ranging from 0.01 to 200 ng/mL. The lowest standard to meet SANTE/12682/2019 criteria ranged, for the selected analytes, from 0.01 to 2 ng/mL.

Figure 2 shows an example calibration curve for 4,4'-DDT (0.5 to 200 ng/mL (ppb)) and cypermethrin I (2.0 to 200 ng/mL (ppb)). Table 2 shows the calibration result for the 20 selected pesticides.

To be compliant with the current regulation, it is essential that analytical testing laboratories meet the MRL of 10 ppb (0.01 mg/kg). To demonstrate the reliability of the instrument at such low concentration, the peak area repeatability of a 10 ppb black tea extract was assessed by using n=12 repeated injections. The % RSD of the calculated concentrations for all 20 compounds was <20%, with the majority of compounds giving RSDs <10%. Figure 3 shows a summary of results at the MRL including the %RSDs for n=12 injections and the average percentage recovery for each compound. Appendix 1 shows the chromatograms of the lowest matrix-matched standard conforming to SANTE/12682/2019 guidance for each of the selected pesticides.

Recovery and precision

Analyte recovery was assessed by spiking black tea at three levels (10, 25, and 50 ppb) before extracting with QuEChERS. Six extractions were performed at each level. Calculated recoveries for the spiked compounds were between 80% and 120%, with calculated precision ≤10% with the exception of folpet, which is thermally labile and therefore known to break down in the GC injector. Utilizing the PTV injector can help reduce the breakdown of labile compounds. Table 3 summarizes the recovery and precision results.
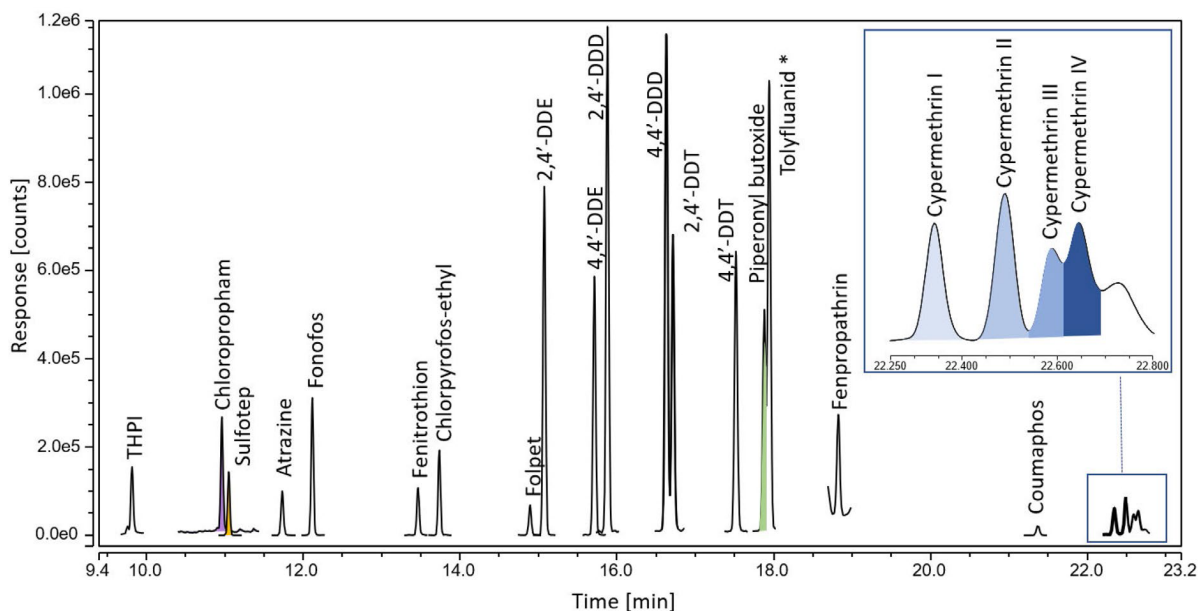
Figure 1. t-SRM acquisition for black tea sample pre-spiked at 5 µg/kg. *A matrix interferent was found to co-elute with tolyfluanid; therefore, the results for this compound were not included in the present work.
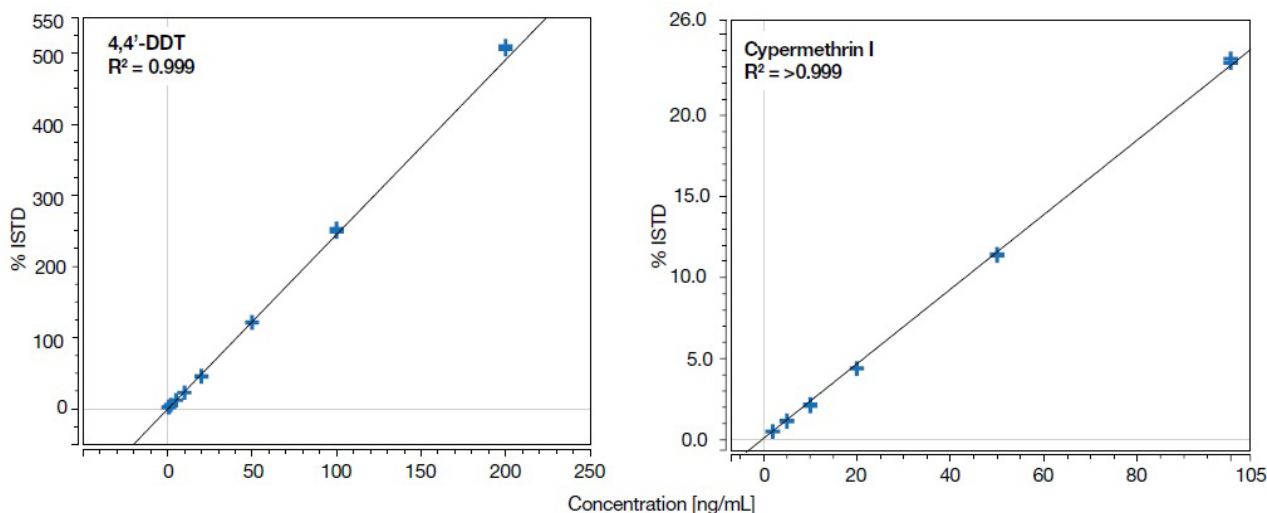
Figure 2. Calibration curve for 4,4'-DDT (range 0.5–200 ng/mL (ppb)) and cypermethrin I (2.0–200 ng/mL (ppb)).

Table 2. Calibration results for 20 selected pesticides in black tea (each point was injected in duplicate)

Peak name	Internal standard	Calibration type	R^2	Linear range (ppb)
Atrazine	Internal PCB 18 ISTD	Lin, WithOffset, 1/A	>0.999	0.5–200
Chlorpropham	Internal PCB 18 ISTD	Lin, WithOffset, 1/A	>0.999	0.5–200
Chlorpyrifos-ethyl	Internal PCB 52 ISTD	Lin, WithOffset, 1/A	0.999	0.5–200
Coumaphos	Internal Triphenylphosphate (TPP) ISTD	Lin, WithOffset, 1/A	0.999	1.0–200

(continues on the next page)

Table 2. Calibration results for 20 selected pesticides in black tea (each point was injected in duplicate) [continuation]

Peak name	Internal standard	Calibration type	R^2	Linear range (ppb)
Cypermethrin I	Internal Triphenylphosphate (TPP) ISTD	Lin, WithOffset, 1/A	>0.999	2.0–200
Cypermethrin II	Internal Triphenylphosphate (TPP) ISTD	Lin, WithOffset, 1/A	>0.999	2.0–200
Cypermethrin III	Internal Triphenylphosphate (TPP) ISTD	Lin, WithOffset, 1/A	0.998	2.0–200
Cypermethrin IV	Internal Triphenylphosphate (TPP) ISTD	Lin, WithOffset, 1/A	0.999	2.0–200
DDD, 2,4'-	Internal Triphenylmethane ISTD	Lin, WithOffset, 1/A	0.999	0.1–200
DDD, 4,4'-	Internal Triphenylmethane ISTD	Lin, WithOffset, 1/A	>0.999	0.5–200
DDE, 2,4'-	Internal Triphenylmethane ISTD	Lin, WithOffset, 1/A	0.999	0.05–200
DDE, 4,4'-	Internal Triphenylmethane ISTD	Lin, WithOffset, 1/A	0.999	0.01–200
DDT, 2,4'-	Internal Triphenylmethane ISTD	Lin, WithOffset, 1/A	0.999	0.5–200
DDT, 4,4'-	Internal Triphenylphosphate (TPP) ISTD	Lin, WithOffset, 1/A	0.999	0.5–200
Fenitrothion	Internal PCB 52 ISTD	Lin, WithOffset, 1/A	0.996	0.5–200
Fenpropathrin	Internal Triphenylphosphate (TPP) ISTD	Lin, WithOffset, 1/A	>0.999	2.0–200
Folpet	Internal PCB 52 ISTD	Lin, WithOffset, 1/A	0.997	2.0–200
Fonofos	Internal PCB 18 ISTD	Lin, WithOffset, 1/A	>0.999	0.5–200
Piperonyl butoxide	Internal Triphenylphosphate (TPP) ISTD	Lin, WithOffset, 1/A	0.999	0.5–200
Sulfotep	Internal PCB 18 ISTD	Lin, WithOffset, 1/A	>0.999	0.1–200
Tetrahydrophthalimide (THPI)	Internal PCB 18 ISTD	Lin, WithOffset, 1/A	0.998	1.0–200
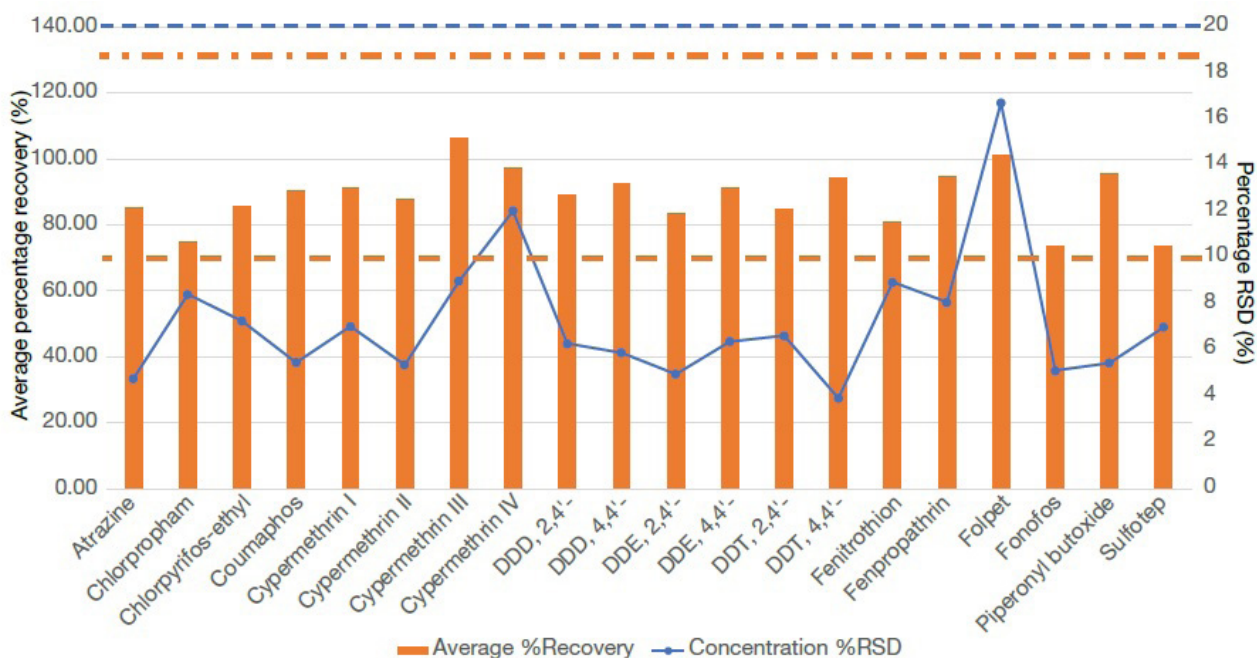
Figure 3. MRL results with %RSDs for n=12 injections and the average percentage recovery for each pesticide.

Table 3. Precision and spike recovery at 10, 25, and 50 ppb (ng/mL) (n=6 extracts at each level)

Compound	Concentration %RSD			Average %Recovery		
	10 ppb spike (n=6)	25 ppb spike (n=6)	50 ppb spike (n=6)	10 ppb spike (n=6)	25 ppb spike (n=6)	50 ppb spike (n=6)
Atrazine	3.4	4.1	5.5	83.3	84.5	85.5
Chlorpropham	7.8	7.0	2.5	77.7	78.7	74.3
Chlorpyrifos-ethyl	4.7	6.0	3.5	84.0	78.9	81.5
Coumaphos	6.1	6.5	5.5	91.3	92.0	91.1
Cypermethrin I	8.0	3.4	4.1	92.9	91.5	91.3
Cypermethrin II	5.0	3.4	3.7	88.3	89.6	89.2
Cypermethrin III	9.7	4.1	3.6	101.2	91.6	90.7
Cypermethrin IV	7.7	5.9	6.2	88.9	87.9	90.1
DDD, 2,4'-	3.4	5.0	2.2	93.3	91.8	91.3
DDD, 4,4'-	3.1	5.7	2.6	97.0	95.3	93.6
DDE, 2,4'-	3.8	4.7	2.2	86.1	83.4	81.6
DDE, 4,4'-	5.8	4.2	3.5	94.5	88.4	85.6
DDT, 2,4'-	3.8	4.4	3.8	89.6	90.2	87.6
DDT, 4,4'-	3.6	3.0	4.2	96.9	92.7	89.3
Fenitrothion	9.8	7.7	3.8	83.2	93.0	90.9

(continues on the next page)

Table 3. Precision and spike recovery at 10, 25, and 50 ppb (ng/mL) (n=6 extracts at each level) [continuation]

Compound	Concentration %RSD			Average %Recovery		
	10 ppb spike (n=6)	25 ppb spike (n=6)	50 ppb spike (n=6)	10 ppb spike (n=6)	25 ppb spike (n=6)	50 ppb spike (n=6)
Fenpropathrin	6.0	7.5	5.0	99.1	92.2	92.6
Folpet	20.6	10.3	6.6	107.6	86.2	61.1
Fonofos	4.4	3.8	6.1	76.0	73.2	72.6
Piperonyl butoxide	4.8	3.6	4.3	98.5	95.7	95.0

Robustness

It is important that the results produced over time are consistent and minimal user intervention is required to operate the system. Mass calibration and resolution tuning are two of the most important aspects ensuring system performance. The Thermo Scientific™ SmartTune™ tool allows the user to check the tune status of the system with a few mouse clicks in an easy and quick fashion. To demonstrate instrument robustness, black tea extracts at a concentration of 50 µg/kg were injected continuously over 124 injections. Neither inlet nor ion source maintenance was performed on the system during this extended sequence, which was equivalent to over 2.5 days of continuous analysis. Peak area %RSDs were <10% for all representative analytes (Figure 4 and Table 4) with the exception of folpet, which produces inconsistent results due to breakdown in the hot GC inlet.
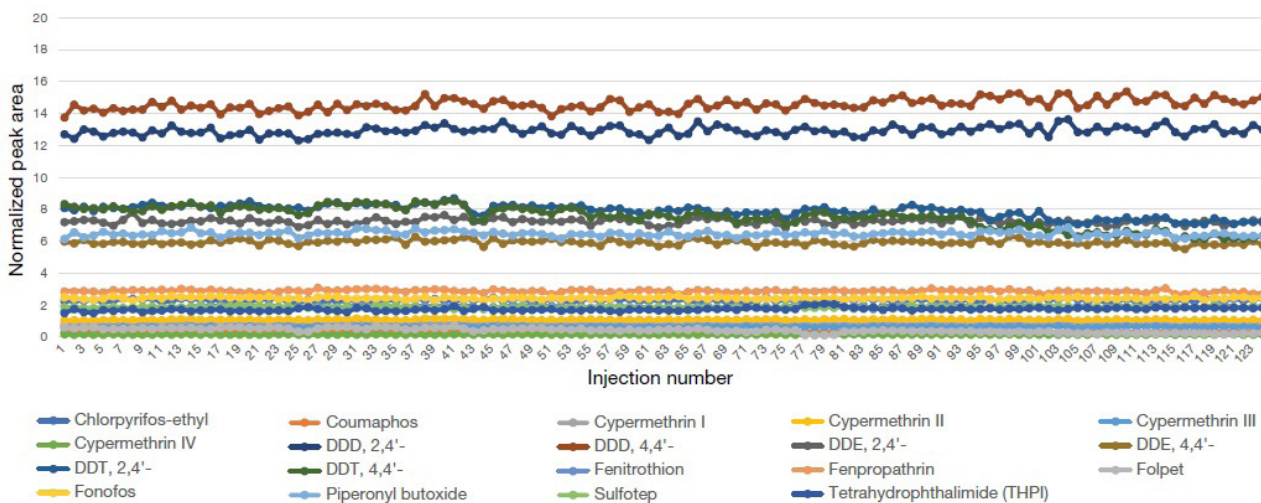
Figure 4. Normalized peak area response (analyte peak area / ISTD peak area) obtained for n=124 consecutive injections of matrix samples spiked at 50 µg/kg.

Table 4. %RSD of pesticides at 50 µg/kg over n = 124 injections

Compound	%RSD (n = 120)
Atrazine	4.3
Chlorpropham	3.6
Chlorpyrifos-ethyl	3.6

(continues on the next page)

Table 4. %RSD of pesticides at 50 µg/kg over n = 124 injections [continuation]

Compound	%RSD (n = 120)
Coumaphos	4.4
Cypermethrin I	2.8
Cypermethrin II	2.9
Cypermethrin III	3.6
Cypermethrin IV	6.0
DDD, 2,4'	2.1
DDD, 4,4'	2.4
DDE, 2,4'	2.3
DDE, 4,4'	2.6
DDT, 2,4'	5.0
DDT, 4,4'	9.0
Fenitrothion	4.1
Fenpropathrin	2.9
Folpet	34.1
Fonofos	2.8
Piperonyl butoxide	2.4
Sulfotep	2.7
Tetrahydrophthalimide (THPI)	5.9

CONCLUSIONS

The results obtained in these experiments demonstrate that the TSQ 9610 mass spectrometer equipped with the NeverVent AEI ion source in combination with the TRACE 1610 GC and the AI/AS 1610 liquid autosampler delivers excellent analytical performance for multi-residue analysis of pesticides in black tea:

- The excellent sensitivity and good linearity between 0.01 ng/mL and 200 ng/mL allowed detection and accurate quantitation of numerous pesticides in the challenging black tea matrix.
- Peak area %RSDs of calculated concentrations at 10 ppb (0.01 mg/kg) were <10%, which are in compliance with SANTE/12682/2019 (Analytical guidelines).
- Calculated recoveries at three different spiking levels (10, 25, 50 ppb (ng/mL)) were within the 80–120% limits established in the SANTE guidelines.
- The TSQ 9610 mass spectrometer uptime is improved due to the NeverVent technology, allowing for laboratory productivity to be maximized with an uninterrupted workflow.

REFERENCE

1. SANTE/12682/2019, Analytical quality control and method validation procedures for pesticide residues analysis in food and feed. https://ec.europa.eu/food/system/files/2020-01/pesticides_mrl_guidelines_ wrkdoc_2019-12682.pdf

Appendix 1. Chromatograms of lowest matrix-matched standard conforming to SANTE guidance

Atrazine, 0.5 ng/mL

Chlorpropham, 0.5 ng/mL

Chlorpyrifos-ethyl, 0.5 ng/mL

Coumaphos*, 1 ng/mL

Cypermethrin I, II, III, IV, 2 ng/mL

DDD, 2,4'-, 0.1 ng/mL

DDD, 4,4'- and DDT, 2,4'-, 0.5 ng/mL

DDE, 2,4'-, 0.05 ng/mL

DDE, 4,4'-, 0.01 ng/mL

DDT, 4,4'-, 0.5 ng/mL

Fenitrothion, 0.5 ng/mL

Fenpropathrin*, 2 ng/mL

Folpet, 2 ng/mL

Fonofos, 0.5 ng/mL

Piperonyl butoxide, 0.5 ng/mL

Sulfotep, 0.1 ng/mL

Tetrahydrophthalimide, 1 ng/mL
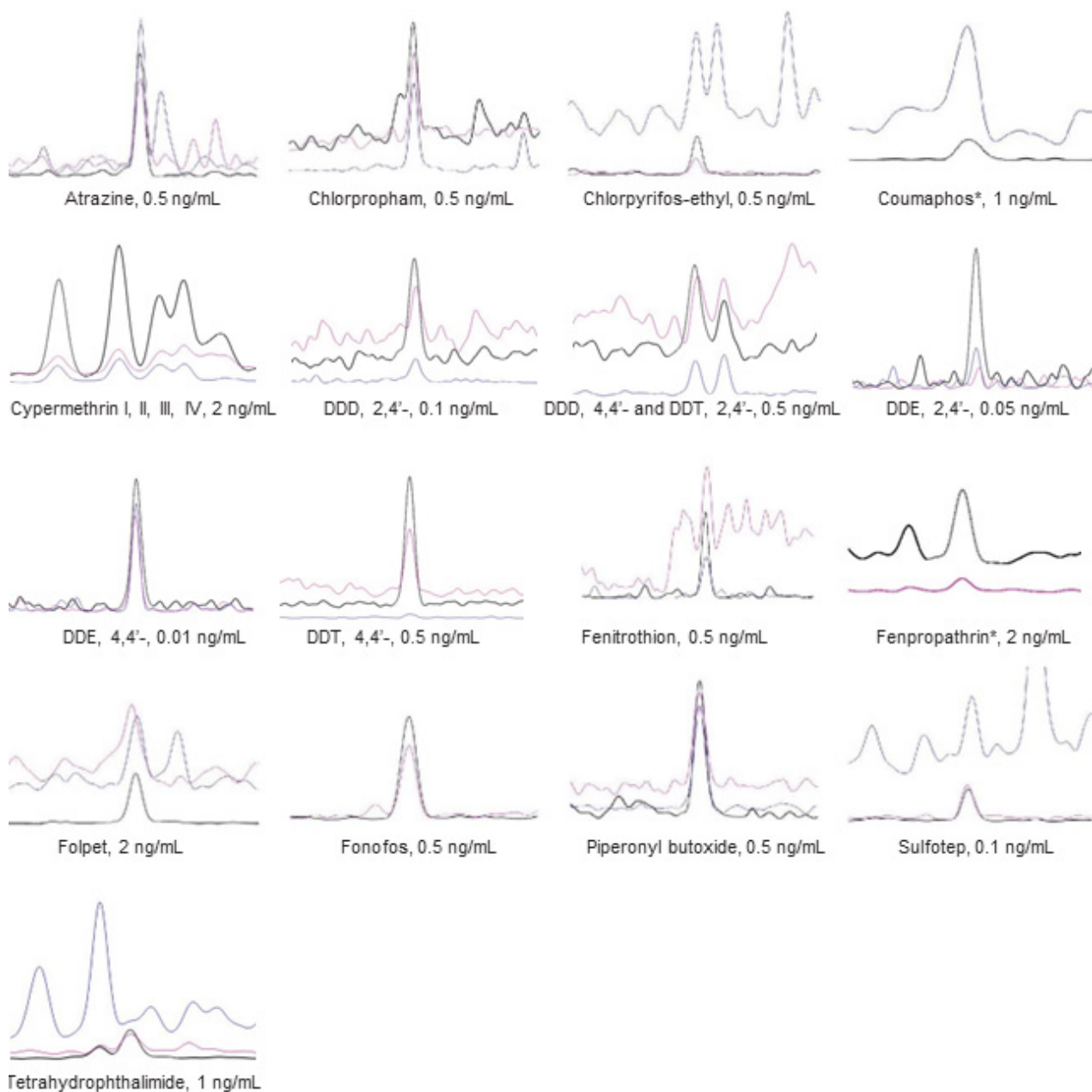
Learn more at thermofisher.com/TSQ9610

This sponsor report is the responsibility of Thermo Fisher Scientific.

BrJAC

SPONSOR REPORT
This section is dedicated for sponsor responsibility articles.

Microwave assisted extraction of pesticides from environmental samples

This report was extracted from the Milestone Application Report ETHOS X - Pesticides - EPA 3546 Method

Pesticides are extensively used in modern agriculture, which could lead to serious consequences due to their biomagnification and persistent nature. Several governments require their analysis in environmental samples. Microwave assisted solvent extraction is a well-established sample preparation technique applied in several official methods. Milestone's ETHOS X equipped with fastEX-24 eT rotor was used in this study to prove its efficacy in the extraction of pesticides from environmental matrices

INTRODUCTION

Pesticides are pivotal chemical compounds for the modern agriculture production, used to control pests' diffusion. Depending on their target function, pesticides are used to treat insects, rodents, fungi and unwanted plants (weeds). For example, since 1940s, organochlorine pesticides and organophosphate pesticides are used extensively not only in agriculture but also for mosquito control.

The action mechanism of these chemicals is mostly designed to disturb the physiological activities of the target organism, leading to dysfunction and reduced vitality. Despite their fundamental use in the modern agriculture, these molecules can cause neurological damage, endocrine disorders, and have acute and chronic health effects on human[1]. Moreover, some of these chemicals belong to the class of persistent organic pollutants (POPs) with high persistence in the environment[2].

EPA 3546[3] outlines the procedure for extracting water insoluble or slightly water-soluble organic compounds from soils, clays, sediments, sludges, and solid wastes.

EPA 3546 is a specific method for Microwave Assisted Solvent Extraction (MASE), a well-established sample preparation technique that enables extractions with reduced solvent volume and time. This application note represents a guideline for the extraction of the priority pesticides from both standard reference materials and spiked materials using the official method EPA 3546.

EXPERIMENTAL
Equipment
- Milestone's ETHOS X.
- fastEX-24 eT rotor.[4]
- 100-mL disposable glass vials.
- SFS-24 (Simultaneous Filtration System).
- GC-MS/MS
- HPLC MS/MS

Figure 1. Milestone ETHOS X with fastex-24 eT (left) and SFS-24 filtration system (right).

Standard and reagents

Standards, surrogates and internal standard were purchased by Sigma Aldrich. Grade solvent pesticide were used. Sodium sulfate anhydrous, silica gel (activated for at least 16 h at 130 °C) and glass wool or paper filter were used in the clean-up procedure. According to the analytical method EPA 8270e[5], internal surrogates and standards were used.

Table 1. Pesticides Stock solution

Analyte	CAS-No	Analyte	CAS-No
α-BHC	319-84-6	Endosulfan Sulfate	1031-07-8
γ-BHC	58-89-9	Endrin aldeide	7421-93-4
β-BHC	319-85-7	Endrin ketone	01/10/7378
δ-BHC	319-86-8	Heptachlor Epoxide	1024-57-3
Aldrin	309-00-2	Methoxychlor	72-43-5
Heptachlor	76-44-8	Demeton	8065-48-3
γ-\α-chlordane	5103-74-2\57-74-9	Dimethoate	60-51-5
α-Endosulfan	1031-07-8	Malathion	121-75-5
4,4'-DDE	72-55-9	Parathion	56-38-2
Dieldrin	60-57-1	Parathion-methyl	298-00-0
Endrin	72-20-8	Mevinphos	7786-34-7
β-Endosulfan II	33213-65-9	Phorate	298-02-2
4,4'-DDD	72-54-8	Fenitrothion	122-14-5
2,4'-DDT	789-02-6	Isocarbophos	24353-61-5
4,4'-DDT	50-29-3	Methidathion	950-37-8
Mirex	2385-85-5	Toxaphene	8001-35-2
Dichlorvos	62-73-7		

Table 2. Internal Standard Solution

Analyte	CAS-No
Isoproturon-d6	217487-17-7
Biphenyl-d10	1486-01-7
Atrazina-d5	163165-75-1
Phenanthrene-d10	1517-22-2
Pirimicarb-d6	1015854-66-6
PCB 138	35065-28-2
Triphenylphosfate	115-86-6

Samples

The clay loam 1 - CRM847 certified reference material were used for the determination of pesticides. For pesticides not included in the certified materials a spiking stock solution on blank soil was used.

Sample preparation

The samples were collected and stored in accordance with the requirements of EPA 3546. Decant and discard any water layer on a sediment sample. Discard any foreign objects such as sticks, leaves, and rocks. Mix the sample thoroughly, especially composited samples. Grind or otherwise reduce the particle size of the waste so that it either passes through a 1 mm sieve or can be extruded through a 1 mm hole.

Ground samples, wet or dried, were weighed directly into the 100 mL extraction disposable glass vials of the fastEX-24 eT rotor. 30 mL of acetone-hexane (1:1) was used as extraction mixture. An aliquot of the internal standard solution was added to the samples just prior to solvent addition then the glass vials were closed (automatic capping tool available).
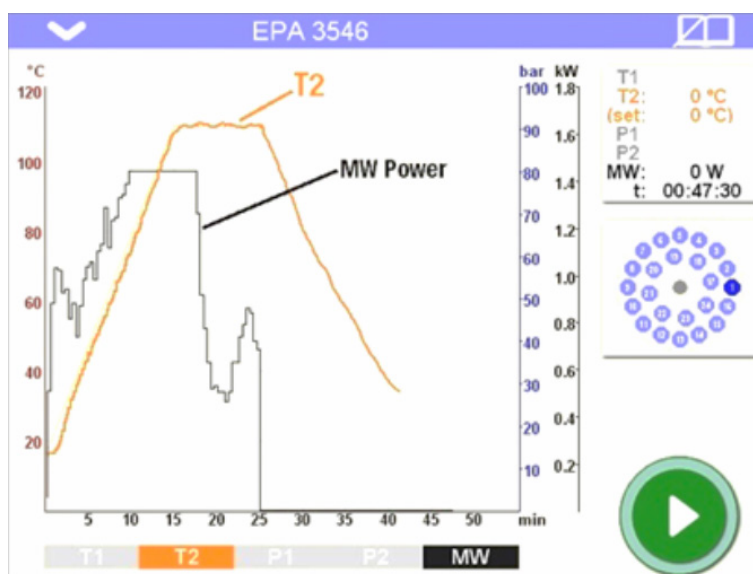
Figure 2. Microwave run profile.

After the extraction, samples were filtered with milestone SFS-24 simultaneous filtration system using sodium sulfate anhydrous. The vials were rinsed with additional solvent aliquots. SFS-24 allows to filter 24 samples simultaneously with different types of filters available. Extracts and rinse solution were collected together.

The extract was subsequently concentrated with nitrogen flow. If purification is not required, concentrate directly until 0.5 mL and add the appropriate surrogate standard solution to achieve the surrogate standard concentration. If purification is necessary, concentrate the extract directly until 2 mL. Purify the solution according to the method (EPA 3610, 3620, 3630, 3640, 3660). Finally, the extracts obtained by ETHOS X were concentrated for analysis.

Analitical conditions

Based on the pesticide compositions both GCMS/MS and HPLC MS/MS with triple quadrupole were used.

GC-MS/MS is equipped with a split-splitless injector, autosampler and triple quadrupole mass spectrometer. Sample injection volume was 1 µl. A 30 m x 0.25 x 0.25 RXI 5MS Capillary column (Restek) was used for the analyses. A five steps ramp oven program was used:

Table 4. GC-MS/MS oven program

Rate (°C/min)	Temperature (°C)	Plateaus (min)
20	50	2
30	150	0
7	260	0
20	290	11

Helium was used as the carrier gas at a linearity velocity of approximately 65 cm/s.
HPLC MS/MS was used to ensure the recovery data and to better quantify some compounds. An oven temperature of 40 °C is used with an injection volume of 0.25 µL.
Mobile phase:
- Water 0,1% formic acid 5 mM ammonium formate.
- Methanol 0,1% formic acid 5 mM ammonium formate.

Table 5. HPLC-MS/MS gradient method

Time (min)	Water (%)	Methanol (%)
0.2	95	5
11	0	100
13	0	100
13.1	95	5

RESULTS AND DISCUSSION

Results from extractions of Clay loam 1 - CRM847 are shown in Table 6. Recovery for all compounds is in the range 70-120% of the certified standard reference material.

Table 6. Pesticides recovery from Clay loam 1 - CRM847 (1g) (n=4)

Analyte	Certified value (µg/kg)	Ethos X (µg/kg)	Recovery (%)	RSD (%)
δ-BHC	138	128.89	93.4	8.7
α-BHC	221	188.95	85.5	7.0
β-BHC	295	342.2	116	2.2
α-Chlordane	309	330.63	107	3.3
γ-Chlordane	171	182.28	106.6	2.4
4.4'-DDD	120	107.28	89.4	3.1
4-4'-DDE	315	290.74	92.3	3.3
4-4'-DDT	92.1	84.27	91.5	11.5
Dieldrin	53.3	54.79	102.8	9.6
Endosulfan I	211	162.25	76.9	4.8
Endosulfan II	225	160.65	71.4	7.9
Endosulfan Sulfate	159	159.63	100.4	4.0
Endrin Ketone	170	139.57	82.1	6.3
Endrin	162	156.81	96.8	4.4
Heptachlor epoxide	127	119.25	93.9	3.7
Methoxychlor	290	260.13	89.7	6.6

Additionally, a pesticide mixture was spiked to a blank soil in order to test the performance of the fastEX-24 eT on a wider list of pesticides (Table 7).

Table 7. Pesticides recovery from Spike solution (n=4)

Analyte	Spike concentration (µg/kg)	Ethos X (µg/kg)	Recovery (%)	RSD (%)
α-BHC	50	52.00	104.0	4.6
γ-BHC	50	50.00	100.0	8.1
β-BHC	50	60.00	120.0	3.2
δ-BHC	50	56.67	113.3	4.1
Aldrin	50	53.33	106.7	5.2
Heptachlor	50	56.67	113.3	2.6
alfa clordano	50	48.40	96.8	4.8
gamma clordano	50	52.67	105.3	6.1
4.4'-DDE	50	56.67	113.3	3.2

Table 7. Pesticides recovery from Spike solution (n=4) [continuation]

Analyte	Spike concentration (µg/kg)	Ethos X (µg/kg)	Recovery (%)	RSD (%)
Dieldrin	50	53.33	106.7	1.3
Endrin	50	52.05	104.1	1.9
β-Endosulfan II	50	50.00	100.0	4.1
4.4'-DDD	50	56.67	113.3	3.8
2.4'-DDT	50	46.65	93.3	2.4
4.4'-DDT	50	45.70	91.4	2.9
Mirex	50	53.05	106.1	5.1
Dichlorvos	50	40.00	80.0	9.3
Demeton	50	41.45	82.9	6.8
Dimethoate	50	52.50	105.0	4.2
Malathion	50	45.70	91.4	3.6
Parathion	50	43.95	87.9	2.7
Parathion-methyl	50	53.33	106.7	2.9
Mevinphos	50	54.20	108.4	3.9
Phorate	50	46.67	93.3	4.6
Fenitrothion	50	56.67	113.3	5.8
Isocarbophos	50	46.25	92.5	6.4
Methidathion	50	43.15	86.3	8.9
Endosulfan Sulfate	50	46.90	93.8	10.6
Endrin aldeide	50	39.45	78.9	3.5
Endrin Ketone	50	39.70	79.4	4.9
Heptachlor Epoxide	50	47.30	94.6	6.3
Methoxychlor	50	53.35	106.7	5.5
Toxaphene	50	41.80	83.6	4.9

CONCLUSION

The results demonstrate the efficiency of the ETHOS X with fastEX-24 eT rotor for the pesticides extraction from environmental matrices. High recovery rate for all the tested molecules showed the great extraction efficiency.

The fastEX-24 eT enables simultaneous solvent extraction of up to 24 samples in only 40 minutes (cooling step included). In turns this means that is able to extract over 200 samples in 8-hour workday. Contamination, memory effects, and cleaning are completely eliminated due to the use of disposable glass vials. The use of contactless temperature control ensures high reproducibility and full recovery of the target analytes for full compliance with Official Methods.

Thanks to the unique design, fastEX-24 eT is easily applied to even more challenging matrices such as solid wastes and plastics. ETHOS X provides extracts with the lowest solvent usage and significant time saving compared to all the other extraction techniques.

The ETHOS X with all its unique features fully addresses the need of environmental laboratories in terms of productivity, ease of use, running costs, and extraction quality.

REFERENCES
1. Chemical Pesticides and Human Health: The Urgent Need for a New Concept in Agriculture. https://www.ncbi.nlm.nih.gov/pmc/articles/PMC4947579/
2. Stockholm Convention – POPs project. http://www.pops.int/
3. EPA 3546-Microwave extraction. https://www.epa.gov/sites/default/files/2015-12/documents/3546.pdf
4. ETHOS X and fastEX 24 eT. https://www.milestonesrl.com/products/microwave-extraction/ethos-x-for-environmental
5. EPA 8270 E – Semivolatile organic compound GC-MS. https://www.epa.gov/esam/epa-method-8270e-sw-846-semivolatile-organic-compounds-gas-chromatographymass-spectrometry-gc

ABOUT MILESTONE
At Milestone we help chemists by providing the most innovative technology for metals analysis, direct mercury analysis and the application of microwave technology to extraction, ashing and synthesis. Since 1988 Milestone has helped chemists in their work to enhance food, pharmaceutical and consumer product safety, and to improve our world by controlling pollutants in the environment.

This sponsor report is the responsibility of Milestone SRL.

RELEASE

TriPlus 500 Headspace Autosampler coupled to the Thermo Scientific™ TRACE™ 1300 Gas Chromatograph

Designed to deliver Superior Repeatability, High Data Quality, Best Reliability

Powered by an innovative new design, the Thermo Scientific™ TriPlus™ 500 GC Headspace Autosampler helps you maximize valuable time with reliable unattended operations and optimize throughput with expanded vial capability.

This modular platform gives today's routine laboratories the productivity they need to succeed – both today and in the future.

For any testing laboratory conducting volatiles analysis, static headspace-gas chromatography, with its simplicity and broad applicability is one of the most reliable and robust techniques. When seeking highly accurate analytical results, the valve-and-loop sampling technique is a must-have. Packed with innovative features, the TriPlus 500 Headspace (HS) autosampler makes the most of daily workflows by addressing the biggest challenges facing today's laboratories doing routine volatiles determination.

Drive reliability through innovation

New pneumatic circuit design – A proprietary pneumatic circuit design and a highly precise heating control work together for an accurate sampling process, increasing the system reliability and robustness. The repeatability of the area counts is the highest in the market. This, coupled with the sample integrity maintained during the injection process, ensure the required data quality is easily achieved.

High precision – Innovative control of the pressure in the sampling loop during filling delivers excellent repeatability of the sample amount injected into the gas chromatograph.

High robustness – Efficient heating of the entire sample path greatly reduces the risk of high boiling solvents contamination, especially through the vent line, which guarantees an extended robustness of the system.

Low carryover – Effective purging over 5 levels of flow rates and short sample path assure minimal to no carryover. An empty blank vial analyzed after undiluted 2-butanol headspace injection shows a carryover <0.0003%.

Find out more at thermofisher.com/TriPlus500

RELEASE

Thermo Scientific TSQ 9610 Triple Quadrupole GC-MS/MS System
Unstoppable confidence for analytical testing

To confidently stay ahead, your GC-MS/MS system must deliver ultimate performance while consistently producing trusted quantitative results. That's the reason for the Thermo Scientific™ TSQ™ 9610 Triple Quadrupole GC-MS/MS System. User-centric Thermo Scientific™ NeverVent™ technology, extended-life detector, and intelligent software eliminate unnecessary downtime to maximize your sample throughput and return on investment (ROI). New extended linear dynamic range combined with proven high sensitivity ensures you keep ahead of the toughest regulatory methods and business demands.

Combine the TSQ 9610 Triple Quadrupole GC-MS/MS System with the Thermo Scientific™ TRACE™ 1600 Series Gas Chromatograph (GC) and Thermo Scientific™ AI/AS 1610 Liquid Autosampler to optimize the performance and productivity of your solution.

Increase instrument uptime
Eliminate unnecessary and unplanned instrument downtime to deliver high-confidence quantitative results, day after day. The TSQ 9610 Triple Quadrupole GC-MS/MS System combines unstoppable robustness with the ability to change the GC column and clean the ion source without interrupting analytical workflows.

Maximize sample throughput
When high sample throughput is essential, the system delivers results on time and with ease. Automated workflows and simplified operation ensure every user produces consistent results, sample after sample. Extended linear range and rapid selected reaction monitoring (SRM) scanning enable method consolidation so you can analyze more compounds in a single run. When these capabilities are combined with best-in-class uptime and sensitivity, you stay ahead of any productivity demand.

Realize rapid return on investment
Ensuring your system delivers results as soon as it's installed is necessary to achieving rapid ROI. With built-in intelligence that simplifies instrument set up, analytical methods, and everyday operation, the TSQ 9610 Triple Quadrupole GC-MS/MS System is designed for accelerated deployment. Reduced needs for operator training and faster time to full productivity together with maximum sample throughput provide fast return on your instrument investment.

Find out more at thermofisher.com/TSQ9610

RELEASE

ETHOS X – Advanced Microwave Extraction System for Environmental Laboratories
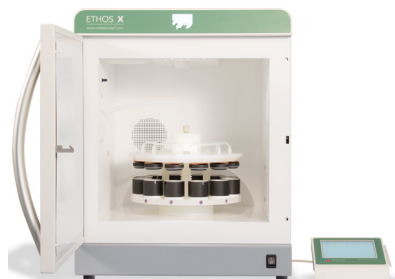
Microwave-assisted solvent extraction offers superior lab efficiency in the determination of organic pollutants with microwave green extraction technique. Typical applications include chlorinated pesticides, semi-volatile organics, PAHs, PCBs, chlorinated herbicides, phenols, organophosphorus pesticides, dioxins and furans.

Determination of organic pollutants in environmental matrices is a common task for thousands of laboratories worldwide, as it leads to controlling and protecting our environment from high levels of contaminants. This analysis is often done to evaluate the effectiveness of a remediation process, to assess the contamination in waste, in waste landfills and for general environmental monitoring. Therefore, every day environmental laboratories deal with several challenges to ensure high quality data and fast turnaround time while maintaining their competitiveness.

Extraction of pollutants from solid matrices is often performed with techniques that limit the productivity and have high running costs. Many laboratories still use the Soxhlet method that was developed in 1879!

Milestone listened to the needs of environmental laboratory professionals by developing the ETHOS X with the fastEX-24 rotor, which allows for simultaneous extraction of 24 samples in 40 minutes with minimal solvent usage. By using large volume disposable glass vials, the fastEX-24 rotor simplifies handling and allows to achieve lower detection limits.

- High throughput: 24 samples in 40 minutes.
- Superior return of investment. Substantial reduction in solvent.
- Simple handling. Disposable glass vials.
- Consistency & Reproducibility. Consistent and reproducible results.
- Safety & Reliability.

Achieving lower detection limits with higher sample amount

The ETHOS X with fastEX-24 rotor extracts up to 30 grams of sample with minimal solvent volume, helping analysts to accomplish their tasks.

The Milestone fastEX-24 rotor uses disposable glass vials, eliminating the need for cleaning and the possibility of memory effect between different runs. The 100 mL vials can accommodate the extraction of a large sample amount. The easy to handle and affordable cost of the vials leads to high productivity at a very low running cost. ETHOS X system easily adapts to existing extraction chemistry through the use of a unique, patented material, called Weflon. Stir bars of Weflon are heated by microwaves and they subsequently transfer this heat to the non-polar solvent, which is not heated by microwaves.

COMPLIANCE

Several official methods describe the use of microwave closed-vessel technology to enhance the extraction efficiency of organic pollutants, such as US EPA 3546, ASTM and other national methods. The ETHOS X with fastEX-24 further enhances the performance of microwave technology for the extraction of water-insoluble or slightly water-soluble organic compounds from soils, clays, sediments, sludges, and solid wastes.

RELEASE

Pittcon Conference & Expo

Pittcon is a catalyst for the exchange of information, a showcase for the latest advances in laboratory science, and a venue for international connectivity.

Pittcon is a dynamic, transnational conference and exposition on laboratory science, a venue for presenting the latest advances in analytical research and scientific instrumentation, and a platform for continuing education and science-enhancing opportunity. Pittcon is for anyone who develops, buys, or sells laboratory equipment, performs physical or chemical analyses, develops analysis methods, or manages these scientists.

Pittcon Awards
Honoring scientists who have made outstanding contributions to Analytical Chemistry

Each year, Pittcon provides a venue where scientists who have made outstanding contributions to laboratory science, analytical chemistry, and applied spectroscopy are honored.

Among these awards is the **Pittcon Heritage Award** which honors those visionaries whose entrepreneurial careers shaped the instrumentation and laboratory supplies community and by doing so have transformed the scientific community at large.

The award has been presented jointly with Pittcon since 2002 and is given out each year at a special ceremony during the Pittcon Conference and Expo. The recipient's name and achievements are added to the Pittcon Hall of Fame, which conference attendees can visit at the show each year.

Pittcon 2025 – Conference on Analytical Chemistry and Applied Spectroscopy
March 1-5, 2025
Boston Convention and Exhibition Center
Boston, Massachusetts, USA

Pittcon
Conference and Exposition
Boston, Massachusetts, USA
March 1-5, 2025

WICKED SMAHT
TO COME TO BOSTON!

Learn More

Why Boston is the Wicked Smaht Choice!

Boston's Logan Airport is conveniently located 2 miles from the Boston Convention and Exhibition Center (BCEC).

Our Attendee Experience Committee is hard at work planning fun evening activities for attendees to continue their networking and collaboration: F1 arcade with 69 full motion simulators, flight club darts and pub, Putt Shack minigolf experience and much more.

Boston's Seaport District is the fastest growing and newest neighborhood in Boston, quickly becoming its new nucleus. It boasts hundreds of new restaurants, trendy hotels, and is highly walkable.

Over 75 Years of Enriching Scientific Endeavor

Important Dates for Attendees

4-1-24
Call for Symposia + Short Courses Opens

5-1-24
Call for General Abstracts Opens

6-1-24
Call for Networking Roundtables + Workshops Opens

10-29-24
Attendee Registration Opens

1-17-25
Early Bird Registration Ends

Pittcon
Conference and Exposition

RELEASE

SelectScience® Pioneers online Communication and Promotes Scientific Success

SelectScience® promotes scientists and their work, accelerating the communication of successful science. Through trusted lab product reviews, virtual events, thought-leading webinars, features on hot scientific topics, eBooks and more, independent online publisher SelectScience® provides scientists across the world with vital information about the best products and techniques to use in their work.

Some recent contributions from SelecScience® to the scientific community

Editorial Article
The next frontier in nanoelectromechanical photothermal infrared spectroscopy

Discover how Invisible-Light Labs is redefining nanoscale analysis with EMILIE, boosting sensitivity and cutting sampling times for breakthroughs in environmental monitoring, nanotechnology, and beyond. EMILIE is a groundbreaking nanoelectromechanical infrared analyzer from Invisible-Light Labs. Access **here**

News & Articles
Optimizing battery testing performance

Learn about the different types of battery testing and explore additional considerations for optimizing performance. The future of battery testing is likely to focus on faster, more efficient methods capable of rapid assessments during operation. This type of assessment will be increasingly valuable as batteries become more integrated into critical industrial applications. While electrochemical impedance spectroscopy is a powerful research tool, its cost and difficulty of use limit its potential. More accessible, streamlined versions of this technology will shape the future of the battery testing industry. Access **here**

Videos at The Scientists' Channel
Sepsis identification and intervention within one hour of infection

Dr. Enrique Hernández, CEO of Loop Diagnostics, recognizes the importance of analyzing the immune system status of a patient in order to accurately detect sepsis early on. Here, Dr. Hernández outlines the challenges in diagnosing sepsis and highlights how the company's *in vitro* cellular immunoassay is designed to detect sepsis within the first hour of bloodstream infection. Access **here**

SelectScience® is the leading independent online publisher connecting scientists to the best laboratory products and applications.
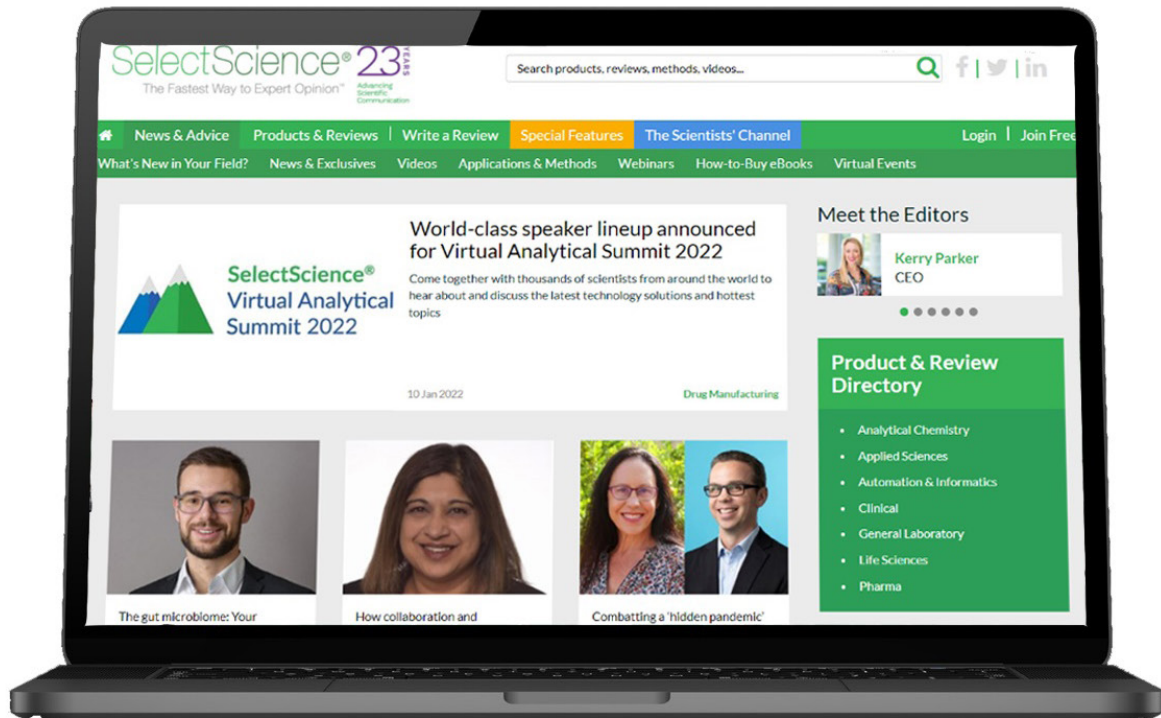
- Working with Scientists to Make the Future Healthier.

- Informing scientists about the best products and applications.

- Connecting manufacturers with their customers to develop, promote and sell technologies.

SelectScience®
The Fastest Way to Expert Opinion

CHROMacademy is the leading provider of eLearning for analytical science
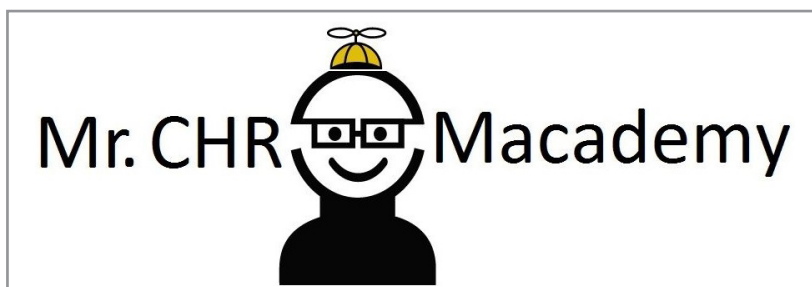
CHROMacademy *helps scientific organizations acquire and maintain excellence in their laboratories*.

For over 10 years, CHROMacademy has increased knowledge, efficiency and productivity across all applications of chromatography. With a comprehensive library of learning resources, members can improve their skills and knowledge at a pace that suits them.

CHROMacademy covers all chromatographic applications – HPLC, GC, mass spec, sample preparation, basic lab skills, and bio chromatography. Each paradigm contains dozens of modules across theory, application, method development, troubleshooting, and more. Invest in analytical eLearning and supercharge your lab.

For more information, please visit www.chromacademy.com/

BrJAC

NOTICES OF BOOKS

Microextraction Techniques – Fundamentals, Applications and Recent Developments

Miguel A. Rodríguez-Delgado, Bárbara Socas-Rodríguez, Antonio V. Herrera-Herrera (Editors)

February, 2024. Springer

This book provides an overview of the two main groups of microextractions, sorbent-based, and solvent-based. Each chapter focuses on the description of the technique fundamentals, the main applications, and the novel developments carried out in recent years written by a renowned expert or group of experts in the field. doi
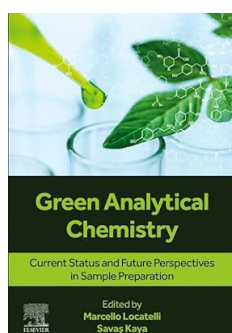
Green Analytical Chemistry – Current Status and Future Perspectives in Sample Preparation

October, 2024. Elsevier

Marcello Locatelli, Savaş Kaya (Eds.)

By proving a theoretical background of novel green technologies and proposing new protocols, this book addresses innovative methodologies in analytical chemistry and sample preparation following the requirements of green analytical chemistry demands. It is a valuable resource for researchers, chemist, students, and all those interested in the allied field. Read more
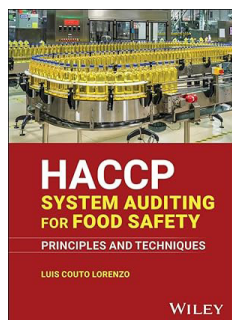
HACCP System Auditing for Food Safety: Principles and Techniques

Luis Couto Lorenzo

August, 2024. Wiley

This book helps readers understand the fundamentals of the Hazard Analysis and Critical Control Point (HACCP) concept and its importance in ensuring food safety, with guidance on how to develop auditing skills including planning, executing, and reporting on HACCP audits effectively. It incorporates many practical examples with accompanying figures and models, along with selected case studies and global practices from Europe, Canada, USA, and New Zealand. Read more
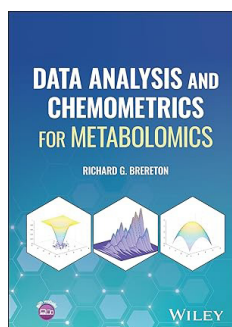
Data Analysis and Chemometrics for Metabolomics

Richard G. Brereton

July, 2024. Wiley

Thoroughly and accessibly written by a leading expert in chemometrics, this book brings robust data analysis into conversation with the metabolomic field to the immense benefit of practitioners. It is ideal for practitioners in the life sciences, clinical sciences and chemistry, as well as metabolomics researchers or developers of research instruments, and statisticians developing methods to design experiments and analyse large datasets of clinical and biological origin. Read more

PERIODICALS & WEBSITES

American Laboratory

American Laboratory® is a platform that addresses basic research, clinical diagnostics, drug discovery, environmental, food and beverage, forensics and other markets, and combines in-depth articles, news, and video to deliver the latest advances in their fields. **Featured Article:** *Researchers Develop New Electrolyte To Improve K-Na/S Battery Performance.* Columbia Engineering researchers have developed a novel electrolyte that improves the performance of K-Na/S batteries, which could provide a much-needed low-cost option for renewable energy storage. **Read more**

LCGC

Chromatographyonline delivers practical, nuts-and-bolts information to help scientists and lab managers become more proficient in the use of chromatographic techniques and instrumentation. *An Integrative Analytical Quality by Design (AQbD), Up-To-Date Greenness, and Whiteness Set of Tools for Evaluation of a Sustainable RP-HPLC Method for Regulated Products.* Hemanth Kumar Chanduluru of the SRM Institute of Science and Technology in Kattankulathur, India, discusses the many issues related to sustainability in analytical separation methods. Read more
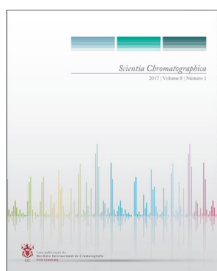
Scientia Chromatographica

Scientia Chromatographica is the first and to date the only Latin American scientific journal dedicated exclusively to Chromatographic and Related Techniques. With a highly qualified and internationally recognized Editorial Board, it covers all chromatography topics in all their formats, in addition to discussing related topics such as "The Pillars of Chromatography", Quality Management, Troubleshooting, Hyphenation (GC-MS, LC-MS, SPE-LC-MS/MS) and others. It also provides columns containing general information, such as: calendar, meeting report, bookstore, etc. Read more

Select Science

SelectScience® has transformed global scientific communications and digital marketing over the last 25 years. Informing scientists about the best products and applications. Connecting manufacturers with their customers to develop, promote and sell technologies promotes scientists and their work, accelerating the communication of successful science. Scientists can make better decisions using independent, expert information and gain easy access to manufacturers. SelectScience® informs the global community through Editorial, Features, Video and Webinar programs. Read more

Spectroscopy

With the *Spectroscopy* journal, scientists, technicians, and lab managers gain proficiency through unbiased, peer-reviewed technical articles, trusted troubleshooting advice, and best-practice application solutions.
Article: *Revolutionizing Dairy Safety: The Role of FT-IR Spectroscopy.* By Will Wetzel. In the review article, the authors highlight the Fourier-transform infrared (FT-IR) spectroscopy high throughput speed, minimal sample preparation, ease of operation, and low variable costs. Read more

EVENTS in 2024

October 6 to 10
34th International Symposium on Chromatography – ISC 2024
Liverpool, UK
https://isc2024.org/

October 20 to 25
SciX Conference 2024
Raleigh, NC, United States
https://www.scixconference.org/scix-future-conferences

October 24 to 25
IV Reunião Bienal da Sociedade Brasileira de Eletroquímica e Eletroanalítica
Center for Agricultural Sciences (CCA), Federal University of São Carlos (UFSCar)
Araras, SP, Brazil
https://www.lsnano.ufscar.br/iv-sbee

November 9 to 12
29th Latin-American Capillary Electrophoresis, Microfabrication and Related Techniques Symposium and Brazilian Symposium on Metabolomics (LACE 2024 / BrMet)
Casa Grande Hotel Guarujá, Guarujá, SP, Brazil
https://www.lace2024.iqm.unicamp.br/

November 10 to 13
9th National Meeting of Forensic Chemistry (ENQFor) and 6th Meeting of the Brazilian Society of Forensic Sciences (SBCF)
Events Center of the Hotel Royal Tulip JP, Ribeirão Preto, SP, Brazil
https://www.enqfor.org.br/

December 8 to 11
4th Iberoamerican Conference on Mass Spectrometry (IberoMS2024)
Grand Carimã Resort & Convention Center, Foz do Iguaçu, PR, Brazil
https://www.iberoms2024.com/

BrJAC

EVENTS in 2025

March 1 to 5
PITTCON Conference & Expo
Boston Convention and Exhibition Center
Boston, Massachusetts, USA
https://pittcon.org/pittcon-2025/

June 8 to 11
48th Annual Meeting of the Brazilian Chemical Society (RASBQ)
Expo Dom Pedro
Campinas, SP, Brazil
https://www.sbq.org.br/48ra/

August 31 to September 4
XXII European Conference on Analytical Chemistry – Euroanalysis
CCIB - Barcelona International Convention Centre
Barcelona, Spain
https://euroanalysis2025.com/index.php

September 23 to 25
Analitica Latin America Expo & Conference
São Paulo Expo, São Paulo, SP, Brazil
https://home.analiticanet.com.br/

October 20 to 23
XXV Brazilian Symposium of Electrochemistry and Electroanalytical
Águas de Lindóia, SP, Brazil
https://www.lsnano.ufscar.br/

October 27 to 31
***Congresso Latino-Americano de Cromatografia e Técnicas Relacionadas* (COLACRO-2025)**
Florianópolis, Brazil
https://www.colacro.org/

November 16 to 21
EspeQ Brasil and Rio Symposium 2025
Nov. 16 to 18 – 8th Brazilian Meeting on Chemical Speciation (EspeQ Brasil 2025)
Nov. 19 to 21 – 17th Rio Symposium on Atomic Spectrometry (RSAS 2025)
Hotel Fazenda Colina Verde, São Pedro, SP, Brazil
Access info

AUTHOR GUIDELINES

Aims & Scope

Brazilian Journal of Analytical Chemistry is a double-blind peer-reviewed research journal dedicated to the diffusion of significant and original knowledge in all branches of Analytical and Bioanalytical Chemistry. It is addressed to professionals involved in science, technology, and innovation projects at universities, research centers and in industry. **BrJAC welcomes** the submission of research papers reporting studies devoted to new and significant analytical methodologies, putting in evidence the scientific novelty, the impact of the research and demonstrating the analytical or bioanalytical applicability. BrJAC **strongly discourages** those simple applications of routine analytical methodologies, or the extension of these methods to new sample matrices, unless the proposal contains substantial novelty and unpublished data, clearly demonstrating advantages over existing ones.

Additionally, there are other submission categories to BrJAC such as:

Reviews: They should be sufficiently broad in scope, but specific enough to permit an appropriate depth discussion, including critical analyses of the bibliographic references and conclusions. Manuscripts submitted for publication as Reviews must be original and unpublished. Reviews undergo double-blind full peer review and are handled by the Editor of Reviews.

Technical Notes: Concise descriptions of developments in analytical methods, new techniques, procedures, or equipment falling within the scope of the BrJAC. Technical notes also undergo double-blind full peer review.

Letters: Discussions, comments, and suggestions on issues related to Analytical Chemistry or Bioanalytical Chemistry. Letters are welcome and will be published at the discretion of the BrJAC Editor-in-Chief.

Point of View: This category is exclusively invited by the Editor-in-Chief.

See the next items for more information on the journal, the documents preparation, manuscript types, and how to prepare the submission.

Professional Ethics

Originality: manuscripts submitted for publication in BrJAC cannot have been previously published or be currently submitted for publication in another journal.

Preprint: BrJAC does not accept manuscripts that have been posted on preprint servers prior to the submission.

Integrity: the submitted manuscripts are the full responsibility of the authors. Manipulation/invention/omission of data, duplication of publications, the publication of papers under contract and confidentiality agreements, company data, material obtained from non-ethical experiments, publications without consent, the omission of authors, plagiarism, the publication of confidential data and undeclared conflicts of interests are considered serious ethical faults.
BrJAC discourages and restricts the practice of excessive self-citation by the authors.
BrJAC does not practice coercive citation, that is, it does not require authors to include references from BrJAC as a condition for achieving acceptance, purely to increase the number of citations to articles from BrJAC without any scientific justification.

Conflicts of interest: when submitting their manuscript for publication, the authors must include all potential sources of bias such as affiliations, funding sources and financial, management or personal relationships which may affect the work.

Copyright: will become the property of the Brazilian Journal of Analytical Chemistry, if and when a manuscript is accepted for publication. The copyright comprises exclusive rights of reproduction and distribution of the articles, including reprints, photographic reproductions, microfilms or any other reproductions similar in nature, including translations.

Request for permission to reuse figures and tables published in the BrJAC: researchers who want to reuse any document or part of a document published in the BrJAC should request reuse permission from the BrJAC Editor-in-Chief, even if they are the authors of such document. A template for requesting reuse permission can be downloaded **here**.

Misconduct will be treated according to the COPE's recommendations (https://publicationethics.org/) and the Council of Science Editors White Paper on Promoting Integrity in Scientific Journal Publications (https://www.councilscienceeditors.org/).

Manuscript submission

The BrJAC does not charge authors an article processing fee.

Manuscripts must be prepared according to the BrJAC manuscript template. Manuscripts in disagreement with the BrJAC guidelines are not accepted for revision.

The BrJAC uses an online manuscript manager system for the submission of manuscripts. This system guides authors stepwise through the entire submission process.

After the submitting author logs in to the system and enters his/her personal and affiliation details, the submission can be started.

All co-authors must be added to the Authors section.

Four documents are mandatorily uploaded by the submitting author: Cover letter, Title Page, Novelty Statement and the Manuscript. Templates for these documents are available for download **here**.

The four documents mentioned above must be uploaded as Word files. The manuscript Word file will be converted by the system to a PDF file which will be used in the double-blind peer review process.

All correspondence, including notification of the Editor's decision and requests for revision, is sent by e-mail to the submitting author through the manuscript manager system.

Documents Preparation

It is highly recommended that authors download and use the templates to create their four mandatory documents to avoid the suspension of a submission that does not meet the BrJAC guidelines.

Cover Letter
The cover letter template should be downloaded and filled out carefully.
Any financial conflict of interest or lack thereof and agreement with BrJAC's copyright policy must be declared.
It is the duty of the submitting author to inform his/her collaborators about the submission of the manuscript and its eventual publication.
The Cover Letter must be signed by the corresponding author.

Title Page
The Title Page must contain information for each author: full name, affiliation and full international postal address, and information on the contribution of each author to the work. Acknowledgments must be entered on the Title Page. The submitting author must sign the Title Page.

Novelty Statement
The Novelty Statement must contain clear and succinct information about what is new and innovative in the study in relation to previously related works, including the works of the authors themselves.

Manuscript (all submission categories)

It is highly recommended that authors download the Manuscript template and create their manuscript in this template, keeping the layout of this file.

- **Language**: **English** is the language adopted by BrJAC. The correct use of English is of utmost importance. In case the Editors and Reviewers consider the manuscript to require an English revision, the authors will be required to send an English proofreading certificate before the final approval of the manuscript by BrJAC.

- **Required items**: the manuscript must include a title, abstract, keywords, and the following sections: Introduction, Materials and Methods, Results and Discussion, Conclusion, and References.

- **Identification of authors**: as the BrJAC adopts a double-blind review, the manuscript file must **NOT** contain the authors' names, affiliations nor acknowledgments. Full details of the authors and their acknowledgements should be on the Title Page.

- **Layout**: the lines in the manuscript must be numbered consecutively and double-spaced.

- **Graphics and Tables**: must appear close to the discussion about them in the manuscript. For **figures** use **Arabic** numbers, and for **tables** use **Roman** numbers.

- **Figure files:** when a manuscript is approved for publication, the BrJAC production team will contact the corresponding author to request separate files of each figure and a graphical abstract. These files must have **good resolution** and the extension **PNG or JPG**. The graphical abstract should preferably be created in landscape format. In the article diagrammed in the journal, the graphical abstract will occupy a space of 8 to 9 cm in length and 6 cm in height. Chemical structures must have always the same dimensions.

- **Permission to use content already published**: to use figures, graphs, diagrams, tables, etc. identical to others previously published in the literature, even if these materials have been published by the same submitting authors, a publication permission from the publisher or scientific society holding the copyrights must be requested by the submitting authors and included among the documents uploaded in the manuscript management system at the time of manuscript submission.

- **Chemical nomenclature, units and symbols**: should conform to the rules of the International Union of Pure and Applied Chemistry (IUPAC) and Chemical Abstracts Service. It is recommended that, whenever possible, the authors follow the International System of Units, the International Vocabulary of Metrology (VIM) and the NIST General Table of Units of Measurement. Abbreviations are not recommended except for those recognized by the International Bureau of Weights and Measures or those recorded and established in scientific publications. Use L for liters. Always use superscripts rather than /. For instance: use mg mL^{-1} and NOT mg/mL. Leave a space between numeric values and their units.

- **References throughout the manuscript:** the references must be cited as superscript numbers. It is recommended that references older than 5 (five) years be avoided, except in relevant cases. Include references that are accessible to readers.

- **References item:** This item must be thoroughly checked for errors by the authors before submission. From 2022, BrJAC is adopting the American Chemical Society's Style in the Reference item. Mendeley Reference Manager users will find the Journal of American Chemical Society citation style in the Mendeley View menu. Non-users of the Mendeley Reference Manager may refer to the ACS Reference Style Quick Guide DOI: https://doi.org/10.1021/acsguide.40303

Review process

Manuscripts submitted to the BrJAC undergo an initial check for compliance with all of the journal's guidelines. Submissions that do not meet the journal's guidelines will be suspended and an alert sent to the corresponding author. The authors will be able to resend the submission within 30 days. If the submission

according to the journal's guidelines is not made within 30 days, the submission will be withdrawn on the first subsequent day and an alert will be sent to the corresponding author.

Manuscripts that are in accordance with the journal's guidelines are submitted for the analysis of similarities by the iThenticate software.

The manuscript is then forwarded to the Editor-in-Chief who will check whether the manuscript is in accordance with the journal's scope and will analyze the similarity report issued by iThenticate.

If the manuscript passes the screening described above, it will be forwarded to an Associate Editor who will also analyze the iThenticate similarity report and invite reviewers.

Manuscripts are reviewed in double-blind mode by at least 2 reviewers. A larger number of reviewers may be used at the discretion of the Editor. As evaluation criteria, the reviewers employ originality, scientific quality, contribution to knowledge in the field of Analytical Chemistry, the theoretical foundation and bibliography, the presentation of relevant and consistent results, compliance with the BrJAC's guidelines, clarity of writing and presentation, and the use of grammatically correct English.

Note: In case the Editors and Reviewers consider the manuscript to require an English revision, the authors will be required to send an English proofreading certificate, by the ProofReading Service or equivalent service, before the final approval of the manuscript by the BrJAC.

The 1st-round review process usually takes around 5-6 weeks. If the manuscript is not rejected but requires corrections, the authors will have one month to submit a corrected version of the manuscript. In another 3-4 weeks, a new decision on the manuscript may be presented to the corresponding author.

The manuscripts accepted for publication are forwarded to the BrJAC production department. Minor changes to the manuscripts may be made, when necessary, to adapt them to BrJAC guidelines or to make them clearer in style, respecting the original content. The articles are sent to the authors for approval before publication. Once published online, a DOI number is assigned to the article.

Final Considerations

Whatever the nature of the submitted manuscript, it must be original in terms of methodology, information, interpretation or criticism.

With regard to the contents of published articles and advertisements, the sole responsibility belongs to the respective authors and advertisers; the BrJAC, its editors, editorial board, editorial office and collaborators are fully exempt from any responsibility for the data, opinions or unfounded statements.

Manuscript submission at www.brjac.com.br